Coordination chemistry of *N*-heterocyclic carbene and thione functionalised calix[4]arene ligands

By Ruth Ann Patchett

A thesis submitted in partial fulfilment of the requirements for the degree of
Doctor of Philosophy in Chemistry

University of Warwick, Department of Chemistry
September 2016

Contents

Acknowledgements

The last four years have been no easy feat and it would be remiss of me not to extend my thanks to the huge number of people who have touched my life over that time. Firstly, I would never have had this opportunity without Dr Adrian Chaplin, who committed much of his time, to even the smallest details of the project. I find such attention to detail a precious trait in a PhD supervisor and am grateful for the time he has committed to my project.

Synthetic work means nothing without the analysis used to confirm products and the teams involved in running the equipment and carrying out complex analysis; as such thanks go to: Dr Ivan Prokes and Robert Perry for their assistance with NMR spectroscopy, in particular weekends of machine time committed to ^{39}K spectroscopy; Dr Ligand Song and Phil Aston for mass spectrometry and their endless patience in making sure the outputs were just right. Robert Jenkins is owed thanks for the vast amount of work he undertook, his amazing support within the chemistry department, specifically how much work he carried out “behind the scenes” with such sincere enthusiasm.

All of the “third floor crew” thank you for making the university feel like home with silly in-jokes and your widespread support I have never once felt alone, or without a biscuit should I need one. Penny and Jo for welcoming me to Warwick and being inspirational WIS. The Chaplin group; Thibault for his vivid use of colour in his technical drawings, Simone for leading by example with her kindness, support and incredible organisation, Rich for his unashamed passion, advice and help, in particular the analytical work which he carried out to an exacting standard. To Lucreo for persevering to be my friend despite problems with my accent, and Matt for his straight talking, encyclopaedic knowledge and no-nonsense Aussie attitude. The many younglings we have adopted, Jack and Caroline who were fantastic additions to the group and in particular Jack for continuing the quest with calix[4]arene complexes, JCB for being my ticket back into the EU and introducing me to LMP. The newest of newbies for arriving with fresh enthusiasm when mine was dwindling. Essentially to

Rhiann, who has shared so many laughs, horrors, ups and inevitable downs. You have spurred me on both with encouragement and by leading as a shining example. Many times all I could do is sit back and be impressed by your passion and ability to constantly turn your hands to new challenges. It has been a privilege to work with you and be your friend. It has been very strange to no longer see you every day.

Outside of the University I would also like to thank my parents for their support and genuine interest, my siblings; Clare, John and, especially David and Hannah; for being so supportive, providing wine and watching Shipwrecked with me. No-one could fill your shoes. Thanks to Evelyn for being my thing to look forward to. Carys who advised me to grab life with both hands. Grainne and Emily for their long distance support, even when it means not asking! Lizzie, Hannah and Mouse for taking me in. James, Martin and Michael for living with, and not murdering me.

Finally I would like to extend my thanks to my examiners; Dr J. Rourke and Dr M Spicer, for reading my work, their helpful and interesting discussion and patience with my corrections.

Abstract

This thesis is a summary of the work carried out exploring the properties and applications of calix[4]arene ligands. Particular attention is given to the flexibility and encapsulation capabilities of these species. Initially synthetic methodology for the incorporation of bis-imidazolinium and imidaolium groups was targeted. The synthesis of imidazolinium functionalised species proved problematic, however pro-ligand **2a·2HI** was readily prepared *via* a six-step synthetic procedure.

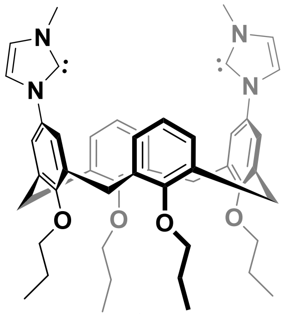
2a

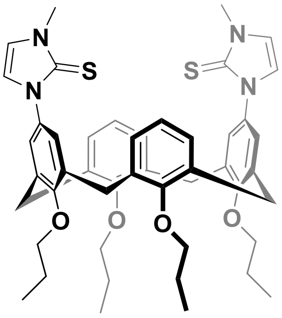
3

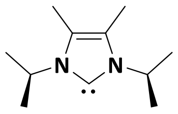
$\mathrm{I}^{i}\mathrm{Pr}_2\mathrm{Me}_2$

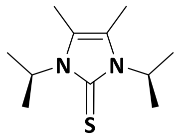
$\mathrm{I}^{i}\mathrm{Pr}_2\mathrm{Me}_2\mathrm{S}$

The coordination chemistry of **2a·2HI** with $[\mathrm{Rh(COD)Cl}]_2$ and $[\mathrm{Rh(CO)_2Cl}]_2$, *via* generation of the free carbene (**2a**) or transmetallation from an isolated silver complex (**6a**) was explored. Both routes resulted in the formation of bimetallic species. The isolation of these complexes highlights the flexibility of the calix[4]arene scaffold. The role of the calix[4]arene was probed though comparison to complexes of the monodentate $\mathrm{I}^{i}\mathrm{Pr}_2\mathrm{Me}_2$ ligand.

Based on these results, the imidazole-2-thione (NHCS) ligand **3** was derived from **2a** and elemental sulfur. Monodentate rhodium and iridium complexes of **3** were readily prepared and found to bind potassium cations within the calix[4]arene cavity. This unusual host-guest chemistry was probed by ^{1}H NMR spectroscopy and in the solid state through comparison to other calix[4]arene hosts.

Common abbreviations

acac	Acetylacetone
Ar^{F}_{4}	3,5-trifluoromethyl)phenyl
Cnt	Centroid
COD	*Cis,cis*-1,5-cyclooctadiene
COE	Cyclooctene
Cp	Cyclopentadienyl
Cp*	Pentamethylcyclopentadienyl
CPR	Calix[4]arene puckering ratio
DCC	*N,N'*-Dicyclohexylcarbodiimide
Dipp	2,6-diisopropylphenyl
DMSO	Dimethyl sulfoxide
DMF	*N,N*-dimethyl formamide
Dtbpm	1,1-bis(di(tert-butyl-phosphino)methane))
ESI-MS	Electrospray Ionisation Mass Spectrometry
HOBT	1-Hydroxybenzotriazole
^{i}Pr	Isopropyl
$I^{i}Pr_2Me_2$	1,3-diisopropyl-4,5-dimethyl-2,3-dihydro-1H-imidazolylidene

$I^{i}Pr_2Me_2S$	1,3-diisopropyl-4,5-dimethyl-2,3-dihydro-1H-imidazol- 2-thione
IR	Infra-red
KHMDS	Potassium bis(trimethylsilyl)amide
Li[TMP]	2,2,6,6-(tetramethylpiperidine)lithium
Mes	Mesitylene
NBD	2,5-Norbornadiene
ROESY	Rotating-frame overhauser effect NMR spectroscopy
TEP	Tollman’s electronic parameter
THF	Tetrahydrofuran
TLC	Thin layer chromatography
J	Coupling constant
RT	Room temperature
NMR	Nuclear magnetic resonance
NOESY	Nuclear Overhauser effect spectroscopy
GC	Gas Chromatography
UV	Ultra-Violet
VT	Variable temperature

Declaration of collaborative and published work

This thesis is submitted to the University of Warwick in support of my application for the degree of Doctor of Philosophy. It has been composed by myself and has not been submitted in any previous application for any degree.

The work presented (including data generated and data analysis) was carried out by the author except in the cases outlined below:

- Crystallographic analysis of all compounds, for which solid-state structures are described, was conducted by Dr. Adrian B. Chaplin, Associate Professor, University of Warwick (Chapters 2, 3, and 4).
- Synthesis and characterisation of pro-ligands **1a·2HCl** and **1b·2HCl** were conducted by Dr Adrian B. Chaplin, Associate Professor, University of Warwick (Chapter 2).
- Synthesis of monoimidazole-calix[4]arene **A418** was conducted by Jack Emerson-King (PhD student), University of Warwick (Chapter 4).
- Competitive ^{1}H NMR experiments and equilibrium constant calculations were carried out by Dr Richard Knighton, post-doctoral research fellow, University of Warwick.

Parts of this thesis have been published by the author:

- **R. Patchett** and A. B. Chaplin. Coordination chemistry of a calix[4]arene-based NHC ligand: Dinuclear complexes and comparison to $I^iPr_2Me_2$. Dalton Trans.2016,**45**, 8945 - 8955.

1.0 Introduction and scope

Overview

This chapter provides a background for the calix[4]arene and N-heterocyclic carbene (NHC) chemistry described in this thesis. A short account of the synthesis, structures, selective functionalisation and host-guest chemistry of calix[4]arenes is outlined. The discussion focuses on previous examples of phosphine- and NHC-based calix[4]arene ligands and their corresponding transition metal complexes. An overview of NHC ligands is also provided, including common structures and topologies of multidentate variants.

1.1 Calixarene synthesis and structure

Calix[n]arenes are a group of cyclic oligomers, their name derives from the Greek 'calix' which translates to 'vase' or 'chalice' due to their characteristic shape. 'Arene' refers to the phenolic units where n denotes the number of repeat units in the oligomer.[1] This naming system was introduced in the 1970s and provides a simple alternative to systematic names, for example pentacyclo[19.3.1.$1^{3,7}$.$1^{9,13}$.$1^{15,19}$]octacosa-1(25),3(28),4,6,9(27),10,12,15(26),16,18,21,23-dodecaene is more simply described as *p*-*tert*butylcalix[4]arene (**Figure 1.1**).

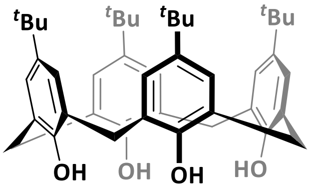

A1

Figure 1.1: Structure of *p*-tertbutylcalix[4]arene (**A1**)

Calixarenes were first synthesised serendipitously as a side product from the Bakelite process in the 1900s.[2, 3] This process was assumed to yield only linear polymeric products until 1944, when Zinke and co-workers postulated that the synthesis yielded semi-rigid cyclic products.[4] This was later confirmed by determination of the molecular weight of the cyclic tetrameric product from the condensation of 4-(1,1,3,3-tetramethylbutyl)phenol and formaldehyde. Calixarenes have since become known as attractive complexing agents and enzyme mimics due to their characteristic 'basket like' shape which makes them well suited for the inclusion of guest molecules.[5-7]

Calix[n]arenes have been isolated in ring sizes ranging from n = 4-16.[8-10] Calix[n]arenes with n = 4 – 8 have been synthesised on a large scale with good yields.[9, 10] This thesis will focus on calix[4]arene structures.

Calix[4]arenes can be synthesised easily by condensation of *p*-substituted phenols and formaldehyde in the presence of a catalytic amount of base. Several systematic studies have been carried out to study the effect of reaction conditions such as reagent ratios, temperature and solvent on the product distribution. For example, KOH, RbOH and CsOH are shown to favour formation of the hexameric products while NaOH favours formation of the tetramers.[9, 11, 12] The Zinke-Cornforth procedure has been developed with conditions favouring formation of calix[4]arene products and is carried out by heating *p-tert*butylphenol in formaldehyde solution with NaOH. It was found that ~ 0.03 – 0.04 equivalents NaOH favoured formation of calix[4]arenes while higher concentrations (>0.3 equivalents) favour the formation of calix[5]arene.[12] Generally it has been concluded that calix[4]arenes are the thermodynamic products and can be formed easily by pyrolysis of higher order oligomers.[13] Calix[4]arenes with identical substituents in the *para*-positions are commonly synthesised by one-pot procedures.[13] Heterofunctionalised calix[4]arenes have been prepared from step-wise procedures; these are broadly separated into non-convergent stepwise synthesis and fragment condensation.[14] Non-convergent syntheses involve alternating hydroxymethylation and condensation of *o*-bromo-*p*-alkylphenol monomers to form linear oligomers which are subsequently cyclised by intramolecular condensation in dilute conditions (**Scheme 1.1**).[15]

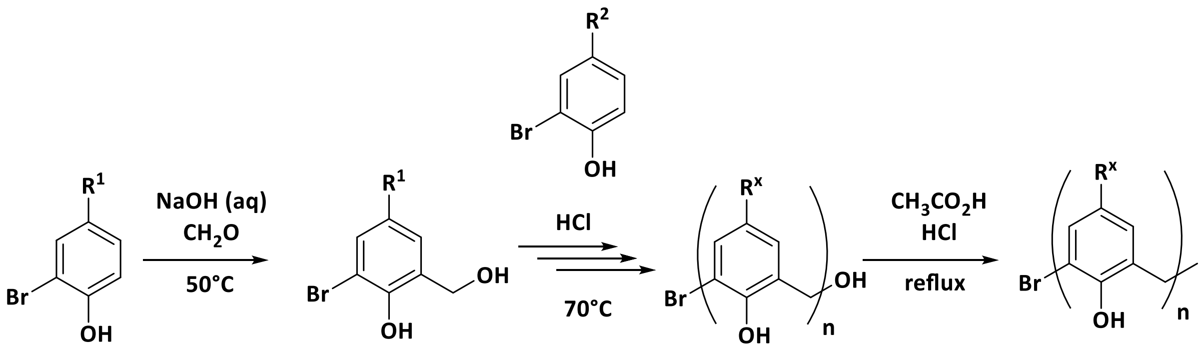

Scheme 1.1*:* Non-convergent stepwise synthesis of calix[4]arenes

Convergent pathways involve a reduced number of steps for the synthesis of asymmetrically functionalised calix[4]arenes. The systematic synthesis of asymmetric calix[4]arenes by fragment condensation in [3+1] or [2+2] processes (**Scheme 1.2**) has been reported, however, both convergent and fragment condensation methods are generally labour intensive and are low yielding.[16, 17]

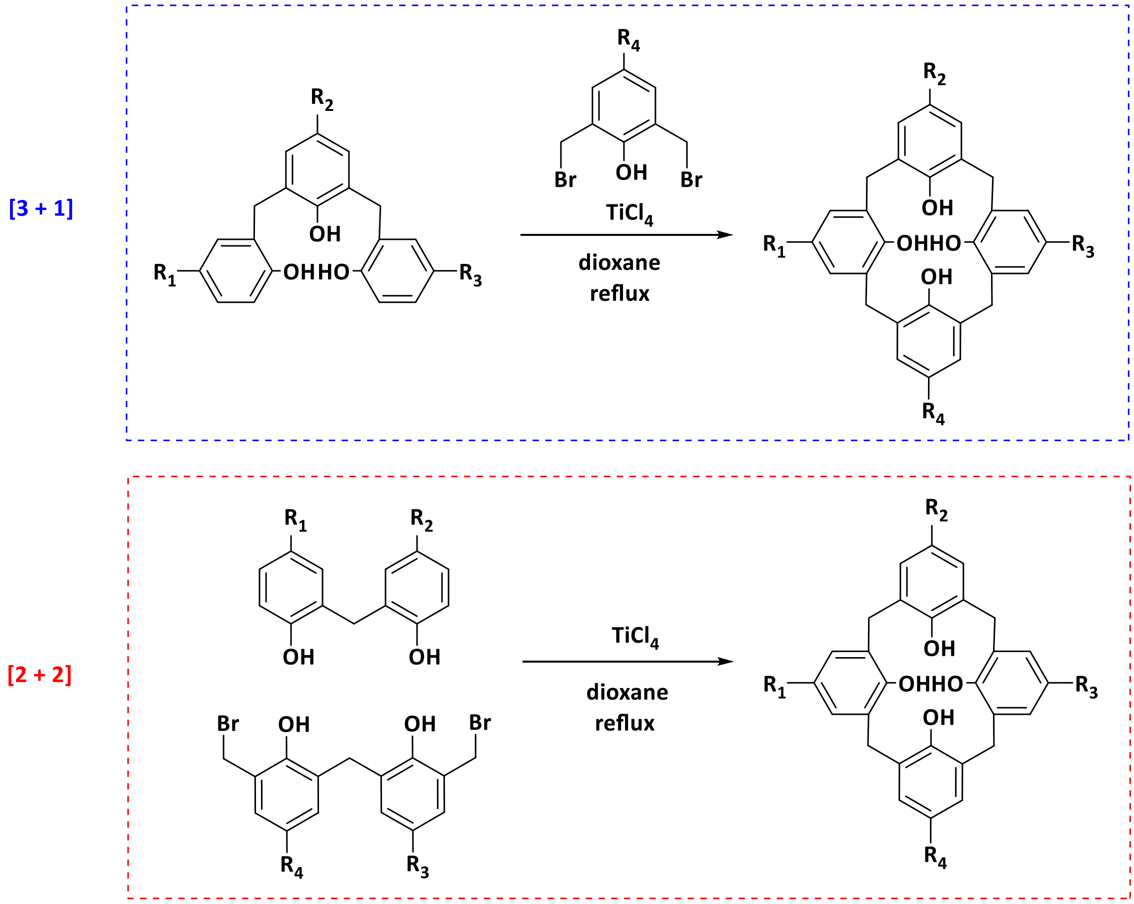

Scheme 1.2: Synthesis of multifunctional calix[4]arenes by fragment condensation; [3+1] (top) and [2+2] (bottom)

Selective functionalisation of symmetric calix[4]arene products can provide a more efficient synthetic route for the preparation of compounds bearing heterofunctionalised products. *p-tert*Butylcalix[4]arene, in particular, is readily synthesised on a large scale and available from most large chemical suppliers, and provided an excellent starting point for the preparation of selectively functionalised calix[4]arene products (*vide infra*).[12]

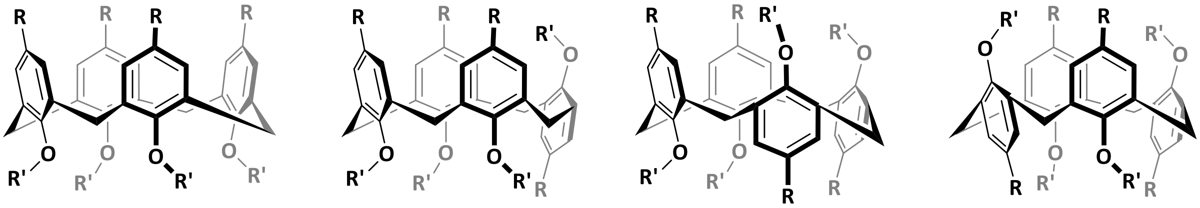

cone **partial cone** **1,2-alternate** **1,3-alternate**

Figure ***1.2:*** Conformational isomers of alkylated calix[4]arenes

Conformational isomers of calix[4]arenes are formed by rotation of the aryl substituents about the bridging methylene units. The resulting isomers are defined as cone, partial cone, 1,2-alternate and 1,3-alternate structures (**Figure 1.2**).[18] The four conformers of the hydroxyl (R' = H) calix[4]arenes are in equilibrium in solution at room temperature. The cone conformation of the phenolic calix[4]arene is the most thermodynamically stable species due to hydrogen bonding between the hydroxyl groups. Interconversion of conformational isomers can be followed by observation of the ^{1}H resonances for the methylene protons of the calix[4]arene, which appear as a pair of germinal doublets below ambient temperatures and a well-defined singlet at elevated temperatures, due to rapid conformational interconversion.[19]

The most common method for producing a well-defined cavity is by trapping the cone or partial cone conformations by substitution of the phenolic hydrogen with a significantly bulky group, such as ^{n}propyl, to sterically prevent rotation of the aryl groups.[20] The nature of *p*-subsituent has little effect on conversion of isomers, for example free energy of conversion of *p-tert*butylcalix[4]arene (**A1**, R = ^{t}Bu, R' = H) is observed at 15.7 kcal/mol in chloroform while the unsubstituted calix[4]arene (R, R' = H) is observed at 14.9 kcal/mol.[19] Cone conformations can be observed in solution by ^{1}H NMR spectroscopy by the observation of the methylene protons as two geminally coupled doublets at approximately 2.5 and 1.2 ppm (**Figure 1.3**), these have been assigned to the equatorial and axial positions, respectively.[21, 22]

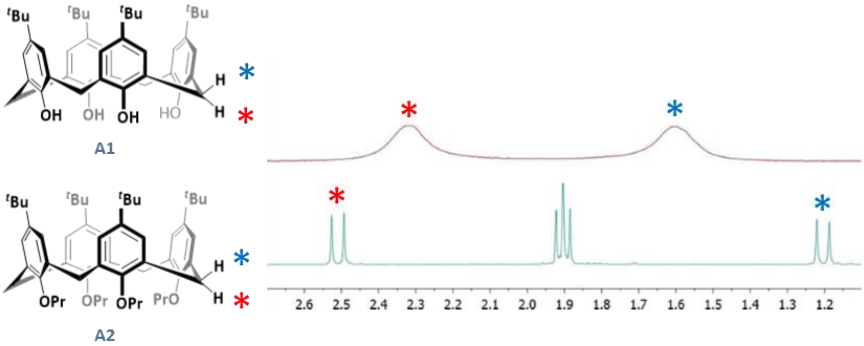

Figure 1.3: *^{1}H NMR spectra showing methylene bridge resonances of* ***A1*** *and* ***A2*** *($CDCl_3$, 298 K, 400 MHz)*

(Triplet observed at 3.85 ppm is assigned to $OC\underline{H}_2$.)

1.2 Functionalisation of calix[4]arenes

Synthetic modification of calixarenes is broadly assigned as either upper or lower rim, where upper rim refers to substitution at the *p*-positions and lower rim refers to the incorporation through the narrow phenol edge. Modification of both upper and lower rim have been extensively investigated.[23-25] In particular, Gutche *et al.* have developed routes for the formation of a wide range of selectively functionalised calix[4]arene products.[12, 26-30] The variety of the appendices and range of ring sizes has led to calixarenes being described as having '(almost) unlimited possibilities' as ligands for metal sensing, receptors for neutral and charged species and catalysts.[31]

As official numbering schemes for calix[4]arene compounds are complex, this thesis will use a simpler system where, for example, substitution of opposing aryl rings will be referred to as '1,3-upper rim substitution' and appendage of adjacent phenol groups will be referred to as '1,2-lower rim substitution' (**Figure 1.4**).

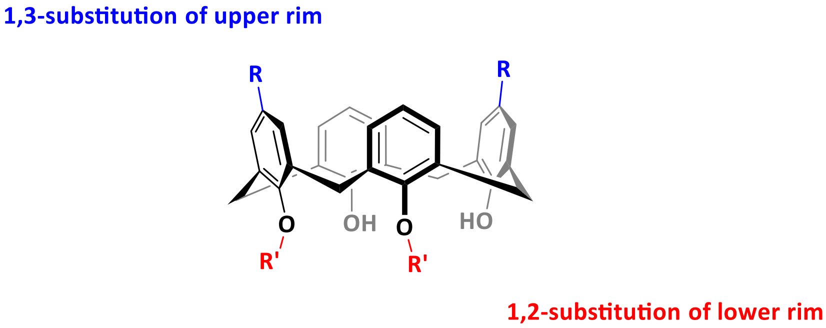

Figure 1.4: *Numbering system adopted for this thesis*

1.2.1 Lower rim functionalisation

The phenolic groups on the lower rim provide an excellent handle for the functionalisation of calix[4]arenes. The simplest reactions involve the formation of phenolic ethers, which increase the solubility of the scaffold and, as discussed above, can be used to 'trap' specific calix[4]arene conformations. Alkylation of the lower rim is readily achieved by S_N2 reactions with alkyl halides under basic conditions with the selectivity controlled by variation of base strength, stoichiometry and reaction conditions (**Scheme 1.3**).[23]

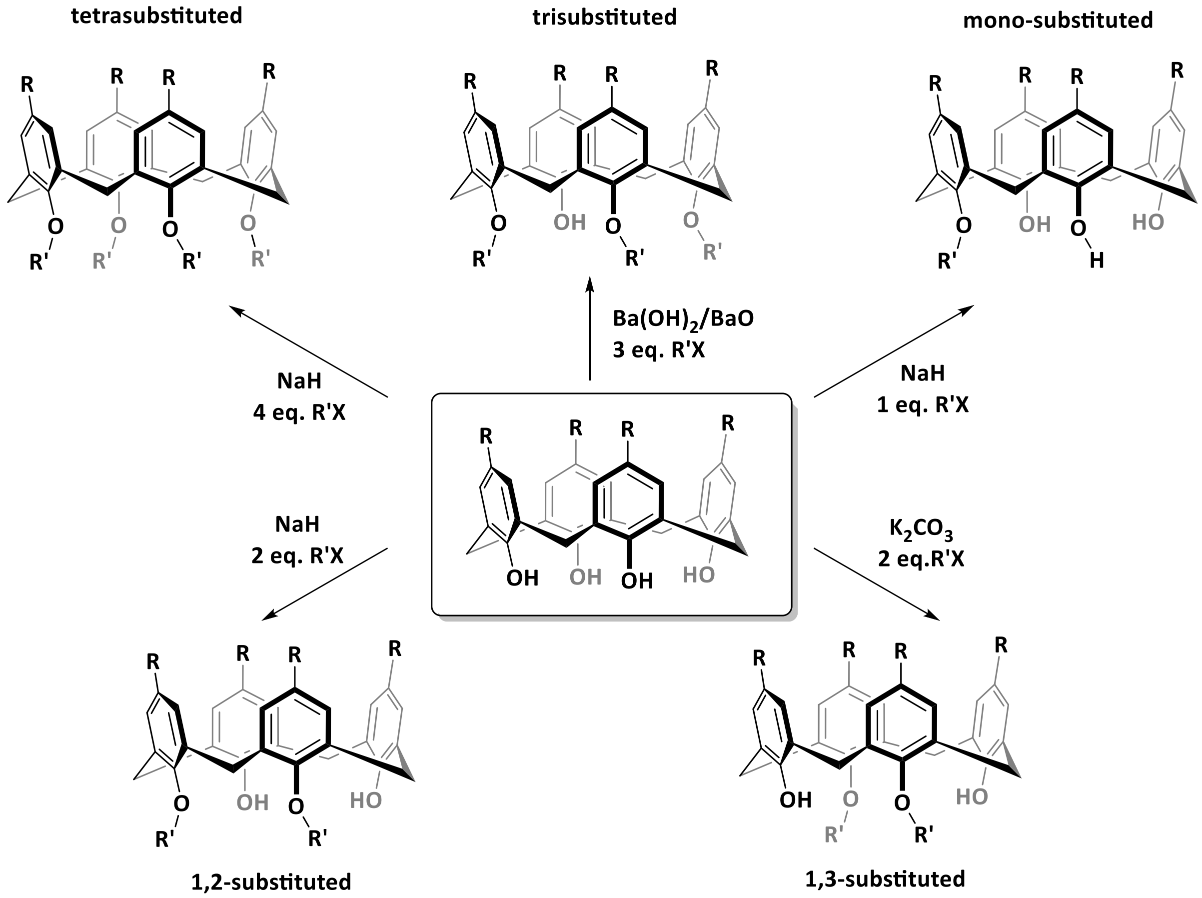

Scheme 1.3: *Selective alkylation of the calix[4]arene lower rim*

Generally an excess of strong base such as NaH can be used to carry out tetra-*O*-alkylation The selectivity of 1,3-distal and 1,2-proximal products is determined by the relative stabilities of Species A and B of the monoalkylated intermediate as shown in **Scheme 1.4**. Weaker bases such as K_2CO_3 can result in the selective formation of 1,3-disubsituted 'distal' products *via* the thermodynamically favoured intermediate, Species A. Stoichiometric addition of stronger bases can be exploited for the formation of 1,2-'proximal' products.[32]

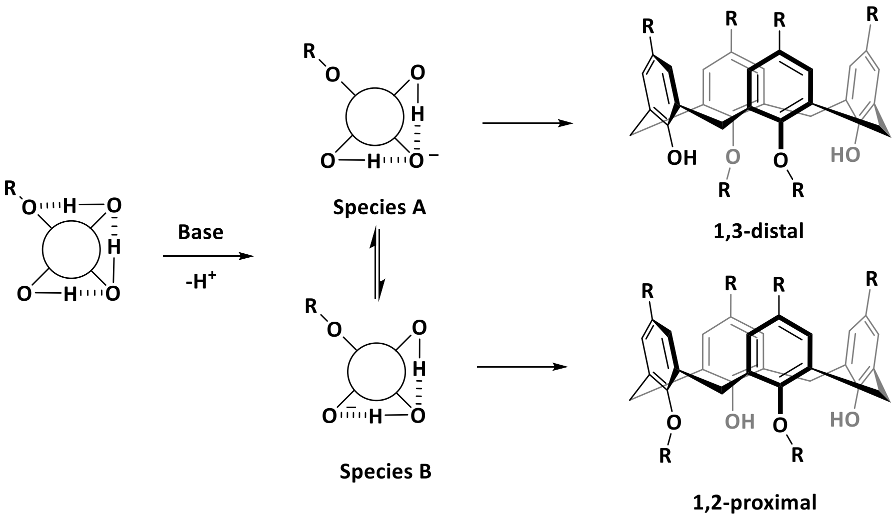

Scheme 1.4: Mechanism for selective alkylation of the lower rim of calix[4]arenes

The potential to functionalise the lower rim with ether, acetate and ester functionalities makes them excellent precursors for the synthesis of biological mimics. For example calix[4]arenes bearing amino acid derivatives on the lower rim have been reported by Yong-bing *et al.* (**Figure 1.5**) which are able to selectively extract transition metal ions over alkali metals from aqueous solution.[33-35] Functionalisation of the lower rim has also been exploited for the synthesis of calix[4]arene ligands bearing coordinating groups including thiones, phosphine, phosphites and NHCs (Section 1.6).[23]

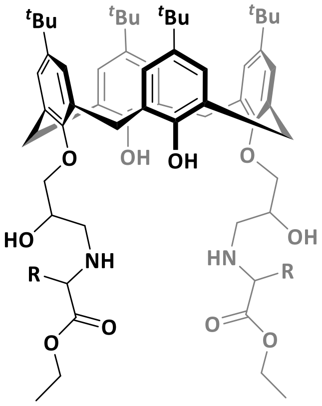

R = CH_3, $CH(CH_3)_2$

A3

Figure 1.5 Calix[4]arene bearing amino acid derivatives in the lower rim

The synthesis of lower rim-functionalised calix[4]arene complexes has been carried out by Matt.[36] For example, the synthesis of distal 1,3-bis-phosphite and 1,3-bis-phosphinite systems which afford both bimetallic and chelated monometallic rhodium complexes (**Scheme 1.5**). Rhodium complexes **A5**, **A6** and **A7** have been synthesised by addition of rhodium precursors to the phosphinite ligand **A4** and have been and used as effective catalysts for the hydroformylation of styrene.[36]

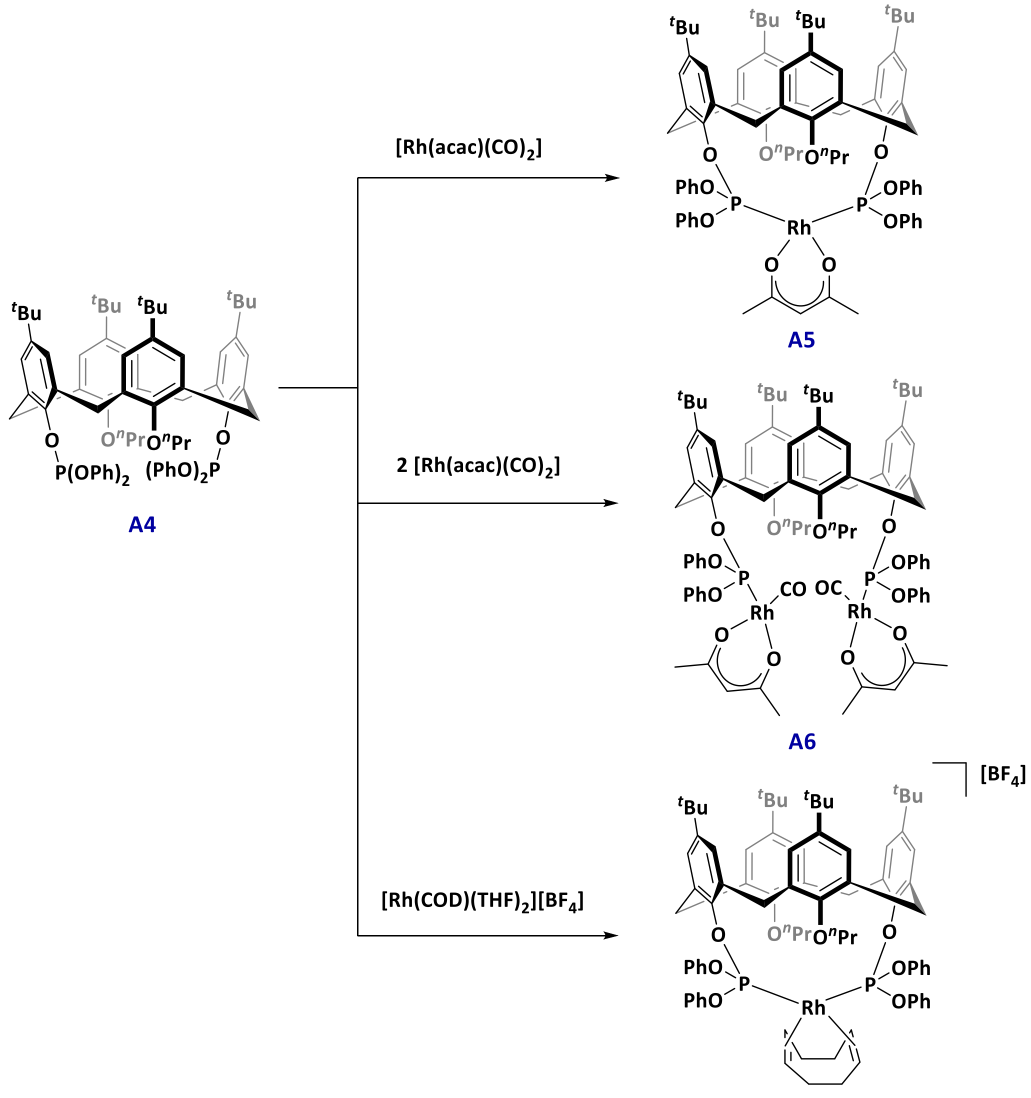

Scheme 1.5*:* Rhodium complexes bearing phosphite-functionalised calix[4]arene ligands

Wieser *et al.* have prepared platinum complexes of lower-rim functionalised calix[4]arene ligands which direct a hydride ligand into the central calix[4]arene cavity (**A9** and **A10**, **Scheme 1.6**). The directed positioning of the hydride has been inferred by ROESY NMR experiments, which indicated positioning of the hydride in close contact with the pendant methylene $OC\underline{H}_2$ groups. X-ray crystal analysis of **A10** was also used to confirm the projection of the hydride into the cavity.[37]

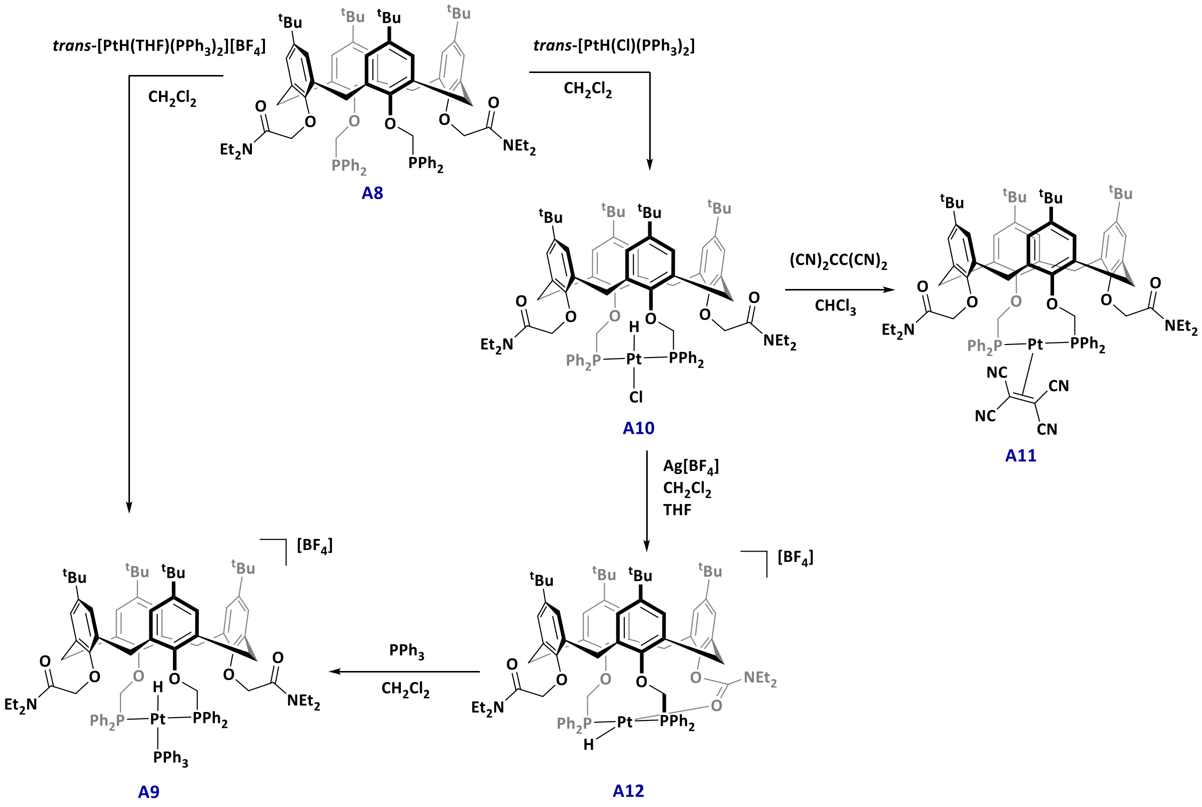

Scheme 1.6: Platinum complexes prepared by Wieser

Hattori and co-workers have also recently reported a series of palladium complexes from ligand **A15** (**Scheme 1.7**).[38] This ligand was prepared from an Ullman-type phosphinoylation from the 1,3-bis(triflate ester), reduction with $HSiCl_3$ and subsequent methylation of the hydroxygroups with alkyl halide in the presence of base. Treatment with two equivalents of

$[PdCl_2(MeCN)_2]$ resulted in the formation of the bis-μ_2-chloro-bridged dinuclear palladium complex in benzonitrile, whereas one equivalent of palladium precursor in acetonitrile resulted in the formation of the mononuclear palladium complex **A16**. The square planar geometry of the central palladium results in the projection of the acetonitrile ligand into the calix[4]arene cavity. The chloride ligand in **A16** was easily abstracted by treatment with $Ag[BF_4]$ in acetonitrile to give **A17**. The acetonitrile ligand in **A16** was easily exchanged with the chloride counterion upon reflux in a non-coordinating solvent to give **A18**. In all cases projection of the acetonitrile and chloride ligands into the calix[4]arene cavity was corroborated by X-ray analysis. ^1H NMR analysis of **A17** was particularly notable for the contrasting shifts observed for the $C\underline{H}_3CN$ resonances at 3.05 and -1.59 ppm ($CDCl_3$/DMSO-d_6 5:1), indicative of the shielding as a result of π-interaction with the inner walls of the calix[4]arene cavity.

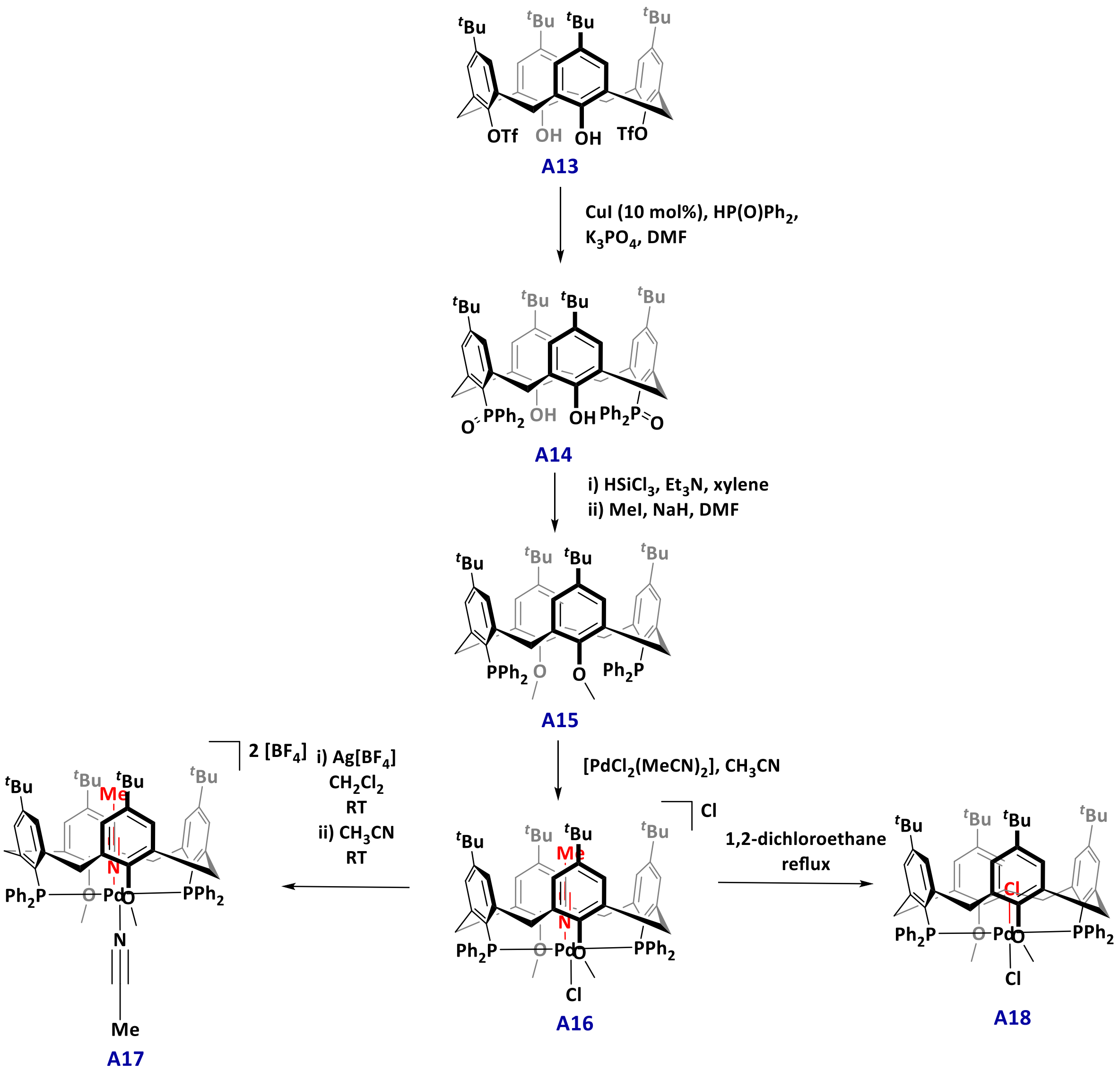
Scheme 1.7: Preparation of palladium complexes reported by Hattori

A number of lower rim functionalised calix[4]arenes bearing bridged polyether appendages or 'calixcrowns' have been reported as strong alkali metal binding ligands. These are discussed in detail in Chapter 4.

1.2.2 Upper rim functionalisation

Typically, synthetic routes for functionalisation of the upper rim of calix[4]arenes involve initial dealkylation by reverse Friedel-Crafts reaction of *p*-alkyl-calix[4]arenes,[12] which enables further functional group transformation, such as incorporation of bromide by use of

N-bromosuccimide (**Route A, Scheme 1.8**).[26] Such halide functionalised calix[4]arenes have been readily used in coupling reactions for the incorporation of imidazole or aromatic functionalities or addition of donor groups by lithium exchange. *Ipso*-nitration of the upper rim has also been explored by Reinhoudt (**Route B, Scheme 1.8**) as a route for the synthesis of amine, imine, amino and sulfanamido functionalities.[30, 39] Use of excess of nitric and acetic acids results in the formation of tetranitrocalix[4]arenes, while lower stoichiometries can be used to form mixtures which are separable by column chromatography.[39]

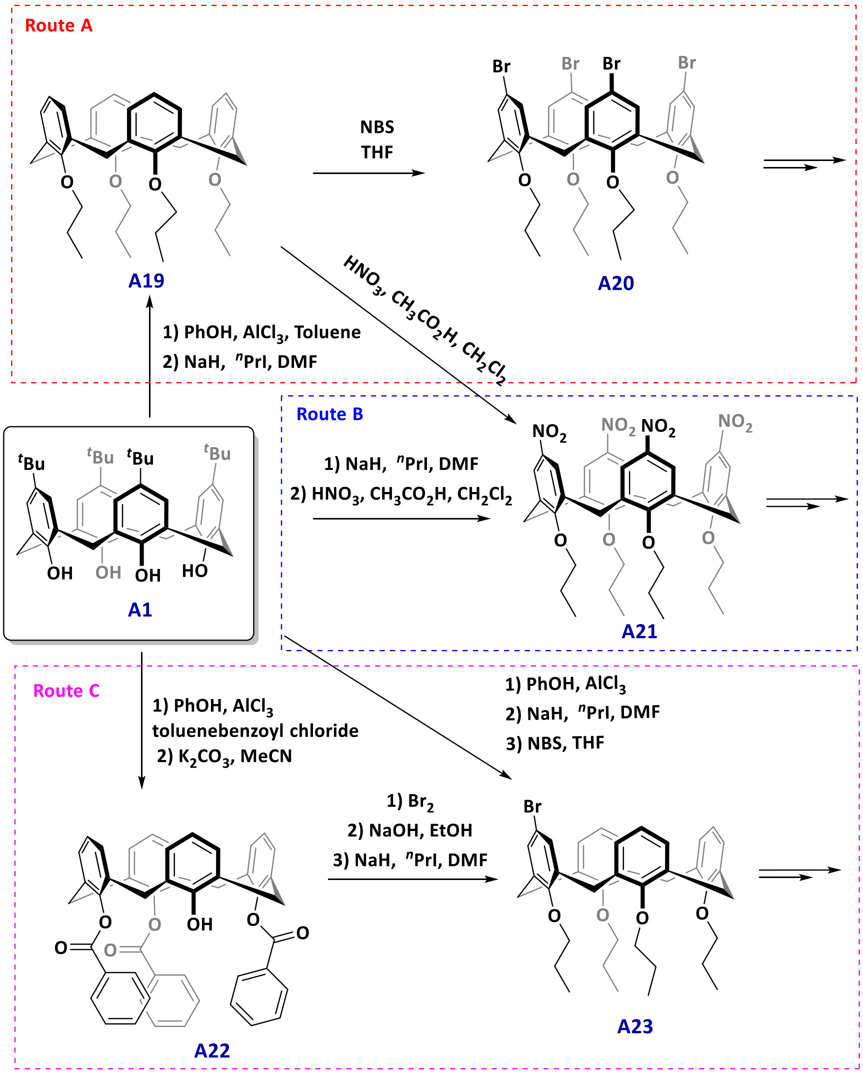

Scheme 1.8: Common routes to upper rim functionalisation of calix[4]arenes from *tert*butylcalix[4]arene

Mono-halogenation of calix[4]arenes has been achieved in low yields by the addition of one equivalent of a halogenating agent and separation of the product mixture by column chromatography.[40] Alternatively monobrominated calix[4]arenes can be synthesised by protection of upper rim positions by tribenzolylation of the lower rim, followed by addition of dibromine (**Route C**, **Scheme 1.8**).[41, 42] Monobrominated calix[4]arenes have been used for the incorporation of coordinating moieties, for example, by lithiation followed by phosphination as described by Harvey *et al.*[43] and subsequently used for the synthesis of Cp*Rh complexes (**Scheme 1.9**).[44,43]

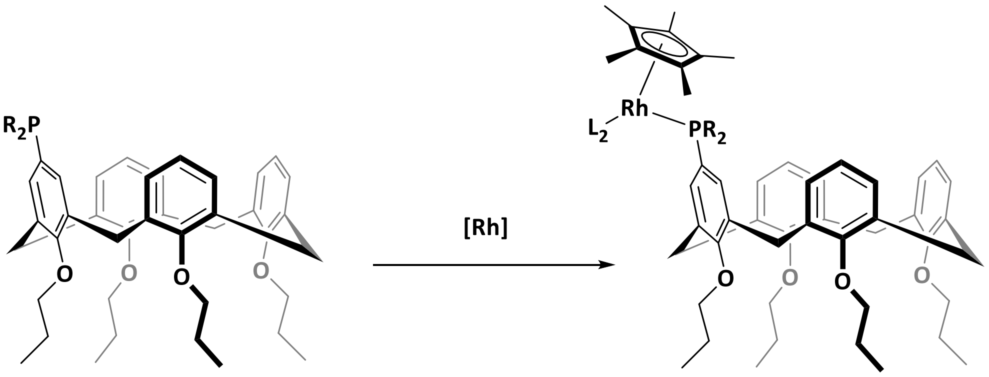

A24

L_2 = CO or Cl_2

[Rh] = [RhCp*$(CO)_2$] R = Ph L = CO A25
[Rh] = [RhCp*$(Cl)_2]_2$ R = ^{i}Pr, Ph L = Cl A26

Scheme 1.9: Cp*Rh complexes of phosphine functionalised calix[4]arenes

Matt *et al.*[45] have developed the coordination chemistry of bis-phosphine calix[4]arene ligand **A27**. Reaction of **A27** with one equivalent of Ag[BF_4] resulted in the formation of silver complex **A28** (**Figure 1.6**), the structure of which was confirmed by mass spectrometry, ^{1}H and ^{31}P NMR spectroscopy. Notably the ^{13}P resonances displayed characteristic coupling to ^{107}Ag ($^{1}J_{AgP}$ = 502 Hz) and ^{109}Ag ($^{1}J_{AgP}$ = 580 Hz).

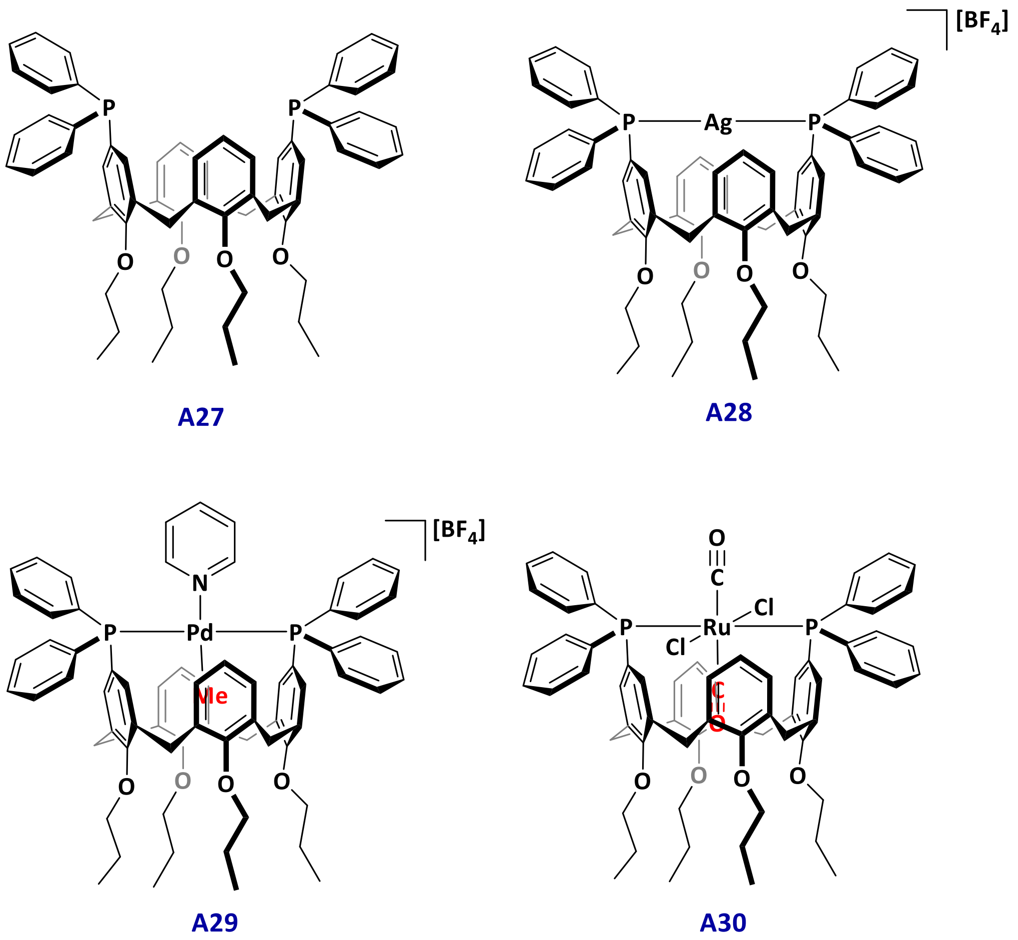

A27 **A28**

A29 **A30**

Figure 1.6: Complexes of **A27**

Treatment of **A27** with [Pd(Me)(COD)(THF)][BF$_4$], followed by addition of pyridine resulted in the formation of **A29** (**Figure 1.6**). The bulky pyridine ligand prevents gyroscopic spinning of the pyridine-Pd-Me fragment resulting in the projection of the methyl group inside the calix[4]arene cavity as established by NOESY NMR experiments. The methyl group is characterised by a triplet ^{1}H NMR signal observed at δ = -0.79 *cf.* related Pd-CH$_3$ resonances observed at δ = -0.60.[46] Reaction of **A27** with ruthenium trichloride and carbon monoxide resulted in a ruthenium(II) complex with *cis*-carbonyl ligands, which slowly isomerise in solution to form *trans*-carbonyl complex **A30**. The X-ray diffraction structure of **A30** is notable for the positioning of the CO ligand within the calix[4]arene cavity.

A calix[4]arene bearing phosphinomethyl donor moieties in the 1,3-positions, **A31**, has been developed by Kubas and co workers and the coordination with palladium, platinum and rhodium investigated (**Scheme 1.10**).[47] Despite the presence of the potentially chelating phosphino groups only polymeric Pd(II) (**A32**) and Pt(II) (**A33**) complexes and a dinuclear rhodium(I) complex (**A34**) were isolated in moderate yields (59-82%). **A31** was analysed in the solid state by X-ray crystallography and the tendency to form bimetallic and polymeric products was attributed to the distance observed between the phosphorus atoms (7.01 Å) and the directionality of the lone pairs, which are projected away from the calix[4]arene centre. However, no detailed analysis was carried out in solution.

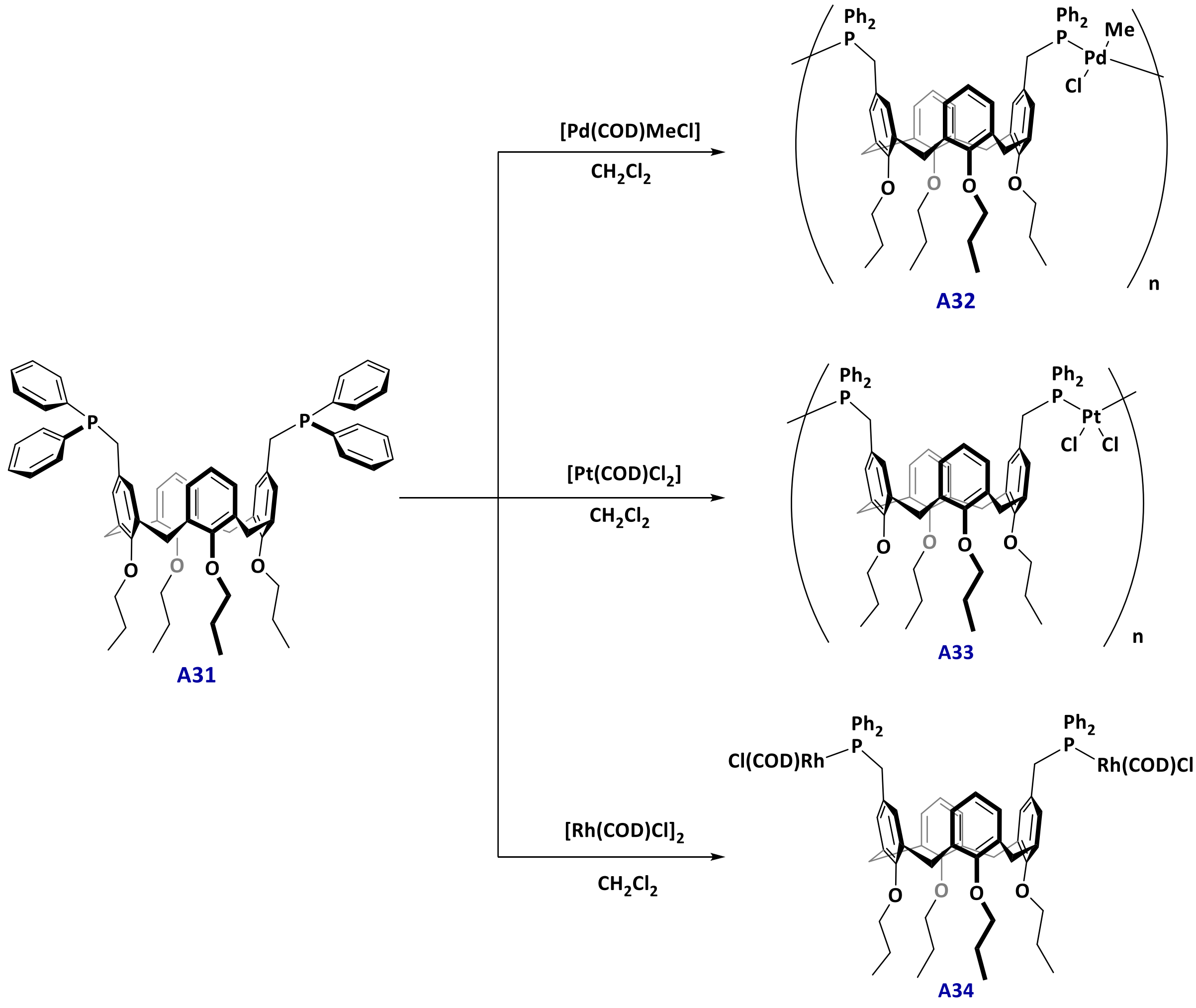

Scheme 1.10: *Polymeric and bimetallic complexes of* ***A31***

Treatment of the relatively bulky 1,3-bisphosphine functionalised calix[4]arene ligand bearing *tert*butyl functionalities in the 2,4-upper rim positions (**A35**) also resulted in the formation of bimetallic transition metal complexes (**A36** to **A38**) (**Scheme 1.11**).[48] Attempts were made to prepare monometallic chelate complexes from **A35**, however, only polymeric products were obtained.

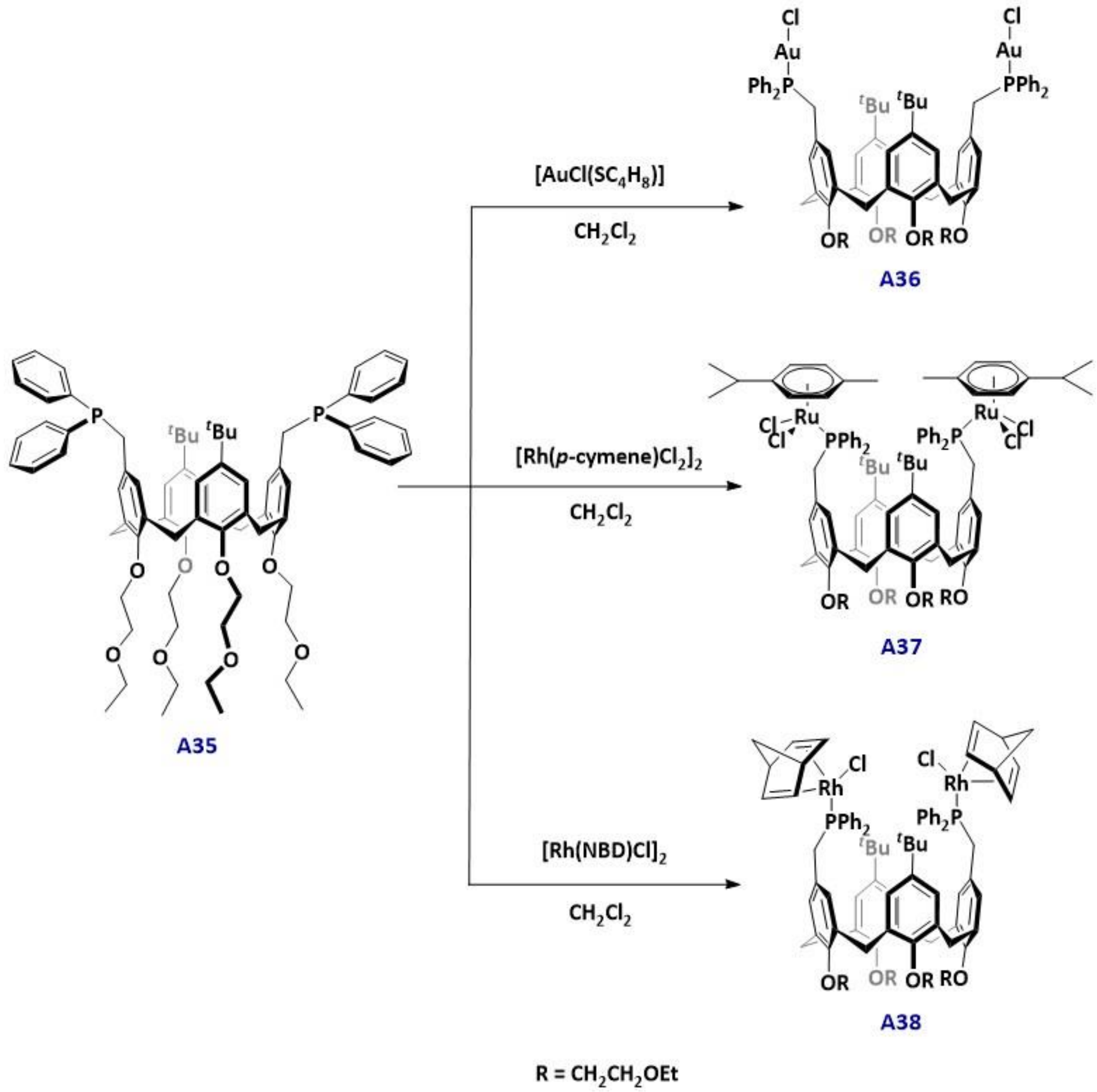

Scheme 1.11: *Au, Ru and Rh complexes of* ***A35***

Reaction of the phosphite ligand, **A39**, with [Pd(η^3-Me-allyl)(THF)$_2$][BF$_4$] was used for the preparation of monometallic chelated species, **A40**, this success was attributed to the extension of the coordinating pendant arms (**Scheme 1.12**).[49]

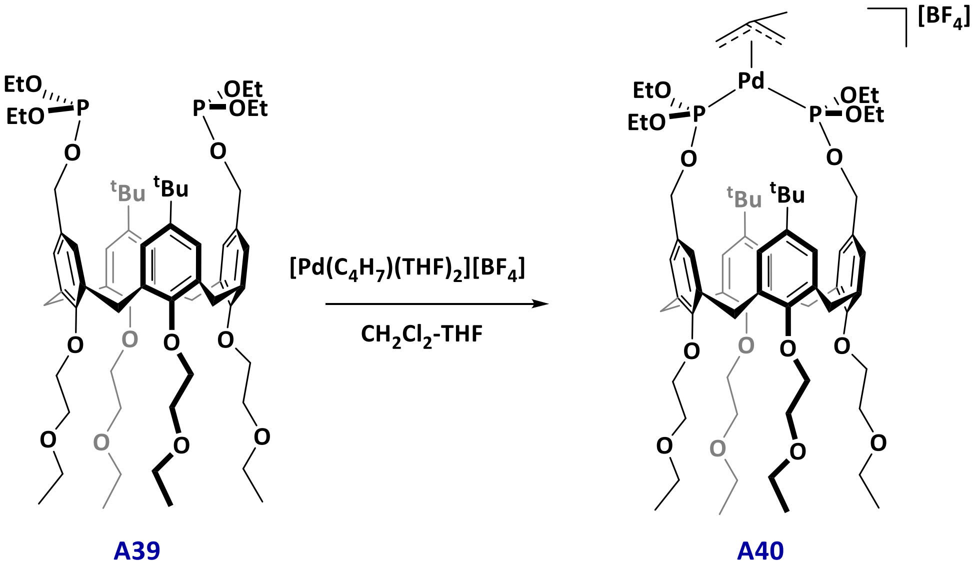

Scheme 1.12: Monometallic palladium complexes reported by Matt

Ongoing unpublished work carried out by the Chaplin group† with ligand **A31** has shown that formation of chelated monomeric complexes is possible, by use of the unusual [Rh(biphen)(dtbpm)] precursor. This resulted in the formation of a monometallic complex which was characterised by NMR spectroscopy and ESI-MS (**Scheme 1.13**).

---

† Ongoing unpublished work by Jack Emerson-King, PhD student and Dr Adrian Chaplin, Associate Professor, University of Warwick.

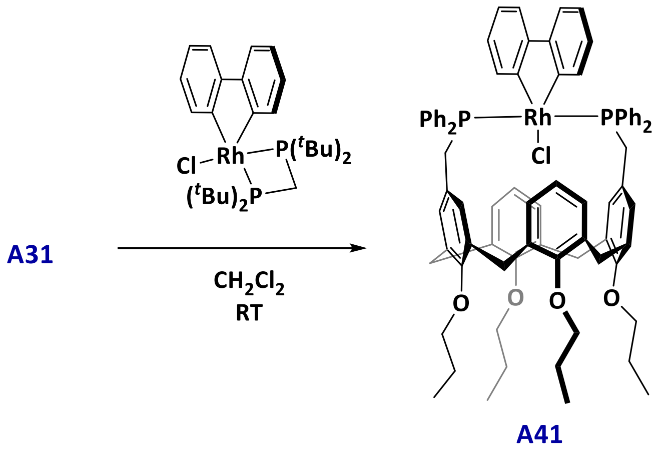

Scheme 1.13*:* Synthesis of monometallic Rh calix[4]arene complexes reported by the Chaplin group

Macrocycles derived from the functionalisation of the calix[4]arene upper rim have also been used for the synthesis of transition metal complexes (**Figure 1.7**). Of particular note is the formation of palladium complexes **A42** and **A43** by Cameron *et al*. which demonstrated the use of an extended cavity resulting in complementarity for large ligands such as pyridine and phenylpyridine within the calix[4]arene cavity.[50] The upfield shift of the pyridine and phenylpyridine resonances, observed by ^{1}H NMR spectroscopy is indicative of an aromatic donor-acceptor interaction between the calix[4]arene and the included ligand.

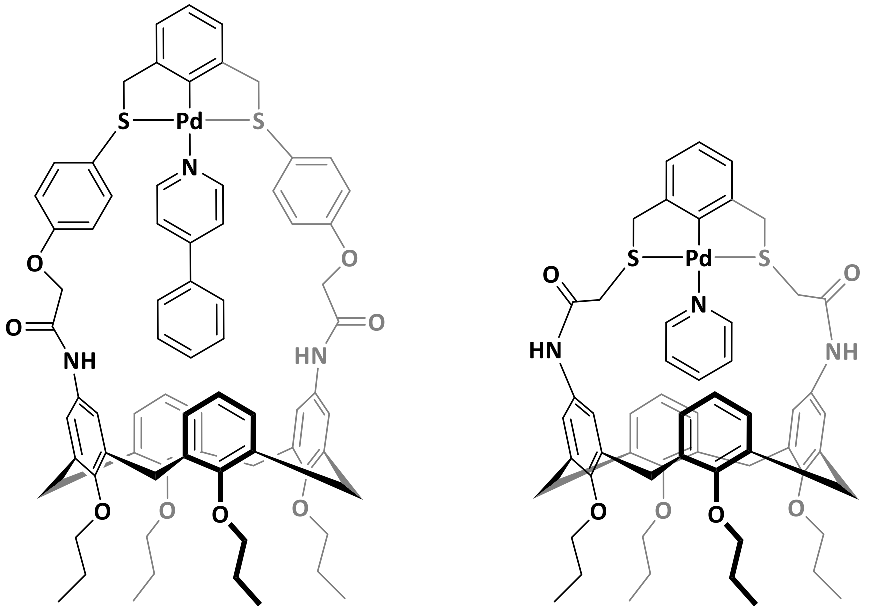

A42 **A43**

Figure 1.7: Palladium complexes of macrocyclic calix[4]arene ligands

1.3 Calix[4]arene inclusion complexes

In addition to intramolecular inclusion complexes, calix[4]arenes have demonstrated an ability to form strong and selective intermolecular inclusion complexes (**Figure 1.8**). This includes the ubiquitous *p-tert*butyl-calix[4]arene (**A1**) which has been used to form host-guest complexes with a variety of small molecules such as chloroform, benzene, 4-fluorotoluene and toluene.[51, 52] Encapsulation of these small molecules was observed by ^{1}H NMR spectroscopy by the upfield shift of the guest protons which interact with the ring currents of the calix[4]arene cavity walls. X-ray diffraction has also been used to confirm the presence of guest molecules within the calix[4]arene cavity.[7, 53] In some cases, guests have been subsequently removed, however this typically requires prolonged heating at high temperatures under vacuum.[12]

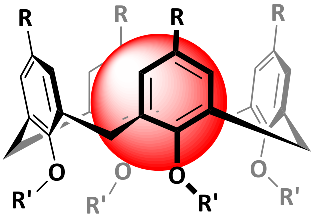

Figure 1.8: Schematic of calix[4]arene inclusion complexes

*p-tert*Butylcalix[4]arene has also been shown to encapsulate anisole in a 2:1 ratio (**A44**, **Figure 1.9**).[54] This host-guest adduct was characterised by X-ray crystallography, indicating the presence of the anisole within the closed cage, created by the two calix[4]arene macrocycles, although the anisole is observed to be disordered over eight possible orientations.

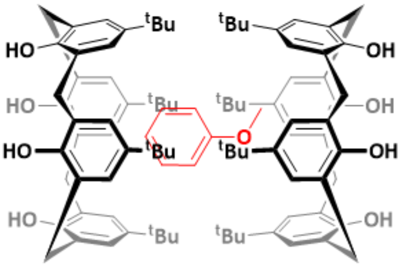

A44

Figure 1.9: *p-tert*Butlycalix[4]arene-anisole host guest complex reported by Ungaro

The encapsulation of xenon within the cavity of **A1** has been reported by Ripmeester, by vapour diffusion into a saturated solution of the calix[4]arene in nitrobenzene.[55] The host-guest complex was characterised in the solid state by X-ray crystallography (**Figure 1.10**) and by ^{129}Xe NMR spectroscopy. Both techniques showed the presence of Xe in two sites, as indicated by disorder in the solid state and the presence of two ^{129}Xe resonances observed at δ 59 and δ 64.

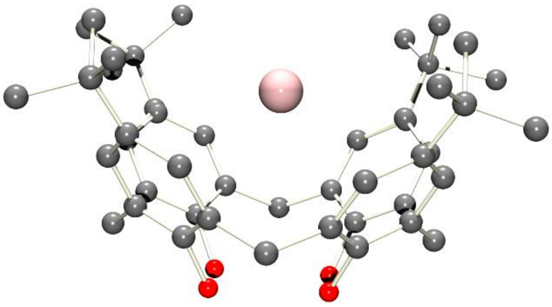

Figure 1.10: X-ray crystal structure of Xe encapsulated within *p-tert*butylcalix[4]arene (**A1**)

In addition to neutral guest molecules, a large number of examples of calix[4]arenes appended with donor or acceptor moieties, capable of acting as cation or anion complexation agents, have been reported. Calix[4]arenes acting as hosts to alkali metal guests are discussed in section 4.1.2.

1.4 N-Heterocyclic carbenes

The growth of the NHC chemistry since the preparation of the first thermally stable NHC by Arduengo in 1991[56] is well established and widely reviewed over the last decade.[57-62] This section will therefore only provide a brief introduction to their structure, binding characteristics and a short discussion of common multidentate NHC topologies.

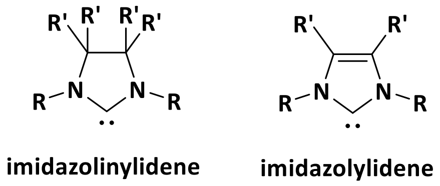

Figure 1.11: General NHC structures

NHCs differ from other carbenes by the presence of heteroatoms, typically nitrogen, in the positions adjacent to the carbenic carbon. The most common examples are based around 5-membered ring structures (**Figure 1.11**), containing either a saturated (imidazolinylidene) or unsaturared backbone (imidazolylidine). N-substituents (R) or variation of the cyclic backbone substituents (R') can be used to tune the properties of the NHC (*vide infra*). The stability of central carbene is thought to be a combination of the steric effects resulting from use of bulky R substituents but, more importantly the stability imparted by the electronic structure. This is widely accepted to be a result of the inductive σ effect which is a result of the electronegativity of the nitrogen resulting in the stabilization of the in-plane pair of unshared electrons and simultaneously the electron donation from the nitrogen p-orbitals into the vacant p-orbital on the carbenic centre.[57, 63] This effect is observed in particular in cyclic carbenes where the carbonic carbon is forced into a more bent sp^2 like arrangement, this favours the formation singlet state carbene structures.[57] Coodination to transition metals then occurs by strong σ-donation from the carbene with complimentary and synergistic π-backbonding from the metal centre (**Figure 1.12**).[58 64, 65] There is also considerable evidence suggesting that NHC ligands can behave as π-donors in the presence of electron deficient metal centres (**Figure 1.12**).[66, 67]

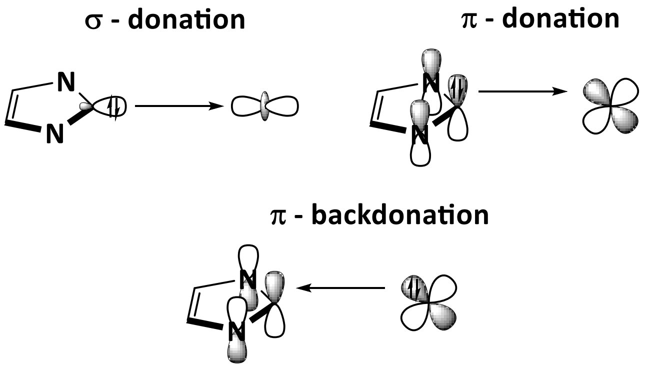

Figure 1.12: *MO diagram showing binding of a singlet NHC to a transition metal*

Although 5 membered NHC rings are the most common, 4, 6 and 7 membered structures are also known (**Figure 1.13**, **A51-A55**). 'Abnormal' C4 binding of 5-membered ring systems are also well established, for example ligand **A47**.[68-71] Abnormal binding can be prevented by the functionalisation of the imidizolylidene backbone, most commonly with relatively inert methyl or benzyl groups. Electronic characteristics of NHC ligands can also be altered by the inclusion of a heteroatoms, such as sulfur or oxygen, or additional heteroatoms in the C4 or C5 positions.[71] These electronic differences have a direct effect on the electron-donating ability of the carbene and can be quantified using Tolman's electronic parameter (TEP).[72]

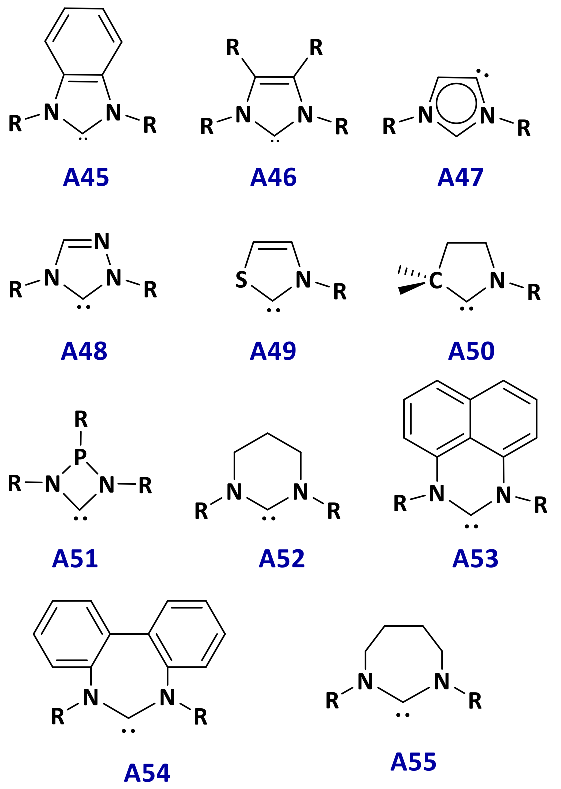

Figure 1.13: Selected *e*xamples of N-heterocyclic carbene structures

NHCs have been extensively investigated in organometallic chemistry and catalysis in recent years, largely due to their structural diversity. As such, a wide range of ligands with specifically designed topology including incorporation of bulky, coordinating and chiral groups have been prepared.[60, 73] Polydentate NHCs have prepared in a wide variety of geometries including pincer, tripodal, ring and cage systems (**Figure 1.14**).[62, 74-76]

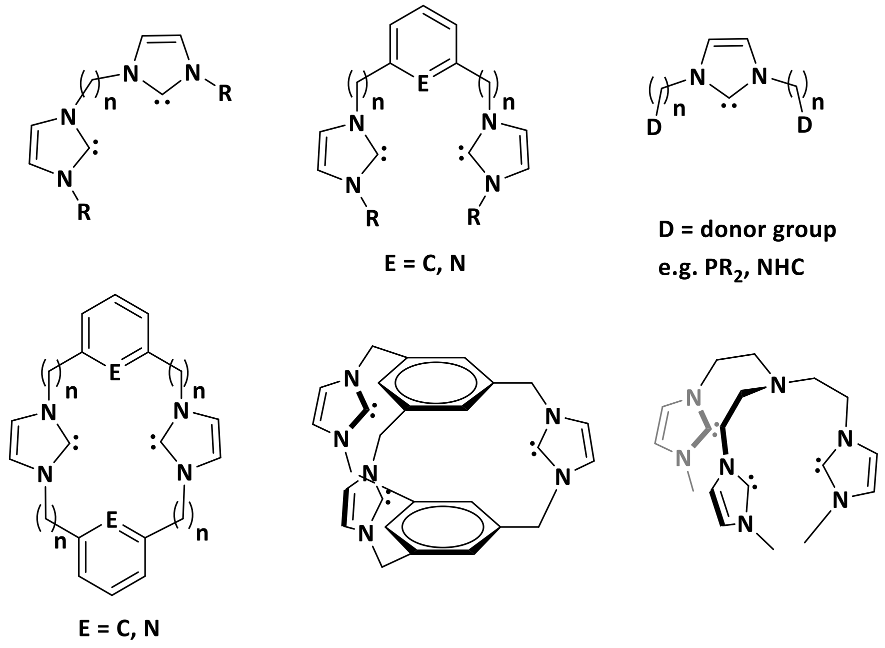

Figure 1.14: Pincer, ring and cage NHC structures

Many chelating NHC ligands have been designed to favour strong binding to a metal centre, such as pincer ligands (**Figure 1.14**), which are held in position by a rigid donor group. The thermal stability and broad range of transition metal centres supported by pincer structures make them excellent systems for catalytic applications.[74, 77] In addition to the popular pincer based motifs, a wide variety of supramolecular motifs have been described, including MOFs,[78, 79] polymers[80] and cage structures.[81] Molecular cylinders from polydentate NHC precursurs have been reported by Hahn *et al.* [82] from a reaction between multidentate imidazolium proligands with Ag_2O to form tri- or tetra- silver stacked complexes (**A56-57**, **Figure 1.15**).

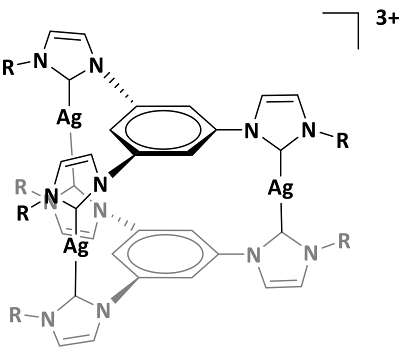

A56

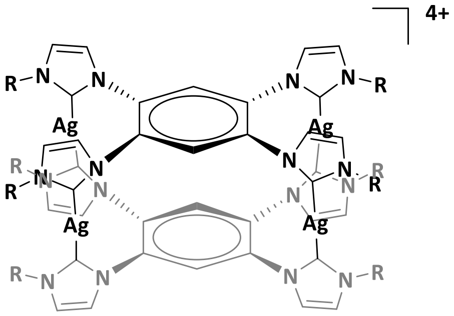

A57

Figure 1.15: Silver cage structures reported by Hahn

The applications of carbenes can be broadly separated into catalysis, materials and medicinal chemistry.[57, 58, 83, 84] The most well-known catalytic application of NHC complexes is undoubtedly Grubb's second generation catalyst, which shows increased TOF and greater thermal stability than the phosphine bearing first generation catalyst (**Figure 1.16**).[85, 86]

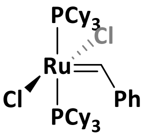

Grubbs
1st Generation

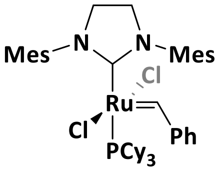

Grubbs
2nd Generation

Figure 1.16: Grubb's first and second generation catalysts

Many examples of NHC metal catalysts have also been described in coupling,[87] hydrogenation,[88] metathesis reactions[58] with good stability in a wide variety of catalytic conditions.[58] For example, pyridine-enhanced precatalyst preparation stabilization and initiation (PEPPSI) is well reported in palladium catalysed coupling reactions such as Negishi and Suzuki coupling reactions (**Figure 1.17**).[87] Ir species have been reported as transfer hydrogenation catalysts e.g. **A58** and **A59**.[88, 89] A large number of Rh(I) and Ir(I) NHC complexes have also shown activity in the hydrosilation of multiple bonds, for example the addition of silanes to alkynes (**A60**) (**Figure 1.17**).

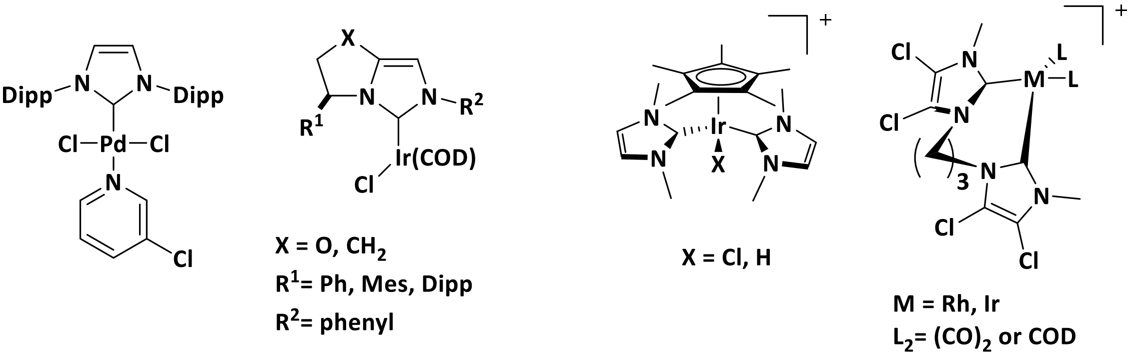

X = O, CH_2
R^1= Ph, Mes, Dipp
R^2= phenyl

X = Cl, H

M = Rh, Ir
L_2= $(CO)_2$ or COD

PEPPSI **A58** **A59** **A60**

Figure 1.17: *Selection of NHC-transition metal catalysts*

1.5 NHC functionalised calix[4]arenes

Despite the prominence of NHC-based complexes in organometallic chemistry, relatively few NHC functionalsed calix[4]arene complexes have been reported. The limited number of known examples are introduced in this section.

Calix[4]arenes bearing NHC substituents on the lower rim have been reported by Katz and Solovyov, which were prepared by addition of dibromoalkanes in the presence of a base, to 1,3-dialkoxylcalix[4]arenes and subsequent alkylation with an excess of 1-alkyl-imidazole (**Scheme 1.14**).[90] The Au(I) complexes of these ligands were then formed using transmetallation from the isolatied Ag(I) complexes **A62**.

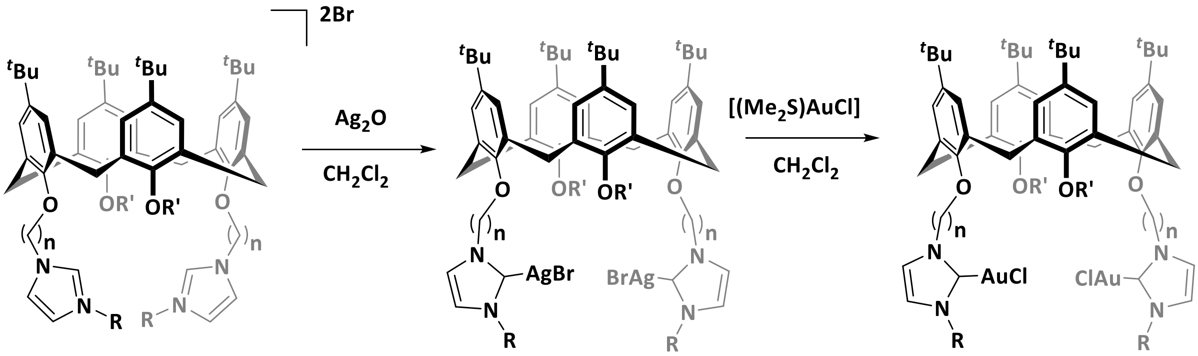

A61 **A62** **A63**

n = 4 R = Bu R' = ^{n}Pr
n = 4 R = Ph R' = ^{n}Pr
n = 3 R = Ph R' = Me

Scheme 1.14: Ag and Au complexes of lower-rim functionalised calix[4]arenes

Pro-ligands bearing methylene bridged imidazolium functionalities on the upper rim have been shown to result in a predisposition for subsequently bound metal fragments to be projected away, rather than over the calix[4]arene cavity (**Scheme 1.15**). These complexes have been investigated by Schatz *et al.*, who synthesised **A65** by addition of $Pd(OAc)_2$ to the bis(imidazolium) salt **A64** in low yield (8%) due to simultaneous formation of polymeric species and **A67** by transmetallation from the isolated complex **[A66][AgCl$_2$]** with *trans*-[Pd(MeCN)$_2$Cl$_2$] in CH$_2$Cl$_2$.[91, 92] The *cis*-palladium complex **A65** was found to catalyse Suzuki cross-coupling of phenylboronic acid and chlorotoluene to yield 4-methylbiphenyl in yields within the range of other chelating NHC systems. The molecular structure of the *cis*-palladium complex was confirmed by X-ray diffraction which showed distortion of the NHC moieties and projection of the chloride ligands away from the central calix[4]arene cavity.

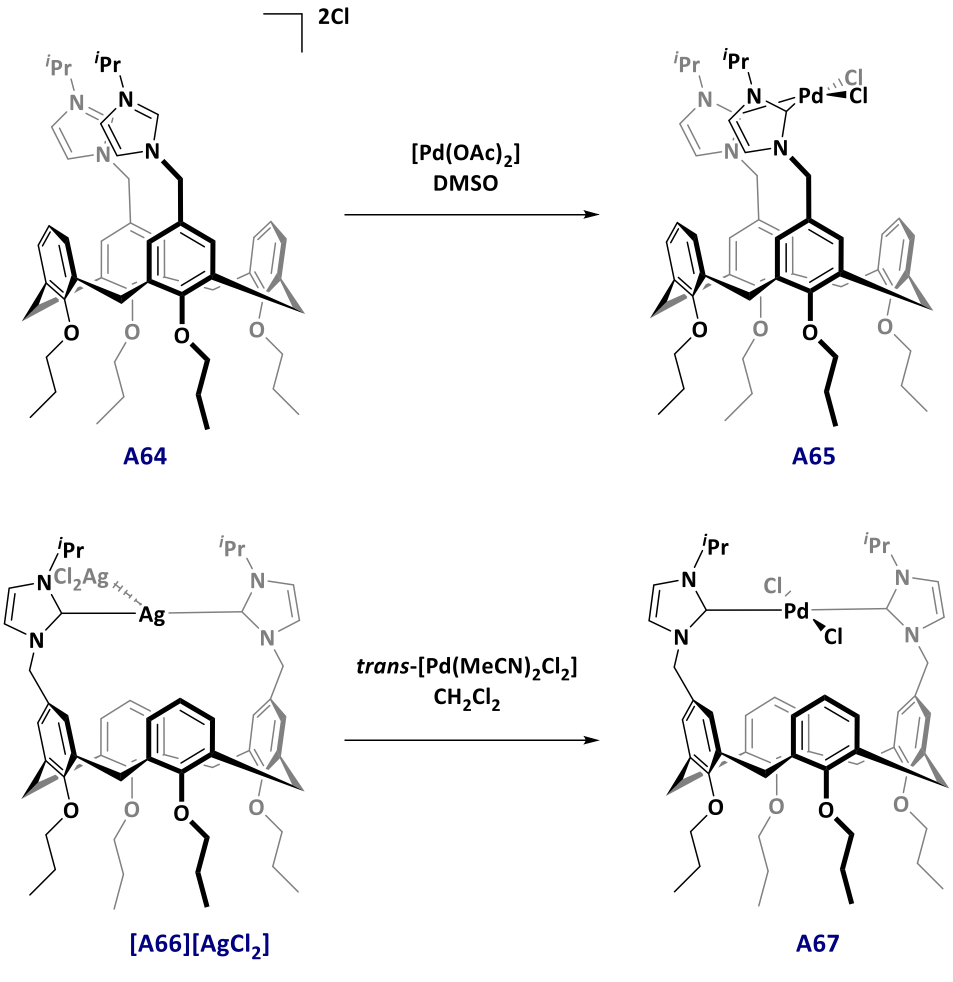

Scheme 1.15: Complexes of upper-rim NHC calix[4]arenes

The structure of the Ag(I) complex **[A66][BF$_4$]** was confirmed by X-ray diffraction.[92] This showed C_s symmetry due to the offset bending of the Ag centre (**Scheme 1.16**). VT ^{1}H NMR spectroscopy showed time averaged C_{2v} symmetry at ambient temperature due to dynamic fluxional behaviour of this unit which was reduced to C_S at temperatures below -33°C.[92]

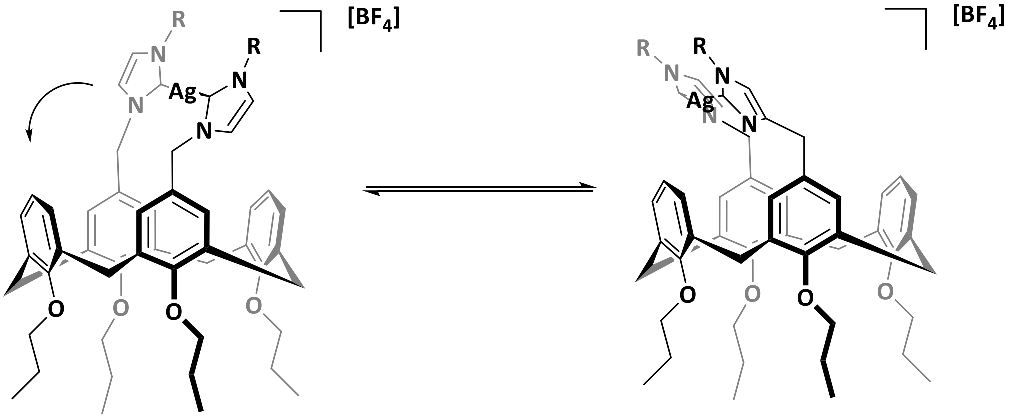

Sche.: Scheme 1.16: Fluctional structures of **[A66][BF$_4$]**

1,3-imidazolium functionalised calix[4]arene structures have been investigated by Dinarès and co-workers.[93] *iso*-Propyl- and butyl-substituted 1,3-bis(imidazolium)calix[4]arenes (**A68·2HX**) have been used as selective anion receptors for carboxylate ions (**Figure 1.18**). These pro-ligands were also used in the preparation of *trans*-palladium complexes **A69**, by addition of [Pd(OAc)$_2$]. The Pd adopts a square planar geometry over the calix[4]arene cavity enabled by the twisting of the NHC functionalities to a perpendicular position to the aromatic calix[4]arene walls. Both **A69** complexes were found to be active catalysts in the Suzuki-Miyaura coupling of 4-bromoacetophenone and phenylboronic acid producing diaryl products in good yields.[94]

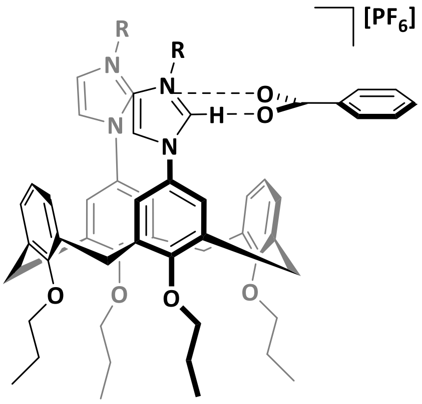

R = ^{n}Bu, ^{i}Pr

[A68.(HO$_2$Ph)][PF$_6$]

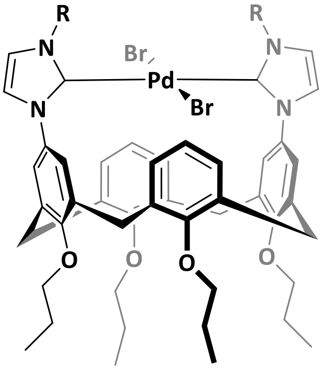

R = ^{n}Bu, ^{i}Pr

A69

Figure 1.18: Carboxylate binding and NHC based Pd calix[4]arene complexes

Complexes of mono-substituted and 1,2-bis-substituted imidazolium calix[4]arene pro-ligands have been described by Brenner and Matt.[95] Palladium complexes **A70** and **A71** were produced by addition of Pd(OAc)$_2$ to the imidazolium salts in *ca.* 37% yield (**Figure 1.19**). These low yields have been attributed to formation of oligometic by-products, however, these were not unambiguously identified. The monosubstituted complex **A72** was formed from PdCl$_2$ and KBr in the presence of Cs$_2$CO$_3$ in pyridine and was isolated in good yield (75%). The *trans* configuration and the C$_s$-symmetry of the monomeric **A70** and **A71** complexes was established by ^{13}C NMR spectroscopy (δ 168 (NCN)) and the three environments observed for the bridging methylene units. Coordination of the mono-substituted calix[4]arene scaffold was also used in the synthesis of a di-calix[4]arene complex **A73** under similar conditions, but in the absence of pyridine and use of 0.5 equivalents of PdCl$_2$.

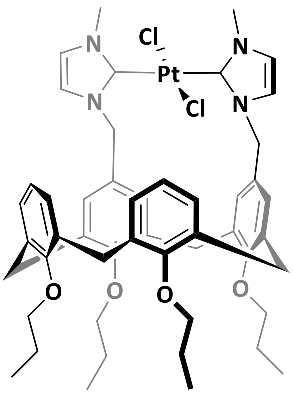

A70

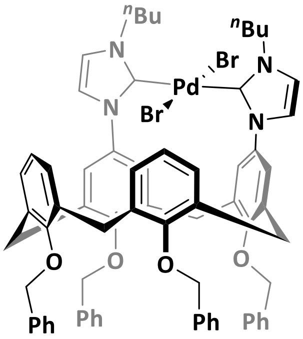

A71

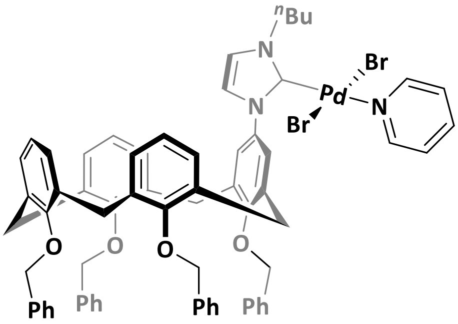

A72

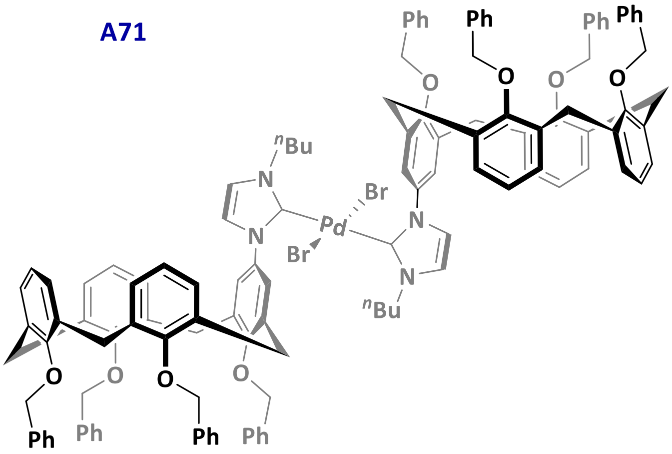

A73

Figure 1.19: Complexes of mono and 1,2-substituted NHC-calix[4]arene ligands

1.6 Thesis scope and objectives

The development of calix[4]arene scaffolds bearing 1,3-fuctionalised donor groups has been identified as a pathway to the formation of chelating NHC ligand systems. With a view of exploiting the flexible and encapsulating characteristics of these structures this thesis aims to explore the coordination chemistry of calix[4]arene structures bearing 1,3-substituted NHC donors on the upper rim. Closely related imidazol-2-thione derivatives were subsequently synthesised and studied during the course of this work. The synthesis of mononucular organometallic species and formation of host-guest complexes were then targeted (**Figure 1.20**).

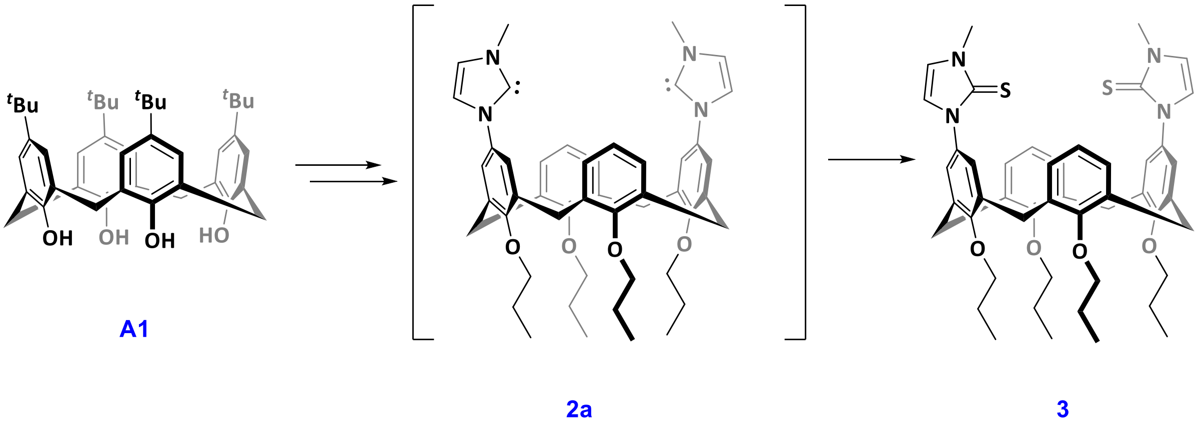

Figure 1.20: 1,3-substituted calix[4]arenes studied in this thesis

1.7 References

1. C. D. Gutsche, R. Muthukrishnan and K. Hyun No, *Tetrahedron Lett.*, 1979, **20**, 2213-2216.
2. A. Baeyer, *Ber.*, 1872, 25.
3. Lebach, H. US Patent 965823 A, 1908.
4. A. Zinke and E. Ziegler, *Ber. Dtsch. Chem. Ges. (A and B Series)*, 1944, **77**, 264-272.
5. K. Araki, T. Watanabe, M. Oda, H. Hayashida, M. Yasutake and T. Shinmyozu, *Tetrahedron Lett.*, 2001, **42**, 7465-7468.
6. H. J. Kim, M. H. Lee, L. Mutihac, J. Vicens and J. S. Kim, *Chem. Soc. Rev.*, 2012, **41**, 1173-1190.
7. J. J. Rebek, *Chem. Commun.*, 2000, 637-643.
8. C. Bavoux, R. Baudry, I. Dumazet-Bonnamour, R. Lamartine and M. Perrin, *J. Incl. Phenom. Macrocycl. Chem.*, 2001, **40**, 221-224.
9. A. Ninagawa and H. Matsuda, *Makromol. Chem. Rapid Comm.,* 1982, **3**, 65-67.
10. Y. Nakamoto and S.-i. Ishida, *Makromol. Chem. Rapid Comm.*, 1982, **3**, 705-707.
11. C. D. Gutsche, M. Iqbal and D. Stewart, *J. Org. Chem.*, 1986, **51**, 742-745.
12. C. D. Gutsche, B. Dhawan, K. H. No and R. Muthukrishnan, *J. Am. Chem. Soc.*, 1981, **103**, 3782-3792.
13. C. D. Gutsche and M. Iqbal, in *Inorg. Synth.*, John Wiley & Sons, Inc., 2003.
14. C. D. Gutsche, *Calixarenes*, The Royal Society of Chemistry, Great Britain, 1st edn., 1989.
15. B. T. Hayes and R. F. Hunter, *J. App. Chem.*, 1958, **8**, 743-748.
16. V. Boehmer, F. Marschollek and L. Zetta, *J. Org. Chem.*, 1987, **52**, 3200-3205.
17. V. Böhmer, P. Chhim and H. Kämmerer, *Makromol.Chem.* 1979, **180**, 2503-2506.
18. K. Araki, K. Iwamoto, S. Shinkai and T. Matsuda, *Chem. Lett.*, 1989, **18**, 1747-1750.
19. C. D. Gutsche and L. J. Bauer, *J. Am. Chem. Soc.*, 1985, **107**, 6052-6059.
20. C. D. Gutsche, *Acc. Chem. Res.*, 1983, **16**, 161-170.
21. S. E. Biali, V. Böhmer, S. Cohen, G. Ferguson, C. Grüttner, F. Grynszpan, E. F. Paulus, I. Thondorf and W. Vogt, *J. Am. Chem. Soc*, 1996, **118**, 12938-12949.

22. S. Simaan and S. E. Biali, *J. Org. Chem.*, 2003, **68**, 7685-7692.

23. P. Jose and S. Menon, *Bioinorg Chem Appl.*, 2007, 65815.

24. B. S. Creaven, T. L. Gernon, J. McGinley, A.-M. Moore and H. Toftlund, *Tetrahedron*, 2006, **62**, 9066-9071.

25. P. D. Harvey, *Coord. Chem. Rev.*, 2002, **233**, 289-309.

26. C. D. Gutsche and P. F. Pagoria, *J. Org. Chem*, 1985, **50**, 5795–5802.

27. C. D. Gutsche, J. A. Levine and P. K. Sujeeth, *J. Org. Chem.*, 1985, **50**, 5802-5806.

28. C. D. Gutsche and L.-G. Lin, *Tetrahedron*, 1986, **42**, 1633-1640.

29. A. Vrielink, P. W. Codding, C. D. Gutsche and L.-G. Lin, *J.inclusion phenom.*, 1986, **4**, 199-207.

30. S. K. Sharma and C. D. Gutsche, *J. Org. Chem.*, 1999, **64**, 998-1003.

31. V. Böhmer, *Angew. Chem. Int. Ed.*, 1995, **34**, 713-745.

32. K. I. Araki, Koji. Shigematsu,Satoshi. Shinkai,Seiji., *Chem. Lett.*, 1992, **21**, 1095-1098.

33. A. M. Krause-Heuer, N. J. Wheate, M. J. Tilby, D. G. Pearson, C. J. Ottley and J. R. Aldrich-Wright, *Inorg. Chem.*, 2008, **47**, 6880-6888.

34. M. Ling-Zhi, H. Huang, H. Yong-bing and C. Yuan-yin, *Wuhan University Journal of Natural Sciences*, 1999, **4**, 216-218.

35. W. He, F. Liu, Y. Mei, Z. Guo and L. Zhu, *New J. Chem.*, 2001, **25**, 1330-1336.

36. S. Steyer, C. Jeunesse, J. Harrowfield and D. Matt, *Dalton Trans.*, 2005, 1301-1309.

37. C. Wieser, D. Matt, L. Toupet, H. Bourgeois and J.-P. Kintzinger, *J. Chem. Soc., Dalton Trans.*, 1996, 4041-4043.

38. K. Hirasawa, S. Tanaka, T. Horiuchi, T. Kobayashi, T. Sato, N. Morohashi and T. Hattori, *Organometallics*, 2016.

39. W. Willem Verboom, A. Alex Durie, R. J. M. Egberink, Z. Asfari and D. N. Reinhoudt, *J. Org. Chem.*, 1992, **57**, 1313-1316.

40. A. Ikeda, M. Yoshimura, P. Lhotak and S. Shinkai, *J. Chem. Soc., Perkin Trans. 1*, 1996, 1945-1950.

41. X. Hu, Y. Li, H. Yang and Y. Luo, *Tetrahedron Lett.*, 2006, **47**, 7463-7465.

42. A. Casnati, M. Fochi and A. Pochini, *Gazz. Chim. Ital.*, 1996, 99-106.

43. M. Vézina, J. Gagnon, K. Villeneuve, M. Drouin and P. D. Harvey, *Organometallics*, 2000, **20**, 273-281.

44. M. Vezina, J. Gagnon, K. Villeneuve, M. Drouin and P. D. Harvey, *Chem. Commun.*, 2000, 1073-1074.

45. C. Wieser-Jeunesse, D. Matt and A. De Cian, *Angew. Chem. Int. Ed.*, 1998, **20**, 2861-2864.

46. M. Feller, E. Ben-Ari, M. A. Iron, Y. Diskin-Posner, G. Leitus, L. J. W. Shimon, L. Konstantinovski and D. Milstein, *Inorg. Chem.*, 2010, **49**, 1615-1625.

47. X. Fang, B. L. Scott, J. G. Watkin, C. A. G. Carter and G. J. Kubas, *Inorg. Chim. Acta*, 2001, **317**, 276-281.

48. I. A. Bagatin, D. Matt, H. Thönnessen and P. G. Jones, *Inorg. Chem.*, 1999, **38**, 1585-1591.

49. C. Jeunesse, C. Dieleman, S. Steyer and D. Matt, *J. Chem. Soc., Dalton Trans.*, 2001, 881-892.

50. B. R. Cameron, S. J. Loeb and G. P. A. Yap, *Inorg. Chem.*, 1997, **36**, 5498-5504.

51. G. D. Enright, E. B. Brouwer, K. A. Udachin, C. I. Ratcliffe and J. A. Ripmeester, *Acta Cryst., Sect. B: Struct. Sci*, 2002, **58**, 1032-1035.

52. G. D. Andreetti, A. Pochini and R. Ungaro, *J. Chem. Soc., Perkin Trans. 2*, 1983, 1773-1779.

53. B. C. Hamann, K. D. Shimizu and J. Rebek, *Angew. Chem. Int. Ed.*, 1996, **35**, 1326-1329.

54. R. Ungaro, A. Pochini, G. D. Andreetti and P. Domiano, *J. Chem. Soc., Perkin Trans. 2*, 1985, 197-201.

55. E. B. Brouwer, G. D. Enright and J. A. Ripmeester, *Chem. Commun.*, 1997, 939-940.

56. A. J. Arduengo, R. L. Harlow and M. Kline, *J. Am. Chem. Soc.*, 1991, **113**, 361-363.

57. M. N. Hopkinson, C. Richter, M. Schedler and F. Glorius, *Nature*, 2014, **510**, 485-496.

58. H. D. Velazquez and F. Verpoort, *Chem. Soc. Rev.*, 2012, **41**, 7032-7060.

59. G. C. Fortman and S. P. Nolan, *Chem. Soc. Rev.*, 2011, **40**, 5151-5169.

60. F. Wang, L.-j. Liu, W. Wang, S. Li and M. Shi, *Coord. Chem. Rev.*, 2012, **256**, 804-853.

61. F. Lazreg, F. Nahra and C. S. J. Cazin, *Coord. Chem. Rev.*, 2015, **293–294**, 48-79.

62. M. Poyatos, J. A. Mata and E. Peris, *Chem. Rev.*, 2009, **109**, 3677-3707.

63. W. A. Herrmann and C. Köcher, *Angew. Chem.Int.Ed.Engl.*, 1997, **36**, 2162-2187.

64. T. Cantat, N. Mezailles, A. Auffrant and P. Le Floch, *Dalton Trans.*, 2008, 1957-1972.

65. H. Jacobsen, A. Correa, A. Poater, C. Costabile and L. Cavallo, *Coord. Chem. Rev.*, 2009, **253**, 687-703.

66. N. S. Antonova, J. J. Carbo and J. M. Poblet, *Dalton Trans.*, 2011, **40**, 2975-2982.

67. N. M. Scott, E. D. Stevens, R. Dorta, A. Correa, L. Cavallo and S. P. Nolan, *J. Am. Chem. Soc.*, 2005, **127**, 3516-3526.

68. R. H. Crabtree, *Coord. Chem. Rev.*, 2013, **257**, 755–766.

69. A. R. Chianese, A. Kovacevic, B. M. Zeglis, J. W. Faller and R. H. Robert H. Crabtree, *Organometallics*, 2005, **23**, 2461-2468.

70. P. L. Arnold and S. Pearson, *Coord. Chem. Rev.*, 2007, **251**, 596-609.

71. O. Schuster, L. Yang, H. G. Raubenheimer and M. Albrecht, *Chem. Rev.*, 2009, **109**, 3445-3478.

72. C. A. Tolman, *Chem. Rev.*, 1977, **77**, 313-348.

73. S. Würtz, C. Lohre, R. Fröhlich, K. Bergander and F. Glorius, *J. Am. Chem. Soc.*, 2009, **131**, 8344-8345.

74. R. E. Andrew, L. Gonzalez-Sebastian and A. B. Chaplin, *Dalton Trans.*, 2016, **45**, 1299-1305.

75. X. Hu and K. Meyer, *J. Organomet. Chem.*, 2005, **690**, 5474-5484.

76. C. E. Ellul, G. Reed, M. F. Mahon, S. I. Pascu and M. K. Whittlesey, *Organometallics*, 2010, **29**, 4097-4104.

77. W. Yao, Y. Zhang, X. Jia and Z. Huang, *Angew. Chem. Int. Ed.*, 2014, **53**, 1390-1394.

78. A. Burgun, R. S. Crees, M. L. Cole, C. J. Doonan and C. J. Sumby, *Chem. Commun.*, 2014, **50**, 11760-11763.

79. F. Carson, E. Martinez-Castro, R. Marcos, G. G. Miera, K. Jansson, X. Zou and B. Martin-Matute, *Chem. Commun.*, 2015, **51**, 10864-10867.

80. B. Karimi and P. Fadavi Akhavan, *Chem. Commun.*, 2011, **47**, 7686-7688.

81. C. Mejuto, G. Guisado-Barrios, D. Gusev and E. Peris, *Chem. Commun.*, 2015, **51**, 13914-13917.

82. A. Rit, T. Pape, A. Hepp and F. E. Hahn, *Organometallics*, 2011, **30**, 334-347.

83. K. M. Hindi, M. J. Panzner, C. A. Tessier, C. L. Cannon and W. J. Youngs, *Chem. Rev.*, 2009, **109**, 3859-3884.

84. L. Mercs and M. Albrecht, *Chem. Soc. Rev.*, 2010, **39**, 1903-1912.

85. M. Scholl, T. M. Trnka, J. P. Morgan and R. H. Grubbs, *Tetrahedron Lett.*, 1999, **40**, 2247-2250.

86. J. Huang, E. D. Stevens, S. P. Nolan and J. L. Petersen, *J. Am. Chem. Soc.*, 1999, **121**, 2674-2678.

87. N. Hadei, E. A. B. Kantchev, C. J. O'Brie and M. G. Organ, *Org. Lett.*, 2005, **7**, 3805-3807.

88. K. Yoshida, T. Kamimura, H. Kuwabara and A. Yanagisawa, *Chem. Commun.*, 2015, **51**, 15442-15445.

89. T. P. Brewster, A. J. M. Miller, D. M. Heinekey and K. I. Goldberg, *J. Am. Chem. Soc.*, 2013, **135**, 16022-16025.

90. M. M. Nigra, A. J. Yeh, A. Okrut, A. G. DiPasquale, S. W. Yeh, A. Solovyov and A. Katz, *Dalton Trans.*, 2013, **42**, 12762-12771.

91. M. Frank, G. Maas and J. Schatz, *Eur. J. Inorg. Chem.*, 2004, **2004**, 607-613.

92. T. Fahlbusch, M. Frank, G. Maas and J. Schatz, *Organometallics*, 2009, **28**, 6183-6193.

93. I. Dinarès, C. Garcia de Miguel, N. Mesquida and E. Alcalde, *J. Org. Chem.*, 2009, **74**, 482-485.

94. I. Dinarès, C. Garcia de Miguel, M. Font-Bardia, X. Solans and E. Alcalde, *Organometallics*, 2007, **26**, 5125-5128.

95. E. Brenner, D. Matt, M. Henrion, M. Teci and L. Toupet, *Dalton Trans.*, 2011, **40**, 9889-9898.

2.0 Synthesis of calix[4]arene N-heterocyclic carbene and imidazol-2-thione ligands

Overview

This chapter discusses the development of the synthetic routes for the preparation of 1,3-functionalised imidazolinium (**1·2HCl**) and imidazolium (**2·2HI**) calix[4]arene pro-ligands. *In situ* generation of the free carbene **2a** (R = Me) is also detailed, the formation of which was substantiated by the isolation of the thione adduct **3** by reaction with elemental sulfur. Comparisons between **2a**, **3** and the monodentate **$I^{i}Pr_{2}Me_{2}$** and **$I^{i}Pr_{2}Me_{2}S$** ligands are also made.

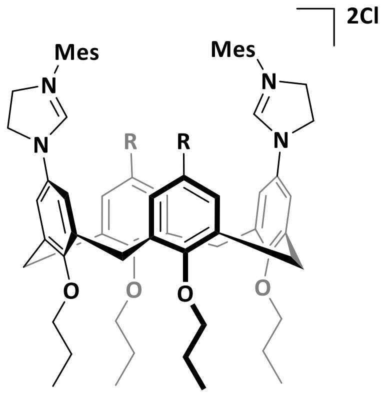

1.2HCl

R = H, ^{t}Bu

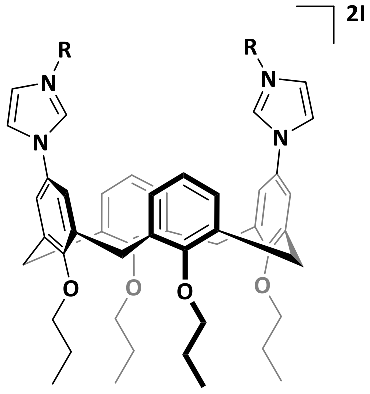

2.2HI

R = Me, ^{n}Pr, $CH_2CH_2OCH_3$

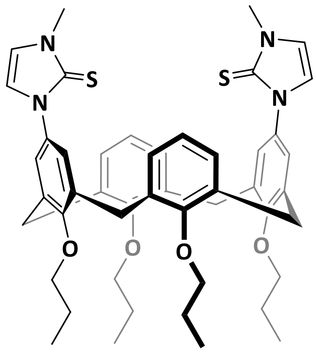

3

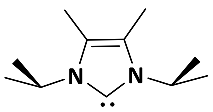

$I^{i}Pr_{2}Me_{2}$

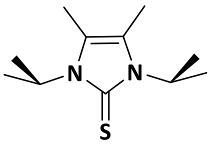

$I^{i}Pr_{2}Me_{2}S$

2.1 Introduction

2.1.1 Preparation of NHC pro-ligands

Imidazolinium and imidazolium salts have been described in recent years as efficient NHC ligand precursors for the synthesis of transition metal complexes. These robust and bench stable salts can be made from a wide range of synthetic routes using commercially available starting materials and are readily converted to the free carbene by deprotonation at the C2 position.[1, 2]

2.1.1.1 Imidazolium pro-ligands

Imidazolium pro-ligands are perhaps the most convenient NHC precursors due, in part, to the commercial availability of imidazole (currently available for £112.50/500 g from Sigma Aldrich, August 2016). Common synthetic routes to the formation of these precursors are outlined in **Scheme 2.1**.[3]

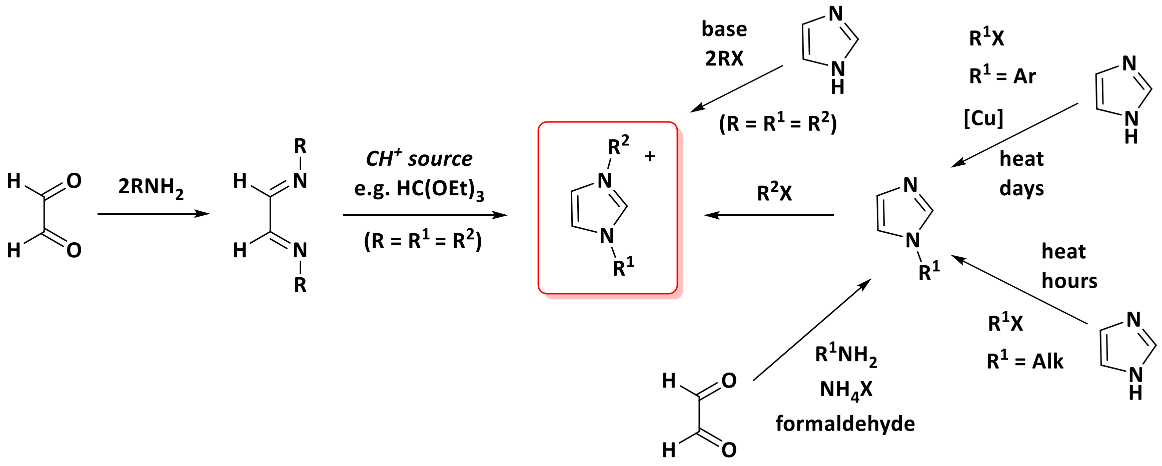

Scheme 2.1*:* Preparation of imidazolium salts

Synthesis of symmetrically substituted imidazolium salts can be achieved from alkyl imidazoles prepared from a reaction between aniline, ammonium salt and aqueous glyoxal in the presence of catalytic quantities of acid to form diazabutadienes which are then cyclised by addition of paraformaldehyde in aqueous conditions.[4, 5] More simply alkylimidazoles can be prepared directly though S_N2 substitution of allyl halides or Ullman coupling reaction of aryl halides.[6-8] Subsequent alkylation of the resulting alkylimidazole readily affords the asymmetric N-functionalised imidazolium salts. Symmetric species can be synthesised *via* adaptions of these protocols or by a simple reaction between glyoxal and primary amines and cyclisation by addition of a CH^+ source such as $CH(OEt)_3$.[9]

2.1.1.2 Imidazolinium pro-ligands

Imidazolinium pro-ligands are chiefly synthesised through the formation of *N,N'*-disubstituted-1,2-diamines, followed by addition of as CH^+ source such as $HC(OEt)_3$ (**Scheme 2.2**).[10] 1,2-diamines are typically prepared by reduction of imines or amides. Other common routes include; formation of N,N'-disubstituted formamidines and cyclisation by addition of an excess of 1,2-dichloroethane, or reaction of lithium formamidinate with biselectrophiles such as 1,3,2-dioxathiolane-2,2-dioxide.[9, 11, 12 13, 14]

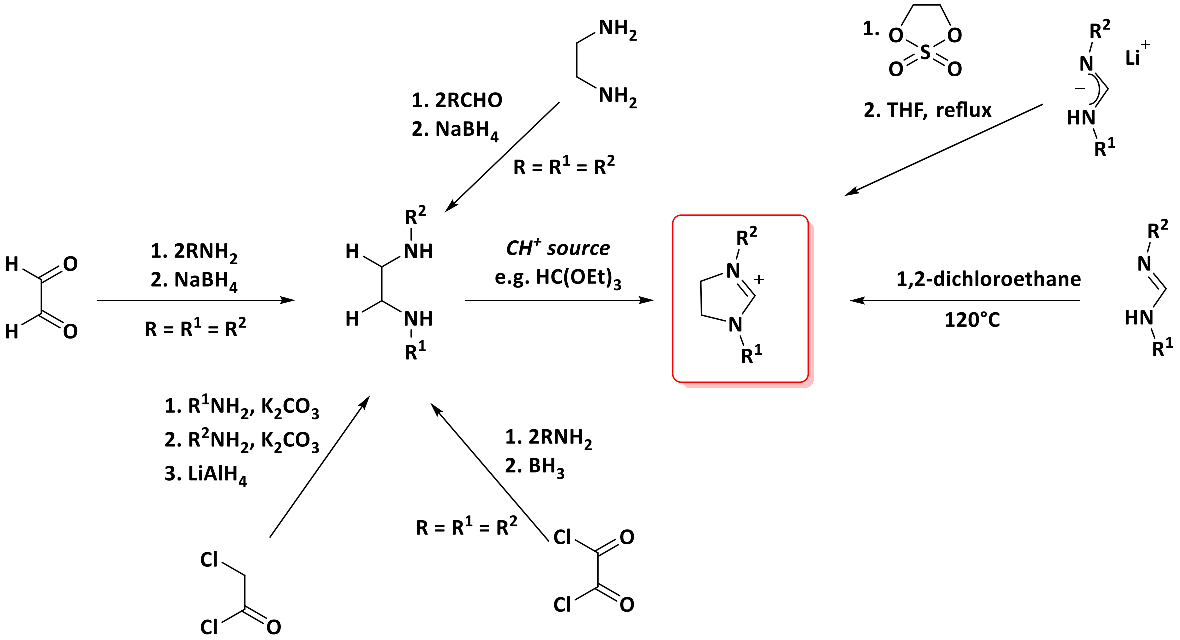

Scheme 2.2*:* Preparation of imidizolinium salts

2.1.1.3 Other precursors

While imidazolium and imidazolinium salts are generally considered the primary precursors for NHC ligands it is also worth noting other established NHC precursors, such as imidazol-2-thiones (NHCSs). These precursors are much more robust than free carbenes and are stable in the presence of water and air. The corresponding free NHC ligands can be produced by reduction of NHCS with potassium.[15] Thione compounds are simply synthesised by condensation of *N,N'*-dialkylthioureas and 3-hydroxy-2-butanone,[15] addition of CS_2 to 1,2-diamines,[16] or addition of 1,1,3,3-tetrakis-(trifluoromethyl)-1,3-dithiethene to alkylimidazoles (although this route is limited NHCSs with $(CF_3)_2CH$ substituents) (**Scheme 2.3**).[17] Formation of imidazole-2-thiones by reaction of a free carbene, isolated or generated *in situ*, with elemental sulfur is another common route, although less useful in this context.[18, 19]

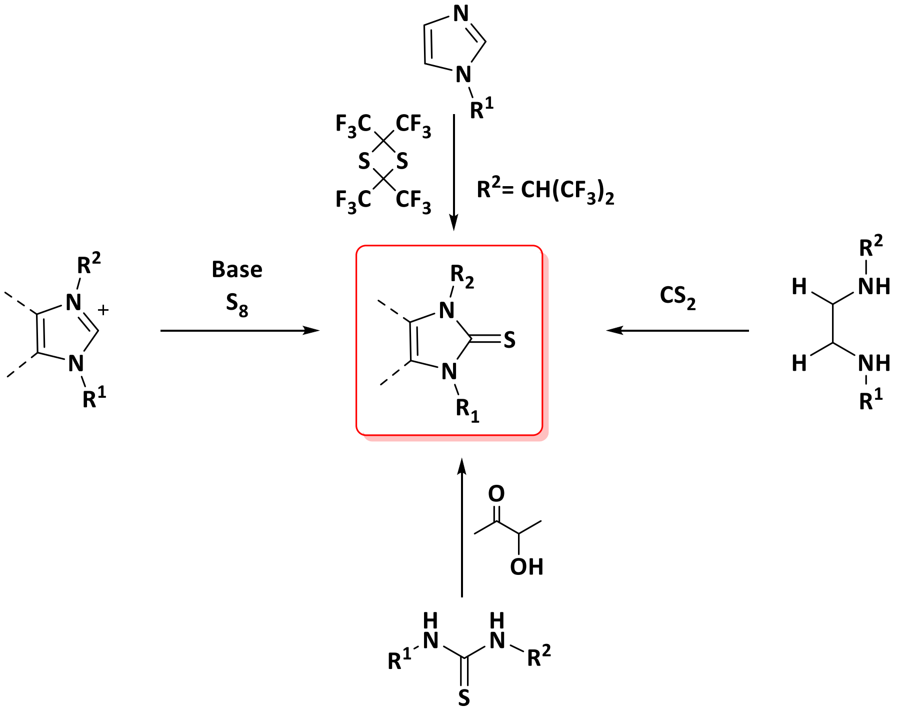

Scheme 2.3: Preparation of NHCS products

Other masked NHCs involve protection of the C2 position by derivatives of CO_2, $HCCl_3$, HC_6F_5 and are discussed in Chapter 3.

2.1.2 Preparation of calix[4]arene-based NHC pro-ligands

Dinarès *et al*. have reported the synthesis 1,3-bis(imidazolium)-calix[4]arene salts **[A68]2[PF$_6$]** by Ullman-type coupling of 1,3-dibromocalix[4]arene **A74** with imidazole (**Scheme 2.4**).[6, 20] Use of 20 mol % CuI, 80 mol % DMEDA, Cs_2CO_3 and heating at 170°C for 2 days resulted in low yields (11 %) of **A75**. An increased yield of 89% was achieved by addition of equimolar CuI and DMEDA (50 mol %) and heating for 7 days at 170°C. Alkylation of **A75** using 1-bromoalkanes and counterion exchange using HPF_6, resulted in the isolation of**[A68]2[PF$_6$]** in good yields R = ^{n}Bu, 80 %; and R = ^{i}Pr =53 %.

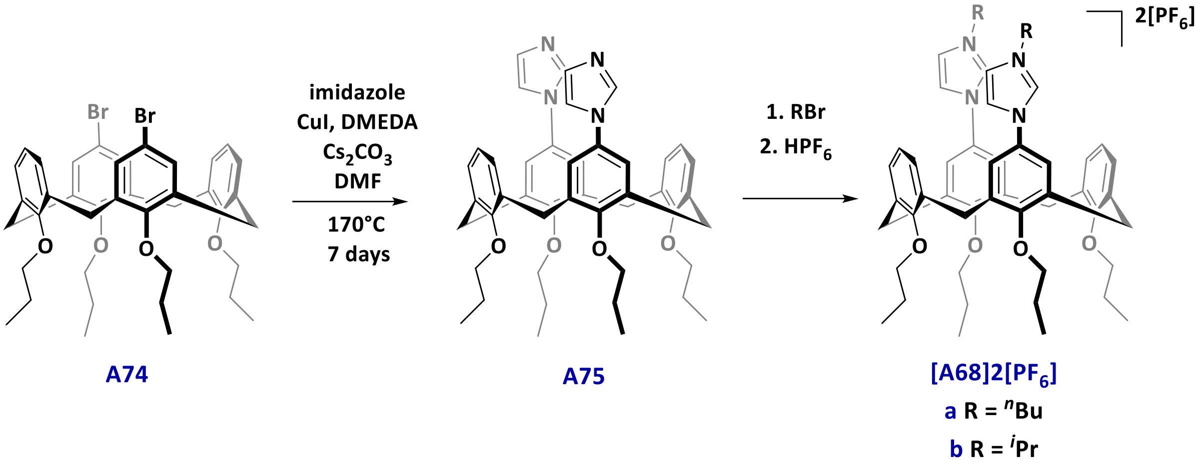

Scheme 2.4: Synthesis of 1,3-bis(imidazolium)calixarene salts **[A68]2[PF$_6$]** described by Dinarès *et al*

Imidazolium salts **A68** (**a** and **b**) have been examined for their anion binding properties: analysis of Job plots for interactions with halides, CN$^-$, acetate and benzoate indicated a 1:1 receptor: anion binding stoichiometry. The **A68** salts have also been used in the synthesis of palladium complexes (**Figure 1.18**, Chapter 1).

The synthesis of methylene bridged tetrakis(imidazole) and tetrakis(imidazolium) calix[4]arenes have been reported by several groups. For example, Willans *et al.* have reported the synthesis of **A77** and **A78** through reaction of tetrakisbromomethylcalix[4]arene **A76** with imidazole or methylimidazole respectively (**Scheme 2.5**).[7] Similar alkylation reactions of 1,2-di(chloromethyl)calix[4]arene **A79** have been used for the preparation of bis(imidazolium) salt **A80**.[21]

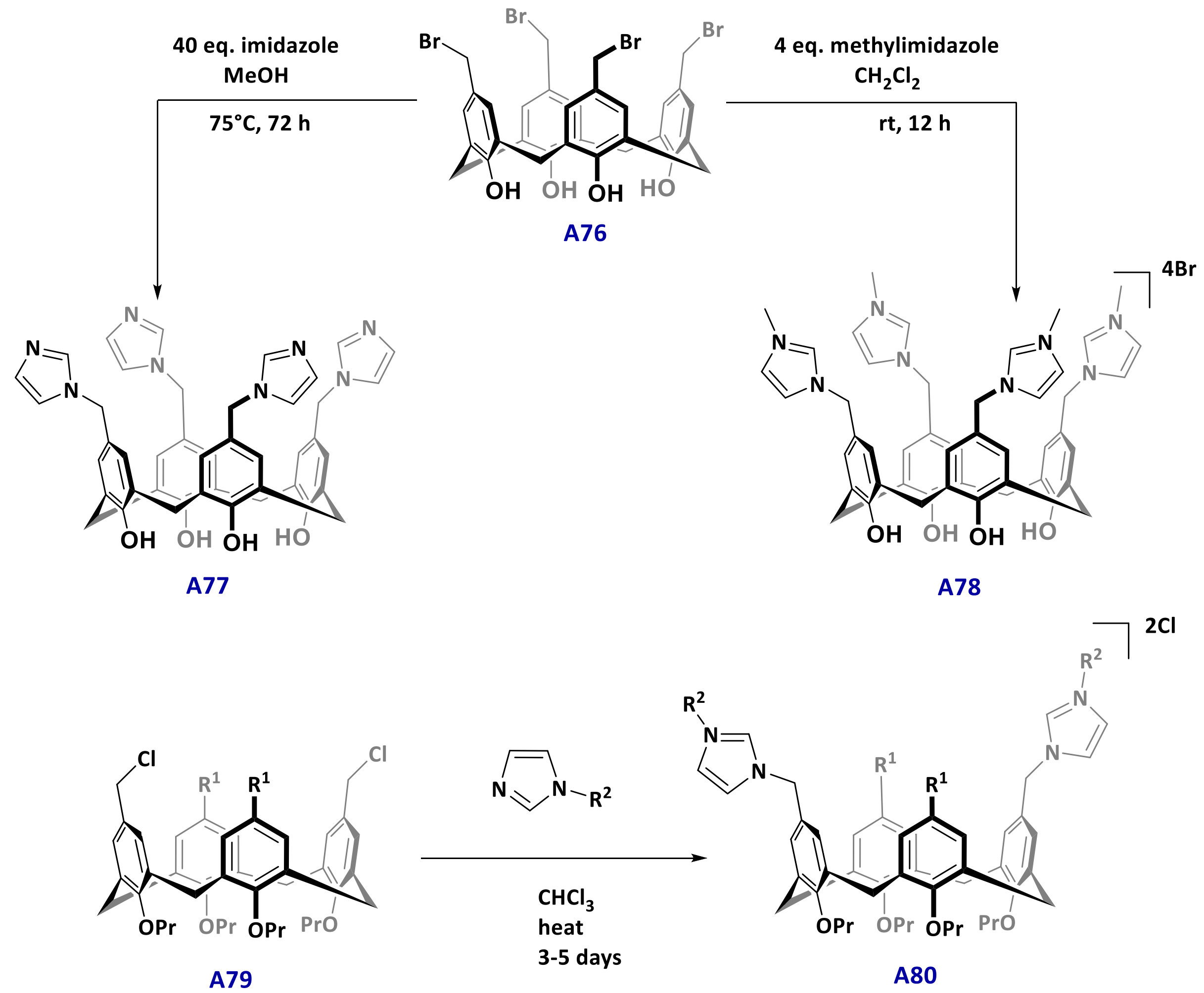

R^1= ^{t}Bu
R^2= Me (70 %), ^{i}Pr (63 %), Mes (43 %), 2,6-Dipp (22 %)

R^1= H,
R_2= Me (96 %), ^{i}Pr (98 %), Mes (91 %), Dipp (96 %), Cy (96 %)

Scheme 2.5: Synthesis of **A77**, **A78**, **A79** and **A80** reported by Willans *et al.*

2.2 Results and discussion

2.2.1 Imidazolinium functionalised calix[4]arenes **1·2HCl**

Based on preliminary work by Dr. Adrian Chaplin, the preparation of 1,3-bis(imidazolinium)calix[4]arene pro-ligands **1·2HCl** were initially targeted. These pro-ligands were prepared over 5-6 steps from *tert*-butylcalix[4]arene in an overall yields of <5% (**Scheme 2.6**).[10,22-24] Formation of **1·2HCl** were apparent by ^{1}H NMR spectroscopy by the appearance of the characteristic high frequency NC<u>H</u>N resonances at δ 9.54 and 9.04 (CD_3CN) for **1a.2HCl** and **1b.2HCl**, respectively.[25] Strong parent ions with half-integer spacing were observed at 483.3018 *m/z* (cald. 483.3006 *m/z*) $[M]^{2+}$ and 539.3631 *m/z* (cald.539.3632 *m/z*) $[M]^{2+}$ by ESI-MS. A low-quality solid state structure (R_1 = 15%) of **1b.2HCl** was also determined by X-ray diffraction (**Figure 2.1**).

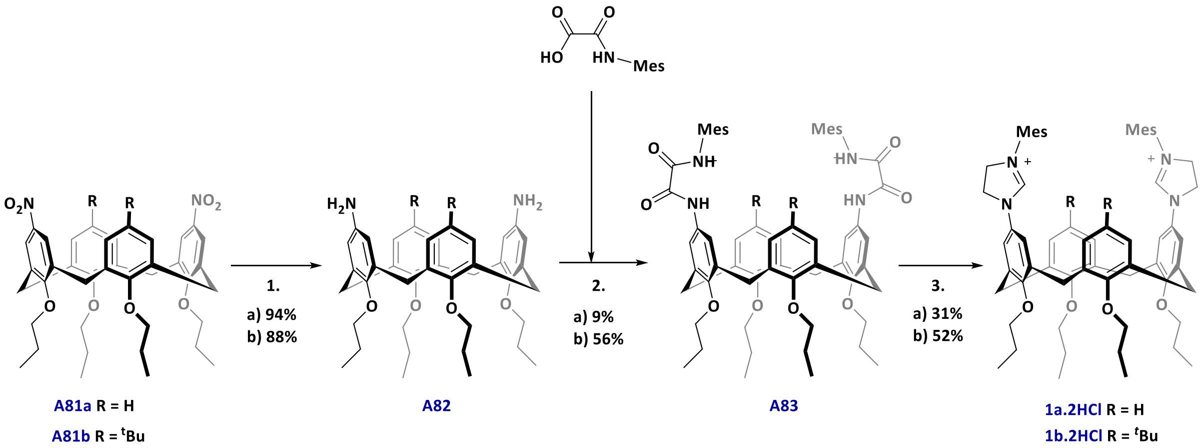

Scheme 2.6: Synthesis of 1,3-substituted bis(imidazolinium)calix[4]arenes **1a.2HCl** and **1b.2HCl.** Conditions: **1)** $SnCl_2.2H_2O$ **2)** DCC, HOBT, THF **3) i)**BH_3.THF **ii)** HCl, MeOH **iii)** $HC(COEt)_3$

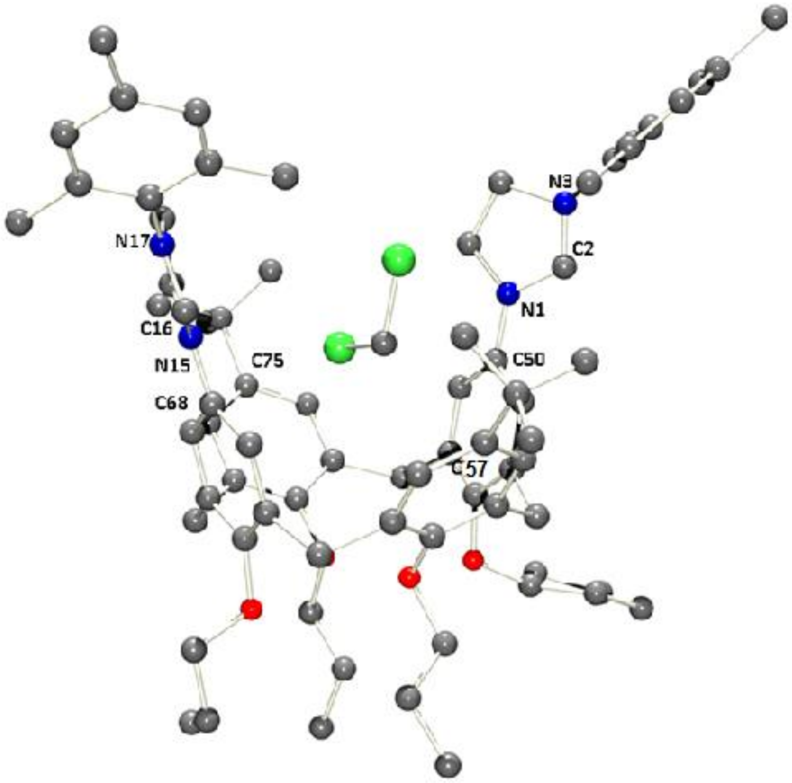

Figure 2.1*:* Solid state structure of **1b.2HCl** in ball and stick view. Hydrogen atoms and anions are omitted for clarity. Selected bond lengths (Å) and angles (°):C2···C16, 8.56(5); C50···C68, 6.55(3); C75···C57, 8.86(3); CPR = 0.739(4)

As well as the inclusion of the CH_2Cl_2 guest within the calix[4]arene cavity, the solid state of **1b.2HCl** is notable for the adoption of a distinct pinched-cone conformation, where the bulky and charged imidazolinium moieties are held at a NCH···NCH distance of 8.56(5) Å. Such pinched-cone conformations of upper rim substituted calix[4]arenes are well documented, can be driven by different factors, and have been shown to result in extensive deformation of the calix[4]arene scaffold.[26] In order to quantify the extent of the calix[4]arene puckering in this thesis a ‘calix[4]arene puckering ratio’ (CPR) has been defined as the ratio of opposing upper rim carbon-carbon distances; CPR = $r_{(CC)substituted}/r_{(CC)unsubstituted}$ (**Figure 2.2**).

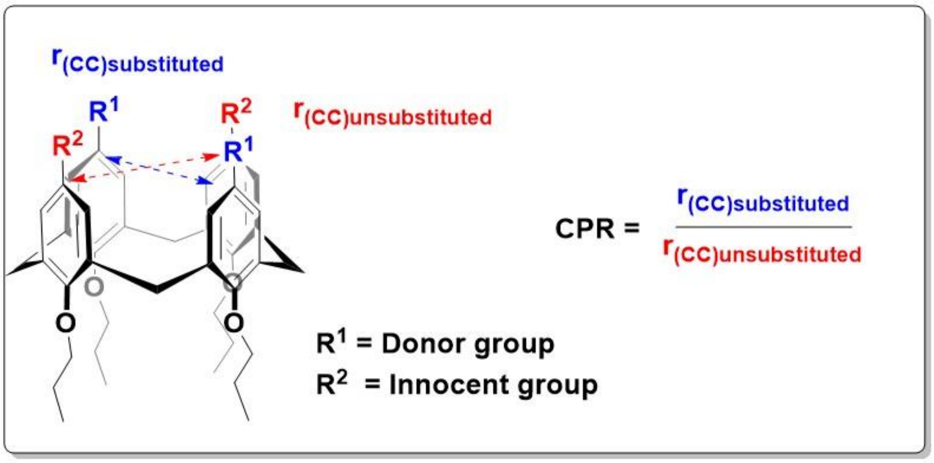

Figure 2.2*:* Calix[4]arene puckering ratio (CPR) definition

For **1b.2HCl** the CPR = 0.739(4), indicates that the calix[4]arene adopts a puckered conformation, driven by the steric repulsion of the *tert*butyl groups rather than electrostatic interactions from the two charged imidazolium donors. Although the presence of the CH_2Cl_2 guest can also be assumed to be a contributing factor.

The preparation of **1·2HCl** on a large scale, however proved problematic. In particular the literature nitration to form **A81** resulted in inconsistent results and crude NMR spectra showed a variation in yield of the 1,3-product from 0-16% (*cf.* literature yields reported at 24% (**A81b**)).[22] Due to the inherent lack of selectivity of the direct nitration of *p*-*tert*butylcalix[4]arene **A2**, synthetic routes to selectively form **A81** were investigated. For example 1,3-di*tert*butylcalix[4]arene **A86** can by synthesised by exploitation of the benzoyl groups on the lower rim. Benzoyl chloride can be used to form the 1,3-substituted product, followed by selective dealkylation of the *para* positions. The benzoyl groups are then easily hydrolysed and the lower rim alkylated. Nitration in this instance selectively proceeds *via* substitution of the bulky *tert*butyl group. In this instance the increased number of steps resulted in only in a marginal increase in yield from 5 to 13% (**Scheme 2.7**).[27, 28]

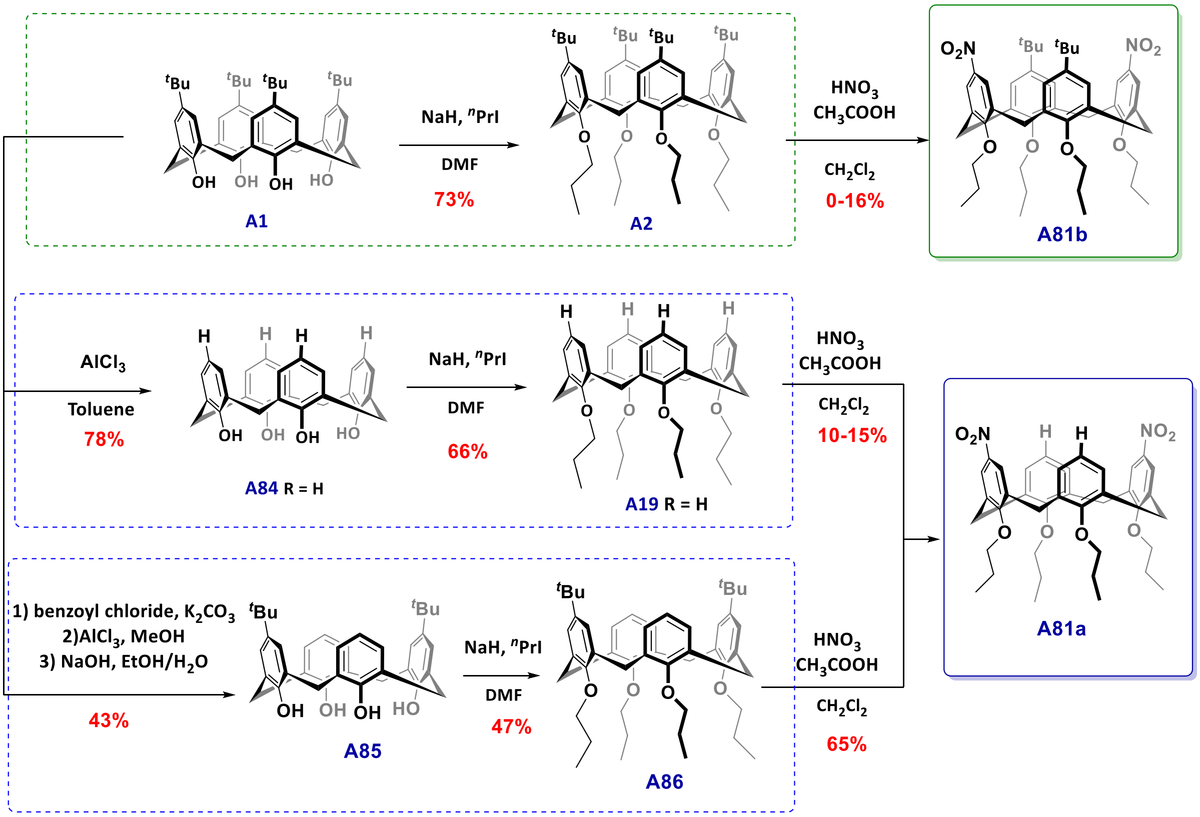

Scheme 2.7: Nitration routes for the formation **A81 a** and **b**

Alternative routes that could theoretically be adapted for the selective formation of 1,3-dinitrocalix[4]arene products are known in literature, such as *via* isolation of boronic acid functionalised intermediates and reaction with bismuth nitrate (proposed route given in **Scheme 2.8**).[29] However, due to the increased number of steps (five from **A1**) this route was not investigated during this project.

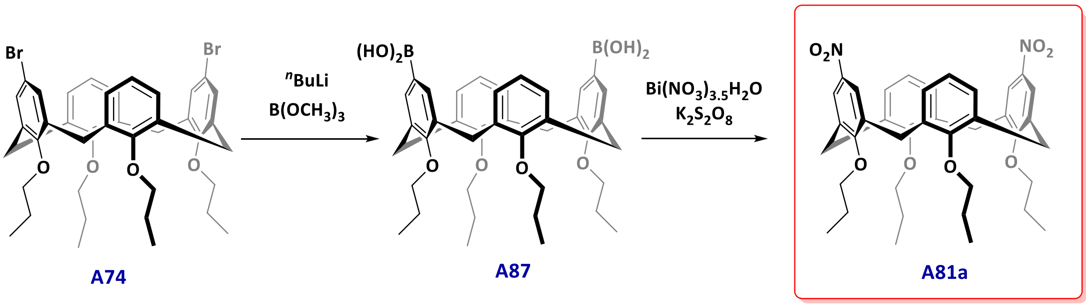

Scheme 2.8: Proposed route for the formation of 1,3-dinitrocalix[4]arene

2.2.2 Imidazolium functionalised calix[4]arenes 2.2HI

Given the low yielding preparation of **1.2HCl** adaptions of known procedures for the preparation of 1,3-functionalised bis(imidazolium) calix[4]arene salts were targeted (**Scheme 2.9**). In this was the synthesis of new salt **2a.2HI** was achieved using a six step synthesis starting from *p-tert*butylcalix[4]arene **A1** over *ca.* two weeks, with an overall yield of 7% (*cf.* <5% for **1·2HCl**).[30-33] Formation of **A75** by Ullman-type coupling of imidazole and 1,3-dibromocalix[4]arene **A74** was achieved with an isolated yield of 62% (lit. 89 %).[6] Subsequent alkylation of **A75** with MeI in THF gave **2a·2HI** in 84% isolated yield. Formation of **2a.2HI** was confirmed by ^{1}H and ^{13}C NMR spectroscopy, in particular a characteristic high frequency NC<u>H</u>N resonance was observed at δ 9.20 (CD_2Cl_2, **Table 2.1**). ESI-MS, which showed the expected parent dication peak at 377.2220 *m/z*, $[M]^{2+}$ (calcd 377.2224 *m/z*) with half integer spacing and microanalysis showed excellent agreement with calculated values.

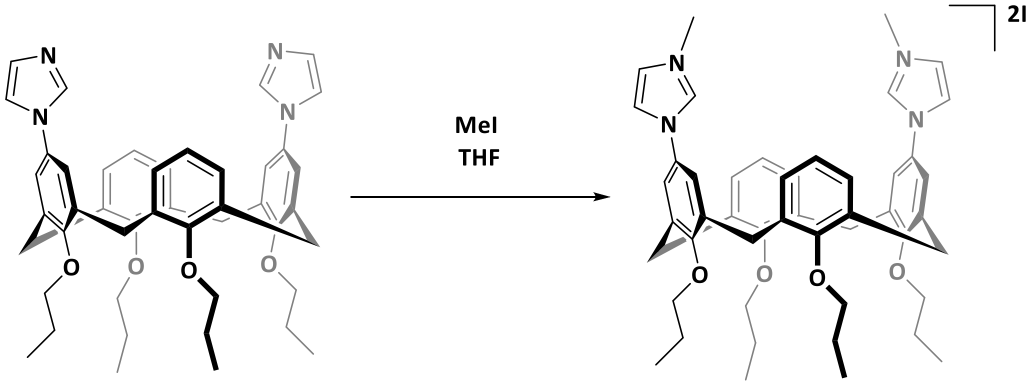

A75 **2a.2HI**

Scheme 2.9: Alkylation of 1,3-diimizadolcalix[4]arene **A75**

Other alkylation reactions were assayed with a range of alkyl halides are summarised in **Table 2.1*Table 2.1***. Alkylations involving ^{n}PrI, $ICH_2CH_2OCH_3$ and $BrCH_2CH_2CH=CH_2$ similarly proceeded with good conversion, however chloro containing ($ClCH_2CH_2OCH_3$) and more bulky X^{i}Bu (X = Br, I) showed no conversion. Due to the relatively high yield and structural simplicity of the methyl product **2a.2HI**, this salt was used for the synthesis of transition metal products.

Table 2.1: Summary of alkylation reactions of **A75**

Reagent	**Solvent**	**Temp (°C)**	**Time (h)**	**Yield (%)**	**δ NC$\underline{H}$N**	**ESI-MS $[M]^{2+}$¥**
MeI	THF	70	14	84 (isolated)	9.20 (CD_2Cl_2)	377.22
^{n}PrI	THF	70	16	71 (isolated)	9.73 (CD_2Cl_2)	405.25
$BrCH_2CH_2CH=CH_2$	Dioxane	100	18	50 (by NMR)	10.35 ($CDCl_3$)	417.3*
$ClCH_2CH_2OCH_3$	THF/ dioxane	70-100	96	25 (by NMR)	10.55 ($CDCl_3$)	-
$ClCH_2CH_2OCH_3$	Dioxane	100	24	Quantitative (by NMR)	9.20 ($CDCl_3$)	421.2*
Br^{i}Bu	Dioxane	100	16	No reaction	-	-
I^{i}Bu	THF	80	16	No reaction	-	-

*LR-ESI-MS ¥ All agree with calculated values

The solid state structure of **2a.2HI** was determined by X-ray diffraction (**Figure 2.3**). The calix[4]arene scaffold notably adopts a pinched cone conformation with a CPR = 2.247(9)/1.838(7) (two independent molecules observed). This puckering contrasts that found for **1b.2HCl** (CPR = 0.739(4), (**Figure 2.3**), presumably a consequence of the reduced steric bulk on the upper rim (lack of *tert*butyl groups). In this instance the distortion is presumably driven by columbic repulsion, resulting in N$\underline{C}$HN···N$\underline{C}$HN separations of 13.43(2)/13.09(1). Although these large distances may superficially suggest that chelation of

2a.2HI may be difficult, it can be assumed that this geometry will not be retained in solution.[34]

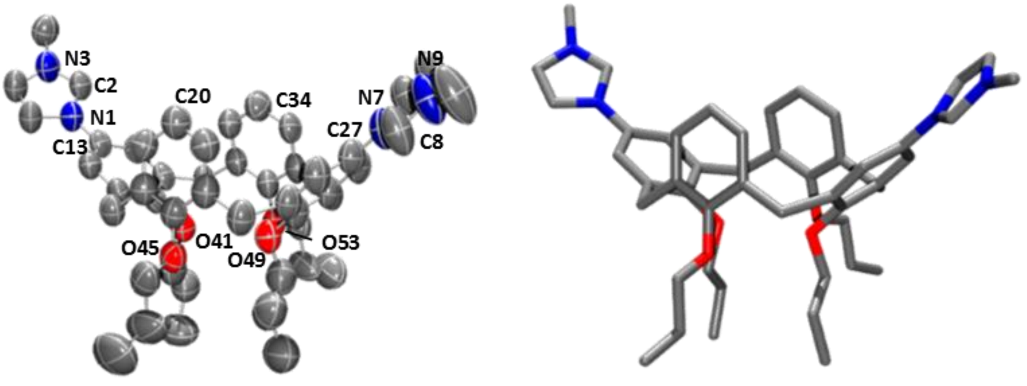

Figure 2.3: *Solid-state structure of* ***2a·2HI*** *Drawn in both thermal ellipsoids and stick for clarity. Ellipsoids drawn at the 30% probability level; only one of the two unique molecules shown (Z′ = 2); hydrogen atoms, anions and minor disordered components are omitted for clarity. Selected bond lengths (Å) and angles (°): C2···C8, 13.43(2); C102···C108, 13.09(2); C13···C27, 9.79(1); C20···C34, 4.27(2); C113···C127, 9.58(1); C120···C134, 5.22(2); CPR = 2.24(1), 1.838(7).*

Deprotonation of **2a.2HI** was carried out using strong hindered bases K[O^{t}Bu] or K[N(SiMe$_3$)$_2$] in C_6D_6 or d_8-THF at 298 K, resulting in quantitative formation of the free carbene **2a** by ^{1}H NMR spectroscopy (**Scheme 2.10**). Although **2a** is stable in solution under argon for 24 h, it could not be isolated and was therefore chatacterised *in situ* using ^{1}H and ^{13}C NMR spectroscopy in C_6D_6 or THF at 298 K. Formation of the free carbene **2a** was confirmed by the loss of the high frequency $NC\underline{H}N$ resonance and the presence of a characteristic ^{13}C carbenic resonance at δ 213.3 (C_6D_6)/ δ 216.0 (d_8-THF). Both ^{1}H and ^{13}C{^{1}H} spectra of **2a** exhibit C_{2v} symmetry with the $N\underline{Me}$ signals located at δ 4.17 and δ 37.8, respectively. The formation of the free carbene was also confirmed by a "trapping" experiment involving the addition of elemental sulfur and formation of a stable thione derivative which was subsequently isolated and fully characterised (*vide infra*).

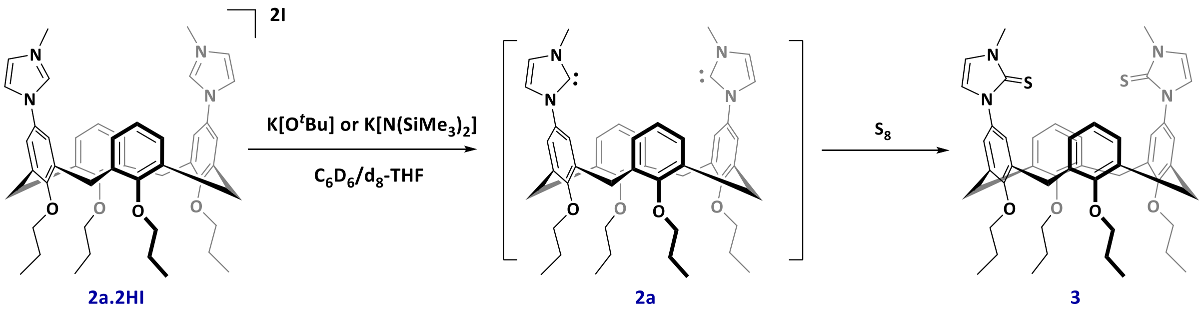

Scheme 2.10: Deprotonation of pro-ligand **2a.2HI** to form free carbene **2a**

2.2.3 Imidazol-2-thione functionalised calix[4]arene **3**

Synthesis of calix[4]arene imidazole-2-thione ligand **3** was initially achieved by reaction of **2a**, generated *in situ* from **2a.2HI** and KO^{t}Bu in THF, with S_8 as described above. The crude product was obtained with an apparent 88% yield, however, this material was later found to contain potassium salt impurities (see Chapter 4) and purification by column chromatography was necessary (silica, CH_2Cl_2, Et_2O 3:1), ultimately leading to a low isolated yield of pure **3** (26 %). The synthesis of **3** was therefore adapted using inspiration from literature and prepared by deprotonation of **2a.2HI** in the presence of S_8 using the weak base K_2CO_3 in refluxing ethanol over 16 hours giving an improved yield of analytically pure **3** in 58 % yield (**Scheme 2.11**).[19, 35]

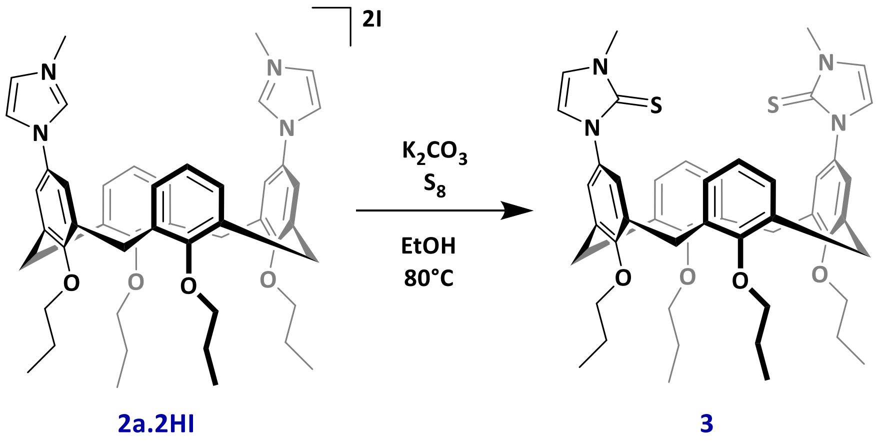

Scheme 2.11: Synthesis of 1,3-NHCS functinonalised calix[4]arene **3**

The formation of **3** was fully corroborated by ^{1}H and ^{13}C NMR spectroscopy, ESI-MS, microanalysis and X-ray diffraction (**Figure 2.4**). Notably in CD_2Cl_2 solution, the $N\underline{C}N$ signal showed a significant downfield shift from δ 134.9 to 163.4 compared to **2a.2HI**, but an upfield shift compared to **2a** (δ 213.3, C_6D_6).

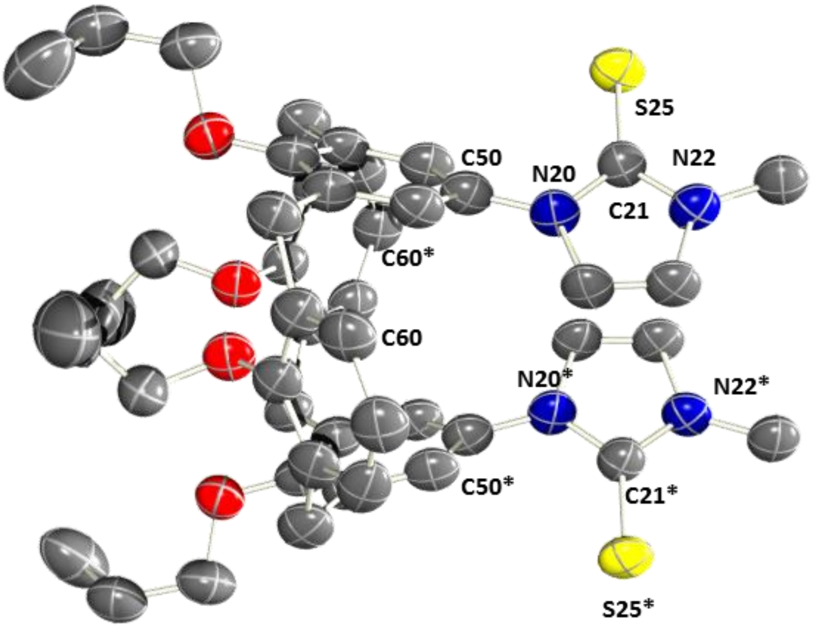

Figure 2.4: Solid state structure of **3** in ellipsoid view. Thermal ellipsoids drawn at the 50% probability level. Atoms denoted with * are generated from symmetry element *1+X,1-Y,1/2-Z* Hydrogen atoms, anions and minor disordered units are omitted for clarity. Selected bond lengths (Å) and angles (°): S25···S25, 7.73(9); C50···C50*, 4.235(11); C60···C60*, 10.118(12); C21···C21*, (4.4816(12), CPR = 0.419(1)

As for **2a.2HI**, the solid state structure of **3** (**Figure 2.4**) shows a pinching of the calix[4]arene scaffold. In this case the functionalised walls are contracted ($N\underline{C}SN$-$N\underline{C}SN$ = 4.85(1), CPR = 0.419(1)) driven by apparent π-stacking of the imidazol-2-thione functionalities (Cnt-Cnt – 3.460(9) Å). The thiones adopt an antiparallel arrangement resulting in an overall *pseudo* C_2 symmetry. The structure was further corroborated by ESI-MS, where a $[MH]^{+}$ peak was observed, and by microanalysis.

2.2.4 Model systems

To help gain an insight into the role of the calix[4]arene scaffold in complexes derived from **2a** and **3**, known "model" monodentate ligands, 1,3-diisopropyl-4,5dimethylimidazol-2-ylidene (**I^{i}Pr$_2$Me$_2$**) and 1,3-diisopropyl-4,5-dimethylimidazol-2-thione (**I^{i}Pr$_2$Me$_2$S**), were prepared for comparison. The preparation of these model ligands was achieved using the procedure reported by Kuhn and Kratz (**Scheme 2.12**). Spectroscopic data of isolated materials showed excellent agreement with literature values.[15]

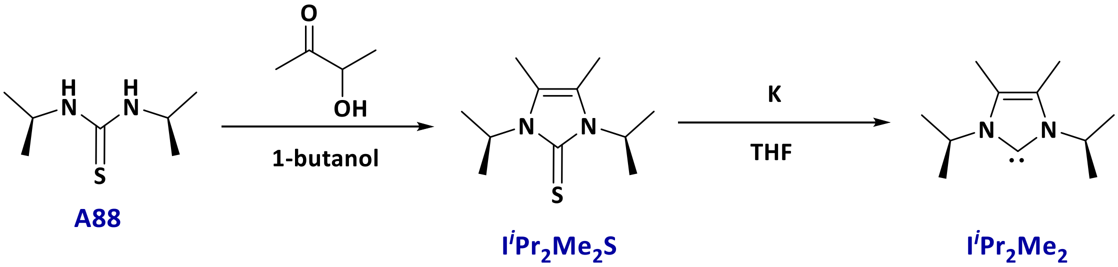

Scheme 2.12: Synthesis of model ligands reported by Kuhn and Kratz

The use of these mono-dentate ligands as models can be justified on the grounds of similar electronic and steric properties of the donor groups. For instance the good agreement of the carbenic and N$\underline{C}$SN resonances can be noted: $\delta_{N\underline{C}N}$ 213.2 (C_6D_6, **2a**) 205.9 (C_6D_6, **I^{i}Pr$_2$Me$_2$**), and $\delta_{N\underline{C}SN}$ 163.4 (CD_2Cl_2, **3**), 160.7 (CD_2Cl_2, **I^{i}Pr$_2$Me$_2$S**) (***Table 2.2***). Tolman's electronic parameter (TEP), which is based on the A_1 carbonyl stretching frequency of $[Ni(CO)_3(L)]$ complexes, can also be used to compare the electronic properties of the molecules.[36] As can be seen from ***Table 2.***, substitution of the N or C4/C5 positions with alkyl or aryl substituents has little effect on this value.[37] Moreover, the TEP value for **I^{i}Pr$_2$Me$_2$** was found to be approximately the average value of those found for IMes and IDM (which can be used as an approximation for the unknown value for **2a**). Percentage buried volume (%V_{bur}) represents the percentage of a sphere around a metal which is occupied by the atoms of the ligand and can be used to approximate the steric effects of the NHC ligand.[38] %V$_{bur}$ values shown in ***Table 2.*** indicate that **I^{i}Pr$_2$Me$_2$** is a suitable model for **2a**, as the %V$_{bur}$ is approximately the average of those of IMes and IDM.

Overall it can be summarised that monodentate ligands **I^{i}Pr$_2$Me$_2$** and **I^{i}Pr$_2$Me$_2$S** can provide a good representation of the donor characteristics of **2a** and **3** and therefore differences in coordination chemistry are likely to be a result of the calix[4]arene scaffold.

Table 2.2*:* Electronic and steric parameters of monodentate NHC and NHCS ligands and calix[4]arenes **2a** and **3**

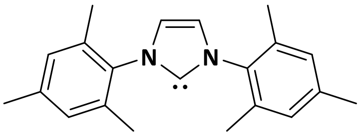

IMES

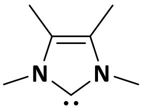

IDM

Ligand	TEP /cm^{-1}	%V$_{bur}$	δ N$\underline{\mathrm{C}}$N / δ N$\underline{\mathrm{C}}$SN
I^{i}Pr$_2$Me$_2$	2051	28.0	205.9 (C_6D_6)
IMes	2050	31.8	219.4 (C_6D_6)[39]
IDM	2052	24.9	214.6 (C_6D_6)[40]
2a	-	-	213.2 (C_6D_6)
I^{i}Pr$_2$Me$_2$S	-	-	160.7 (CD_2Cl_2)
3	-	-	163.4 (CD_2Cl_2)

2.3 Conclusion

Synthetic methodology for the preparation of **1·2HCl** has been investigated. Formation of the 1,3-dinitrocalix[4]arene **A82** proved to be a significant challenge and encumbered synthesis of meaningful quantities of **1·2HCl**. Instead, adaption of literature procedures for closely related 1,3-substituted *N*-alkylimidazolium calix[4]arenes resulted in the reliable synthesis of satisfactory quantities of pro-ligand **2a.2HI**. The corresponding free carbene **2a** was readily formed in solution by addition of strong bases, characterised *in situ* and trapped by addition of elemental sulfur resulting in the formation of the imidazol-2-thione adduct **3**. The donor characteristics of **2a** and **3** are comparable to those of the mono-dentate ligands $\mathrm{I^{\mathit{i}}Pr_2Me_2}$ and $\mathrm{I^{\mathit{i}}Pr_2Me_2S}$, which will be used in parallel to assess the role of the calix[4]arene scaffold in the subsequent study of the coordination chemistry of **2a** and **3**.

2.4 Experimental section

2.4.1 General considerations

Unless otherwise stated all organic manipulations were carried out under a nitrogen atmosphere using standard Schlenk techniques. "Hi-dry" solvents were bought from Acros or Sigma Aldrich and unless otherwise stated used as received. THF and C_6D_6 were dried over Na, vacuum distilled, freeze-pump-thaw degassed three times and stored under argon. CD_2Cl_2 was distilled over CaH_2, freeze-pump-thaw degassed three times under argon and stored over 3 Å molecular sieves under argon. *d*$_8$-THF was dried over 3 Å molecular sieves and freeze–pump–thaw degassed three times before being placed under argon. **A75** was synthesised by adaption of literature procedures.[20, 27, 31-33] All other solvents and reagents are commercial products and were used as received. NMR spectra were recorded on Bruker DPX-400, AV-400, AV-500 spectrometers at 298 K. Chemical shifts are quoted in ppm and coupling constants in Hz. ESI-MS were recorded on a Bruker MaXis mass spectrometer. Microanalysis were performed by Stephen Boyer at London Metropolitan University.

2.4.2 Preparation of isolated products

Pro-ligand (2a.2HI)

A solution of **A75** (1.00 g, 1.38 mmol) was stirred with iodomethane (0.84 mL, 13.8 mmol) in THF (30 mL) in a sealed J. Young's flask 70°C for 14 hours. The resulting suspension was diluted with diethyl ether (*ca.* 20 mL), the solvent removed by filtration and the remaining precipitate washed with diethyl ether (2 x 20 mL). Volatiles were removed *in vacuo*. Yield = 1.17 g (84%, fine off-white powder). **^{1}H NMR** (CD_2Cl_2, 400 MHz) δ 9.20 (br, 2H, NC$\underline{H}$N), 8.04 (t, $^3J_{HH}$ = 1.8, 2H, Imid), 7.23 (d, $^3J_{HH}$ = 7.5, 4H, Ar), 7.05 (t, $^3J_{HH}$ = 7.5, 2H, Ar), 6.72 (t, J_{HH} = 1.8, 2H, imid), 6.61 (s, 4H, $\underline{Ar}$-imid), 4.54 (d, $^2J_{HH}$ = 13.5, 4H, ArC$\underline{H}_2$Ar), 4.17 (s, 6H, NCH_3), 4.03 – 4.09 (m, 4H, OCH_2), 3.74 (t, $^3J_{HH}$ = 6.8, 4H, OCH_2), 3.28 (d, $^2J_{HH}$ = 13.5, 4H, ArC$\underline{H}_2$Ar), 1.87 – 2.06 (m, 8H, C$\underline{H}_2$CH$_3$), 1.12 (t, $^3J_{HH}$ = 7.4, 6H, CH$_2$C$\underline{H}_3$), 0.93 (t, $^3J_{HH}$ = 7.5, 6H, CH$_2$C$\underline{H}_3$).

$^{13}C\{^1H\}$ NMR (CD_2Cl_2, 101 MHz) δ 157.5 ($\underline{C}OCH_2$), 157.3 ($\underline{C}OCH_2$), 137.7 (Ar{$\underline{C}CH_2$}), 135.7 (Ar{$\underline{C}CH_2$}), 134.9 (NCHN), 130.2 (Ar), 129.2 (Ar{$\underline{C}N$}), 125.6 (Imid), 124.4 (Ar), 120.8 (Ar), 119.9 (Imid), 78.1 (OCH_2), 77.4 (OCH_2), 37.8 (NCH_3), 31.4 (Ar$\underline{C}H_2$Ar), 23.9 ($\underline{C}H_2CH_3$), 23.5 ($\underline{C}H_2CH_3$), 10.9 ($CH_2\underline{C}H_3$), 10.2 ($CH_2\underline{C}H_3$). **ESI-MS** (CH_3CN, 180 °C, 3 kV) Positive ion 377.222 *m/z*, $[M]^{2+}$ (calc 377.222). **Anal.** Calcd. For $C_{48}H_{58}I_2N_4O_4$ (1008.81 $g{\cdot}mol^{-1}$): C, 57.13; H, 5.80; N, 5.55. Found: C, 56.88; H, 6.00; N, 5.55.

General procedure for alkylation reactions of A75

A solution of **A75** and alkylhalide (5 equivalents) in THF or dioxane (5 mL) was heated. The resulting suspension was diluted with diethyl ether (*ca.* 20 mL), the solvent removed by filtration and the remaining precipitate washed with diethyl ether (2 x 20 mL). Volatiles were removed *in vacuo*. Yields and characterisation of products are summarised in ***Table 2.1***.

In situ generation of free carbene (2a)

A suspension of **2a·2HI** (10.2 mg, 0.0101 mmol) and K[O^{t}Bu] (3.1 mg, 0.0276 mmol) in d_8-THF (0.5 mL) was agitated and sonicated for several minutes inside a sealed J. Young's NMR tube. Analysis by NMR spectroscopy indicated quantitative formation of **2a** with the concomitant formation of ^{t}BuOH (δ^{1}H 5.33, OH; 1.15, CH_3; δ^{13}C 68.1, $\underline{C}CH_3$; 31.6, CH_3). The reaction was repeated in C_6D_6 with the same outcome. The ^{1}H NMR spectra remained unchanged on standing at 293 K for 24 h in both cases. **^{1}H NMR** (d_8-THF, 500 MHz): δ 7.41 (s, 4H, Ar), 7.24 (d, $^3J_{HH}$ = 1.6, 2H, imid.), 6.94 (d, $^3J_{HH}$ = 1.6, 2H, imid.), 6.40 (d, $^3J_{HH}$ = 7.5, 4H, Ar), 6.31 (app t, 2H, J = 8, Ar), 4.51 (d, $^2J_{HH}$ = 13.1, 4H, ArC$\underline{H}_2$Ar), 4.00 – 4.04 (m, 4H, OCH_2), 3.76–3.79 (m, 4H, OCH_2), 3.76 (s, 6H, NCH_3), 3.20 (d, $^2J_{HH}$ = 13.1, 4H, ArC$\underline{H}_2$Ar), 1.99 – 2.07 (m, 4H, $C\underline{H}_2CH_3$), 1.92–1.99 (m, 4H, $C\underline{H}_2CH_3$), 1.10 (t, $^3J_{HH}$ = 7.4, 6H, $CH_2C\underline{H}_3$), 0.98 (t, $^3J_{HH}$ = 7.5, 6H, $CH_2C\underline{H}_3$). **$^{13}C\{^1H\}$ NMR** (d_8-THF, 126 MHz): δ 216.0 (s, NCN), 156.7 (s, $\underline{C}OCH_2$), 156.3 (s, $\underline{C}OCH_2$), 137.9 (s, Ar{$\underline{C}N$}), 137.6 (s, Ar{$\underline{C}CH_2$}), 134.5 (s, Ar{$\underline{C}CH_2$}),128.9 (s, Ar), 123.1 (s, Ar), 121.6 (s, Ar), 121.1 (s, imid.), 118.1 (s, imid.), 77.9 (s, OCH_2), 77.7 (s, OCH_2), 38.3 (s, NCH_3), 32.0 (s, $Ar\underline{C}H_2Ar$), 24.5 (s, $\underline{C}H_2CH_3$), 24.2 (s, $\underline{C}H_2CH_3$), 11.2 (s, $CH2\underline{C}H_3$), 10.7 (s, $CH_2\underline{C}H_3$).

^{1}H NMR (C_6D_6, 500 MHz): δ 7.40 (s, 4H, Ar), 6.74 (d, $^3J_{HH}$ =7.5, 4H, Ar), 6.71 (br, 2H, imid.), 6.61 (t, $^3J_{HH}$ = 7.5, 2H, Ar), 6.18 (br, 2H, imid.), 4.53 (d, $^2J_{HH}$ = 13.2, 4H, $ArC\underline{H}_2Ar$), 3.87 (t, $^3J_{HH}$ = 7.6, 4H, OCH_2), 3.76 (t, $^3J_{HH}$ = 7.4, 4H, OCH_2), 3.42 (s, 6H, NCH_3), 3.17 (d, $^2J_{HH}$ = 13.3, 4H, $ArC\underline{H}_2Ar$), 1.84–1.95 (m, 8H, $C\underline{H}_2CH_3$), 0.93 (app. t, J = 7, 12H, $CH_2C\underline{H}_3$). **^{13}C{^{1}H} NMR** (C_6D_6, 126 MHz): δ 213.2 (s, NCN), 156.7 (s, $\underline{C}OCH_2$), 155.5 (s, $\underline{C}OCH_2$), 137.1 (s, Ar{$\underline{C}$N}), 136.4 (s, Ar{$\underline{C}CH_2$}), 134.7 (s, Ar{$\underline{C}CH_2$}), 128.8 (s, Ar), 123.0 (s, Ar),121.5 (s, Ar), 120.1 (s, imid.), 117.8 (s, imid.), 77.1 (s, OCH_2),77.0 (s, OCH_2), 37.8 (s, NCH_3), 31.6 (s, $Ar\underline{C}H_2Ar$), 23.7 (s, $\underline{C}H_2CH_3$), 23.6 (s, $\underline{C}H_2CH_3$), 10.6 (s, $CH_2\underline{C}H_3$), 10.5 (s, $CH_2\underline{C}H_3$).

Deprotonation using $K[N(SiMe_3)_2]$ in C_6D_6:

Prepared *in situ* as described above.

^{1}H NMR (C_6D_6, 400 MHz) δ 7.45 (s, 4H, Ar), 6.77 (d, $^3J_{HH}$ = 1.6, 2H, Imid), 6.70 (d, $^3J_{HH}$ = 7.5, 4H, Ar), 6.58 (t, $^3J_{HH}$ = 7.5, 2H, Ar), 6.21 (d, $^3J_{HH}$ = 1.6, 2H, Imid), 4.52 (d, $^2J_{HH}$ = 13.2, 4H, $ArC\underline{H}_2Ar$), 3.86 (t, $^3J_{HH}$ = 7.6, 4H, OCH_2), 3.75 (t, $^3J_{HH}$ = 7.3, 4H, OCH_2), 3.42 (s, 6H, NCH_3), 3.14 (d, $^2J_{HH}$ = 13.2, 4H, $ArC\underline{H}_2Ar$), 1.82 - 1.97 (m, 8H, $C\underline{H}_2CH_3$), 0.92 (t, $^3J_{HH}$ = 7.4, 6H,$CH_2C\underline{H}_3$). Co-formation of $HN(SiMe_3)_2$ *δ* 0.1 (s, $HN(SiMe_3)_2$). **^{13}C{^{1}H} NMR** (C_6D_6, 101 MHz) δ 215.8 (N$\underline{C}$N), 156.7 ($\underline{C}OCH_2$), 155.4 ($\underline{C}OCH_2$), 137.4 (Ar{$\underline{C}$N}), 136.4 (Ar{$\underline{C}CH_2$}), 134.7 (Ar{$\underline{C}CH_2$}), 128.7 (Ar), 123.0 (Ar), 121.3 (Ar), 120.0 (imid), 117.6 (imid), 77.1 (OCH_2), 77.0 (OCH_2), 37.9 (NCH_3), 31.6 ($Ar\underline{C}H_2Ar$), 23.7 ($\underline{C}H_2CH_3$), 23.6 ($\underline{C}H_2CH_3$), 10.6 ($CH_2\underline{C}H_3$), 10.5 ($CH_2\underline{C}H_3$).

Thione (3)

A solution of **2a.2HI** (495.0 mg, 0.4907 mmol), K_2CO_3 (400.0 mg, 0.894 mmol) and sulfur (40 mg, 1.203 mmol) in ethanol (15 mL) was stirred at 90°C for 16 hours. The solvent was removed *in vacuo* and the resulting white powder extracted with CH_2Cl_2 and layered with pentane. Yield = 58% (231.0 mg, colourless crystals). **^{1}H NMR** (CD_2Cl_2, 400 MHz) δ 6.95 (s, 4H, Ar), 6.69 (d, $^3J_{HH}$ = 7.4 , 4H, Ar), 6.60 (m, 2H, Ar) , 6.57 (d, $^3J_{HH}$ =2.4 , 2H), 6.31 (d, $^3J_{HH}$ = 2.4 , 2H), 4.51 (d, $^2J_{HH}$ = 13.3 , 4H, ArC$\underline{H}_2$Ar), 3.94, (t, $^3J_{HH}$=7.5, 4H, OC$\underline{H}_2$), 3.87 (t, $^3J_{HH}$ =7.5, 4H, OC$\underline{H}_2$), 3.55 (s, 6H, C$\underline{H}_3$N), 3.24 (d, $^2J_{HH}$= 13.4 , 4H, ArC$\underline{H}_2$Ar), 1.99 (m, 8H, C$\underline{H}_2$CH$_3$), 1.02 (m, 12H, CH$_2$C$\underline{H}_3$). **^{13}C{^{1}H} NMR** (CD$_2$Cl$_2$, 101 MHz) δ 163.4 (N$\underline{C}$N), 157.0 ($\underline{C}$OCH$_2$), 156.6 ($\underline{C}$OCH$_2$), 136.4 (Ar{$\underline{C}$CH$_2$}), 135.2 ($\underline{C}$CH$_2$Ar), 132.9 ($\underline{C}$NCH), 128.9 (Ar), 125.5 (Ar), 122.8 (Ar), 118.2 ($\underline{C}$HN), 118.0 ($\underline{C}$HNCH$_3$), 77.7 (OCH$_2$), 77.5 (OCH$_2$), 35.6 (CH$_3$N), 31.4 (Ar$\underline{C}$H$_2$Ar), 23.9 ($\underline{C}$H$_2$CH$_3$), 23.8 ($\underline{C}$H$_2$CH$_3$), 10.7 (CH$_2\underline{C}$H$_3$), 10.6 (CH$_2\underline{C}$H$_3$). **ESI-MS** (CH$_3$CN, 180°C, 4 kV) Positive ion: 817.3818 *m/z* [MH]$^+$ (calcd. 817.3816 *m/z*). **Anal.** Calcd. For $C_{48}H_{56}N_4O_4S_2$ (MW 816.37 g mol^{-1}) (calc. C; 70.55, H; 6.91,N; 6.86) Found: C,70.69; H,6.74; N,7.71.

2.4.2 Crystallography

Structure determinations were carried out by Dr. A. B. Chaplin. Relevant crystallographic data are given in **Table 2.3**. Data were collected on an Oxford Diffraction Gemini Ruby CCD diffractometer using graphite monochromated CuKα radiation and a low-temperature device. Data were collected and reduced using CrysAlisPro. All non-hydrogen atoms were refined anisotropically using SHELXL,[41] through the Olex2 interface.

Table 2.3: Crystallographic data for **1b·2HCl**, **2a·2HI** and **3**

	1b.2HCl	**2a.2HI**	**3**
CCDC / ID	**001abc12**	1448987	**0112abc14**
Figure	**Figure 2.2**	**Figure 2.5**	**Figure**
Formula	$C_{75}H_{100}Cl_8N_4O_4$	$C_{51}H_{64}Cl_6I_2N_4O_4$	$C_{48}H_{56}N_4O_4S_2$
M	1405.18	1263.56	817.08
Crystal System	Orthorhombic	monoclinic	tetragonal
Space group	$P2_12_12_1$	$P2_1/c$	$I4_1/acd$
Radiation	CuKα (λ = 1.54184)	CuKα (λ = 1.54184)	CuKα (λ = 1.54178)
T [K]	100(2)	150(2)	150(2)
a [Å]	16.8495(6)	24.1609(13)	30.2825(9)
b [Å]	18.0909(7)	32.4937(10)	30.2825(9)
c [Å]	25.3132(14)	16.4506(4)	20.5618(5)
α[deg]	90	90	90
β [deg]	90	101.091(4)	90
γ [deg]	90	90	90
V [Å^3]	7716.0(6)	12673.8(9)	18855.8(12)
Z [*Z'*]	4	8	16
Density [gcm^{-3}]	1.210	1.324	1.151
μ (mm^{-1})	3.040	10.439	1.375
θ range [deg]	12.712 to 79.934	12.712 to 133.202	12.798 to 120.022
Reflns collected	8499	77500	40099
R_{int}	0.0682	0.0837	0.0946
Completeness	90.3%	99.8%	99.8
No. of data/restr/param	4214/1222/777	22354/1339/1265	3497/0/265
R_1 [$I > 2\sigma(I)$]	0.1523	0.0843	0.1099
wR_2 [all data]	0.4269	0.2691	0.3304
GoF	1.660	0.951	1.261
Largest diff. pk and hole [eÅ^{-3}]	0.95/-0.47	1.55/-0.79	0.99/-0.33
Flack (*x*)	0.05(3)	-	-

2.5 References

1. A. J. Arduengo, R. L. Harlow and M. Kline, *J. Am. Chem. Soc.*, 1991, **113**, 361-363.

2. A. J. Arduengo Iii, J. R. Goerlich, R. Krafczyk and W. J. Marshall, *Angew. Chem. Int. Ed.*, 1998, **37**, 1963-1965.

3. M. C. Jahnke and F. Ekkehardt Hahn, in *N-Heterocyclic Carbenes: From Laboratory Curiosities to Efficient Synthetic Tools*, The Royal Society of Chemistry, 2011, pp. 1-41.

4. B. Bildstein, M. Malaun, H. Kopacka, K. Wurst, M. Mitterböck, K.-H. Ongania, G. Opromolla and P. Zanello, *Organometallics*, 1999, **18**, 4325-4336.

5. B. Bildstein, M. Malaun, H. Kopacka, K.-H. Ongania and K. Wurst, *J. Organomet. Chem.*, 1999, **572**, 177-187.

6. I. Dinarès, C. G. Miguel, N. Mesquida and E. Alcalde, *J. Org. Chem.*, 2008, **74**, 482–485.

7. E. K. Bullough, C. A. Kilner, M. A. Little and C. E. Willans, *Org. Biomol. Chem.*, 2012, **10**, 2824-2829.

8. B. K. M. Chan, N. Chang and M. R. Grimmett, *Aust. J. Chem.*, 1977, **30**, 2005-2013.

9. A. J. Arduengo Iii, R. Krafczyk, R. Schmutzler, H. A. Craig, J. R. Goerlich, W. J. Marshall and M. Unverzagt, *Tetrahedron*, 1999, **55**, 14523-14534.

10. A. W. Waltman and R. H. Grubbs, *Organometallics*, 2004, **23**, 3105-3107.

11. A. Paczal, A. C. Bényei and A. Kotschy, *J. Org. Chem.*, 2006, **71**, 5969-5979.

12. M. B. Dinger, P. Nieczypor and J. C. Mol, *Organometallics*, 2003, **22**, 5291-5296.

13. L. C. Benhamou, E. Lavigne,G.Bellemin-Laponnaz,S, César,V., *Chem. Rev.*, 2011, **111**, 2705–2733.

14. E. A. B. Kantchev and J. Y. Ying, *Organometallics*, 2009, **28**, 289-299.

15. N. Kuhn and T. Kratz, *Synthesis*, 1993, 561-562.

16. D. Kremzow, G. Seidel, C. W. Lehmann and A. Fürstner, *Chem. Eur. J.*, 2005, **11**, 1833-1853.

17. V. A. Petrov, W. Marshall and R. Dooley, *J. Fluorine Chem.*, 2014, **167**, 159-165.

18. J. Huang, H.-J. Schanz, E. D. Stevens, S. P. Nolan, K. B. Capps, A. Bauer and C. D. Hoff, *Inorg. Chem.*, 2000, **39**, 1042-1045.

19. G. E. Tyson, K. Tokmic, C. S. Oian, D. Rabinovich, H. U. Valle, T. K. Hollis, J. T. Kelly, K. A. Cuellar, L. McNamara, N. I. Hammer, C. E. Webster, A. G. Oliver and M. Zhang, *Dalton Trans.*, 2015, **44**, 14475-14482.

20. I. Dinarès, C. Garcia de Miguel, N. Mesquida and E. Alcalde, *J. Org. Chem.*, 2008, **74**, 482-485.

21. T. Fahlbusch, M. Frank, J. Schatz and H. Schmaderer, *Eur. J. Inorg. Chem.*, 2006, 1899-1903.

22. W. Willem Verboom, A. Alex Durie, R. J. M. Egberink, Z. Asfari and D. N. Reinhoudt, *J. Org. Chem.*, 1992, **57**, 1313-1316.

23. E. Kelderman, W. Verboom, J. F. J. Engbersen, D. N. Reinhoudt, G. J. T. Heesink, N. F. van Hulst, L. Derhaeg and A. Persoons, *Angew. Chem. Int. Ed.*, 1992, **31**, 1075-1077.

24. D. M. Rudkevich, W. Verboom and D. N. Reinhoudt, *J. Org. Chem.*, 1994, **59**, 3683-3686.

25. G. Grieco, O. Blacque and H. Berke, *Beilstein J. Org. Chem.* 2015, **11**, 1656-1666.

26. M. O. Vysotsky, V. Böhmer, F. Würthner, C.-C. You and K. Rissanen, *Org. Lett.*, 2002, **4**, 2901-2904.

27. C. D. Gutsche and L.-G. Lin, *Tetrahedron*, 1986, **42**, 1633-1640.

28. J.-O. Dalbavie, J.-B. Regnouf-de-Vains, R. Lamartine, S. Lecocq and M. Perrin, *Eur. J. Inorg. Chem.*, 2000, 683-691.

29. S. Manna, S. Maity, S. Rana, S. Agasti and D. Maiti, *Org. Lett.*, 2012, **14**, 1736-1739.

30. A. Arduini, A. Pochini, S. Reverberi, R. Ungaro, G. D. Anreetti and F. Ugozzoli, *Tetrahedron*, 1986, **42**, 2089-2100.

31. A. Dondoni , C. Ghiglione, A. Marra and M. Scoponi, *Macromol. Chem. Phys*, 1999, **200**, 77-86.

32. C. D. Gutsche and P. F. Pagoria, *J. Org. Chem*, 1985, **50**, 5795–5802.

33. M. Larsen and M. Jørgensen, *J. Org. Chem*, 1996, **61**, 6651-6655.

34. X. Fang, B. L. Scott, J. G. Watkin, C. A. G. Carter and G. J. Kubas, *Inorg. Chim. Acta*, 2001, **317**, 276-281.

35. D. J. Williams, D. Vanderveer, R. L. Jones and D. S. Menaldino, *Inorg. Chim. Acta*, 1989, **165**, 173-178.

36. C. A. Tolman, *Chem. Rev.*, 1977, **77**, 313-348.

37. D. G. Gusev, *Organometallics*, 2009, **28**, 6458-6461.

38. H. Clavier and S. P. Nolan, *Chem. Commun.*, 2010, **46**, 841-861.

39. M. Movassaghi and M. A. Schmidt, *Org. Lett.*, 2005, **7**, 2453-2456.

40. E. A. Giner, A. Santiago, M. Gómez-Gallego, C. Ramírez de Arellano, R. C. Poulten, M. K. Whittlesey and M. A. Sierra, *Inorg. Chem.*, 2015, **54**, 5450-5461.

41. G. M. Sheldrick, *Acta Cryst.*, 2008, **A64**, 112-122.

3.0 Coordination chemistry of NHC pro-ligand (2a·2HI)

Overview

This chapter presents the coordination chemistry of the 1,3-bis(imidazolium)calix[4]arene pro-ligand **2a.2HI** with rhodium(I) precursors $[Rh(COD)Cl]_2$ and $[Rh(CO)_2Cl]_2$. *In situ* generation of the free carbene and reaction with Rh(I) precursors results in the formation of neutral bimetallic complexes, whereas transmetallation from an isolated silver transfer agent **6a** yields unusual μ^2-Cl bridged dinuclear complexes (**7a** and **8a**). The structures of the bimetallic products are supported by the synthesis and characterisation of model complexes bearing the monodentate **I^{i}Pr$_2$Me$_2$** ligand. This comparison provides a platform for understanding the influence of the calix[4]arene backbone on the binding properties and reactivity of the NHC moieties (*c.f.* section 2.2.4).

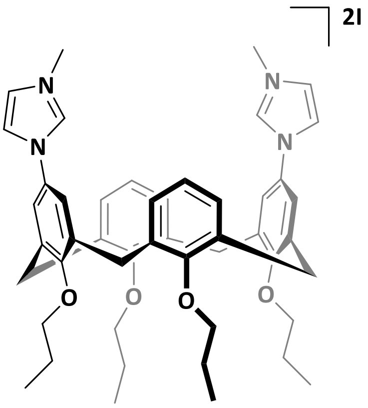

2a.2HI

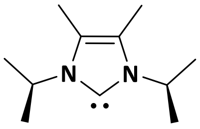

I^{i}Pr$_2$Me$_2$

3.1 Introduction

3.1.1 Complexes of NHC Ligands

3.1.1.1 Deprotonation of azolium salts

While many methods for the preparation of NHC complexes have been reported, the most common proceed *via* deprotonation of azolium salts at the most acidic C2 position. These and other notable synthetic routes for the formation of NHC complexes are outlined in **Scheme 3.1**.[1]

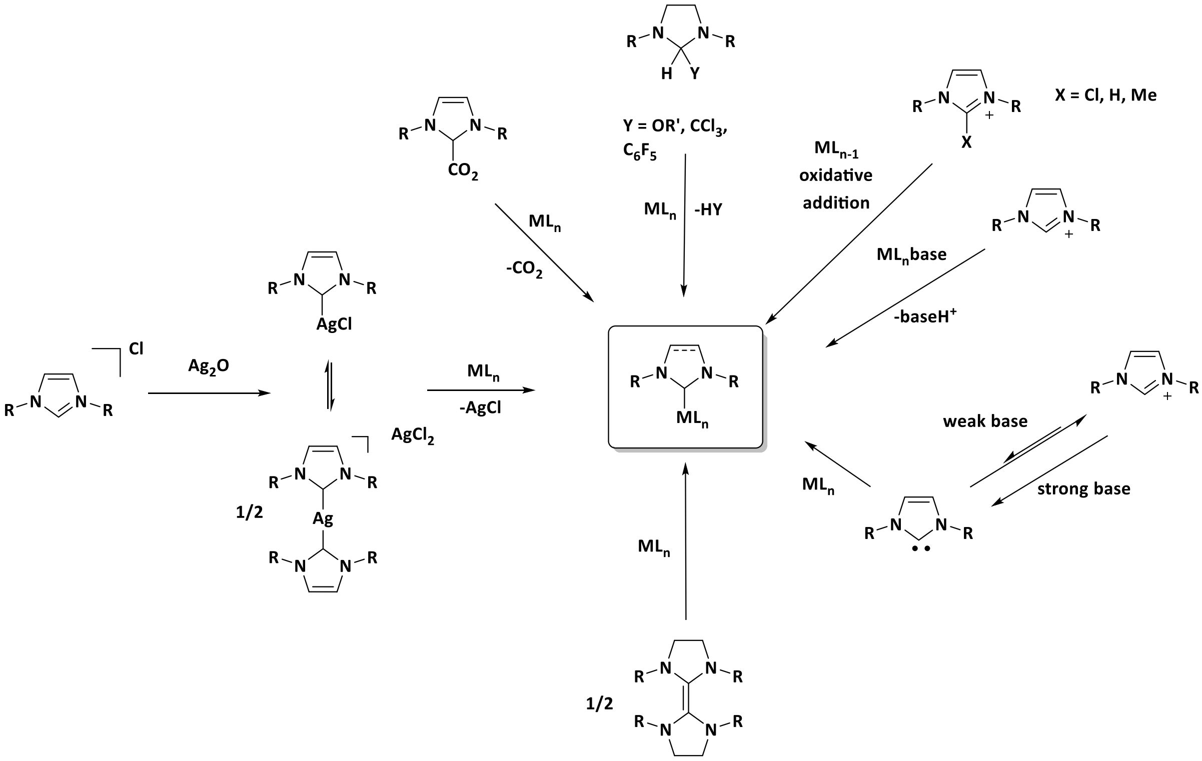

Scheme 3.1: Common synthetic routes for the formation of NHC complexes

Isolable free carbenes have been used to substitute relatively labile ligands such as THF, tmeda, py on monometallic precursors or fragment bimetallic metal precursors bridged by halides.[1] *In situ* deprotonation of azolium salts followed by addition of metal precursors is a desirable alternative to the isolation of the free carbene as this route avoids the handling of potentially air and moisture sensitive carbenes.

In cases where the use of a strong base may result in deprotonation at multiple positions, weaker bases such as Cs_2CO_3 may be used *in situ*.[2-5] Although the addition of a weak base to an azolium salt is unlikely to result in the formation of a high concentration of free carbene, metallation of these species *in situ* has been shown to proceed with good yields. This success has been attributed to thermodynamically favourable formation of the resulting NHC complexes.[4, 6]

Another well-established synthetic route for the formation of NHC complexes is by the use of metal precursors containing basic ligands such as acetate, alkoxides or hyrides. Wanzlick and Öfele used this method in the synthesis of the first imidazolylidene complexes in the late 1960s, using $Hg(OAc)_2$ and $[CrH(CO)_5]^-$.[7, 8]

3.1.1.2 Transmetallation reactions

One of the most effective methods for the formation of late transition metal NHC complexes is by transmetallation from complexes containing a weak metal-carbene bond (**Scheme 3.2**). These so-called carbene transfer agents can be isolated or generated *in situ*. The use of transfer agents is often favoured in order to avoid unwanted reactions resulting from the use of strong bases and storage of unstable free carbenes.

Silver NHC complexes are the most common transfer agents and are typically formed by reaction between imidizolium salts and Ag_2O.[1, 4, 9] These complexes can be difficult to handle in some cases due to their instability in light.[10-13] Previously reported products obtained in this manner include Au, Cu, Ni, Pd, Rh, Ir and Ru complexes.[14-17] Typically *bis*-NHC_2 complexes of Ag(I) adopt a linear conformation with $\underline{Ag}$-N$\underline{C}$N bond lengths of 2.05-2.15 Å and N$\underline{C}$N-$\underline{Ag}$-N$\underline{C}$N bond angles of 170-180°. ^{13}C carbene resonances are typically observed between δ 170-180, and $^1J_{AgC}$ coupling to both spin active, ^{107}Ag and ^{109}Ag isotopes can be observed (both spin = ½): coupling constants range from 180 to 234 Hz and 204 to 270 Hz, respectively.[9] Ag-carbene signals have not been observed for some complexes, this is speculated to be due to dynamic behaviour on the NMR timescale.[9] Imidazolinylidenes have been observed to be relatively inert to transmetallation compared to their unsaturated counterparts. This is thought to be a consequence of the relatively strong Ag-C bonds, which are not readily cleaved.

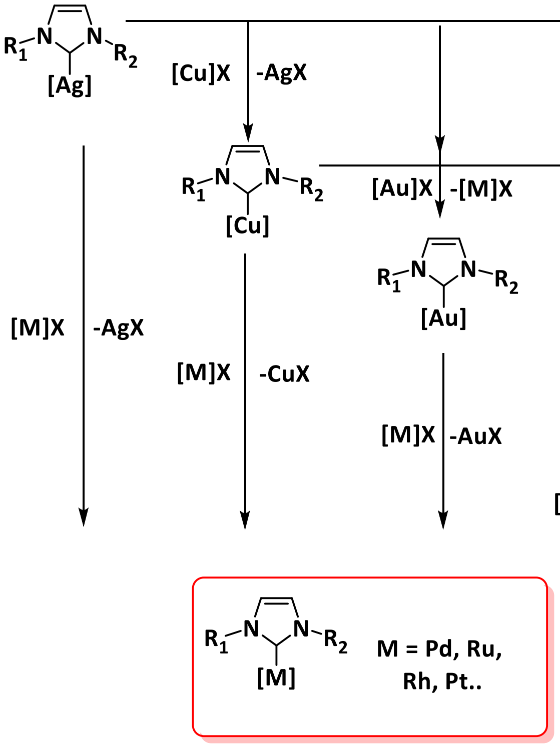

Scheme 3.2: *Transmetallation reactions of carbene transfer agents*

Although less common, copper(I), gold(I), nickel(I) and zirconium(IV)-NHC complexes can also be used as transfer agents (**Scheme 3.2**).[13, 18-21] Copper complexes can result in cleaner formation of transition metal complexes and are more cost effective than the corresponding silver complexes (Cu_2O £114/25 g *cf.* Ag_2O £217/25 g, Sigma Aldrich 20/06/2016). Copper complexes are most commonly synthesised from the corresponding free carbene and therefore suffer from the issues described above, however, they can also be prepared from Cu_2O in a method analogous to that described for Ag complexes, or by transmetallation from isolated Ag complexes.[18, 22] Transmetallation from Au(I) complexes is rare and requires the use of PPh_3 and an oxygen free atmosphere.[4, 18] The relative strength of NHC-M bonds decrease in order Au>Cu>Ag, and indeed Cu and Ag-NHC complexes have been used in the formation of Au-NHC complexes.[19, 23] Nickel NHC-complexes can be formed by transmetallation from silver or copper complexes or by reaction of imidazolium salts with Raney Nickel powder.[13, 17, 24]

3.1.1.3 Other routes

Non-bulky imidazolinylidenes readily dimerize to form enetetramines. These dimers can be used as NHC precursors and a range of mono-, bis-, tris- and tetrakiscarbene complexes have been prepared in this way.[25, 26]

As the isolation of a stable free carbene is not always viable, the reversible formation of NHC adducts of HY (Y = OR', CCl_3, C_6F_5) or CO_2 can be exploited, these compounds are often referred to as "masked carbenes". Oxidative addition of C2-X bonds (X = Me, H or halogen) to low valent transition metal complexes has been established since the 1970s as an operable route to NHC-M-X complexes. The majority of examples involve group 10 M(0) complexes, however, examples including Ir also exist.[27, 28]

3.1.2 Rhodium complexes of NHC ligands

A wide range of NHC complexes have been reported over the last 20 years and their synthesis, stability and catalytic applications are well reported.[29-32] This introduction does not attempt to cover all of this vast quantity of work, but instead provide a brief overview to give an impression of known monodentate and polydentate Rh and Ir-NHC complexes.

3.1.2.1 Monodentate NHC ligands

Monodentate NHC ligands have been used in a wide range of complexes, including bulky and fused ring structures which have been used to form low valent complexes featuring, agostic interactions or which undergo cyclometallation (**Scheme 3.3**).

Raubenheimer *et al*. prepared a series of cationic and neutral Rh-NHC complexes by addition of isolated carbenes to $[Rh(COD)Cl]_2$ (**Scheme 3.3**, **A89** to **A92**).[33] Use of an excess of $[Rh(COD)Cl]_2$ resulted in the formation of neutral mono-NHC chloride complexe **A89**, whereas addition of half an equivalent resulted in the formation of cationic bis-carbene complexes **A91**. Carbonyl species **A90** and **A92** were readily prepared by substitution of the COD by bubbling with CO and removal of free COD by pentane washing. Complexes **A91** and **A92** were tested for their activity in the catalytic hydroformylation of 1-hexene.

Chaplin *et al.* have recently investigated a series of Rh and Ir complexes based on the conformationally rigid $IBioxMe_4$ ligand first prepared by Glorius (**Scheme 3.3**, **A93** to **A100**).[34-37] Formation of mono-, bis- and tris- functionalised Rh and Ir complexes were described.[34] The rigid structure of the NHC ligand has enabled the formation of formally 14 valence electron rhodium(I) complex (**Scheme 3.3**, **A98**). The equivelent iridium(I) complex activates the C-H bonds of fluoroarenes resulting in the formation of 16 valance electron iridium(III) species.[35] Nolans' double C-H activated *tert*butyl NHC Rhodium complexes **A101** to **A103** are also of particular interest due to their low coordination numbers and were formed by reaction of the I^tBu ligand with a chloride bridged Rh(I)-olefin dimer (**Scheme 3.3**).[38]

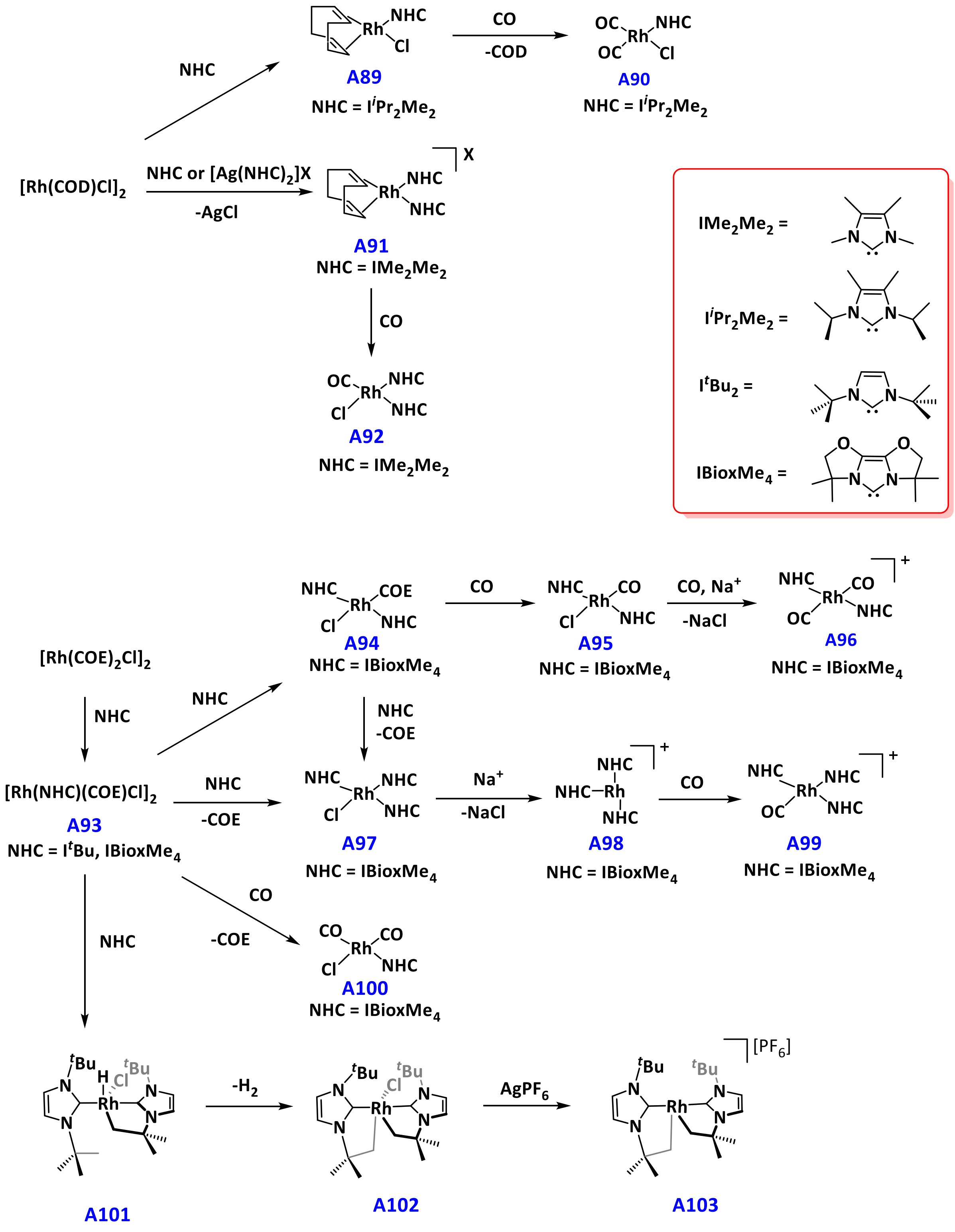

Scheme 3.3: Preparation of selected Rh-NHC complexes

Several groups have generated mixed NHC-phosphine complexes, for example Douglas *et al.* have studied the reaction of I^{i}Pr$_2$Me$_2$ with [HRh(PPh$_3$)$_4$], which results in the formation of a mixture of mono and bis-NHC complexes (**Scheme 3.4**).[39] By contrast reaction of $[HRh(CO)(PPh_3)_3]$ with **$I^{i}Pr_2Me_2$** resulted in a mixture of *cis* and *trans* bis-NHCcomplexes (**A108** and **A109**) as well as the formation of an unsymmetrical μ-CO bridged dimer **A110** (**Scheme 3.4**).

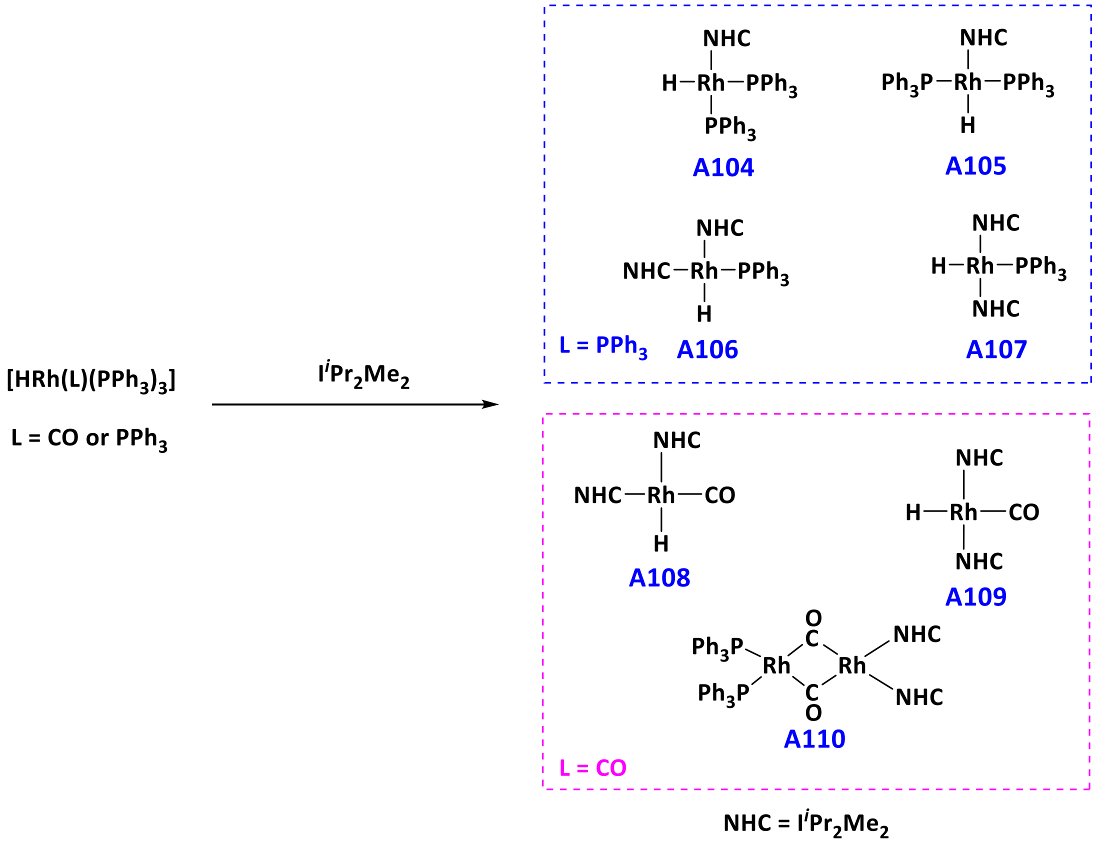

Scheme 3.4: Synthesis of mixed NHC-Phosphine complexes reported by Douglas

3.1.2.2 Multidentate NHC ligands

Multidentate NHC ligands have been designed to adopt pincer, chain, ring and cage-based structures, which have been used to enhance catalytic selectivity, for stabilisation of low coordinate species and in the preparation of conjugated organometallic polymers with desirable electronic and mechanical properties.[35, 40, 41] Pincer complexes are used extensively in catalysis due to their high stability under a range of catalytic conditions.[42]

An excellent demonstration of the effect of co-ordination routes on complex geometry is the reactivity of the bis-NHC pincer ligand **A111**, reported by Hollis and co-workers (**Scheme 3.5**).[43] In this example a monometallic pincer type product was easily synthesised by transmetallation using a Zr(IV) transfer agent, providing a template for the pincer architecture (**A112**). Addition of the same rhodium based precursor to the free carbene generated *in situ* resulted in the direct formation of a bimetallic product **A114**.

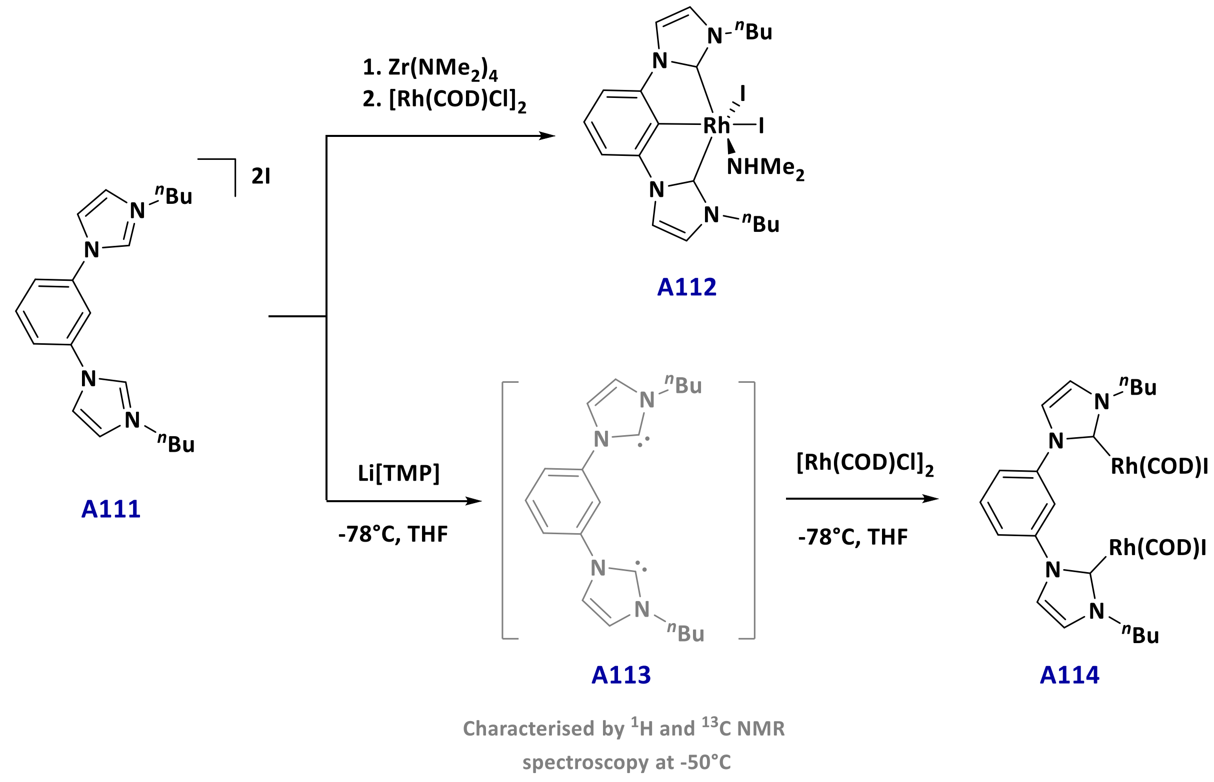

Scheme 3.5: Synthesis of pincer and bimetallic Rh NHC complexes reported by Hollis and co-workers

Veige and coworkers have reported the synthesis of rhodium(I) complexes based upon a chiral bis-NHC pro-ligand **A115** (**Scheme 3.6**). Here they found that presence of an ^{i}Pr group is sufficiently bulky to prevent the formation of an enetetramine structure, as evidenced by the N$\underline{C}$N resonances observed at δ 226, **A118** *cf.* 126, **A116**.[44, 45] Reaction of the enetetramine with one equivalent of $[Rh(NBD)_2][BF_4]$ under mild conditions resulted yielded the C_1 symmetric mononuclear complex **A117**. NBD was displaced by heating under a pressure of CO (100 bar) to yield *cis*-carbonyl species **A120**. Reaction of **A116** or **A118** with dinuclear $[Rh(COD)Cl]_2$ yielded the C_2 symmetric products **A119**. Complexes **A117, A119** and **A120** were found to be active in the hydroformylation of styrene.

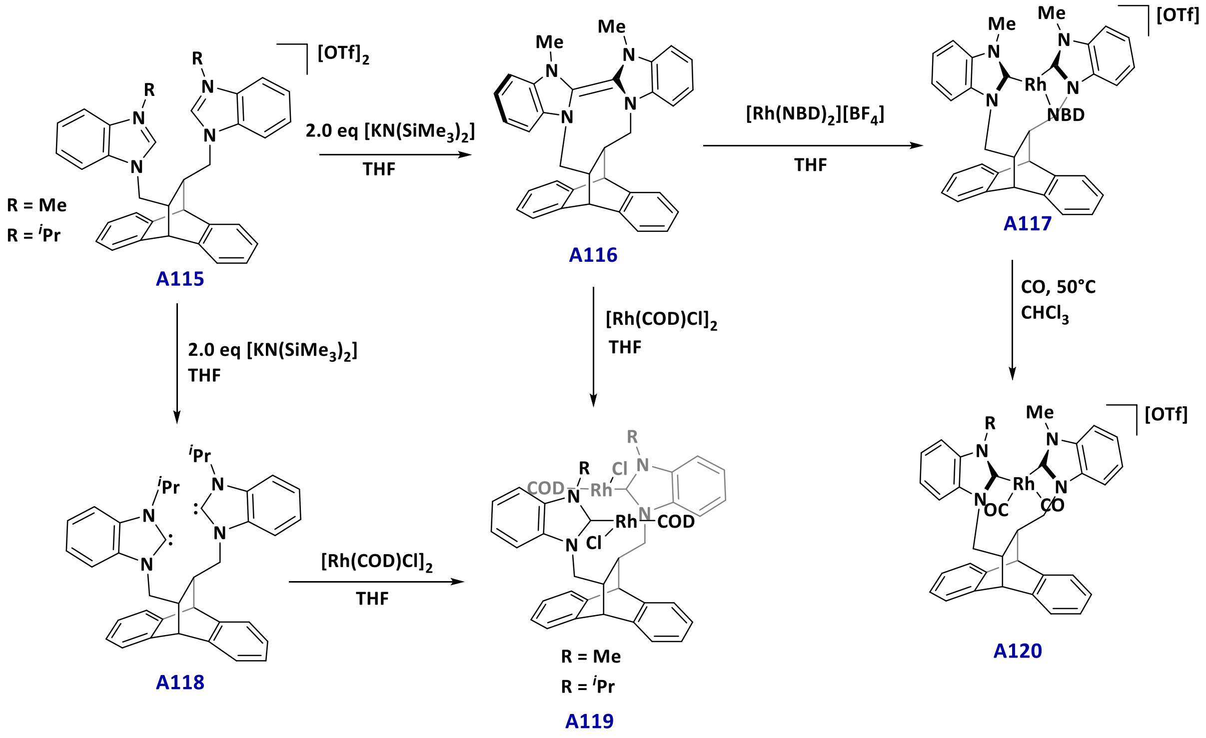

Scheme 3.6: Synthesis of chiral Rh(I) complexes

3.2 Results and discussion

3.2.1 Coordination of free carbene 2a

Based on proceeding work (Chapter 2) the free carbene **2a** was prepared *in situ* by deprotonation of **2a.2HI** with K[O^{t}Bu] in THF and reacted with rhodium(I) dimers $[Rh(COD)Cl]_2$ and $[Rh(CO)_2Cl]_2$ in the presence of excess KI, to avoid formation of mixed halide products (**Scheme 3.7**). In the absence of excess KI mixed chloro and iodide species were observed. Halide exchange of this kind has been observed by Hollis and co-workers during the synthesis of bimetallic NHC complexes (**Scheme 3.5**).[43]

Use of 1 equivalent of $[Rh(L_2)Cl]_2$ (L_2 = COD or $(CO)_2$) per **2a** resulted in the isolation of dinuclear complexes **4a** and **5a**. Reaction with 0.5 equivalents of dimer also resulted in the formation of these dimeric species, but alongside a significant quantity of **2a.2HI**, formed by protonation of the carbene produced during work-up, as confirmed by the presence of a high frequency NC$\underline{H}$N resonance at δ 8.81 (CD_2Cl_2) in the ^{1}H NMR spectra of the crude reaction mixture.

Complex **4a** was purified over by column chromatography using a short alumina plug and isolated in good yield (53 % *cf.* similar bimetallic pincer-type products **A114** isolated in 61 % yields).[43] However, **5a** isolated by the same method was obtained in a relatively low yield (17%). An alternative synthesis of **5a** was therefore developed *via* displacement of the COD ligand by CO (1 atm) in CH_2Cl_2. This reaction proved to be quantitative as determined by ^{1}H NMR spectroscopy leading to an improved isolated yield of 37% (slightly improved yield of 20 % over two steps from the starting **2a.2HI** pro-ligand) with displaced COD removed by successive washings with pentane. The low isolated yield of **5a** from **4a** is attributed to non-negligable solubility of **5a** in pentane.

Model complex **4b** was readily synthesised in an analogous fashion by reaction of **I^{i}Pr$_2$Me$_2$** with $[Rh(COD)Cl]_2$ and KI in THF. Subsequent purification over silica gave **4b** in a 31% isolated yield. Model complex **5b** was then easily formed by displacement of the COD ligand in **4b** with CO (1 atm) and subsequent pentane washing and obtained in a good yield (59 %). The structure of complexes **4** and **5** were fully corroborated by ^{1}H, ^{13}C NMR and IR spectroscopy (for **5** *vide infra*) and microanalysis. NCN signals for **4a** and **4b** showed good agreement to those observed by Hollis and co-corkers for **A114**, δ 180.4 (**4a**), δ178.4 (**4b**) and 182.0 (**A114**).[43]

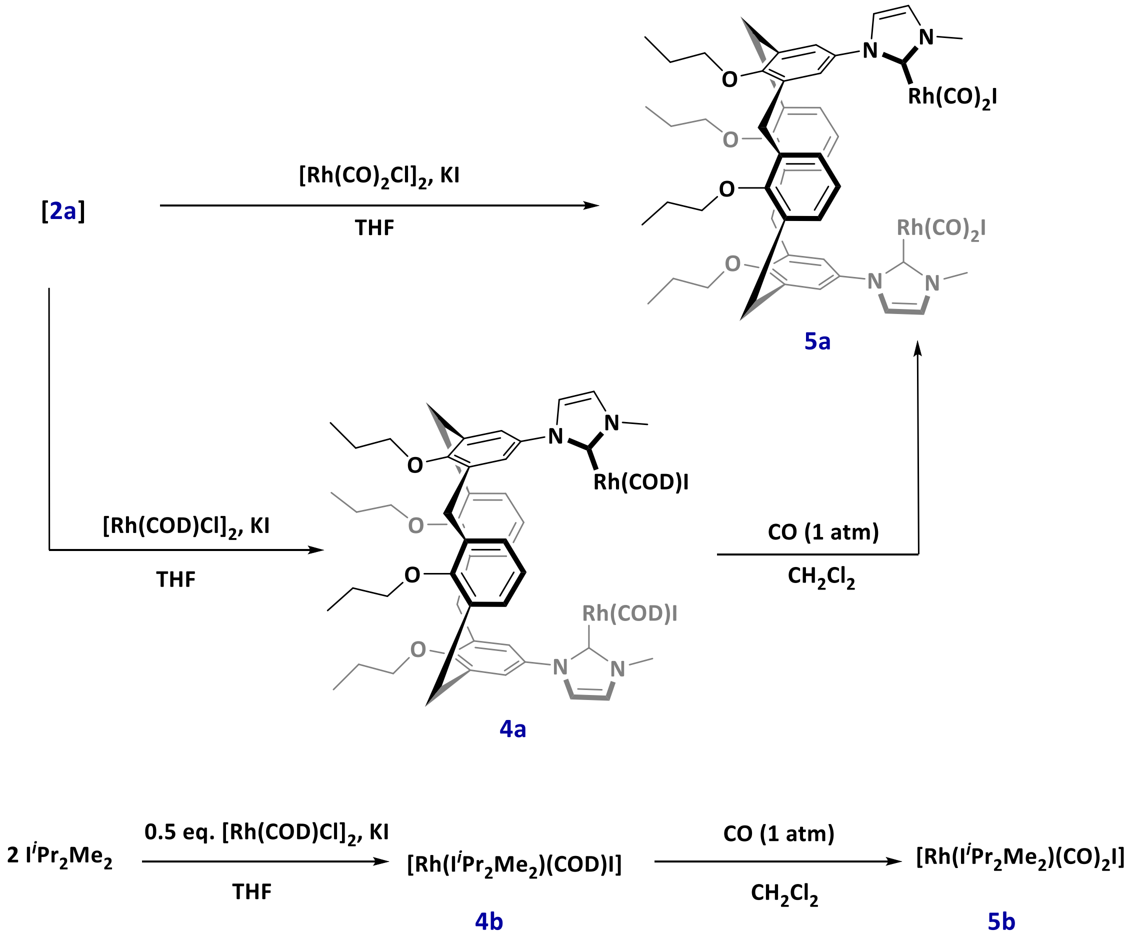

Scheme 3.7: Reactions of **2a** and **I^{i}Pr$_2$Me$_2$** with rhodium(I) dimers

The structures of new complexes **4a** and **4b** were determined in the solid state by X-ray crystallography (**Figure 3.1**). In comparison to **2a.2HI**, the calix[4]arene scaffold has undergone a conformational inversion in **4a**, whereby the previously distant imidazolium groups of the pro-ligand are drawn together in an antiparallel arrangement, apparently driven by π-stacking interactions between the imidazolyidene rings Cnt - Cnt = 3.608(5) Å, giving a CPR value of 0.4317(5) and *pseudo* C_2 symmetry in the solid state.

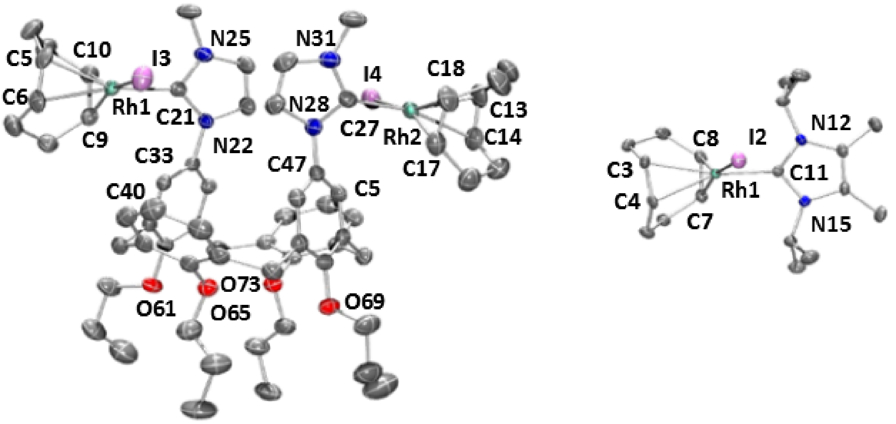

Figure 3.1: Solid state structures of **4a** and **4b** Thermal ellipsoids drawn at the 50% probability level. Hydrogen atoms, anions and minor disordered components are omitted for clarity. Selected bond lengths (Å)and angles (°):**4a**: Rh1–I3, 2.6905(3); Rh1–Cnt(C5,C6), 2.089(3); Rh1–Cnt(C9,C10), 2.001(3); Rh1–C21, 2.021(3); Rh2–I4, 2.6934(3); Rh2–Cnt(C13,C14), 2.098(3); Rh1–Cnt(C17,C18), 1.990(4); Rh2–C27, 2.024(3); Rh1···Rh2, 8.5698(3); Cnt(C21–N25)–Cnt(C27–N31), 3.608(5); CPR = 0.3609(5) **4b**: Rh1–I2, 2.6729(2); Rh1–Cnt(C3,C4), 2.109(2); Rh1–Cnt(C7,C8), 2.00(3); Rh1–C11, 2.021(3)

^{1}H and ^{13}C{^{1}H} NMR spectra of **4a** both exhibit a single resonance for the methyl moiety at δ 3.85 and 39.1, respectively. Together with the observation of the ArC$\underline{H}_2$Ar ^{1}H resonances as two diastereotopic signals at δ 4.62, 4.50, 3.38, 3.19 ($^2J_{HH}$ ~14 Hz) (**Figure 3.2**), it is apparent that C_2 symmetry is retained in solution. Moreover, the now inequivelent ^{1}H resonances of the imidazolylidene functionalised aryl ring show a large divergence from that observed for the pro-ligand (δ 7.95 and 5.92 *cf.* 6.61 in **2.2HI**). This is assumed to be a consequence of the proximity of the halogen atom $\underline{C}$H···$\underline{I}$ = 4.139(3)/4.295(3) Å.

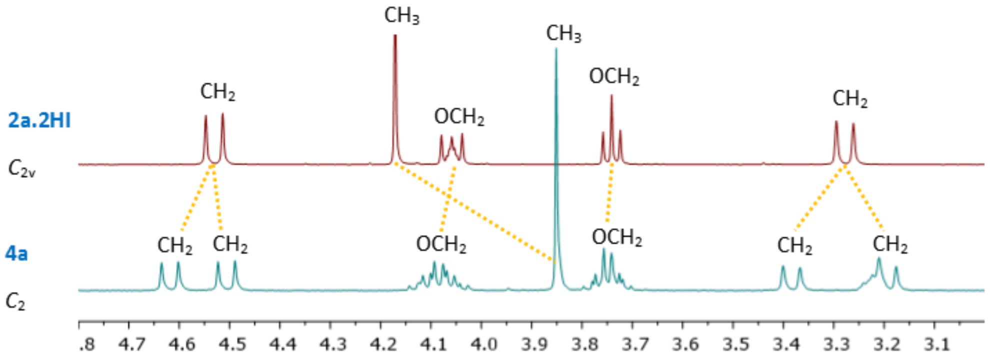

Figure 3.2: ^{1}H NMR spectra of **2a.2HI** and **4a** (CD_2Cl_2, 400 MHz, 298K)

Adoption of square planar geometries, as expected for d^8-metal complexes of this type, is seen in both **4a** and **4b**. The NHC binding is also in good agreement, with Rh-N$\underline{C}$N bond lengths of 2.021(3)/2.024(3) Å and 2.021(3) Å, and CRhI bond angles of 89.8(6)/89.4(9)° and 87.1(4)° for **4a** and **4b**, respectively. ^{13}C NMR data resonances also show good agreement with the carbenes observed at δ 180.4 ($^1J_{RhC}$ = 49 Hz) and δ 178.4 ($^1J_{RhC}$ = 49 Hz) and diene signals at δ 95 ($^1J_{RhC}$ = 7 Hz) and 72 ($^1J_{RhC}$ = 14 Hz) for **4a** and **4b** respectively.

Suitable samples of carbonyl complexes **5a** and **5b** have not yet been grown for structural elucidation by X-ray crystallography, however, solution data suggests that both adopt structures that are similar to **4a** and **4b**. The *cis*-configuration of the carbonyl ligands has been confirmed by the observation of two corresponding bands by IR spectroscopy (ν(CO)): 2071, 2002 (**5a**) and 2072, 1998 cm^{-1} (**5b**)) and two high frequency doublets observed the ^{13}C{^{1}H} NMR spectrum (δ 188.4 ($^1J_{RhC}$ = 54 Hz) and 181.6 ($^1J_{RhC}$ = 78 Hz); (**5a**) 188.7 ($^1J_{RhC}$ ~53 Hz) and 182.7 ($^1J_{RhC}$ = 78 Hz)) (**5b**) The ^{1}H and ^{13}C NMR data of **5a** also shows evidence for C_2 symmetry as observed for the COD analogue. Both **5a** and **5b** show lower frequency ^{13}C carbene resonances and reduction in coupling to ^{103}Rh compared to **4a** and **4b** (e.g. δ 180.4 ($^1J_{RhC}$ ~49 Hz) (**4a**) *cf.* 171.5 ($^1J_{RhC}$ ~44 Hz) (**5a**).

3.2.2 Transmetallation reactions

In order to further investigate the coordination chemistry of pro-ligand **2a.2HI** with rhodium(I) precursors, the silver calix[4]arene transfer agent **6a** was synthesised (**Scheme 3.8**). This was achieved by reaction between **2a.2HI**, Ag_2O and $Na[BAr^F_4]$, in a 1:1:0.99 ratio in CH_2Cl_2 . The resulting product was recrystallised from CH_2Cl_2/pentane to give **6a** as colourless crystals in good yield (73 %). The use of an excess of $Na[BAr^F_4]$ per **2a.2HI** resulted in the formation of a mixture of species, which could be bimetallic or multimetallic species or involve co-ordination of Na^+ to the lower rim O^nPr groups (Chapter 4).[46, 47] Such species are evident by the presence of more than one equivalent of $[BAr^F_4]^-$ per **2a** by ^1H NMR spectroscopy. Addition of a less than one equivalent of $Na[BAr^F_4]$ per **2a.2HI** resulted in the formation of a mixture of products which were difficult to separate. The colourless crystalline **6a** was stored without decomposition in a glovebox under argon with the exclusion of light for several months. For comparison the model **$I^iPr_2Me_2$**-based complex **6b** was synthesised directly from the free carbene, Ag[OTf] and $Na[BAr^F_4]$ (**Scheme 3.8**). This biscarbene complex, bearing instead a tetrafluoroborate anion has been previously described by Abram (**A121**), however, for accurate comparison incorporation of the $[BAr^F_4]^-$ counterion was more desirable.[14] The solid-state structure of both **6a** and **6b** were obtained by X-ray diffraction (**Figure 3.4**).

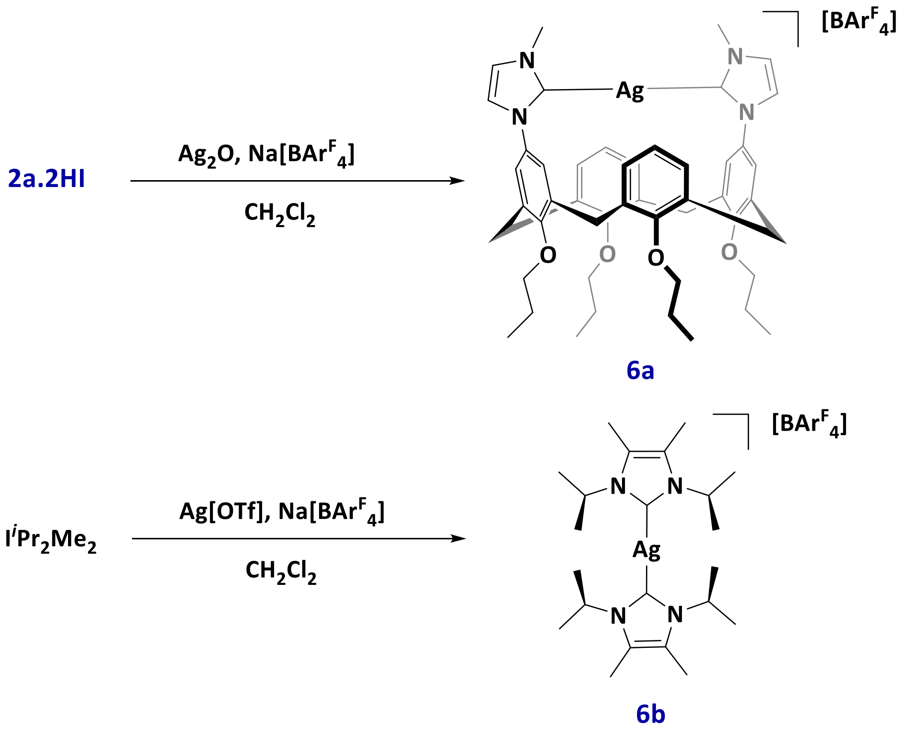

Scheme 3.8: Synthesis of Ag(I) complexes **6a** and **6b**

The structure of silver complex **6a** was fully confirmed by ^1H and ^{13}C NMR spectroscopy, microanalysis and ESI-mass spectrometry, which showed a parent cation signal at 859.3340 *m/z* $[M]^+$ (calcd. 859.3347 *m/z*) with integer mass spacing and excellent agreement with the predicted isotope pattern (**Figure 3.3**).

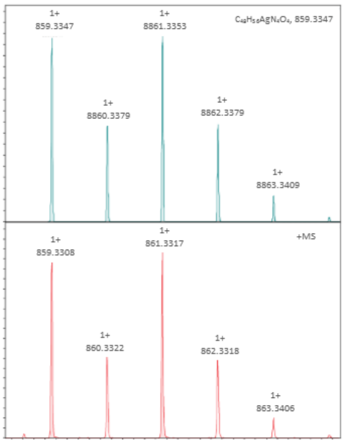

Figure 3.3: ESI-MS of **6a;** observed $[M]^+$ ion (bottom) and predicted pattern (top)

Complex **6a** was characterised in solution by the presence of two coincident doublet carbene ^{13}C resonances centred at δ 180.7, as a result of coupling to ^{107}Ag and ^{109}Ag. The observed coupling constants for Ag^{107} and Ag^{109} of $^{1}J_{CAg}$ = 183 Hz and 211 Hz, respectively, are in good agreement with literature values.[9] However, the equivalent carbene signal could not be determined for **6b**, presumably because it is too broad to be observed.[14, 48] The X-ray structure of **6a** shows a distorted linear geometry about the Ag centre of 170.00(14)° *cf.* 176.81(15)° for **6b**. The deviation from linearity in **6a** is presumably a consequence of the chelating calix[4]arene scaffold. N$\underline{\text{C}}$N-Ag bond lengths of **6a** and **6b** were in good agreement 2.085(4)/2.083(4) Å (**6a**) *cf.* 2.078(11) Å (**6b**). The structure of **6a** shows a near coplanar arrangement of the NHC donors and a puckering of the calix[4]arene scaffold as a result of chelation to the Ag centre, CPR = 0.5708(7). The solid-state structure of **6b** is notable for a significantly more orthogonal orientation of the NHC ligands in comparison to **6a** and **A121**, for example N6–C2–C8–N12 = 3.7(5)°, **6a**; N3–C2–C15–N19 = 77.0(5)°, **6b**; N–C–C–N = 20.6(6)°, **A121**]. These differences are presumably due to crystal packing effects, induced by disparate anion sizes, and enabled through low-energy Ag– NHC bond rotation.

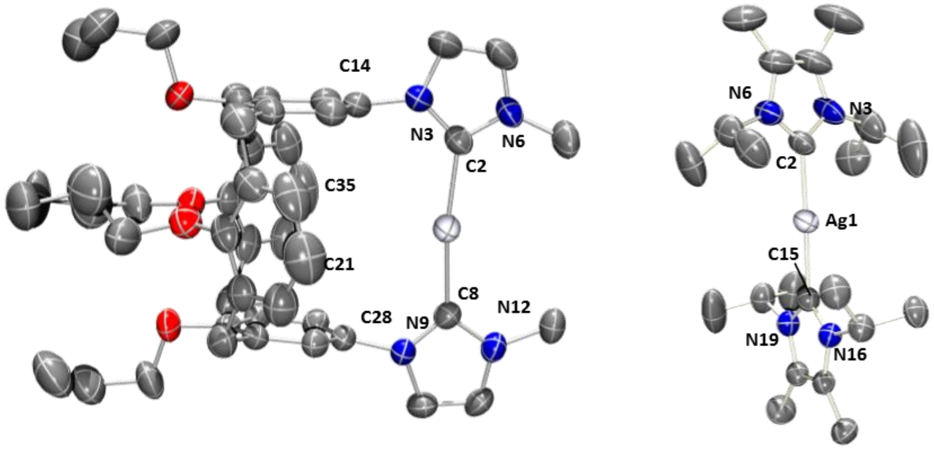

Figure 3.4: Solid state structure of **6a** and **6b**. Thermal ellipsoids drawn at the 30% probability level. Hydrogen atoms, anions and minor disordered components are omitted for clarity. Selected bond lengths (Å) and angles (°) **6a**: Ag1–C2, 2.085(4); Ag1–C8, 2.083(4); C2–Ag1–C8, 171.00(14); **6b**: Ag1–C2, 2.093(4); Ag1–C15, 2.092(4); C2–Ag1–C15, 176.81(15) CPR = 0.5708(7).

Transmetallation reactions of **6a** with one equivalent of rhodium(I) dimers $[Rh(COD)Cl]_2$ and $[Rh(CO)_2Cl]_2$ in 1,2-difluorobenzene resulted in the formation of bimetallic complexes **7a** and **8a** respectively as the only isolable products in moderate yields of 63% and 59% (**Scheme 3.9**). Reaction of **6a** with 0.5 equivalents of the rhodium(I) dimer resulted in the formation of mixtures of **2a.2HI** and **7a** or **8a** in equal measure, as determined by ^{1}H NMR spectroscopy, showing that the bimetallic complexes are formed selectively. These products were difficult to purify due to low stability in solution, but were characterised *in situ* using ^{1}H, ^{13}C NMR and IR spectroscopy, and ESI-MS. A low resolution X-ray structure of **8a** was also collected (**Figure 3.5**). The monocationic character of both species was confirmed by integration of ^{1}H NMR data which confirmed the presence of one equivalent of $[BAr^F{}_4]$ anion per calix[4]arene ligand. Parent cation signals were observed by ESI-MS with integer mass spacing and showed good agreement with calculated values (1209.3986 *m/z* $[M]^+$, calcd. 1209.3973 *m/z* for **7a** and 1105.1680 *m/z* $[M]^+$, calcd. 1105.1891 *m/z* for **8a**).

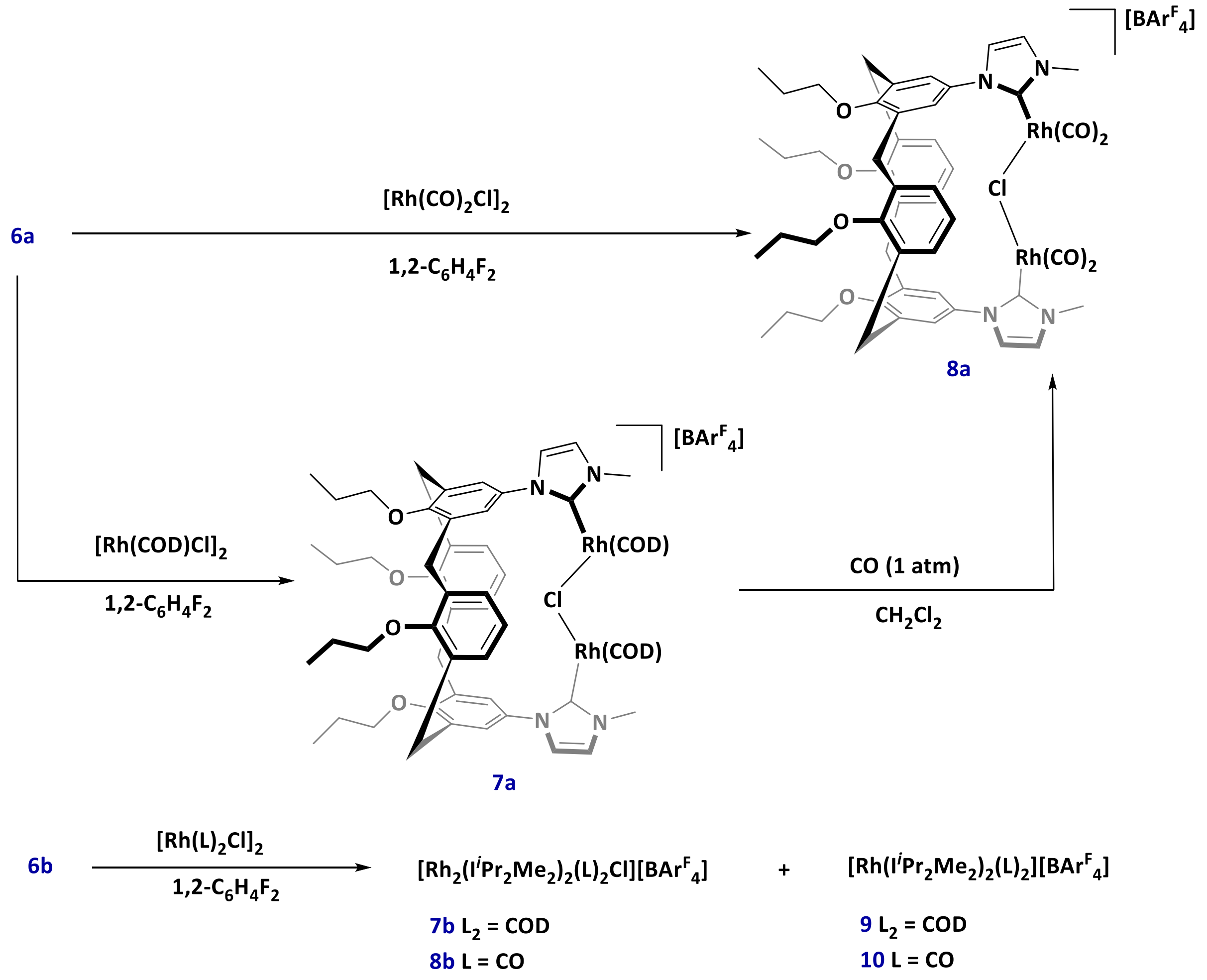

Scheme 3.9: Transmetallation reactions of **6a** and **6b**

The presence of two inequivalent CO ligands can be identified in **8a** from the observation of two ^{13}C resonances at δ 182.7 ($^1J_{RhC}$ = 53 Hz) and 181.0 ($^1J_{RhC}$ = 80 Hz) (1,2-difluorobenzene). Inequivalent COD{CH} signals were observed by ^{13}C NMR spectroscopy at δ 100.3, 96.4, 78.5 and 71.8 for **7a**. This data, alongside the presence of single ^{1}H and ^{13}C resonances for the N-CH_3 group and two sets of diastereotopic $ArC\underline{H}_2Ar$ resonances, indicates the adoption of C_2 symmetry in solution for both **7a** and **8a**. The low quality solid state structure of **8a** (R_1 = 27%) shows *pseudo* C_2 symmetry and pinching of the calix[4]arene scaffold with a CPR = 0.6371(4), a direct consequence of the presence of the μ-Cl bond.

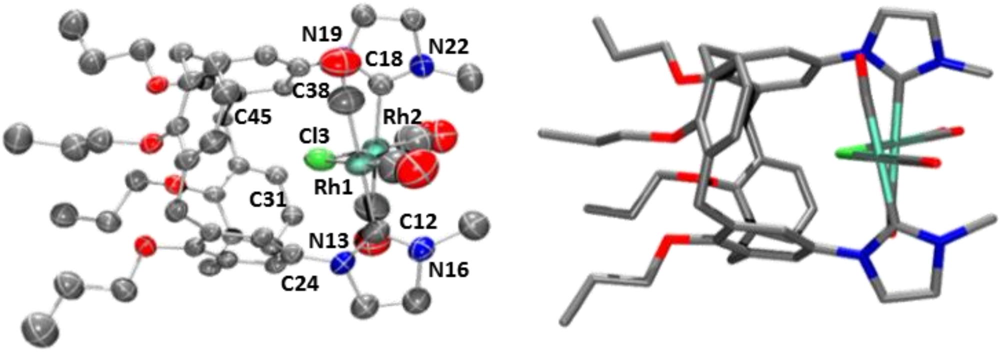

Figure 3.5: Low resolution solid state structure of **8a** in ellipsoid and stick view for clarity. Thermal ellipsoids drawn at the 50% probability level. Hydrogen atoms and anions are omitted for clarity. Selected bond lengths (Å) and angles (°):Rh1–Cl3, 2.353(5); Rh2–Cl3, 2.360(5); Rh1···Rh2, 3.861(3); Rh1–Cl3–Rh2, 110.0(3); CPR = 0.6371(4)

In contrast to the selective transmetallation reactions of **6a**, reactions of **6b** with [Rh(COD)Cl]$_2$ and [Rh(CO)$_2$Cl]$_2$ in 1,2-difluorobenzene resulted in the formation of **7b**/**9** (2:1 ratio) and **8b**/**10** (5:2 ratio) respectively, as determined by ^{1}H NMR spectroscopy (**Scheme 3.9**).

To authenticate the structures of the μ-Cl bridged I^{i}Pr$_2$Me$_2$ complexes **7b** and **8b**, these species were independently synthesised by reactions of known precursors **A89** and **A90**,[33] with 0.5 equivalents of halide extractor Na[BAr$^F{}_4$] in CH$_2$Cl$_2$ (**Scheme 3.10**). Complexes **7b** and **8b** were subsequently isolated as single products in 69% and 66% yield, respectively, and fully characterised by ^{1}H, ^{13}C NMR and IR spectroscopy, ESI-MS, microanalysis and X-ray crystal diffraction (**Figure 3.6**).

Complexes **7b** and **8b** were also used to help verify the structures of the calix[4]arene complexes **7a** and **8a** as their spectroscopic data showed excellent agreement. For instance, the carbene resonances for **7a** and **7b** were observed at δ 176.9 ($^1J_{\mathrm{RhC}}$ = 50 Hz) and 175.6 ($^1J_{\mathrm{RhC}}$ = 50 Hz), and the carbonyl ^{13}C signals and IR bands of **8a** and **8b** located at δ 182.7 ($^1J_{\mathrm{RhC}}$ = 53 Hz), 181.0 ($^1J_{\mathrm{RhC}}$ = 80 Hz) and δ 185.4 ($^1J_{\mathrm{RhC}}$ = 53 Hz), 181.0 ($^1J_{\mathrm{RhC}}$ = 84 Hz) and 2083/2016 and 2090/2019 cm^{-1}, respectively. Conformational differences, associated with the relative orientation of the NHC ligands about the Rh–Cl–Rh bridge, are evident by comparison of the solid-state structures of **8a** (anti) **7b** (syn) and **8b** (anti); ^{1}H and ^{13}C NMR data for **7a** and **8a** are consistent with anti-configurations in solution.

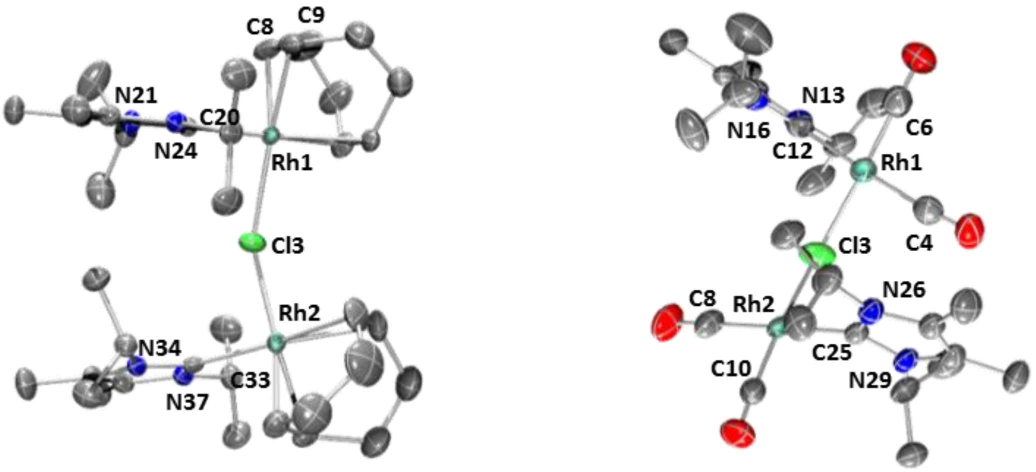

Figure 3.6*:* Solid state structures of **7b** and **8b**. Thermal ellipsoids drawn at the 50% probability level. Hydrogen atoms, anions, minor disordered components and solvent molecules are omitted for clarity. Selected bond lengths (Å)and angles (°):**7b**: Rh1–Cl3, 2.3988(9); Rh1–Cnt(C4,C5), 2.092(5); Rh1–Cnt(C8,C9), 1.974(4); Rh1–C20, 2.025(3); Rh2–Cl3, 2.4067(9); Rh2–Cnt(C12,C13), 2.101(4); Rh2–Cnt(C16,C17), 1.972(4); Rh2–C33, 2.022(3); Rh1–Cl3–Rh2, 144.13(4); **8b**: Rh1–Cl3, 2.4045(9); Rh1–C4, 1.915(4); Rh1–C6, 1.833(4); Rh1–C22, 2.069(3); Rh2–Cl3, 2.3987(9); Rh2–C8, 1.920(4); Rh2–C10, 1.817(4); Rh2–C25, 2.069(3); Rh1–Cl3–Rh2, 122.26(4).

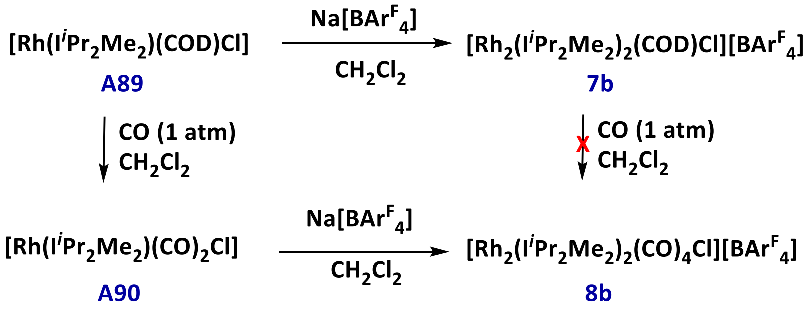

Scheme 3.10: Synthesis of μ-Cl bridged I^{i}Pr$_2$Me$_2$ complexes **6b** and **7b**

Reaction of **7b** with CO (1 atm) resulted in the formation of a mixture of products, including **A90**, in agreement with reactivity observed for IDipp and IMes complexes reported by James *et al.*[33] [49]

bis-(I^{i}Pr$_2$Me$_2$) Complexes **9** and **10**, formed during transmetallation reactions of **6b** with Rh(I) dimers, containing the [BAr$^F_4$] counter anions were independently prepared in 56% and 66% yields, respectively (**Scheme 3.11**). The structures of both compounds were fully characterised by ^{1}H and ^{13}C NMR spectroscopy, IR spectroscopy, ESI-MS, microanalysis and in the solid state by X-ray crystal diffraction (**Figure 3.7**). Complexes **9** and **10** show carbene N$\underline{\text{C}}$N resonances were observed at δ 178.1 ($^1J_{\text{RhC}}$ = 55.8 Hz) and 168.2 ($^1J_{\text{RhC}}$ = 47 Hz), respectively and ESI-MS showed parent ions at 571.3215 *m/z* [M]$^+$ (calcd 571.3242 *m/z*) for **9** and 519.2249 *m/z* [M]$^+$ (calcd 519.2201 *m/z*) for **10**. Additionally the IR spectrum of **10** showed carbonyl bands at 2077 and 2018 cm^{-1} (CH_2Cl_2), supporting the assertion that a *cis* complex was formed. X-ray structures showed the expected square planar binding and confirmed *cis*-binding of the CO ligands (**Figure 3.7**).

$$\text{I}^i\text{Pr}_2\text{Me}_2 \xrightarrow[\text{1,2-C}_6\text{H}_4\text{F}_2]{\substack{\text{0.5 eq. [Rh(COD)Cl]}_2 \\ \text{0.5 eq. Na[BAr}^\text{F}_4]}} \underset{\textbf{9}}{[\text{Rh}(\text{I}^i\text{Pr}_2\text{Me}_2)_2(\text{COD})][\text{BAr}^\text{F}_4]} \xrightarrow{\text{CO}} \underset{\textbf{10}}{cis\text{-}[\text{Rh}(\text{I}^i\text{Pr}_2\text{Me}_2)_2(\text{CO})_2][\text{BAr}^\text{F}_4]}$$

Scheme 3.11: Synthesis of bis(I^{i}Pr$_2$Me$_2$) complexes **9** and **10**

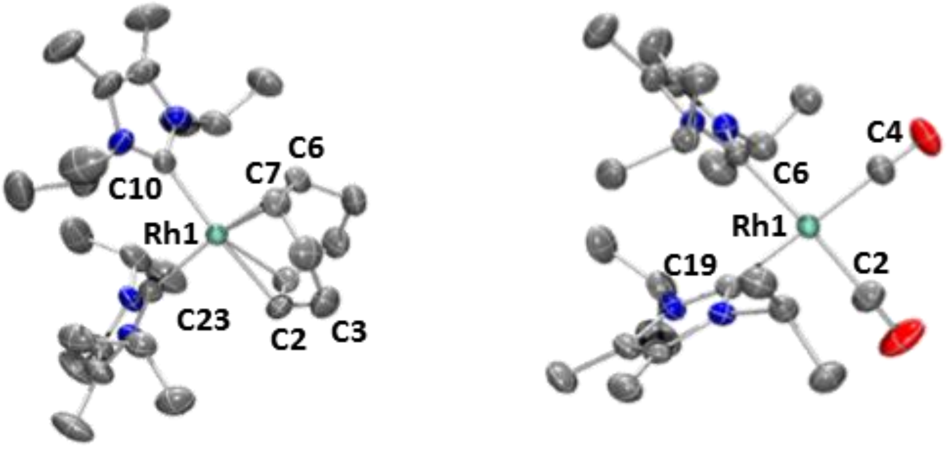

Figure 3.7: Solid state structures of **9** and **10**. Thermal ellipsoids drawn at the 50% probability level. Hydrogen atoms and anions are omitted for clarity. Selected bond lengths (Å) and angles (°): **8**: Rh1–C10, 2.086(3); Rh1—C23, 2.073(3); Rh1–Cnt(C7,C6), 2.07(3); Rh1–Cnt(C2,C3) 2.06(9); **9**: Rh1–C4, 1.89(3); Rh1–C4, 1.893(3); Rh1–C6, 2.09(3); Rh1–C19, 2.08(3).

3.3 Conclusion

A series of neutral and cationic calix[4]arene complexes have been synthesised from the 1,3-bis(imidazolium) functionalised calix[4]arene proligand **2a.2HI** described in Chapter 2, by *in situ* reactions of the free carbene or *via* transmetallation of the isolated monometallic silver(I) transfer agent (**6a**) with rhodium(I) dimers $[Rh(COD)Cl]_2$ and $[Rh(CO)_2Cl]_2$. Both methods resulted in the formation of bimetallic structures, which have been characterised in solution using NMR and IR spectroscopy (CO derivatives), and ESI-MS (cationic complexes). Verification of their structural formulation was aided by excellent agreement with data from simpler and well-defined model complexes containing **I^{i}Pr$_2$Me$_2$**. Several solid-state structures, determined using X-ray diffraction, highlight the flexibility of the calix[4]arene scaffold, which can undergo significant conformational distortion as a result of charge repulsion (**2a.2HI**), π-stacking of the imidazolylidene rings (**4a**), *trans*-coordination to silver (**6a**), or presence of a bridging μ_2-Cl ligand (**8a**).

Comparisons of the transmetallation reactions of **2a** and **I^{i}Pr$_2$Me$_2$**-based demonstrates the selectivity enforced by the presence of the calix[4]arene scaffold.

3.4 Experimental

3.4.1 General Considerations

All manipulations were performed under an atmosphere of argon, using Schlenk and glove box techniques unless otherwise stated. Glassware was oven dried at 150 °C overnight and flamed under vacuum prior to use. Anhydrous CH_2Cl_2, Et_2O, and pentane (<0.005% H_2O) were purchased from ACROS or Aldrich and freeze–pump–thaw degassed three times before being placed under argon. THF was dried over sodium/benzophenone, vacuum distilled, and freeze–pump–thaw degassed three times before being placed under argon. 1,2-$C_6H_4F_2$ was stirred over neutral alumina, filtered, dried over CaH_2, vacuum distilled, and freeze–pump–thaw degassed three times before being placed under argon over 3 Å molecular sieves. CD_2Cl_2 was dried over CaH_2, vacuum distilled, and freeze–pump–thaw degassed three times before being placed under argon. C_6D_6 was dried over Na, vacuum distilled, and freeze–pump–thaw degassed three times before being placed under argon. $[Rh(COD)Cl]_2$, $[Rh(CO)_2Cl]_2$, $Na[BAr^F_4]$, **A89**, and **A90** were synthesised using adapted literature protocols.[33, 50-54] All other solvents and reagents are commercial products and were used as received. NMR spectra were recorded on Bruker AV spectrometers at 298 K unless otherwise stated. ^1H NMR spectra recorded in 1,2-$C_6H_4F_2$ were referenced using the highest intensity peak of the highest (δ 6.865) frequency fluoro-arene multiplets. $^{13}C\{^1H\}$ NMR spectra recorded in 1,2-$C_6H_4F_2$ were referenced using an internal sealed capillary of C_6D_6. Chemical shifts are quoted in ppm and coupling constants in Hz. IR spectra were recorded on a PerkinElmer Spectrum One FT-IR spectrometer at 293 K. ESI-MS analyses were recorded on Bruker Maxis Impact instrument. Microanalyses were performed by Stephen Boyer at London Metropolitan University.

3.4.2 Preparation of isolated complexes

[2a(Rh(COD)I)$_2$] (4a)

A solution of **2a·2HI** (99.7 mg, 0.0987 mmol) and K[O^{t}Bu] (27.8 mg, 0.248 mmol) was stirred in THF (10 mL) for 1 hour then added to a flask charged with [Rh(COD)Cl]$_2$ (51.6 mg, 0.105 mmol) and KI (165.1 mg, 1.42 mmol). After a further hour the volatiles were removed *in vacuo*. The product was extracted with CH_2Cl_2 (2 × 10 mL) and purified by column chromatography (over alumina with 1 : 1 EtOAc/CH_2Cl_2, in air). Yield = 75.5 mg (53%, yellow powder). **^{1}H NMR** (CD_2Cl_2, 400 MHz): δ 7.95 (d, $^4J_{HH}$ = 2.8, 2H, Ar), 7.29–7.39 (m, 2H, Ar), 7.04 – 7.14 (m, 2H, Ar), 6.97 (t, $^3J_{HH}$ = 7.4, 2H, Ar), 6.44 (d, $^3J_{HH}$ = 2.0, 2H, imid.), 6.19 (d, $^3J_{HH}$ = 2.0, 2H, imid.), 5.92 (d, $^4J_{HH}$ = 2.8, 2H, Ar), 5.24 – 5.29 (m, 2H, COD{CH}), 4.92 – 5.09 (m, 2H, COD{CH}), 4.62 (d, $^2J_{HH}$ = 13.3, 2H, $ArC\underline{H}_2Ar$), 4.50 (d, $^2J_{HH}$ = 13.5, 2H, $ArC\underline{H}_2Ar$), 3.99 – 4.18 (m, 4H, OCH_2), 3.85 (s, 6H, NCH_3), 3.65 – 3.82 (m, 4H, OCH_2), 3.38 (d, $^2J_{HH}$ = 13.4, 2H, $ArC\underline{H}_2Ar$), 3.21 – 3.26 (m, 2H, COD{CH}), 3.19 (d, $^2J_{HH}$ = 13.7, 2H, $ArC\underline{H}_2Ar$), 2.29 – 2.39 (m, 2H, COD{CH}), 2.09–2.29 (m, 6H, COD{CH_2}), 1.97 – 2.09 (m, 4H, $C\underline{H}_2CH_3$), 1.83 – 1.97 (m, 6H, $C\underline{H}_2CH_3$ + COD{CH_2}), 1.58 – 1.79 (m, 4H, COD{CH_2}), 1.27 – 1.46 (m, 4H, COD{CH_2}), 1.15 (t, $^3J_{HH}$ = 7.4, 6H, $CH_2C\underline{H}_3$), 0.95 (t, $^3J_{HH}$ = 7.5, 6H, $CH_2C\underline{H}_3$). **^{13}C{^{1}H} NMR** (CD_2Cl_2, 101 MHz): δ 180.4 (d, $^1J_{RhC}$ = 49, NCN), 158.2 (s, $\underline{C}OCH_2$), 155.0 (s, $\underline{C}OCH_2$), 137.0 (s, Ar{$\underline{C}CH_2$}), 136.9 (s, Ar{$\underline{C}CH_2$}), 134.9 (s, Ar{C}), 134.7 (s, Ar{C}), 134.3 (s, Ar{C}), 131.5 (s, Ar), 129.6 (s, Ar), 123.6 (s, Ar), 123.4 (s, imid.), 122.9 (s, Ar), 122.5 (s, imid.), 122.5 (s, Ar), 95.0 (d, $^1J_{RhC}$ = 7, COD{CH}), 95.0 (d, $^1J_{RhC}$ = 7, COD{CH}), 77.7 (s, OCH_2), 77.3 (s, OCH_2), 71.4 (d, $^1J_{RhC}$ = 14, 2 × COD{CH}), 39.1 (s, $N\underline{C}H_3$), 33.9 (s, COD{CH_2}), 31.7 (s, CH_2), 31.4 (s, CH_2), 31.0 (s, CH_2), 30.7 (s, CH_2), 29.2 (s, COD{CH_2}), 23.8 (s, $\underline{C}H_2CH_3$), 23.4 (s, $\underline{C}H_2CH_3$), 11.3 (s, $CH_2\underline{C}H_3$), 10.3 (s, $CH_2\underline{C}H_3$). **Anal.** Calcd For $C_{64}H_{80}I_2N_4O_4$ (1428.24 g mol^{-1}): C, 53.79; H, 5.64; N, 3.92. Found: C, 53.71; H, 5.75; N, 4.04.

[(I^{i}Pr$_2$Me$_2$)Rh(COD)I] (4b)

A solution of I^{i}Pr$_2$Me$_2$ (61.2 mg, 0.336 mmol), [Rh(COD)Cl]$_2$ (166.1 mg, 0.337 mmol) and KI (1072.2 mg, 6.46 mmol) in THF (10 mL) was stirred for 1 hour. The volatiles were removed *in vacuo* and the product obtained after purification by column chromatography (over silica, with CH_2Cl_2, in air) and subsequent recrystallisation from CH_2Cl_2/ pentane. Yield = 55.0 mg

(31%, yellow crystals). **^{1}H NMR** (CD_2Cl_2, 500 MHz): δ 5.97 (sept, $^{3}J_{\mathrm{HH}}$ = 7.1, 2H,NCH), 5.03 – 5.09 (m, 2H, COD{CH}), 3.50–3.57 (m, 2H, COD{CH}), 2.26–2.36 (m, 4H, COD{CH_2}), 2.16 (s, 6H, $C\underline{H}_3$), 1.87 – 1.98 (m, 2H, COD^{1}{CH_2}), 1.73–1.83 (m, 2H, COD{CH_2}), 1.56 (d, $^{3}J_{\mathrm{HH}}$ = 7.1, 6H, $CHC\underline{H}_3$), 1.50 (d, $^{3}J_{\mathrm{HH}}$ = 7.1, 6H, $CHC\underline{H}_3$).**^{13}C{^{1}H} NMR** (CD_2Cl_2, 126 MHz): δ 178.4 (d, $^{1}J_{\mathrm{RhC}}$ = 49, NCN), 126.0 (s, $\underline{C}CH_3$), 95.2 (d, $^{1}J_{\mathrm{RhC}}$ = 7, COD{CH}), 71.5 (d, $^{1}J_{\mathrm{RhC}}$ = 14, COD{CH}), 53.7 (s, NCH), 32.8 (s, COD{CH_2}), 30.0 (s, COD{CH_2}), 22.4 (s, $CH\underline{C}H_3$), 21.4 (s, $CH\underline{C}H_3$), 10.7 (s, $C\underline{C}H_3$). **Anal.** Calcd for $C_{19}H_{32}I_2N_2Rh$ (518.29 g mol^{-1}): C, 44.03; H, 6.22; N, 5.41. Found: C, 44.11; H, 6.14; N, 5.47.

[2a(Rh(CO)$_2$I)$_2$] (5a)

Method A: A solution of **2a·2HI** (102.1 mg, 0.101 mmol) and K[O^{t}Bu] (28.9 mg, 0.258 mmol) was stirred in THF (10 mL) for 1 hour then added to a flask charged with $[Rh(CO)_2Cl]_2$ (40.7 mg, 0.105 mmol) and KI (165.4 mg, 0.996 mmol). After a further hour the volatiles were removed *in vacuo*. The product was extracted with CH_2Cl_2 (2 × 10 mL) and purified by column chromatography (over alumina, with 1 : 1 Et_2O/CH_2Cl_2, in air). Yield = 22.4 mg (17%, yellow powder).

Method B: A solution of **2a** (121.2 mg, 0.0848 mmol) in CH_2Cl_2 (10 mL) was stirred under CO (1 atm) for 12 hours, resulting in a colour change from bright to pale yellow. The mixture was dried *in vacuo* and washed with pentane (3 × 5 mL). Yield = 42.1 mg (37%, yellow powder). **^{1}H NMR** (CD_2Cl_2, 500 MHz): δ 7.26 (s, 2H, Ar), 7.02 (br, 4H, Ar), 6.82 (t, $^{3}J_{\mathrm{HH}}$ = 7.4, 2H, Ar), 6.77 (s, 2H, imid.), 6.46 (s, 2H, imid.), 6.41 (s, 2H, Ar), 4.51 (d, $^{2}J_{\mathrm{HH}}$ = 13.3, 2H, $ArC\underline{H}_2Ar$), 4.48 (d, $^{2}J_{\mathrm{HH}}$ = 13.6, 2H, $ArC\underline{H}_2Ar$), 3.80 – 4.09 (m, 8H, OCH_2), 3.77 (s, 6H, NCH_3), 3.24 (d, $^{2}J_{\mathrm{HH}}$ = 14.1, 2H, $ArC\underline{H}_2Ar$), 3.22 (d, $^{2}J_{\mathrm{HH}}$ = 14.1, 2H, $ArC\underline{H}_2Ar$), 1.79 – 2.16 (m, 8H, $C\underline{H}_2CH_3$), 1.03 – 1.13 (m, 6H, $CH_2C\underline{H}_3$), 0.92 – 1.03 (m, 6H, $CH_2C\underline{H}_3$). **^{13}C{^{1}H} NMR** (CD_2Cl_2, 126 MHz): δ 188.4 (d, $^{1}J_{\mathrm{RhC}}$ = 54,CO), 181.6 (d, $^{1}J_{\mathrm{RhC}}$ = 78, CO), 171.5 (d, $^{1}J_{\mathrm{RhC}}$ = 44, NCN), 157.5 (s, $\underline{C}OCH_2$), 156.3 (s, $\underline{C}OCH_2$), 136.2, 136.1, 135.9, 135.6, 130.6,129.4, 123.8, 123.4, 123.2, 122.8, 77.8 (OCH_2), 77.4(OCH_2), 40.0 (s, NCH_3), 31.5 (br, $Ar\underline{C}H_2Ar$), 24.0 ($\underline{C}H_2CH_3$), 23.7 ($\underline{C}H_2CH_3$), 11.0 (s, $CH_2\underline{C}H_3$), 10.4 (s,

$CH_2\underline{C}H_3$). Not all signals were unambiguously identified. **IR** (CH_2Cl_2, cm^{-1}): ν(CO) 2071, 2002. **Anal.** Calcd for $C_{52}H_{56}I_2N_4O_8Rh_2$ (1324.02 g mol^{-1}): C, 47.15; H, 4.26; N, 4.23. Found: C, 46.91; H, 4.12; N, 4.25.

$[(I^{i}Pr_2Me_2)(Rh(CO)_2I)]$ (5b)

A solution of 4b (40.1 mg, 0.0774 mmol) in CH_2Cl_2 (10 mL) was placed under an atmosphere of CO (1 atm) for 2 hours. The volatiles were removed *in vacuo* to afford the product, which was washed with pentane (3 × 10 mL) and dried thoroughly under vacuum. Yield = 21.4 mg (59%, fine yellow powder).**^{1}H NMR** (CD_2Cl_2, 500 MHz): δ 5.26 (sept, $^3J_{HH}$ = 7.1, 2H, NCH), 2.22 (s, 6H, CCH_3), 1.501 (d, $^3J_{HH}$ = 7.1, 6H, $CHC\underline{H}_3$), 1.496 (d, $^3J_{HH}$ = 2.7, 6H, $CHC\underline{H}_3$). **^{13}C{^{1}H} NMR** (CD_2Cl_2, 126 MHz): δ 188.7 (d, $^1J_{RhC}$ = 53, CO), 182.7 (d, $^1J_{RhC}$ = 78, CO), 166.8 (d, $^1J_{RhC}$ = 41, NCN), 127.2 (s, $\underline{C}CH_3$), 54.3 (s, $\underline{C}HCH_3$), 22.2 (s, $CH\underline{C}H_3$), 21.1 (s, $CH\underline{C}H_3$), 10.7 (s, $C\underline{C}H_3$). **IR** (CH_2Cl_2, cm^{-1}): ν(CO) 2072, 1998. **Anal.** Calcd for $C_{13}H_{20}I_2N_2O_2Rh$ (466.12 g mol^{-1}): C, 33.50; H, 4.33; N, 6.01. Found: C, 33.41; H, 4.25; N, 6.03.

$[(2a)Ag][BAr^F_4]$ (6a)

A suspension of **2a·2HI** (79.5 mg, 0.0788 mmol), Ag_2O (20.0 mg, 0.0862 mmol) and $Na[BAr^F_4]$ (69.0 mg, 0.0778 mmol) in CH_2Cl_2 (20 mL) was sonicated periodically over 2 hours. The solution was filtered and the solvent was removed *in vacuo* to afford the product. Yield = 100.0 mg (73%, white crystals). **^{1}H NMR** (400 MHz, CD_2Cl_2): δ 7.72–7.76 (m, 8H, Ar^F), 7.57 (br, 4H, Ar^F), 7.10 (d, $^3J_{HH}$ = 7.4, 4H, Ar), 6.92 (d, $^3J_{HH}$ = 1.7, 2H, imid.), 6.85 (t, $^3J_{HH}$ = 7.5, 2H, Ar), 6.81 (d, $^3J_{HH}$ = 1.7, 2H, imid.), 6.40 (s, 4H, Ar), 4.57 (d, $^2J_{HH}$ = 12.8, 4H, $ArC\underline{H}_2Ar$), 4.10–4.22 (m, 4H, OCH_2), 3.80 (s, 6H, NCH_3), 3.74 (t, $^3J_{HH}$ = 7.1, 4H, OCH_2), 3.24 (d, $^2J_{HH}$ $^2J_{HH}$ = 12.8, 4H, $ArC\underline{H}_2Ar$), 2.10–2.21 (m, 4H, $C\underline{H}_2CH_3$), 1.99 (app. sex., J = 7, 4H, $C\underline{H}_2CH_3$), 1.12 (t, $^3J_{HH}$ = 7.4, 6H, $CH_2C\underline{H}_3$), 0.98 (t, $^3J_{HH}$ = 7.5, 6H, $CH_2C\underline{H}_3$). **^{13}C{^{1}H} NMR** (CD_2Cl_2, 101 MHz): δ 180.7 (two coincident d,$^1J_{109AgC}$ = 211, $^1J_{107AgC}$ = 183, NCN), 162.3 (q, $^1J_{BC}$ = 50.5, Ar^F), 157.8 ($\underline{C}OCH_2$), 156.7 (s, $\underline{C}OCH_2$), 136.5 (s, 2 × Ar{C}), 135.4 (s, Ar^F), 134.3 (s, Ar{C}), 129.4 (qq, $^2J_{FC}$ = 32, $^3J_{BC}$ = 3, Ar^F),129.3 (s, Ar), 118.0 (sept, $^3J_{FC}$ = 4, Ar^F), 126.4 (s, Ar), 125.2 (q, $^1J_{FC}$ = 272, Ar^F), 124.7 (d,

$^{3}J_{\mathrm{AgC}}$ = 6, imid.), 123.4 (s, Ar), 121.9 (d, $^{3}J_{\mathrm{AgC}}$ = 6, imid.), 118.0 (sept, $^{3}J_{\mathrm{FC}}$ = 4, $\mathrm{Ar^F}$), 78.7 (s, $\mathrm{OCH_2}$), 77.2 (s, OCH2), 38.8 (d, $^{3}J_{\mathrm{AgC}}$ = 3, $\mathrm{NCH_3}$), 31.4 (s, $\mathrm{Ar\underline{C}H_2Ar}$), 24.0 (s, $\mathrm{\underline{C}H_2CH_3}$), 23.5 (s, $\mathrm{\underline{C}H_2CH_3}$), 11.0 (s, $\mathrm{CH_2\underline{C}H_3}$), 10.1 (s, $\mathrm{CH_2\underline{C}H_3}$). **ESI-MS** ($\mathrm{CH_3CN}$, 180 °C, 3 kV) positive ion: 859.3340 m/z, $[\mathrm{M}]^+$ (calcd 859.3347 *m/z*). **Anal.** Calcd For $\mathrm{C_{80}H_{68}AgBF_{24}N_4O_4}$ (1724.09 g $\mathrm{mol^{-1}}$):C, 55.73; H, 3.98; N, 3.25. Found: C, 55.85; H, 4.08; N, 3.33.

$\mathbf{[(2a)Rh_2(COD)_2Cl][BAr^F_4]}$ (7a)

A solution of 6a (29.9 mg, 0.0173 mmol) and $\mathrm{[Rh(COD)Cl]_2}$ (9.4 mg, 0.0191 mmol) in 1,2-$\mathrm{C_6H_4F_2}$ (0.5 mL) was stirred for 1 hour with the exclusion of light. The solvent was removed *in vacuo* and the resulting crude material washed with pentane and dried *in vacuo*. Yield = 22.3 mg (63%, yellow powder). The product was characterised *in situ*, although has limited stability in solution. **^{1}H NMR** (1,2-$\mathrm{C_6H_4F_2/C_6D_6}$, 500 MHz): δ 8.09 – 8.15 (m, 8H, $\mathrm{Ar^F}$), 7.49 (br, 4H, $\mathrm{Ar^F}$) 5.44 (br, 2H, COD{CH}), 5.38 (br, 2H, COD{CH}), 4.58 (d, $^{2}J_{\mathrm{HH}}$ = 13.6, 2H, $\mathrm{ArC\underline{H}_2Ar}$), 4.49 (d, $^{2}J_{\mathrm{HH}}$ = 13.6, 2H, $\mathrm{ArC\underline{H}_2Ar}$), 4.20 (s, 6H, $\mathrm{NCH_3}$), 3.96 – 4.24 (m), 3.67–3.76 (m), 3.55 – 3.63 (m), 3.49–3.55 (m), 3.46 (d, $^{2}J_{\mathrm{HH}}$ = 13.6, 2H, $\mathrm{ArC\underline{H}_2Ar}$), 3.23 – 3.33 (m), 3.09 (d, $^{2}J_{\mathrm{HH}}$ = 13.6, 2H, $\mathrm{ArC\underline{H}_2Ar}$), 1.35–2.50 (m, $\mathrm{CH_2}$), 1.03 (t, $^{3}J_{\mathrm{HH}}$ = 6.9, 6H, $\mathrm{CH_2C\underline{H}_3}$), 0.85 (t, $^{3}J_{\mathrm{HH}}$ = 6.9, 6H, $\mathrm{CH_2C\underline{H}_3}$), 0.7–1.1 (m, COD{$\mathrm{CH_2}$}). Not all signals unambiguously assigned and some signals obscured by solvent peak. **^{13}C{^{1}H} NMR** (1,2-$\mathrm{C_6H_4F_2/C_6D_6}$, 126 MHz, selected signals only): δ 176.9 (d, $^{1}J_{\mathrm{RhC}}$ = 50, NCN), 100.3 (br, COD{CH}), 96.4 (br, COD{CH}), 78.5 (d, $^{1}J_{\mathrm{RhC}}$ = 14, COD{CH}), 71.8 (d, $^{1}J_{\mathrm{RhC}}$ = 13, COD{CH}), 97.7 (d, $^{1}J_{\mathrm{RhC}}$ = 7, COD{CH}), 70.2 (d, $^{1}J_{\mathrm{RhC}}$ = 16, COD{CH}), 37.8 (s, $\mathrm{NCH_3}$). **ESI-MS** ($\mathrm{CH_3CN}$, 180 °C, 3 kV): positive ion: 1209.3986 *m/z*, $[\mathrm{M}]^+$ (calcd 1209.3973 *m/z*).

$\mathbf{[(I^{\mathit{i}}Pr_2Me_2)_2Rh_2(COD)_2Cl]}$ (7b)

A solution of A89 (23.6 mg, 0.0553 mmol) and $\mathrm{Na[BAr^F_4]}$ (24.5 mg, 0.0275 mmol) in $\mathrm{CH_2Cl_2}$ (10 mL) was stirred for 1 hour. The solution was then filtered and layered with pentane to afford the product on diffusion. Yield = 32.0 mg (69%, yellow crystals). **^{1}H NMR** ($\mathrm{CD_2Cl_2}$, 500 MHz): δ 7.70–7.74 (m, 8H, $\mathrm{Ar^F}$), 7.56 (br, 4H, $\mathrm{Ar^F}$), 5.91 (sept, $^{3}J_{\mathrm{HH}}$ = 7.1, 4H, NCH), 4.75 (s, 4H, COD{CH}), 3.51 (s, 4H, COD{CH}), 2.22–2.36 (m, 8H, COD{CH$_2$}), 2.11 (s, 12H, CCH$_3$), 1.81–1.93 (m, 8H, COD{CH$_2$}), 1.57 (d, $^3J_{\mathrm{HH}}$ = 7.0, 12H, CHC$\underline{\mathrm{H}}_3$), 1.36 (d, $^3J_{\mathrm{HH}}$ = 7.0, 12H, CHC$\underline{\mathrm{H}}_3$). **^{13}C{^{1}H}NMR** (CD$_2$Cl$_2$, 126 MHz): δ 175.6 (d, $^1J_{\mathrm{RhC}}$ = 50, NCN), 162.3 (q, $^1J_{\mathrm{BC}}$ = 51, Ar$^{\mathrm{F}}$), 135.4 (s, Ar$^{\mathrm{F}}$), 129.4 (qq, $^2J_{\mathrm{FC}}$ = 31, $^3J_{\mathrm{BC}}$ = 3, Ar$^{\mathrm{F}}$), 126.3 (s, $\underline{\mathrm{C}}$CH$_3$), 125.2 (q, $^1J_{\mathrm{FC}}$ =272, Ar$^{\mathrm{F}}$), 118.0 (sept, $^3J_{\mathrm{FC}}$ = 4, Ar$^{\mathrm{F}}$), 97.7 (d, $^1J_{\mathrm{RhC}}$ = 7, COD{CH}), 70.2 (d, $^1J_{\mathrm{RhC}}$ = 16, COD{CH}), 54.3 (s, NCH), 33.1 (s, COD{CH$_2$}), 29.1 (s, COD{CH$_2$}), 22.5 (s, CH$\underline{\mathrm{C}}$H$_3$), 22.2 (s, CH$\underline{\mathrm{C}}$H$_3$), 10.5 (s, C$\underline{\mathrm{C}}$H$_3$). **ESI-MS** (CH$_3$CN, 180 °C, 3 kV) positive ion: 817.2872 *m/z*, [M]$^+$ (calcd 817.2924 *m/z*). **Anal.** Calcd For C$_{70}$H$_{76}$BF$_{24}$N$_4$Rh$_2$Cl (1434.39 g mol^{-1}): C, 49.97; H, 4.56; N, 3.33. Found: C, 50.18; H, 4.52; N, 3.23.

[2a·Rh$_2$(CO)$_4$Cl][BAr$^{\mathrm{F}}_4$] (8a)

A solution of **6a** (32.0 mg, 0.0186 mmol) and [Rh(CO)$_2$Cl]$_2$ (7.8 mg, 0.0201 mmol) in 1,2-C$_6$H$_4$F$_2$ (10 mL) was stirred for one hour with the exclusion of light. The cloudy yellow solution was filtered, reduced to dryness and the resulting residue washed with pentane. Yield = 21.4 mg (31%, yellow powder). The product was characterised *in situ*, although has limited stability in solution. **^{1}H NMR** (1,2-C$_6$H$_4$F$_2$/C$_6$D$_6$, 500 MHz): δ 8.11 – 8.15 (m, 8H, Ar$^{\mathrm{F}}$), 7.49 (br, 4H, Ar$^{\mathrm{F}}$), 4.52 (d, $^2J_{\mathrm{HH}}$ = 12.6, 2H, ArC$\underline{\mathrm{H}}_2$Ar), 4.51 (d, $^2J_{\mathrm{HH}}$ = 12.6, 2H, ArC$\underline{\mathrm{H}}_2$Ar), 4.05 – 4.19 (m, 2H, OCH$_2$), 3.88 – 3.99 (m, 2H, OCH$_2$), 3.84 (s, 6H, NCH$_3$), 3.51 – 3.65 (m, 4H, OCH$_2$), 3.18 (d, $^2J_{\mathrm{HH}}$ = 12.6, 2H, ArC$\underline{\mathrm{H}}_2$Ar), 3.15 (d, $^2J_{\mathrm{HH}}$ = 12.6, 2H, ArC$\underline{\mathrm{H}}_2$Ar), 2.11 – 2.23 (m, 4H, C$\underline{\mathrm{H}}_2$CH$_3$), 1.79 – 1.92 (m, 4H, C$\underline{\mathrm{H}}_2$CH$_3$), 0.94 (t, $^3J_{\mathrm{HH}}$ = 7.5, 6H, CH$_2$C$\underline{\mathrm{H}}_3$), 0.93 (t, $^3J_{\mathrm{HH}}$ = 7.5, 6H, CH$_2$C$\underline{\mathrm{H}}_3$). Some signals obscured by solvent peak. **^{13}C{^{1}H} NMR** (1,2-C$_6$H$_4$F$_2$/C$_6$D$_6$, 126 MHz, selected signals only): δ 182.7 (d, $^1J_{\mathrm{RhC}}$ = 53, CO), 181.0 (d, $^1J_{\mathrm{RhC}}$ = 80, CO), 168.1 (d, $^1J_{\mathrm{RhC}}$ = 43, NCN), 36.3 (s, NCH$_3$). **ESI-MS** (CH$_3$CN, 180 °C, 3 kV) positive ion: 1105.1680 *m/z*, [M]$^+$ (calcd 1105.1891 *m/z*). **IR** (CH$_2$Cl$_2$, cm^{-1}): ν(CO) 2083, 2016.

[(I^{i}Pr$_2$Me$_2$)$_2$Rh$_2$(CO)$_4$Cl][BAr$^{\mathrm{F}}_4$] (8b)

A solution of **A90** (26.5 mg, 0.709 mmol) and Na[BAr$^{\mathrm{F}}_4$] (32.6 mg, 0.368 mmol) in CH$_2$Cl$_2$ (5 mL) was stirred for 1 hour. The solution was then filtered and layered with pentane to afford the product on diffusion. Yield = 37.1 mg (66%, yellow crystals). **^{1}H NMR** (CD_2Cl_2, 400 MHz): δ 7.67 – 7.77 (m, 8H, Ar^F), 7.56 (br, 4H, Ar^F), 5.20 (sept, $^3J_{HH}$ = 7.1, 4H, NCH), 2.18 (s, 12H $CC\underline{H}_3$), 1.55 (d, $^3J_{HH}$ = 7.1, 12H, $CHC\underline{H}_3$), 1.50 (d, $^3J_{HH}$ = 7.0, 12H, $CHC\underline{H}_3$).**^{13}C{^{1}H} NMR** (CD_2Cl_2, 101 MHz): δ 185.4 (d, $^1J_{RhC}$ = 53, CO), 181.0 (d, $^1J_{RhC}$ = 84, CO), 162.3 (q, $^1J_{BC}$ = 50, Ar^F), 135.4 (s, Ar^F), 129.4 (qq, $^2J_{FC}$ = 32, $^3J_{BC}$ = 3, Ar^F), 128.0 (s, CCH_3), 125.2 (q, $^1J_{FC}$ = 272, Ar^F), 54.8 (s, NCH), 22.8 (s, $CH\underline{C}H_3$), 22.4 (s, $CH\underline{C}H_3)_2$, (s, 10.6 $C\underline{C}H_3$). The carbene resonance was not located. **ESI-MS** (CH_3CN, 180 °C, 3 kV) positive ion: 713.0829 *m/z*, $[M]^+$ (calcd 713.0843 *m/z*). **IR** (CH_2Cl_2, cm^{-1}): ν(CO) 2090, 2019. **Anal.** Calcd For $C_{58}H_{52}BClF_{24}N_4O_4Rh_2Cl$ (1577.11 g mol^{-1}): C, 44.17; H, 3.32; N, 3.55. Found: C, 44.51; H, 3.57; N, 3.49.

$[(I^iPr_2Me_2)_2Rh(COD)][BAr^F_4]$ (9)

A solution of $I^iPr_2Me_2$ (50.8 mg, 0.282 mmol), $[Rh(COD)Cl]_2$ (34.3 mg, 0.0696 mmol) and $Na[BAr^F_4]$ (123.4 mg, 0.139 mmol) was stirred in 1,2-$C_6H_4F_2$ (5 mL) for 2.5 h. The solution was then filtered and layered with pentane to afford the product on diffusion. Yield = 114.0 mg (56%, yellow crystals). **^{1}H NMR** (CD_2Cl_2, 500 MHz): δ 7.71 – 7.75 (m, 8H, Ar^F), 7.56 (br, 4H, Ar^F), 5.56 (sept, $^3J_{HH}$ = 7.1, 4H, NCH), 4.27 (s, 4H, COD{CH}), 2.31 – 2.40 (m, 4H, COD{CH_2}), 2.16 (s, 12H, CCH_3), 2.01 – 2.11 (m, 4H, COD{CH_2}), 1.55 (d, $^3J_{HH}$ = 7.1, 12H, $CHC\underline{H}_3$), 1.22 (d, $^3J_{HH}$ = 7.1, 12H, $CHC\underline{H}_3$). **^{13}C{^{1}H} NMR** (CD_2Cl_2, 126 MHz): δ 178.1 (d, $^1J_{RhC}$ = 55.8, NCN), 162.3 (q, $^1J_{BC}$ = 50, Ar^F), 135.4 (s, Ar^F), 129.4 (qq, $^2J_{FC}$ = 32, $^3J_{BC}$ = 3, Ar^F), 127.1 (s, $\underline{C}CH_3$), 125.2 (q, $^1J_{FC}$ = 272, Ar^F), 118.0 (sept, $^3J_{FC}$ = 4, Ar^F), 87.2 (d, $^1J_{RhC}$ = 8, COD{CH}), 54.5 (s, NCH), 31.8 (s, COD{CH_2}), 22.9 (s, $CH\underline{C}H_3$), 21.6 (s, $CH\underline{C}H_3$), 10.9 (s, $C\underline{C}H_3$). **ESI-MS** (CH_3CN, 180 °C, 3 kV) positive ion: 571.3215 *m/z* $[M]^+$ (calcd 571.3242 *m/z*). **Anal.** Calcd For $C_{62}H_{64}BF_{24}N_4Rh$ (1434.39 g mol^{-1}): C, 51.96; H, 4.49; N, 3.90. Found: C, 52.05; H, 4.59; N, 3.93.

$[(I^iPr_2Me_2)_2Rh(CO)_2][BAr^F_4]$ (10)

A solution of 9 (113.9 mg, 0.0794 mmol) in 1,2-$C_6H_4F_2$ (5 mL) was stirred under an atmosphere of CO (1 atm) for 24 hours. The solvent was removed *in vacuo* and the resulting crude material washed with pentane and recrystallised from CH_2Cl_2/ pentane. Yield = 72.4

mg (66%, orange powder). **^{1}H NMR** (CD_2Cl_2, 500 MHz): δ 7.71–7.75 (m, 8H, Ar^F), 7.56 (br, 4H, Ar^F), 5.05 (sept, $^3J_{HH}$ = 7.1, 4H, NCH), 2.20 (s, 12H, CCH_3), 1.46 (d, $^3J_{HH}$ = 7.1, 12H, $CHC\underline{H}_3$), 1.19 (d, $^3J_{HH}$ = 7.1, 12H, $CHC\underline{H}_3$). **^{13}C{^{1}H} NMR** (CD_2Cl_2, 126 MHz): δ 186.9 (d, $^1J_{RhC}$ = 57, CO), 168.2 (d, $^1J_{RhC}$ = 47, NCN), 162.3 (q, $^1J_{BC}$ = 50, Ar^F), 135.3 (s, Ar^F), 129.4 (qq, $^2J^{FC}$ = 32, $^3J_{BC}$ = 3, Ar^F), 128.2 (s, $\underline{C}CH_3$), 125.2 (q, $^1J_{FC}$ = 272, Ar^F), 118.0 (sept, $^3J_{FC}$ = 4, Ar^F), 55.3 (s, NCH), 22.0 (s, $CH\underline{C}H_3$), 21.1 (s, $CH\underline{C}H_3$), 10.9 (s, $C\underline{C}H_3$). **ESI-MS** (CH_3CN, 180 °C, 3 kV) positive ion: 519.2249 *m/z* $[M]^+$ (calcd 519.2201 *m/z*). **IR** (CH_2Cl_2, cm^{-1}): ν(CO) 2077, 2018. **Anal.** Calcd For $C_{56}H_{52}BF_{24}N_4Rh$ (1382.29 g mol^{-1}): C, 48.64; H, 3.79; N, 4.05. Measured: C, 48.51; H, 3.63; N, 4.15.

3.4.3. In situ reactions

Generation of $[(I^iPr_2Me_2)_2Ag][BAr^F_4]$ (6b)

A suspension of $I^iPr_2Me_2$ (9.9 mg, 0.0549 mmol), Ag[OTf] (7.2 mg, 0.0277 mmol) and $Na[BAr^F_4]$ (24.0 mg, 0.0271 mmol) in 1,2-difluorobenzene (0.5 mL) was agitated for several minutes. Analysis *in situ* by NMR spectroscopy indicated quantitative formation of **6b** (data below). Solutions of **6b**, prepared in this way, was then filtered onto either $[Rh(COD)Cl]_2$ (13.6 mg, 0.0276 mmol) or $[Rh(CO)_2Cl]_2$ (10.8 mg, 0.0278 mmol), resulting in the formation of **5b** : **7** (2 : 1) and **6b**/**8** (5:2). **^{1}H NMR** (1,2-$C_6H_4F_2$, 500 MHz): δ 8.11–8.13 (m, 8H, Ar^F), 7.49 (br, 4H, Ar_F), 4.20 (sept, $^3J_{HH}$ = 6.8, 4H, NCH), 1.87 (s, 12H, CCH_3), 1.31 (d, $^3J_{HH}$ = 6.8, 24H, $CHC\underline{H}_3$).**^{13}C{^{1}H} NMR** (1,2-$C_6H_4F_2$, 126 MHz): δ 162.5 (q, $^1J_{BC}$ = 50, Ar^F), 135.1 (s, Ar^F), 129.7 (qq, $^2J_{FC}$ = 32, $^3J_{BC}$ = 3, Ar^F), 124.9 (q, $^1J_{FC}$ = 272, Ar^F), 124 (obscured, $\underline{C}CH_3$), 117.6 (sept, $^3J_{FC}$ = 4, Ar^F), 50.1 (s, NCH), 23.3 (s, $CHC\underline{H}_3$), 8.1 (s, $C\underline{C}H_3$). The carbene resonance was not located. **^{19}F{^{1}H} NMR** (1,2-$C_6H_4F_2$, 282 MHz): δ-62.25 (Ar^F). No signal for $[OTf]^-$ detected. **ESI-MS** (CH_3CN, 180 °C, 3 kV) positive ion: 467.2297 *m/z*, $[M]^+$ (calcd 467.2298 *m/z*).

3.4.4 Crystallography

Structure determinations were carried out by Dr. A. B. Chaplin. Relevant crystallographic data are given in **Table 3.1**. Data were collected on an Oxford Diffraction Gemini Ruby CCD diffractometer using graphite monochromated Mo Kα (λ = 0.71073 Å) radiation and a low-temperature device. Data were collected and reduced using CrysAlisPro. All non-hydrogen atoms were refined anisotropically using SHELXL,[55] through the Olex2 interface.

Table 3.1: Key crystallographic data for structures **3** - **9**

	4a	**4b**	**6a**	**6b**	**8a**	**7b**	**8b**	**9**	**10**
CCDC / ID	1448988	1448989	1448990	1448991	1448993	1448992	1448994	1448995	1448996
Figure	**Figure 3.1**	**Figure 3.1**	**Figure 3.4**	**Figure 3.4**	**Figure 3.5**	**Figure 3.6**	**Figure 3.6**	**Figure 3.7**	**Figure 3.7**
Formula	$C_{64}H_{80}I_2N_4O_4Rh_2$	$C_{19}H_{32}IN_2Rh$	$C_{80}H_{68}AgBF_{24}N_4O_4$	$C_{54}H_{52}AgBF_{24}N_4$	$C_{84}H_{68}BClF_{24}N_4O_8Rh_2$	$C_{71}H_{78}BCl_3F_{24}N_4Rh_2$	$C_{58}H_{52}BClF_{24}N_4O_4Rh_2$	$C_{62}H_{64}BF_{24}N_4Rh$	$C_{56}H_{52}BF_{24}N_4O_2Rh$
M	1428.94	518.27	1724.06	1331.67	1969.50	1766.35	1577.11	1433.89	1382.73
Crystal System	monoclinic	monoclinic	triclinic	monoclinic	monoclinic	monoclinic	triclinic	monoclinic	triclinic
Space group	$P2_1/n$	$P2_1/c$	P-1	$P2_1/c$	$P2_1/c$	$P2_1/n$	P-1	$P2_1/n$	P-1
Radiation	Mo Kα (λ = 0.71073 Å)	Mo Kα (λ = 0.71073 Å)	Mo Kα (λ = 0.71073 Å)	Mo Kα (λ = 0.71073 Å)	Mo Kα (λ = 0.71073 Å)	Mo Kα (λ = 0.71073 Å)	Mo Kα (λ = 0.71073 Å)	Mo Kα (λ = 0.71073 Å)	Mo Kα (λ = 0.71073 Å)
***T* [K]**	200(2)	150(2)	250(2)	150(2)	150(2)	150(2)	150(2)	150(2)	150(2)
***a* [Å]**	13.07898(15)	10.94671(13)	11.5261(8)	10.29827(16)	19.6345(4)	14.1084(4)	12.2319(3)	12.8630(2)	17.0878(3)
***b* [Å]**	27.7640(3)	13.02535(13)	19.1677(9)	20.4557(3)	22.6778(5)	25.7959(7)	13.2693(3)	24.2781(5)	18.9928(3)
***c* [Å]**	17.30754(19)	14.51455(15)	20.4328(7)	29.5742(4)	20.0799(4)	21.8486(7)	21.7143(4)	20.3511(4)	19.5695(4)
α[deg]	90	90	85.952(3)	90	90	90	100.9872(15)	90	79.1970(13)
β [deg]	99.4834(11)	96.9118(10)	77.095(5)	95.6910(14)	109.352(3)	105.666	94.9257(17)	90.0784(15)	87.6582(15)
γ [deg]	90	90	80.605(5)	90	90	90	91.7507(12)	90	76.2505(14)
V [Å^3]	6198.92(12)	2054.51(4)	4338.4(4)	6199.34(16)	8435.8(3)	7656.2(4)	3443.08(12)	6381.6(2)	6062.41(18)
Z [Z']	4	4	2	4	4	4	2	4	4
Density [gcm^{-3}]	1.531	1.676	1.320	1.427	1.551	1.532	1.521	1.493	1.515
μ (mm^{-1})	1.577	2.336	0.331	0.435	0.533	0.637	0.628	0.380	0.399
θ range [deg]	5.87 to 52.744	5.864 to 52.744	6.714 to 51.364	6.348 to 52.742	5.82 to 50.054	6.582 to 52.744	6.62 to 52.744	6.686 to 52744	6.612 to 52.744
Reflns collected	75467	25165	38190	89535	46355	65779	133482	66093	124137
R_{int}	0.0376	0.0343	0.0584	0.0512	0.0801	0.0369	0.0764	0.0388	0.0494
Completeness	99.9%	99.9%	99.8%	99.8%	99.8%	99.8%	99.8%	99.8%	99.8%
No. of data/restr/param	12663/262/713	4192/0/214	16436/883/1269	12657.714/879	14873/1923/1224	15632/633/1042	14061/760/1001	13011/324/897	24757/1056/1806
R_1 [$I > 2\sigma(I)$]	0.0304	0.0183	0.0618	0.0586	0.2744	0.0446	0.0429	0.0534	0.0445
wR_2 [all data]	0.0943	0.0636	0.1860	0.1672	0.6304	0.1139	0.1152	0.1240	0.1161
GoF	1.165	1.231	1.010	1.020	2.559	1.052	1/037	1.154	1.019
Largest diff. pk and hole [eÅ^{-3}]	1.05/-1.03	0.7/-0.85	1.02/-0.46	1.19/-0.66	17.15/-1.80	0.74/-1.16	0.73/-0.52	0.58/-0.42	0.81/-0.58
Flack (*x*)	-	-	-	-	-	-	-	-	-

3. 5 References

1. E. Peris, *Topics in Organomet. Chem.*, 2007, **21**, 83-116.
2. M. Raynal, C. S. J. Cazin, C. Vallée, H. Olivier-Bourbigou and P. Braunstein, *Organometallics*, 2009, **28**, 2460-2470.
3. A. Collado, A. Gomez-Suarez, A. R. Martin, A. M. Z. Slawin and S. P. Nolan, *Chem. Commun.*, 2013, **49**, 5541-5543.
4. R. Visbal, A. Laguna and M. C. Gimeno, *Chem. Commun.*, 2013, **49**, 5642-5644.
5. K. Namitharan, T. Zhu, J. Cheng, P. Zheng, X. Li, S. Yang, B.-A. Song and Y. R. Chi, *Nat. Commun.*, 2014, **5,** 3982.
6. M. Poyatos, M. Sanaú and E. Peris, *Inorg. Chem.*, 2003, **42**, 2572-2576.
7. K. Öfele, *J. Organomet. Chem.*, 1968, **12**, P42-P43.
8. H. W. Wanzlick and H. J. Schönherr, *Angew. Chem. Int. Ed.*, 1968, **7**, 141-142.
9. J. C. Garrison and W. J. Youngs, *Chem. Rev.*, 2005, **105**, 3978-4008.
10. F. Lazreg, M. Lesieur, A. J. Samson and C. S. J. Cazin, *Chem. Cat. Chem*, 2016, **8**, 209-213.
11. M. R. L. Furst and C. S. J. Cazin, *Chem. Commun.*, 2010, **46**, 6924-6925.
12. X. Hu, I. Castro-Rodriguez and K. Meyer, *Chem. Commun.*, 2004, 2164-2165.
13. B. Liu, X. Liu, C. Chen, C. Chen and W. Chen, *Organometallics*, 2012, **31**, 282-288.
14. E. Oehlke, T. Kückmann and U. Abram,*Z. Anorg. Allg. Chem.*, 2007, **633**, 830-834.
15. I. J. B. Lin and C. S. Vasam, *Comments Inorg. Chem.*, 2004, **25**, 75-129.
16. P. L. Arnold, *Heteroatom Chem.*, 2002, **13**, 534-539.
17. R. E. Andrew, C. M. Storey and A. B. Chaplin, *Dalton Trans.*, 2016, **45**, 8937-8944.
18. Y. D. Bidal, O. Santoro, M. Melaimi, D. B. Cordes, A. M. Z. Slawin, G. Bertrand and C. S. J. Cazin, *Chem. Eur. J.*, 2016, **22**, 9404-9409.
19. S.-T. Liu, C.-I. Lee, C.-F. Fu, C.-H. Chen, Y.-H. Liu, C. J. Elsevier, S.-M. Peng and J.-T. Chen, *Organometallics*, 2009, **28**, 6957-6962.
20. S. W. Reilly, C. E. Webster, T. K. Hollis and H. U. Valle, *Dalton Trans.*, 2016, **45**, 2823-2828.
21. S. T. Liddle, I. S. Edworthy and P. L. Arnold, *Chem. Soc. Rev.*, 2007, **36**, 1732-1744.
22. B. R. M. Lake and C. E. Willans, *Organometallics*, 2014, **33**, 2027-2038.
23. C. Boehme and G. Frenking, *Organometallics*, 1998, **17**, 5801-5809.

24. Z. Xi, X. Zhang, W. Chen, S. Fu and D. Wang, *Organometallics*, 2007, **26**, 6636-6642.

25. B. Cetinkaya, P. Dixneuf and M. F. Lappert, *J.Chem. Soc., Dalton Trans.*, 1974, 1827-1833.

26. P. B. Hitchcock, M. F. Lappert and P. L. Pye, *J. Chem. Soc., Dalton Trans.*, 1978, 826-836.

27. D. Kremzow, G. Seidel, C. W. Lehmann and A. Fürstner, *Chem. Eur. J.*, 2005, **11**, 1833-1853.

28. M. Viciano, M. Poyatos, M. Sanaú, E. Peris, A. Rossin, G. Ujaque and A. Lledós, *Organometallics*, 2006, **25**, 1120-1134.

29. L. Mercs and M. Albrecht, *Chem. Soc. Rev.*, 2010, **39**, 1903-1912.

30. G. C. Fortman and S. P. Nolan, *Chem. Soc. Rev.*, 2011, **40**, 5151-5169.

31. H. D. Velazquez and F. Verpoort, *Chem. Soc. Rev.*, 2012, **41**, 7032-7060.

32. M. N. Hopkinson, C. Richter, M. Schedler and F. Glorius, *Nature*, 2014, **510**, 485-496.

33. A. Neveling, G. R. Julius, S. Cronje, C. Esterhuysen and H. G. Raubenheimer, *Dalton Trans.*, 2005, 181-192.

34. A. B. Chaplin, *Organometallics*, 2014, **33**, 3069-3077.

35. S. A. Hauser, I. Prokes and A. B. Chaplin, *Chem. Commun.*, 2015, **51**, 4425-4428.

36. S. Würtz, C. Lohre, R. Fröhlich, K. Bergander and F. Glorius, *J. Am. Chem. Soc.*, 2009, **131**, 8344-8345.

37. G. Altenhoff, R. Goddard, C. W. Lehmann and F. Glorius, *J. Am. Chem. Soc*, 2004, **126**, 15195-15201.

38. R. Dorta, E. D. Stevens and S. P. Nolan, *J. Am. Chem. Soc.*, 2004, **126**, 5054-5055.

39. S. Burling, S. Douglas, M. F. Mahon, D. Nama, P. S. Pregosin and M. K. Whittlesey, *Organometallics*, 2006, **25**, 2642-2648.

40. A. B. Chaplin, *Organometallics*, 2014, **33**, 624-626.

41. L. Mercs, A. Neels, H. Stoeckli-Evans and M. Albrecht, *Dalton Trans.*, 2009, 7168-7178.

42. R. E. Andrew, L. Gonzalez-Sebastian and A. B. Chaplin, *Dalton Trans.*, 2016, **45**, 1299-1305.

43. G. T. S. Andavan, E. B. Bauer, C. S. Letko, T. K. Hollis and F. S. Tham, *J. Organomet. Chem.*, 2005, **690**, 5938-5947.

44. M. S. Jeletic, I. Ghiviriga, K. A. Abboud and A. S. Veige, *Organometallics*, 2007, **26**, 5267-5270.

45. M. S. Jeletic, M. T. Jan, I. Ghiviriga, K. A. Abboud and A. S. Veige, *Dalton Trans.*, 2009, 2764-2776.

46. S. G. Bott, A. W. Coleman and J. L. Atwood, *J. Am. Chem. Soc*, 1986, **108**, 1709-1710.

47. J. W. Steed and J. L. Atwood, in *Supramol. Chem.*, John Wiley & Sons, Ltd, 2009, pp. 105-222.

48. T. Fahlbusch, M. Frank, G. Maas and J. Schatz, *Organometallics*, 2009, **28**, 6183-6193.

49. X.-Y. Yu, H. Sun, B. O. Patrick and B. R. James, *Eur. J. Inorg. Chem.*, 2009, 1752-1758.

50. I. Dinarès, C. G. Miguel, N. Mesquida and E. Alcalde, *J. Org. Chem.*, 2008, **74**, 482–485.

51. N. Kuhn and T. Kratz, *Synthesis*, 1993, **1993**, 561-562.

52. G. Giordano and R. H. Crabtree, *Inorg. Synth.*, 1990, **28**, 88-90.

53. W. E. Buschmann and J. J. Miller, *Inorg. Synth.*, 2002, **33**, 83-85.

54. J. A. McCleverty, G. Wilkinson, L. G. Lipson, M. L. Maddox and H. D. Kaesz, *Inorg. Synth.*, John Wiley & Sons, Inc., 1990, pp. 84-86.

55. G. M. Sheldrick, *Acta Cryst.*, 2008, **A64**, 112-122.

4.0 Coordination chemistry and potassium binding of calix[4]arene NCHS ligand **3**

Overview

This chapter presents the synthesis, characterisation and reactivity of rhodium and iridium complexes based on imidazol-2-thione functionalised calix[4]arene 3, and **I^{i}Pr$_2$Me$_2$S** ligands. Their ability to host potassium guests within the central cavity, despite, in some cases, unfavourable coulombic repulsion is then detailed. For comparison the potassium binding of calix[4]arenes bearing 0, 1 and 2 imidazol-2-thione donor groups have been studied in solution and the solid state.

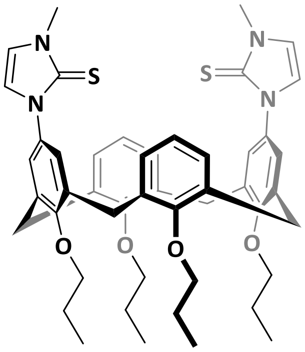

3

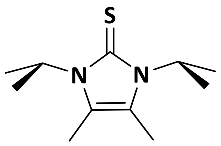

I^{i}Pr$_2$Me$_2$S

4.1 Introduction

4.1.1 Imidazol-2-thione complexes

In addition to their role as NHC precursors, imidazol-2-thiones find applications in the pharmaceutical industry (in particular 1-methylimidazol-2-thione and carbimazole are used for their antithyroid activity)[1, 2] and have received attention as ligands for the formation of transition metal complexes. An array of thione complexes of transition metals, such as Cu, Fe, Pd and Rh have been prepared, in addition to main-group elements such as Bi, Sb and alkali metals.[3-8] This section will describe the binding properties of imidazole-2-thione ligands and provide representative examples of their complexes.

4.1.1.1 Structure and binding

The coordination of thiones to metal centres occurs *via* donation of one or two filled p-orbitals on sulfur. This can result in dymanic behaviour in solution, observed by broadening of resonances observed by ^{1}H NMR spectroscopy, and is reflected by small C-S-M angles observed in the solid state (**Figure 4.1**, **Table 4.1**). NHCS ligands show quite different steric and electronic donor properties to their parent carbenes (**Table 4.1**) including increased S/C-M bond lengths and a distinct upfield shift of the N$\underline{C}$(S)N resonance.[9, 10] Notably NHCS ligands can be used to bridge transition metal centres (*vide infra*).

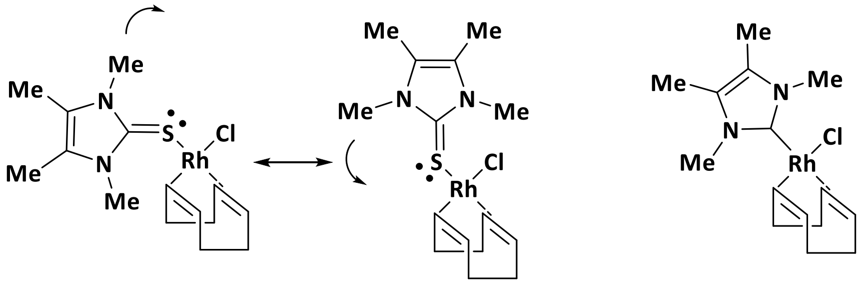

Figure 4.1: [Rh(L)(COD)Cl] complexes L = IMe$_2$Me$_2$S (left), IMe$_2$Me$_2$ (right)

Table 4.1: Comparison of bond lengths (Å) and angles (°) and ^{13}C NMR data of [Rh(L)(COD)Cl] complexes

L = **IMe_2Me_2** or **IMe_2Me_2S**

L	C-S	S/C-Rh	C-S-Rh	S/C-Rh-Cl	δ $N\underline{C}N/N\underline{C}SN$
IMe_2 Me_2S	1.725(2)	2.3602(7)	108.81(7)	92.95(2)	156.3 (CD_2Cl_3)
IMe_2Me_2	-	2.016(2)	-	166.00(4)	178.8 (CD_2Cl_2)

4.1.1.2 Complexes of monodentate NHCS ligands

A range of complexes of monodentate imidazol-2-thione complexes have been reported. Raubenheimer *et al*. have reported the synthesis of rhodium(I) complexes by reaction between $[Rh(COD)Cl]_2$ and **$I^iPr_2Me_2S$** (**A122**), subsequent displacement of the cyclooctadiene ligand with CO affords **A123**, which is also a precursor to complex **A124** (**Scheme 4.1**).[4] The authors have also reported the synthesis of mixed thione-NHC Rh(I) complexes such as **A125** (**Figure 4.2**).[4] Monodentate imidazole-2-thione ligands have also been used in the synthesis of di- and tetra- substituted complexes (**A126** and **A127**),[8] and μ-halide bridged complexes (**A128**) (**Figure 4.2**) which, upon transmetallation, form a μ-S bridged complex (**A129**).[11] Bridging thione ligands, notably show an increase in M=S bond length compared to terminal modes (2.331(2) and 2.335(2) Å *cf.* 2.318(2) Å) respectively.

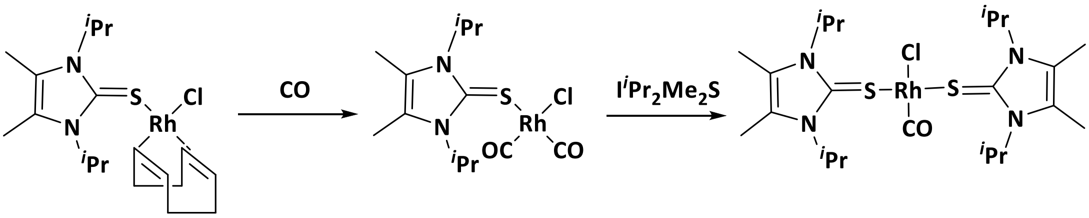

A122 **A123** **A124**

Scheme 4.1: Rh(I) imidazol-2-thione complexes reported by Raubenheimer

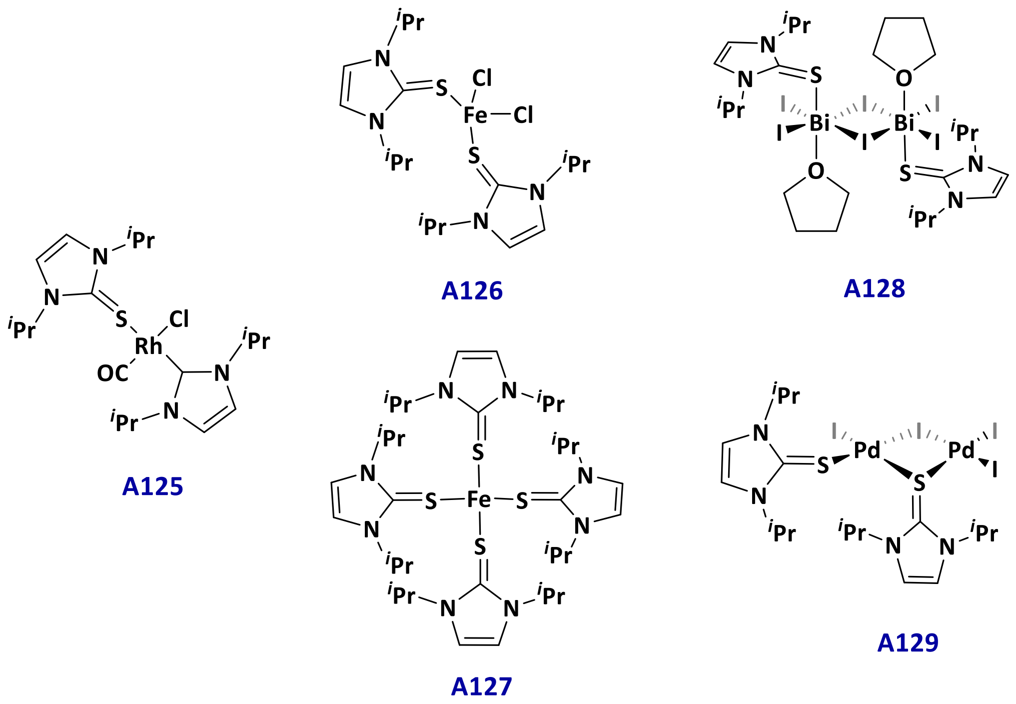

Figure 4.2: Monodentate imidazole-2-thione complexes

4.1.1.3 Complexes of multidentate NHCS ligands

A number of complexes containing multidentate imidazole-2-thione ligands, including pincer type ligands are known (**A130** and **A131**, **Figure 4.3**).[6, 12] Miecznikowski *et al*. used the zinc pincer complex of an SNS pincer ligand as a model for the zinc active site in liver dehydrogenase (that adopts a *pseudo*-tetrahedral geometry). The gold-based SNS pincer has been used in the reduction of 4-nitrophenol by Jia.[6] The tri-dentate hydrotris(methimazolyl)borate ligand **A132** has been reported in the formation of a large range of transition metal and main group complexes. These adopt a variety of motifs including mono metallic complexes such as **A133** to **A138** which adopt a sandwich motif. The indium complex **A133** in particular forms an almost regular S_6 octohadral complex (S-In-S angles found between 86.1 and 87.7°). μ-Halide bridged bimetallic complexes based on the ligand **A132** have also been reported e.g. **A139** to **A141**.[13, 14]

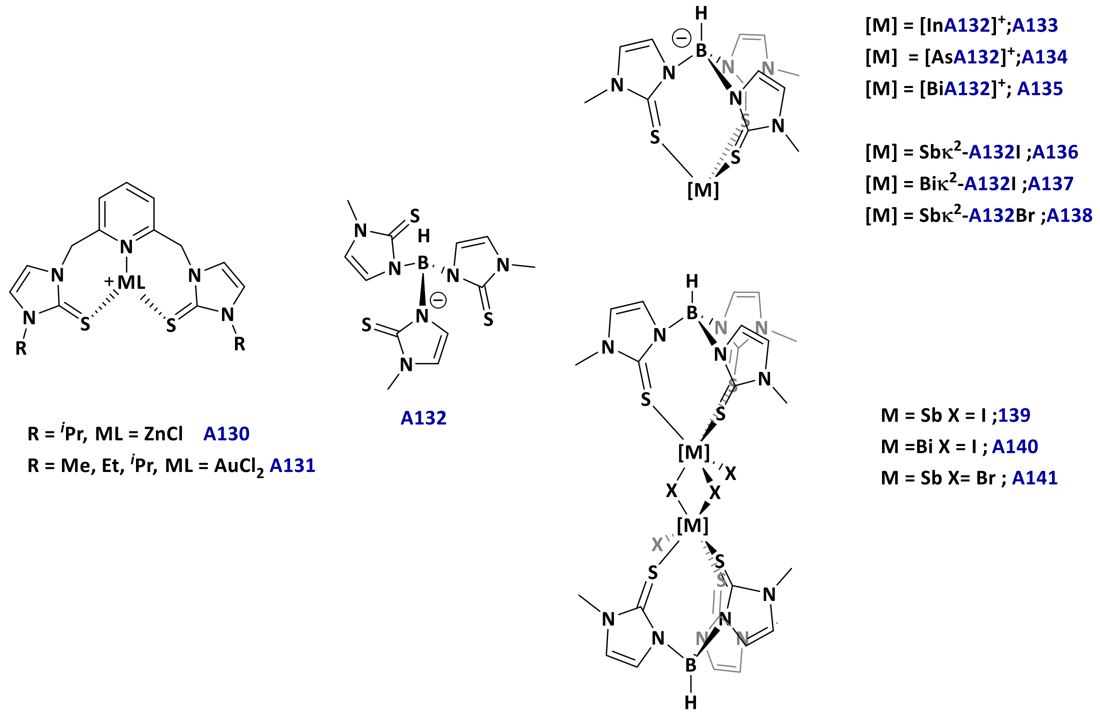

Figure 4.3 Multidentate imidazol-2-thione complexes

4.1.2 Alkali metal binding

Alkali metal cations, in particular Na^+ and K^+, play vital roles in many physiological systems including modulating enzyme activity.[15] As such, development of supramolecular systems which are able to bind to alkali metal cations by non-covalent interactions have been a focus of investigation. Such investigations have led to the development of cation sensors, molecular switches and methods for disposal of radioactive ^{137}Cs.[16-20] A plethora of supramolecular species have therefore been developed with complementary cavity sizes and chelating structures resulting in highly selective binding properties.[15,21-23]

One of the most common groups of alkali metal hosts are crown ethers (**Figure 4.4**). These simple macrocylic structures form well defined complexes with alkali metals by coordination of the ether functionalities: the hydrophobic ring exterior also results in good solubility in non-polar solvents.[24-26] Variation of the ring size allows selective binding for example 15-crown-5 binds most strongly to Na^+, whereas 16-crown-8 shows a greater affinity for K^+

cations. Increased binding strengths have been found for cryptands, initially developed by Lehn.[27] Cryptands typically contain two bridging nitrogen atoms joined by three oligo oxa chains of different lengths, resulting in spherical, ellipsoidal or cylindrical supramolecular capsules. The increased number of ligating atoms relative to that in crown ethers results in higher binding affinity for cation guests although the cage structure results in slower kinetics (**Table 4.2**).[28,29]

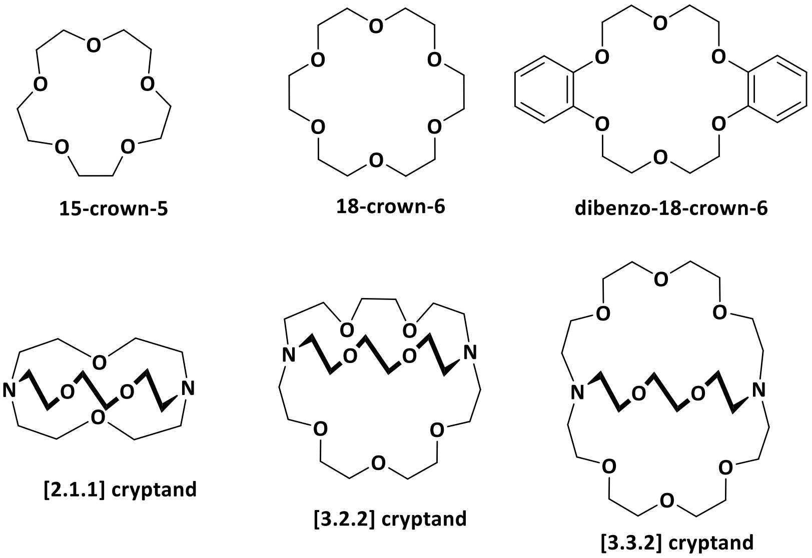

15-crown-5 **18-crown-6** **dibenzo-18-crown-6**

[2.1.1] cryptand **[3.2.2] cryptand** **[3.3.2] cryptand**

Figure 4.4: Structures of common crown ethers and cryptands

Table 4.2: 18-crown-6 and cryptand Na^+ and K^+ binding constants

Host	Cavity size	Na^+	K^+
18-crown-6	2.60	4.35	6.07
[2.1.1]	1.6	6.4	2.3
[3.2.2]	3.6	4.8	>7
[3.3.2]	4.2	3.2	6.0

(a) K_S ($\log_{10}$) for anhydrous methanol at 25°C. (b) Na^+ ~ 2.0 Å and K^+~2.8 Å

Spherands, rigid macrocycles consisting of sp^2 hybridised atoms show higher selectivity for alkali metal cations than crown ether and cryptands due to their pre organised and more rigid structures. Many other species have been adapted for the coordination of alkali metal cations by functionalisation with crown-ether type chains.[30-33]

4.1.3 Alkali metal binding by calix[4]arene hosts

The ability of calix[4]arenes to bind alkali metals has been well explored, this largely consists of variants bearing donor appendages, most commonly oxygen-based substituents, supported by π-donation from the calix[4]arene scaffold.[21, 22, 34] Calix[4]arenes bearing no formally donating functionality in the upper rim, for example **A1** or **A2** have also been shown to bind alkali metal cations, presumably stabilised by cation-π interactions.[35] Binding of alkali metal cations has been shown to be highly dependent on the calix[4]arene conformation, for example extraction of aqueous alkali metal picrates into CH_2Cl_2 has been used to determine the selectivity of the isomers of bisethoxycarbonylmethoxycalix[4]arene **A142** (**Figure 4.4**), the results of which are outlined in **Table 4.2**.[36]

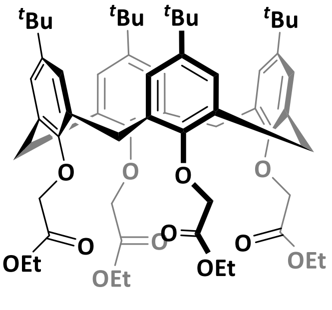

A142

Figure 4.4: Structure of bisethoxycarbonylmethoxycalix[4]arene

Table 4.2: Percent extraction of alkali metal picrates reported by Shinkai *et al.*

Isomer	Li^+ /% extr.	Na^+ /% extr.	K^+ /% extr.	Cs^+ /% extr.
cone	17.6	100	86.1	24.6
partial cone	5.2	62.1	94.3	49.9
1,2-alternate	0	22.1	70.0	54.0
1,3-alternate	1.5	88.8	100	98.9

Calix[4]tubes were first introduced by Beer and co-workers in 1997 and consist of rigid ether-bridged bis-calix[4]arene structures (**A143**, **Figure 4.5**).[37] These calix[4]tubes show a high selectivity for the coordination of potassium ions over other alkali metal ions (O···K bond distances of 2.8 Å *cf.* 2.8 Å observed in [K·18-crown-6], *vide infra*). Binding of the potassium cation within the ether channel was observed by ^1H NMR spectroscopy and in the solid state by X-ray diffraction. Molecular mechanics calculations showed the preference for the potassium to pass through the tube along the main axis. This directionality was presumed to be a result of weak complexation within the calix[4]arene cavities.

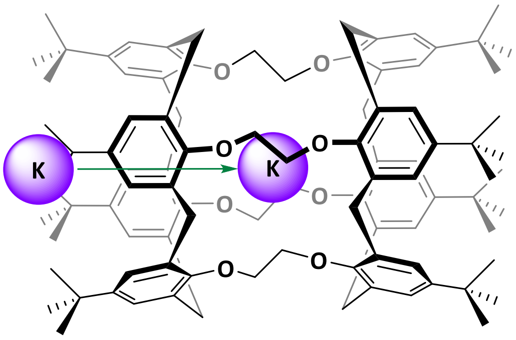

A143

Figure 4.5: Calix[4]tube reported by Beer *et al.*

1,3-Alternate scaffolds have been exploited by a large number of groups for example, Beer *et al*. have appended 1,3-alternate calix[4]arenes with amide functionalities in order to form inclusion complexes with one or two equivalents of potassium cation.[38, 39] Cone and 1,3-calix[4]arene structures are also readily adapted to include crown and azocrown species, for example the synthesis of 1,3-dialkoxy-*p*-*tert*butylcalix[4]arenes in both cone and 1,3-alternate conformations have been described by Rheinhoudt *et al*. resulting in the selective coordination of potassium along the lower rim (**A144**, **Figure 4.6**).[40] Wu *et al*. have also developed a number of calix[4]crown complexes based upon phenolate ligands which allow free rotation of the phenol units.[41] Both 1,2- and 1,3-functionalised calix[4]arene complexes **A145** and **A146** are obtained upon deprotonation one of the phenolic groups. The resulting anionic phenolate donor is therefore able to stabilise of the potassium cation within the calix[4]arene cavity.

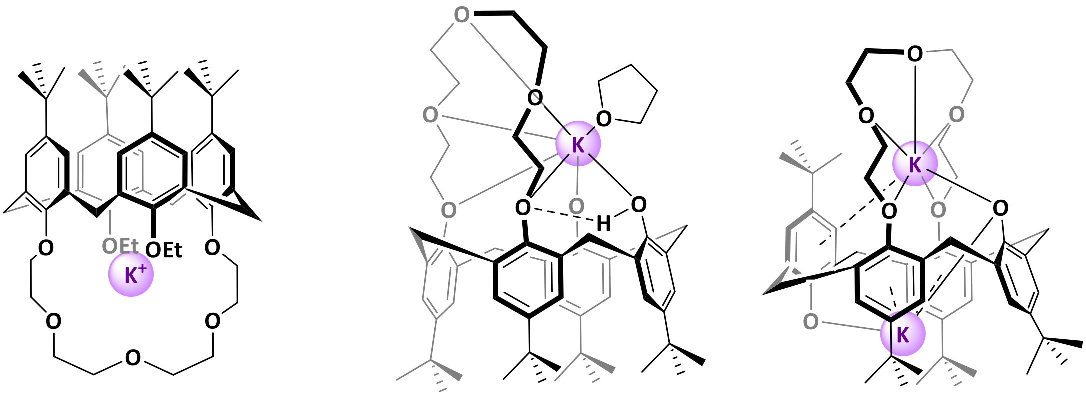

A144 **A145** **A146**

Figure 4.6: Calix[4]crown potassium complexes

The presence of charged phenolate groups has also been shown to promote binding of alkali metals within calix[4]arene cavites. For example, the caesium complex **A147** has been reported by White *et al*. The solid state structure of **A147** was determined by X-ray diffraction, where short Cs-C distances of 3.57 Å, indicative of strong stabilisation from the calix[4]arene scaffold, were observed (**Figure 4.7**).[42] Another example, **A148**, reported by Wu *et al*. features two coordinated potassium cations, one within the calix[4]arene cavity and one coordinated to the lower rim with or without further stabilisation from an 18-crown-6 auxiliary ligand.[41]

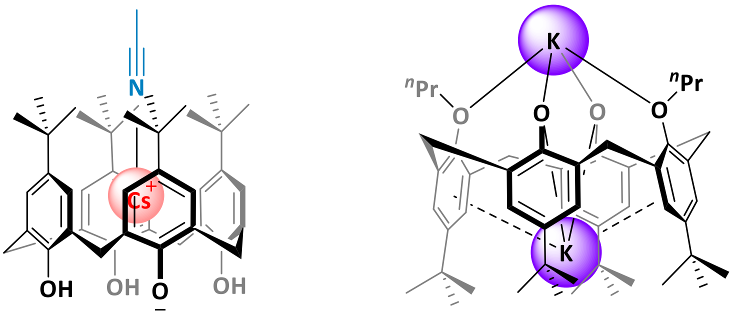

A147 **A148**

Figure 4.7: Anionic calix[4]arene host-guest complexes

4.2 Results and discussion

4.2.1 Synthesis and characterisation of NHCS complexes

Reaction of ligand **3** with $[M(COD)Cl]_2$ dimers (M = Rh or Ir) in CH_2Cl_2 at room temperature in the presence of $Na[BAr^F{}_4]$ as a halide extractor resulted in the formation of mononuclear complexes **11a** and **12a** in acceptable yields (52% and 45% respectively, **Scheme 4.2**). **I^{i}Pr$_2$Me$_2$S** was found to react in an analogous fashion and **11b** and **12b** were formed in 74% and 67% yields, respectively. All of these new complexes were fully characterised by ^1H, ^{13}C NMR spectroscopy, ESI-MS, microanalysis and X-ray diffraction (**Figure 4.8**).

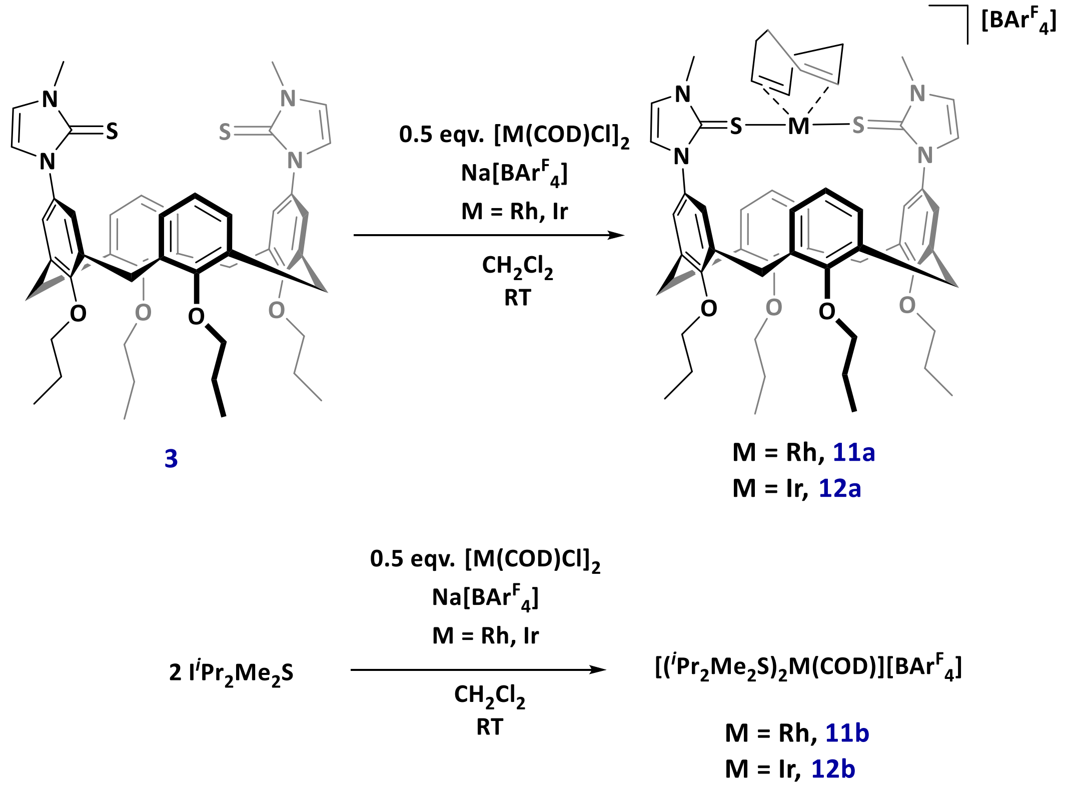

Scheme 4.2: Synthesis of Rh and Ir complexes of **3** and **I^{i}Pr$_2$Me$_2$S**

The solid state structures of **11a** and **12a** determined by X-ray diffraction, are less puckered than the free ligand **3**. This clear from the increased CPR values of = 0.5500(3) and 0.5500(6) for **11a** and **12a** respectively, compared to **3** (0.419(1)). Rotation of the imidazole-2-thione appendages from their antiparallel positions in **3** and the “bent” coordination mode of the thione donors (M-S-C *ca.* 100°) results in the positioning of the transition metal to one side of the calix[4]arene cavity (**Figure 4.9**, **Table 4.3**). Very similar bonding metrics are observed for the model complexes **11b** and **12b**, as seen in **Table 4.3**, although S-M-S and C-S-M bond angles are slightly larger, than in **11a** and **12a**, presumably because the latter thione donors are partially constrained by the calix[4]arene scaffold.

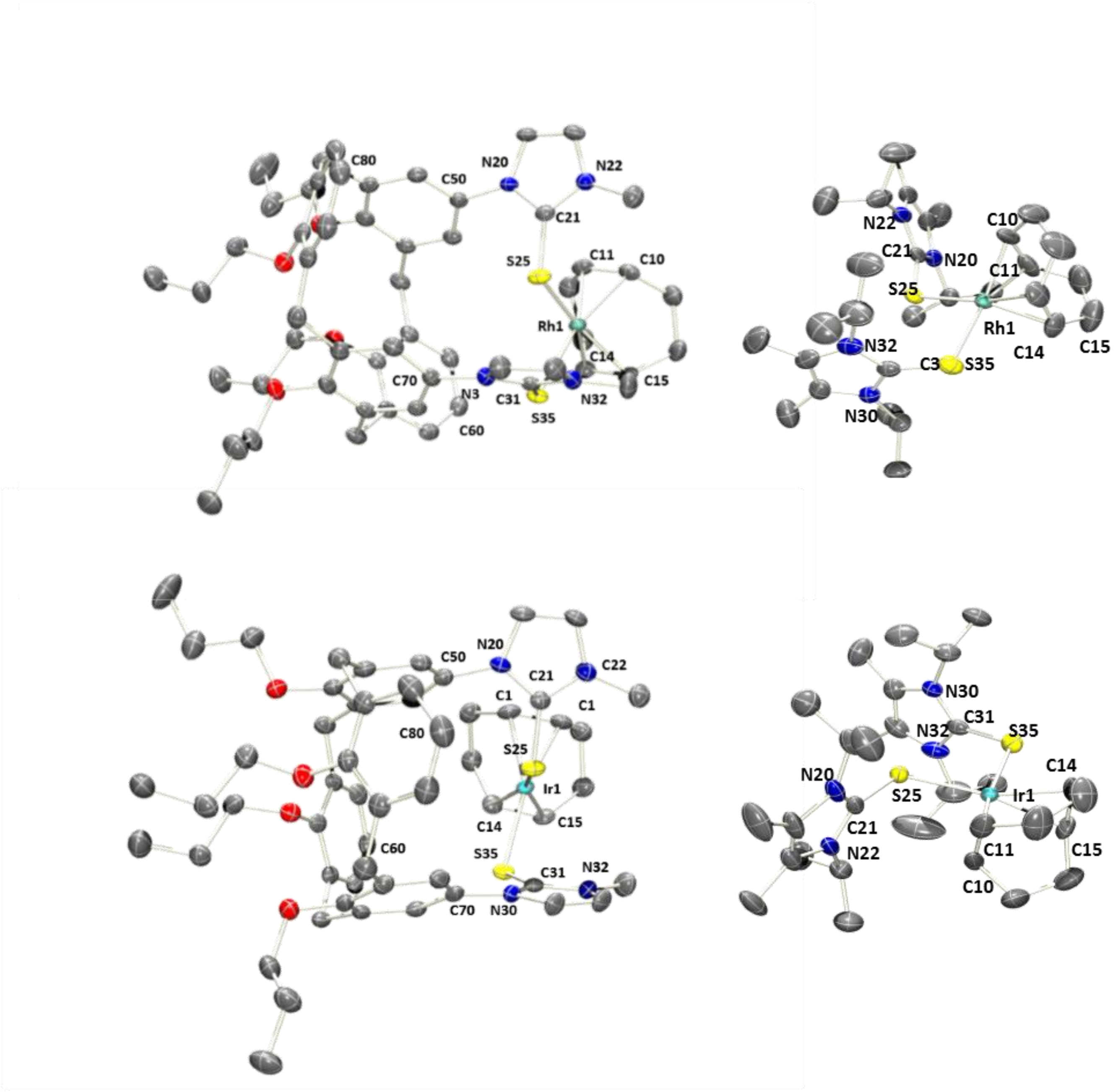

Figure 4.8: Solid-state structures of **11a** (top left)**, 12a** (bottom left), **11b** (top right) and **12b** (bottom right). Thermal ellipsoids for selected atoms drawn at the 50% probability level. Hydrogen atoms, anions, minor disordered components and solvent molecules are omitted for clarity. Selected bond lengths (Å) and angles (°): S25··S35, 3.1572(6); C21··C31, 4.621 ; Rh1-S25, 2.3515(5); Rh1-S35, 2.3756(5); Rh1-C10, 2.158(2); Rh-C11, 2.120(2); Rh1-C14, 2.132(2); Rh1-C15, 2.132(2); S25-C21, 1.705(2); S35-C31, 1.720(2); S25-Rh1-S35, 83.808(18), C21-S25-Rh1, 109.72(7); C31-S35-Rh1, 108.76(6); CPR = 0.5500(3) . **11b** Rh1-S25, 2.3706(6); Rh1-S35, 2.3671(7); Rh1-C10, 2.120(3); Rh1-C11, 2.130(3); Rh1-C14, 2.133(3); Rh1-C15, 2.137(3); S25-C21, 1.727(3); S35-C31, 1.729(3); S35-Rh1-S25, 89.06(2);C11-Rh1-S35, 158.90(11); C11-Rh1-C14, 81.12(13); C21-S25-Rh1, 111.44(8); C31-S35-Rh1, 110.23(9). **12a** S25··S35, 3.1568(12); C21··C31, 4.618(4); Ir1-S25, 2.3390(8); Ir1-S35, 2.3604(8); Ir1-C10, 2.150(3); Ir1-C11, 2.122(3); Ir1-C14, 2.124(3); Ir1-C15, 2.131(3); S25-C21, 1.709(3), S35-C31, 1.732(3); S25-Ir1-S35, 84.40(3); C10-Ir1-S25, 101.71(10); C10-Ir1-S35, 165.21(10); C11-Ir1-S25, 97.24(9); C11-Ir1-S35, 154.99(11); C11-Ir1-C10, 38.45(13); C11-Ir1-C14, 81.51(13); C11-Ir1-C15; 96.95(13); C14-Ir1-S25, 160.36(10); C14-Ir1-S35, 88.66(10); C14-Ir1-C10, 89.53(14); C14-Ir1-C15, 39.05(13); C15-Ir1-S25, 158.50(10); C15-Ir1-S35, 89.51(10); C15-Ir1-C10, 79.91(13); C21-S25-Ir1, 109.63(11); C31-S35-Ir1, 108.46(11) CPR = 0.5500(6). **12b** Ir1-S25, 2.3496(8); Ir1-S35, 2.3459(9); Ir1-C10, 2.109(3); Ir1-C11, 2.117(4); Ir1-C14, 2.119(3); Ir1-C15, 2.129(3); S25-C21, 1.728(3); S35-C31, 1.732(3); S35-Ir1-S25, 89.50(3); C21-S25-Ir1, 111.20(10); C31-S35-Ir1, 110.02(11).

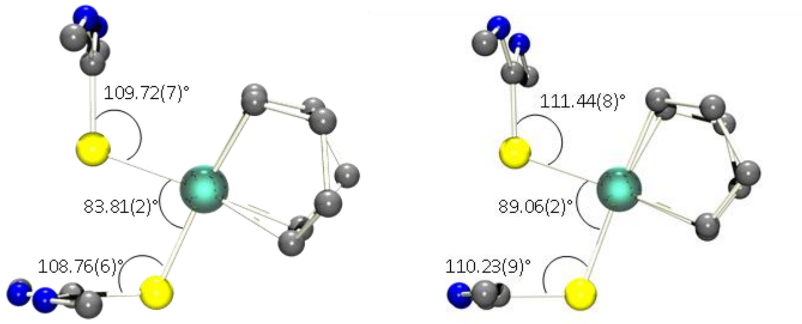

11a **11b**

Figure 4.9: Comparison of partial crystal structures of **11a** and **11b**

Table 4.3*:* Bond lengths and angles of complexes **11a**, **11b**, **12a** and **12b** observed in the solid state structures

Complex	S-M-S /°	C-S-M /°	S-M /Å	C-S/Å	M-CC$_{nt}$(COD) / Å	NCSN/δ	δ CH {COD}
11a	83.808(18)	109.72/108.76	2.3515(5)/2.3756(5)	1.705(2)/1.720(2)	2.030(2)/2.)15(2)	156.4	82.9/81.4
11b	89.06(2)	111.44/110.23	2.3706(6)/2.3671(7)	1.727(3)/1.729(3)	2.010(3)/2.020(3)	151.8	81.1
12a	84.40(3)	109.63/108.46	2.3390(8)/2.3604(8)	1.709(3)/1.732(3)	2.017(3)/2.005(3)	156.6	66.2/63.0
12b	89.50(3)	111.20/110.02	2.3496(8)/2.3459(9)	1.728(3)/1.732(3)	1.994(4)/2.005(3)	149.2	64.6

In solution **11a** and **12a** show C_s symmetry, most likely due to dynamic interconversion of the C-S-M angle about the sulfur atom at room temperature. This symmetry is evidenced by the two sets of diastereotopic ArCH$_2$Ar methylene bridge resonances by ^{1}H NMR spectroscopy (4.60, 4.56, 3.34, 3.22, $^2J_{HH}$ = *ca.* 13 Hz, **11a**; Ir: 4.59, 4.57, 3.35, 3.29, $^2J_{HH}$ = *ca.* 13 Hz, **12a**) and single ^{1}H and ^{13}C{^{1}H}resonances for the NMe group observed at δ 3.76 and 37.2 (**11a**) and δ 3.73, δ 37.1 (**12a**) respectively. Similar dynamics and C_{2v} symmetry is observed in solution for model complexes **11b** and **12b**, which have only one ^{13}C COD{$\underline{C}$H} resonance due to fluxional behaviour of **I^{i}Pr$_2$Me$_2$S** in solution **Table 4.4**. N$\underline{C}$SN and COD{$\underline{C}$H} resonances for **11b** and **12b** show a slight upfield shift with respect to **11a** and **12a**.

4.2.2 Reactivity of NHCS complexes

Reactivity of the isolated thione complexes **11** and **12** was then followed, primarily by ^{1}H NMR spectroscopy (**Scheme 4.3**). No notable reactions were observed on placing **11** and **12** under H_2 at room temperature. The COD ligand, however, was easily displaced by stirring under an atmosphere of CO (1 atm). In this way, bis-carbonyl derivatives **13** and **14** were isolated, with excess COD removed by subsequent washings with hydrocarbon (yields: 53% (**13a**) and 58% (**14a**), 77% (**13b**) and 77% (**14b**)). Although the *cis*-carbonyl adducts could not be crystallised for analysis in the solid state, the *cis*-geometry of the carbonyl ligands was confirmed by IR spectroscopy **13a**: 2068, 2001 **14a**: 2055, 1984 **13b**: 2067, 2002 **14b**: 2052, 1983 cm^{-1}. The remarkable similarity of these stretching frequencies is demonstrative of their electronic similarities of the calix[4]arene and model complexes.

Addition of two equivalents of **I^{i}Pr$_2$Me$_2$S** to **11a** and **12a** in CD_2Cl_2 was used to determine the relative binding strengths of **3** to the transition metal centre. This resulted in approximate 1:6 **11a**:**11b** and 1:2.4 **12a**:**12b** ratios observed in solution by ^{1}H NMR spectroscopy. This suggests that despite the chelating nature of **3**, the **I^{i}Pr$_2$Me$_2$S** binds significantly more strongly to the rhodium(I) or iridium(I) centres. It is possible that this equilibrium is driven by relief of the strain about the S-M-S bonds observed in the calix[4]arene complexes **11a** and **12a**. Similarly, addition of bipyridine to **11a** or **11b** resulted in the rapid and quantitative formation of [Rh(bipy)(COD)][BAr$^F_4$] (**15a**) by ^{1}H NMR spectroscopy, the structure of which was confirmed by independent synthesis in the Chaplin group.[‡] The ^{1}H NMR resonances of **3** were found to be slightly shifted, presumably due to binding of bipy in solution; data showed good agreement with that obtained from mixing free **3** and bipy in solution. Intriguingly neither **12a** nor **12b** showed the same reactivity with bipy but instead single products that could not be attributed to either **3**, **12a** or [Ir(bipy)(COD)][BAr$^F{}_4$]. Further scrutiny suggests that in fact the adduct **16a** or **16b** (**Scheme 4.3**) was formed. This product independently formed, as observed by ^{1}H NMR spectroscopy, by addition of **3** to [Ir(COD)(bipy)][BAr$^F{}_4$] in CD_2Cl_2.

[‡] Synthesis from [Rh(COD)Cl]$_2$/[Ir(COD)Cl]$_2$, bipy, Na[BAr$^F{}_4$] in CH_2Cl_2 at r.t. by Jack Emerson-King, PhD student University of Warwick

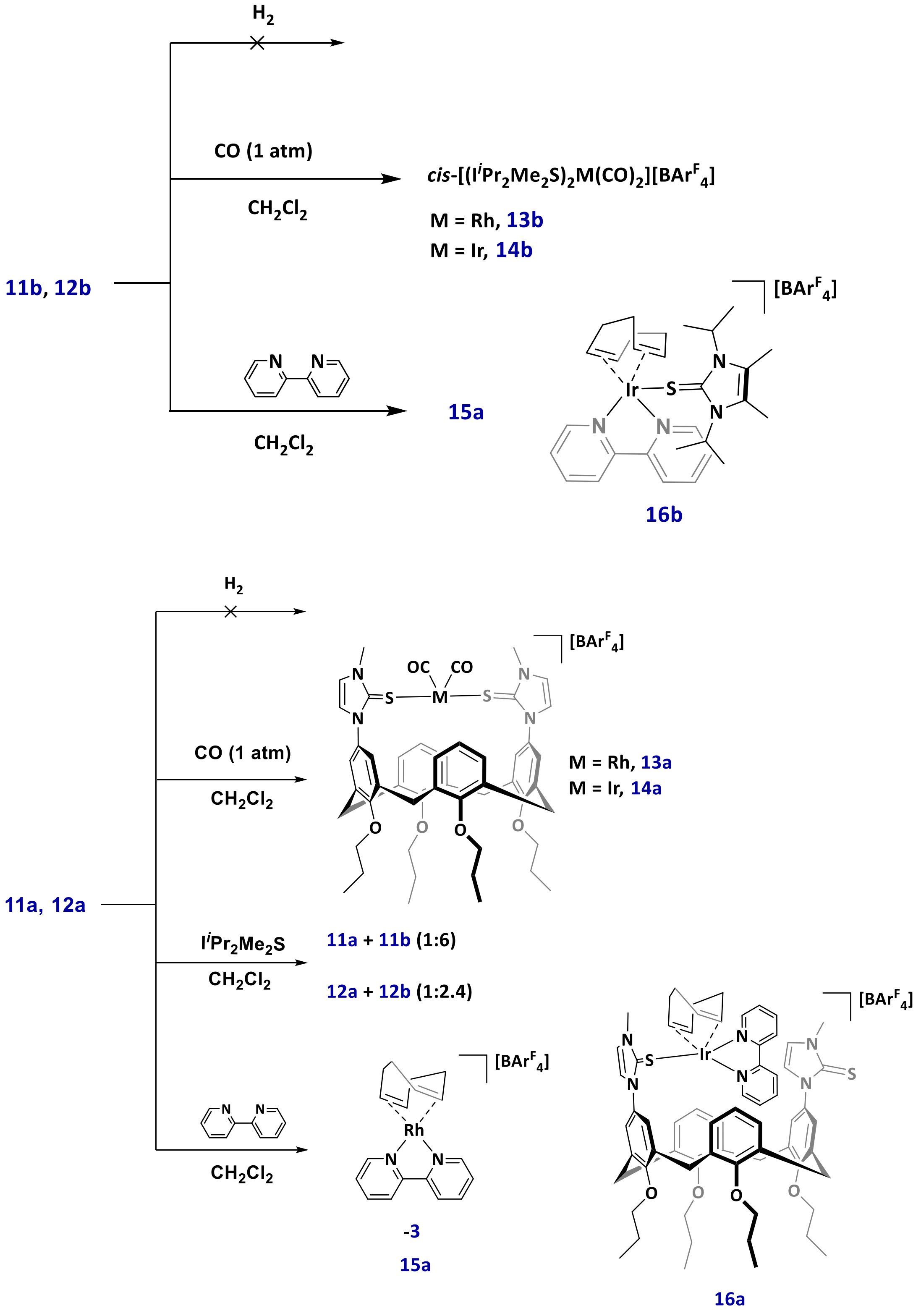

Scheme 4.3: Reactivity of **11**, **12**

4.2.3 Potassium binding studies

Early synthesis of the **11a** and **12a**, synthesised by deprotonation of **1a·2HI** using KHMDS in THF, resulted in the formation of crystalline products which confirmed the presence of potassium cations within the calix[4]arene cavity. Calix[4]arenes bearing potassium cations within the central cavity were then systematically produced by reaction of **A2**, **3**, **18**, **11a** and **12a** with K[BAr^F$_4$] in CH_2Cl_2 at room temperature (**Scheme 4.4**). Analysis by ^{1}H NMR spectroscopy indicated the formation of potassium adducts in each case, notably by the appearance of ^{1}H resonances for the [BAr^F$_4$] counter anion, at δ 7.71 – 7.75 and 7.56. 1:1 stochiometry for potassium binding was confirmed by ^{1}H NMR experiments with addition of 0.5, 1.1 and 5.0 equivalents of K[BAr^F$_4$] per calix[4]arene, which indicated slow exchange and formation of adducts in a 1:1 ratio as determined by integration of BAr^F resonances. Further confirmation of the presence of these complexes were observed by ESI-MS (not observable for **[11a·K][BAr^F$_4$]** or **[12a·K][BAr^F$_4$]**), and in the solid state by X-ray diffraction (**Table 4.4**). Bulk purity in each case was confirmed by microanalysis and reactions of the isolated product with an excess of 18-crown-6. This resulted in the reformation of the potassium free calix[4]arene host and K[18-crown-6]. The 1:1 ratio of the calix[4]arene host and K guest could therefore be monitored integration of BAr^F$_4$$^-$ signals measured by ^{1}H NMR spectroscopy.

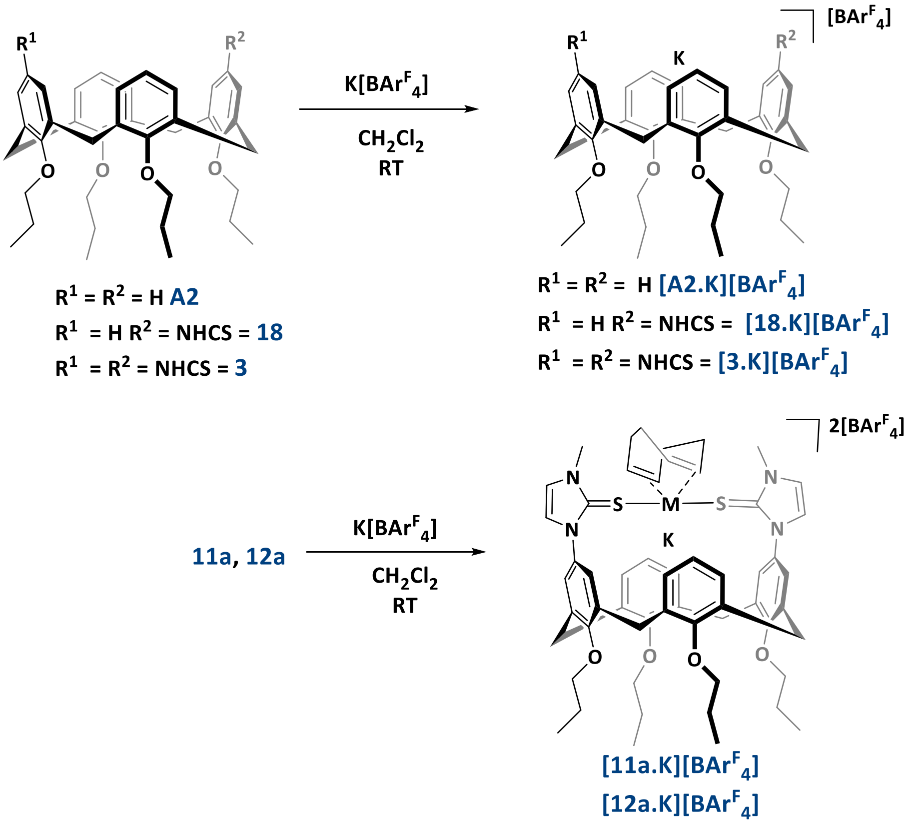

$R^1 = R^2 =$ H **A2**

R^1 = H R^2 = NHCS = **18**

$R^1 = R^2$ = NHCS = **3**

$R^1 = R^2 =$ H **[A2.K][BAr$^F_4$]**

R^1 = H R^2 = NHCS = **[18.K][BAr$^F_4$]**

$R^1 = R^2$ = NHCS = **[3.K][BAr$^F_4$]**

[11a.K][BAr$^F_4$]

[12a.K][BAr$^F_4$]

Scheme 4.4: Reactions of **A2**, **3**, **18**, **11a** and **12a** with K[BAr$^F_4$]

Table 4.4: Summary of characteristic ^{1}H resonances and bond lengths (Å) observed by X-ray diffraction

	[A2·K][BAr$^{F}_{4}$]	[18·K][BAr$^{F}_{4}$]	18	[3·K][BAr$^{F}_{4}$]	3	[11a·K][BAr$^{F}_{4}$]	11a	[12a·K][BAr$^{F}_{4}$]	12a
δ ^{1}H N$\underline{\text{C}}$SN	-	163.8	163.3	164.2	163.4	158.5	156.4	158.9	156.6
δ ^{1}H N$\underline{\text{C}}$H$_3$	-	35.6	35.5	35.4	35.6	37.4	37.2	37.3	37.1
δ ^{1}H NC$\underline{\text{H}}_3$	-	3.41	3.51	3.22	3.55	3.75	3.76	3.77	3.74
S···S (Å)	-	-	-	3.9644	7.739	2.9897	3.1572(6)	2.9933	3.1568(12)
C=S (Å)	-	1.686(2)	-	1.681(2)/1.679(2)	1.688(6)	1.718(4)/1.717(4)	1.720(2)/1.705(2)	1.729(5)/1.720(5)	1.709(3)/1.732(3)
K-Ar$_{Cnt}$ (Å)	2.791(11)	2.825(2)	-	2.712(2)	-	3.084(4)	-	3.068(5)	-
K-Ar$_{Cnt}$ (Å)	-	2.788(2)	-	2.711(2)	-	3.078(4)	-	3.065(5)	-
K-O56 (Å)	3.929(8)	3.9056(12)	-	4.001(15)	-	4.264(3)	-	4.245(4)	-
K-O66 (Å)	2.832(7)	2.8471(13)	-	2.8451(13)	-	3.149(3)	-	3.087(4)	-
K-O76 (Å)	-	3.9239(13)	-	3.9512(15)	-	4.212(3)	-	4.184(4)	-
K-O86 (Å)	-	2.8826(14)	-	2.8069(16)	-	3.534(3)	-	3.514(4)	-
K-S25 (Å)	-	3.2083(6)	-	3.4019(7)	-	3.4722(14)	-	3.5207(19)	-
K-S35 (Å)	-	-	-	3.4102(6)	-	3.5854(15)	-	3.6324(19)	-
K-M (Å)	-	-	-	-	-	3.7153(10)	-	3.6901(13)	-
SMS (°)	-	-	-	-	-	77.99(3)	83.808(18)	78.80(4)	84.40(3)
CPR	0.5827(20)	0.6092(4)	-	0.5536(4)	0.419(1)	0.7156(8)	0.5500(3)	0.7113(10)	0.5500(6)

18-crown-6 was chosen to probe the bulk purity of the calix[4]arene complexes due to its strong and selective binding to potassium. For comparison the unknown 18-crown-6 adduct of K[BAr$^F{}_4$] was isolated by recrystalisation from DCM/pentane. The colourless crystals were analysed by ^{1}H and ^{13}C NMR spectroscopy, ESI-MS, microanalysis and in the solid state by X-ray diffraction (**Figure 4.10**).

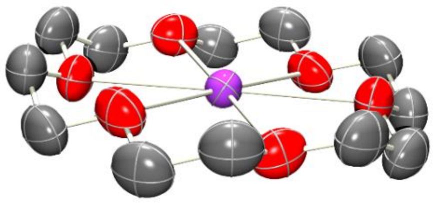

Figure 4.10: [18-crown-6·K][BAr$^F{}_4$] Thermal ellipsoids for selected atoms drawn at the 50% probability level. Hydrogen atoms, disordered components and anions omitted for clarity. Selected bond lengths (Å) and angles (°): K1-O2, 2.774(7); K1-O5, 2.747(7); K1-O8, 2.774(8); K1-O11, 2.783(7); K1-O14, 2.770(7); K1-O17, 2.778(7).

4.2.3.1 Calix[4]arene (A2)

[A2·K][BAr$^F{}_4$] was readily formed by addition of K[BAr$^F{}_4$] to **A2**, despite its lack of stabilising functionalities such as phenolate or thione donors. ^{1}H NMR spectra showed a downfield shift of all resonances, but most notably the aryl, ArC$\underline{H}_2$Ar and OCH$_2$ resonances, consistent with binding through cation-π and ether functionalities (**Figure 4.11**).

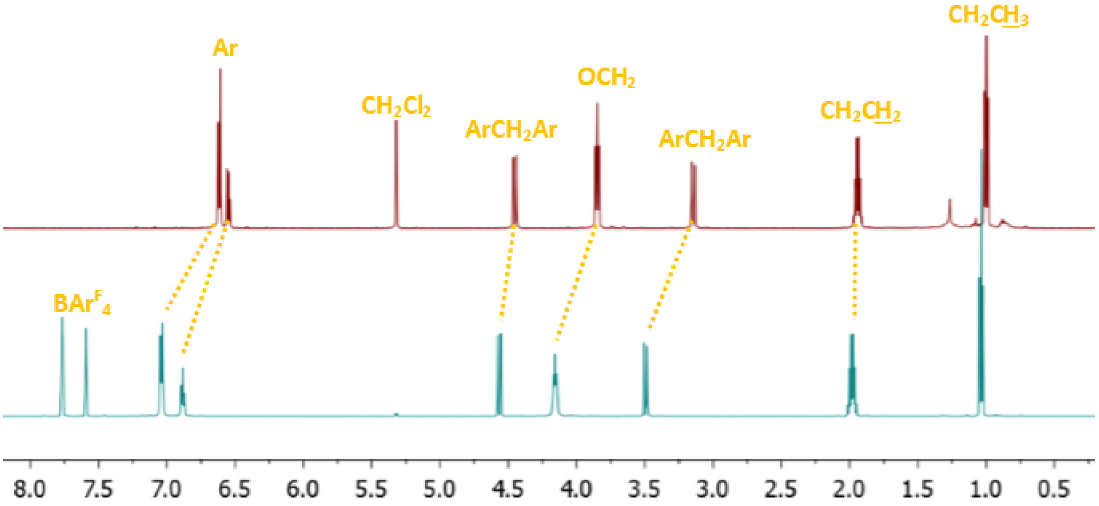

Figure 4.11: ^{1}H NMR spectra of **A2** (top) and isolated **[A2.K][BAr$^F{}_4$]** (CD_2Cl_2, 600 MHz)

In the solid-state structure of [**A2**·K][BAr^F$_4$] the potassium cation is observed well within the calix[4]arene cavity, with short K-Cnt bond distances of 2.791(11) Å for two opposing aryl rings (**Figure 4.12**). K-O bond of lengths 3.929(8) Å and 2.832(7) Å indicate only two of the phenol-ether groups bind strongly to the potassium. C_{4V} symmetry is observed in solution by ^{1}H and ^{13}C NMR spectroscopy indicating that the interactions observed in the solid state (C_{2v}) are dynamic in solution.

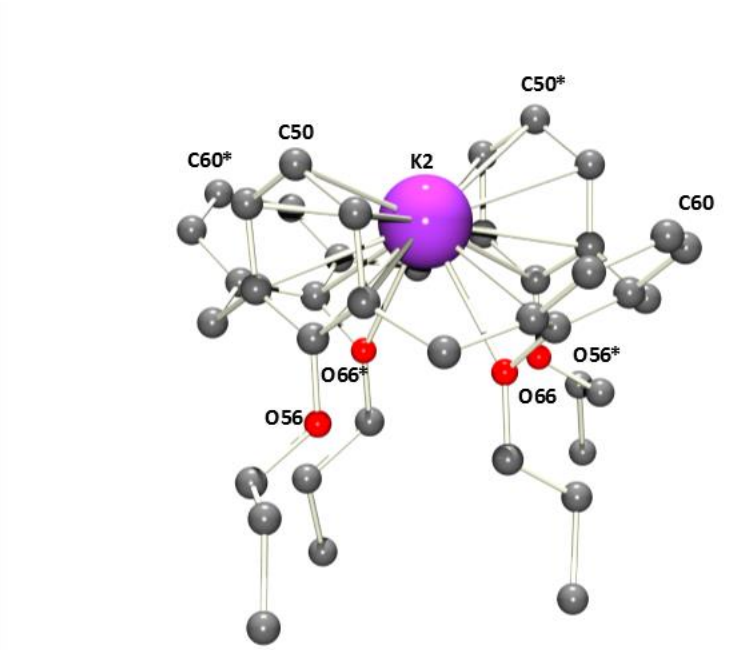

Figure 4.12: Solid-state structure of **[A2·K][BAr^F$_4$]** in ball and stick representation. Structure is disordered equally over special positions, anion, solvent and minor disordered components are omitted for clarity. Atoms denoted * are generated using the symmetry operation *3-X,3/2-Y,+Z* Selected bond lengths (Å) and angles (°): K-Cnt(C50C55), 2.791(11); K-O56, 3.929(8); K-O66, 2.832(7), CPR = 0.5899(3).

4.2.3.2.1 Synthesis of CalixImidMe$_1$S **18** and potassium binding of **3** and **18**

For comparison of potassium binding strengths of **3** and **A2**, mono-functionalised calix[4]arene **18** was synthesised. This synthesis proceeded in a similar way to **2a·2HI**, from the alkylation of known imidazole[*] **A149** to give imidazolium salt **17**, which was characterised by ^{1}H, ^{13}C NMR spectroscopy, ESI-MS and microanalysis (**Scheme 4.5**).[43-45] Thione ligand **18** was then prepared using an analogous procedure to that used for the formation of **3** (Chapter 2) and was isolated in 71% yield and fully characterised by ^{1}H, ^{13}C NMR spectroscopy, ESI-MS and microanalysis.

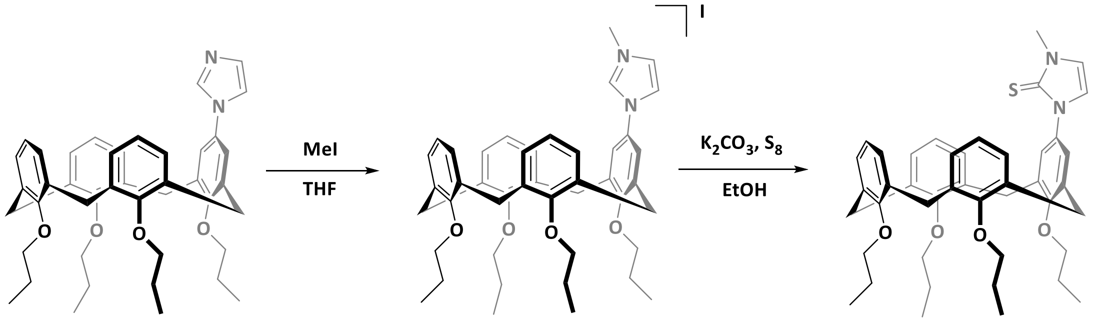

A149 **17** **18**

Scheme 4.5: Preparation of of **18**

Compounds **3** and **18** readily form potassium complexes, which were isolated by recrystalisation as colourless crystalline products. Coordination of the potassion cation was observable by ^{1}H NMR spectroscopy, for example in **3** by the downfield shift of one set of $OC\underline{H}_2$ resonances (δ 3.94 to 4.41) and an upfield shift of the NCH_3 resonance (δ 3.55 to 3.22) (**Figure 4.13**).

---

[*] Synthesised my Jack Emerson-King, PhD student, University of Warwick.

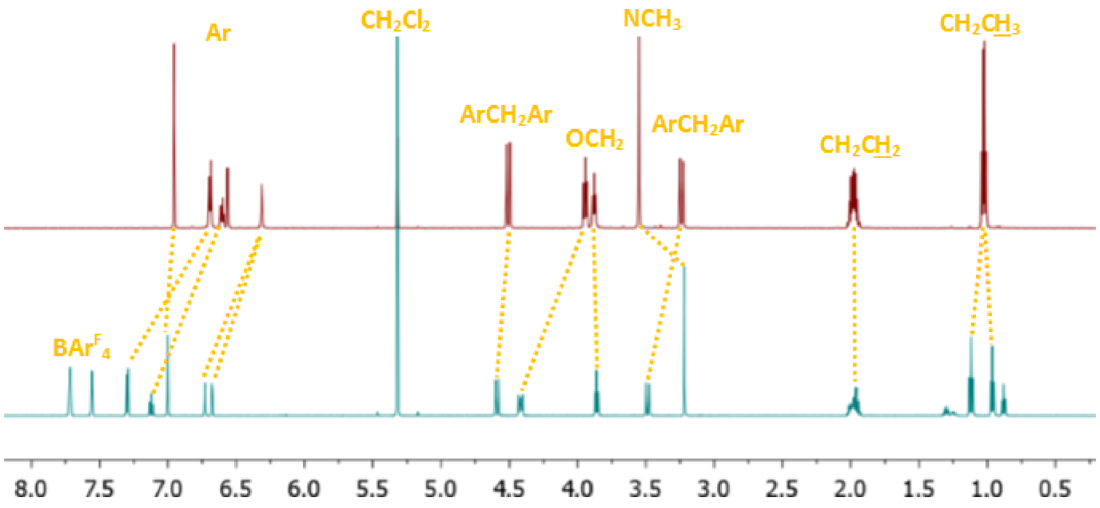

Figure 4.13: ^1H NMR spectra of **3** (top) and isolated **[3·K][BArF$_4$]** (bottom) (CD_2Cl_2, 600 MHz)

In the solid state **[18·K][BAr$^F_4$]** and **[3·K][BAr$^F_4$]** show strong potassium binding, with S-K bond lengths of 3.2083(6) Å and 3.4019(7)/3.4102(6) Å, and CPR values of 0.6092(4) and 0.5536(4), respectively (*cf.* CPR **3** = 0.419(1)) (**Figure 4.14**). The binding of potassium is associated with the shortening of the interspacial S···S distances that drop from 7.739(3) Å in **3** to 3.9644(8) Å for **[3·K][BAr$^F_4$]**. The monofunctionalised calix[4]arene complex **[18·K][BAr$^F_4$]** shows a CPR value which is comparable with that found for **[A2·K][BAr$^F_4$]** (0.6092(4) *cf.* 0.5827(20)). The CPR value for the bis-imidazol-2-thione complex **[3·K][BAr$^F_4$]** shows a dramatic decrease of S···S distance (7.739 to 3.9644 Å) and shift in CPR from 0.419(1) to 0.5536(4)), reflecting the inclusion of potassium guest and breaking of the thione-thione π-stacking interactions observed in **3**. As observed for complex **[A2·K][BAr$^F_4$]**, only two of the phenol-ether moieties participate in the binding of potassium with interspatial K···O distances of 3.9056(12)/3.9239(13)/2.8471(13)/2.8826(14) and 4.001(15)/3.9512(15)/2.8451(13)/2.8069(16) for **[18·K][BAr$^F_4$]** and **[3·K][BAr$^F_4$]** respectively.

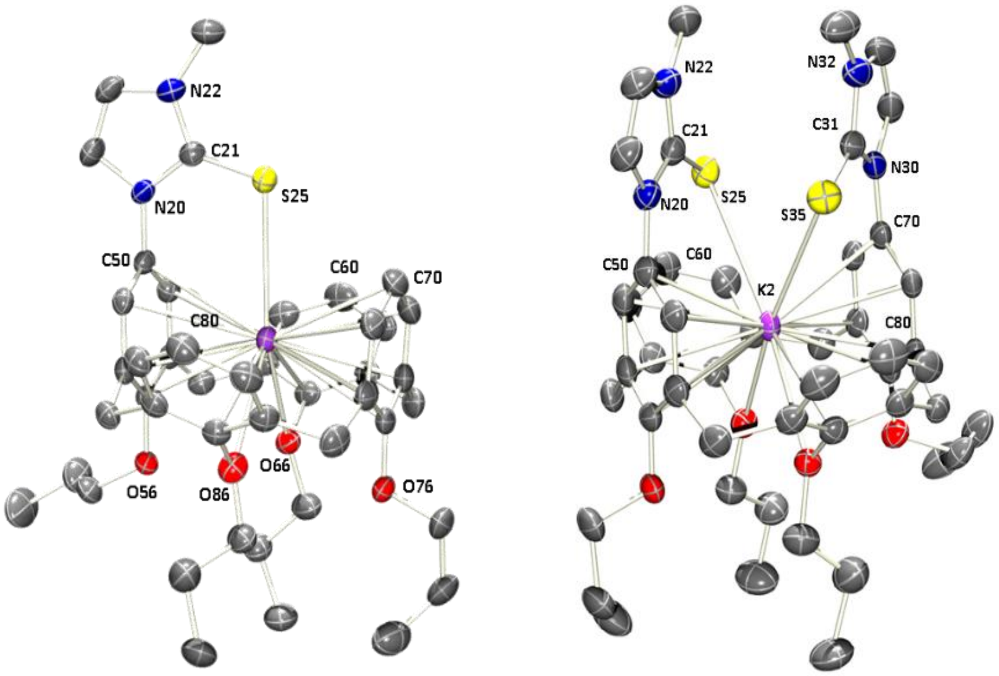

Figure 4.14: Solid-state structures of **[18·K][BAr$^{F}_{4}$]** (left) and **[3·K][BAr$^{F}_{4}$]** (right). Thermal ellipsoids for selected atoms drawn at the 50% probability level. Hydrogen atoms, anions and minor disordered components are omitted for clarity. Selected bond lengths (Å) and angles (°): **[18·K][BAr$^{F}_{4}$]** S25-K2, 3.2083(6); K2-O66, 2.8472(13); K2-O86, 2.8826(15); K2-C52, 3.1288(17); K2-C53, 3.1288(17); K2-C54, 3.0928(17); K2-C63, 3.0698(18); K2-C71, 3.116(2); K2-C72, 3.0748(19); K2-C73, 3.0951(18); K2-C74, 3.0873(19); K2-C75, 3.142(2); K2-C83, 3.1005(18); S25-C21, 1.6857(19). **[3·K][BAr$^{F}_{4}$]** S25-K2, 3.4019(7); S35-K2, 3.4102(6); K2-O66, 2.8451(14); K2-O86, 2.8069(15); K2-C50, 3.0124(18); K2-C51, 3.0037(18); K2-C52, 3.0515(18); K2-C54, 3.0568(17); K2-C55, 3.0383(18); K2-C70, 3.0214(18); K2-C71, 3.0080(19); K2-C72, 3.0566(19); K2-C74, 3.0631(18); K2-C75, 3.0440(18); S25-C21, 1.679(2); S35-C31, 1.681(2).

4.2.3.3 Rhodium and iridium complexes **11a** and **12a**

Both 11a and 12a appear to bind potassium less strongly than 3 or 18. Coordination is observed in solution, however, both the “free” host complexes and host-guest complexes were observable by ^{1}H NMR spectroscopy upon the addition of five equivalents of K[BAr$^{F}_{4}$] (0.13:1 11a:[11a·K][BAr$^{F}_{4}$] and 0.17:1 12a:[12a·K][BAr$^{F}_{4}$] ratios) (**Figure 4.15**). Pure materials were obtained however, by reaction of 11a or 12a with K[BAr$^{F}_{4}$] and subsequent recrystalisation from CH_2Cl_2/pentane, presumably aided by the highly charged nature of the potassium adducts.

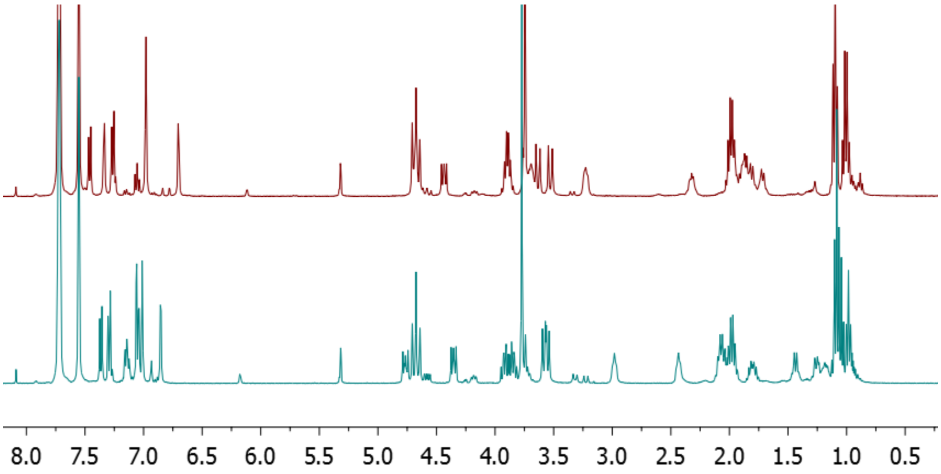

Figure 4.15: ^{1}H NMR specta of **11a** + 5.0 eq. K[BAr^F$_4$] (top) 1**2a** + 5.0 eq. K[BAr^F$_4$] (CD$_2$Cl$_2$, 400 MHz)

Solid state analysis of **[11a·K][BAr^F$_4$]** and **[12a·K][BAr^F$_4$]** both show inclusion of the potassium cation within the calix[4]arene cavity, mediated by interaction with the thione donors, arene rings and adjacent oxygen atoms (**Figure 4.16**). The presence of the included potassium inside the calix[4]arene cavity also results in the shift of CPR values from 0.5499(3) to 0.7156(8) **[11a·K][BAr^F$_4$]** and 0.5500(6) to 0.7114(10) **[12a·K][BAr^F$_4$]** and subsequently a decrease in SMS bond angles from 83.808(18) to 77.99(3) and 84.40(3) to 78.80(4)°. The M···K (M = Rh or Ir) contacts are 3.7153(10) Å and 3.6903(13) Å for **11a** and **12a** respectively, this is unusually close given the cationic nature of the species although greater than the sum of their ionic/covalent radii (K$^+$ = 1.40, Rh = 1.34 Ir = 1.36).[46, 47]

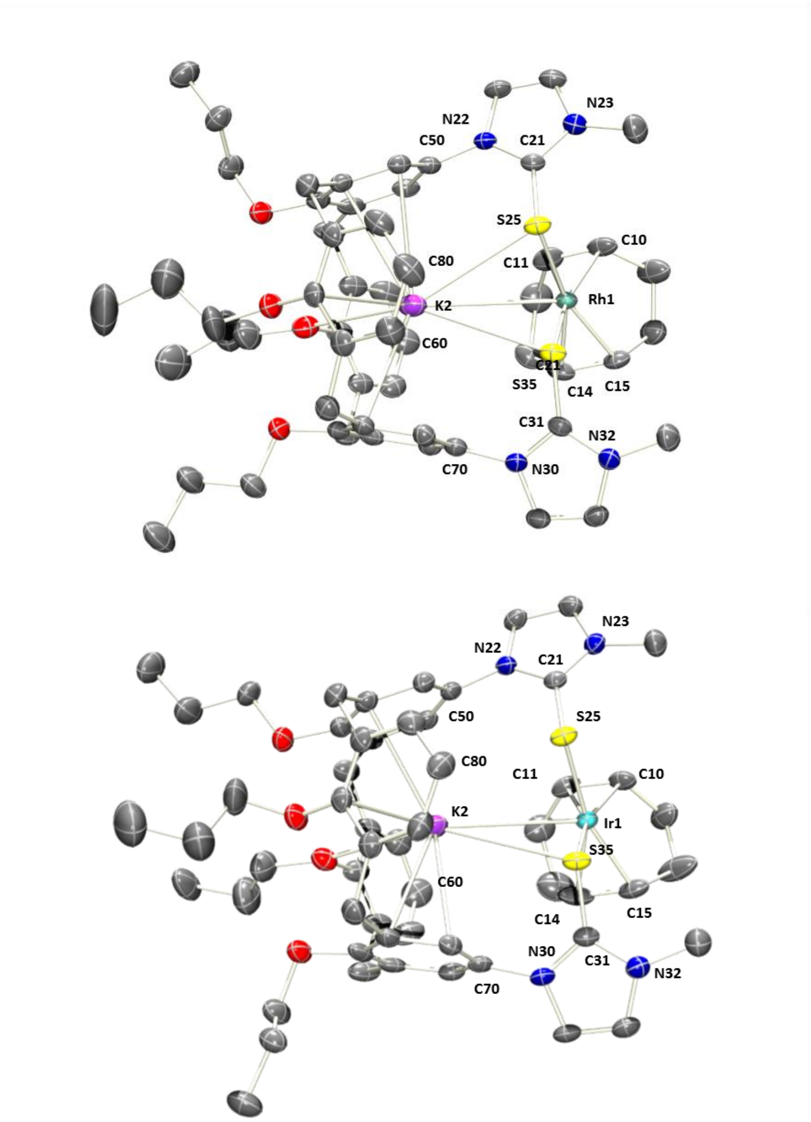

Figure 4.16: Solid-state structures of **[11a·K][BAr$^F_4$]** (top) and **[12a·K][BAr$^F_4$]** (bottom). Thermal ellipsoids for selected atoms drawn at the 50% probability level. Hydrogen atoms, anions, minor disordered components and solvent molecules are omitted for clarity. Selected bond lengths (Å) and angles (°) **[11a·K][BAr$^F_4$]**:Rh1-K2, 3.7153(10); Rh1-S25, 2.3662(10); Rh1-S35, 2.3850(9); Rh1-C10, 2.137(4); Rh1-C11, 2.140(4); Rh1-C14, 2.141(4); Rh1-C15, 2.146(4); K2-O66, 3.149(3); K2-C50, 3.415(3); K2-C51, 3.307(4); K2-C52, 3.299(4); K2-C53, 3.419(4); K2-C54, 3.421(4); K2-C55, 3.433(4); K2-C72, 3.398(4); K2-C73, 3.373(4); K2-C74, 3.276(4); K2-C75, 3.328(4); K2-C83, 3.252(4); S25-C21, 1.716(4); S35-C31, 1.718(4); S25-Rh1-K2, 65.30(3); S25-Rh1-S35, 77.99(3); S35-Rh1-K2, 68.01(3); CPR = 0.7156(8). **[12a·K][BAr$^F_4$]**: Ir1-S35, 2.3640(12); Ir1-S25, 2.3516(12); Ir1-C15, 2.131(5); Ir1-C10, 2.130(5); Ir1-C11, 2.135(5); Ir1-C14, 2.130(5); Ir1-K2, 3.6903(13); S35-C31, 1.729(5); S35-K2, 3.6324(19); S25-C21, 1.720(5); S25-K2, 3.5207(18); C70-K2, 3.445(5); C75-K2, 3.337(5); C71-K2, 3.432(5); C72-K2, 3.359(5); C74-K2, 3.275(5); C55-K2, 3.400(5); C54-K2, 3.386(5); C51-K2, 3.319(5); C50-K2, 3.409(4); C73-K2, 3.344(5); C52-K2, 3.295(5); C53-K2, 3.398(5); C82-K2, 3.498(5); 83-K2, 3.266(5); S35-Ir1-K2, 69.84(4); S25-Ir1-S35, 78.80(4); S25-Ir1-K2, 67.10(4); C15-Ir1-S35, 98.55(15); C15-Ir1-S25, 160.83(16); CPR = 0.7114(10).

Relatively few examples of Rh/Ir···K distances distances <4 Å have been reported.[48-51] Anionic rhodium complex **A150** has been described by Grutzmacher, in which the $[\mathrm{K(THF)_3}]^+$ fragment is embedded in the anionic ligand resulting in a Rh···K distance of 3.36 Å (**Figure 4.17**). The iridium complex , **A151**, reported by Balch and co-workers features a crown ether receptor which binds K$^+$. X-ray crystallography showed an Ir···K distance of 3.33 Å (**Figure 4.17**).

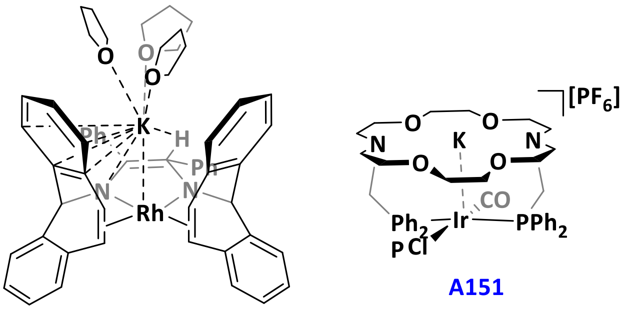

A150

A151

Figure 4.17: Previously reported Rh and Ir complexes with potassium binding characteristics

To the authors' knowledge no structures of bearing positively charged Rh/Ir centres within 4 Å of a potassium cation have been reported. †

4.2.3.4. I^{i}Pr$_2$Me$_2$S and 11b/12b

Attempts to prepare potassium complexes of the **I^{i}Pr$_2$Me$_2$S** ligand through reaction with K[BAr^F$_4$] in CH_2Cl_2 resulted in no observable reaction by ^{1}H NMR spectroscopy at room temperature. Addition of an excess of K[BAr^F$_4$] at room temperature resulted in the appearance of weak [BAr^F$_4$]$^-$ signals in the ^{1}H NMR spectra indicative of the formation of an adduct, however in a 1:40 ratio (**I^{i}Pr$_2$Me$_2$S**:[BAr^F$_4$]$^-$). Addition of 0.5 equivalents of K[BAr^F$_4$] to **I^{i}Pr$_2$Me$_2$S** and heating at 50°C for 24 hours resulted in the formation of a single complex in solution. This was attributed to the formation of **19**. This unexpected adduct was characterised by X-ray diffraction (**Figure 4.18**) and fully characterised by ^{1}H and ^{13}C NMR spectroscopy.

---

† Based on search for Ir/Rh(I) K distances <4 Å using ICSD Web and Conquest (I. J. Bruno, J. C. Cole, P. R. Edgington, M. Kessler, C. F. Macrae, P. McCabe, J. Pearson and R. Taylor, Acta Cryst., B58, 389-397, 2002)

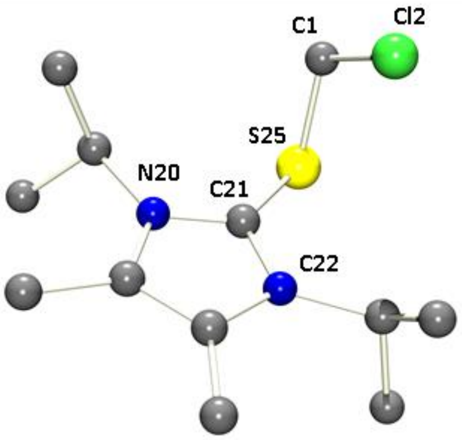

Figure 4.18: Solid-state structures of **19**. Ball and stick representation. Hydrogen atoms and anion ($[BAr^F_4]^-$) omitted for clarity. Selected bond lengths (Å) and angles (°): Cl2-C1, 1.742(6); S25-C1, 1.810(6); S25-C21, 1.739(5); C21-S25-C1, 100.9(3); N20-C21-N22, 108.3; Cl2-C1-S52, 114.3(3).

The model complexes **11b** and **12b** complexes showed no reactivity with 0.5, 1 or 5 equivalents of $K[BAr^F_4]$ in CD_2Cl_2 at room temperature.

Dichloromethane behaving as a non-innocent ligand in the presence of imidazole-2-thione ligands has previously been described be Hill.[14, 52] For example, addition of ligand **A132** to CH_2Cl_2 resulted in the slow formation of a heterocyclic salt **[A132.CH$_2$][Cl]** (**Scheme 4.6**).

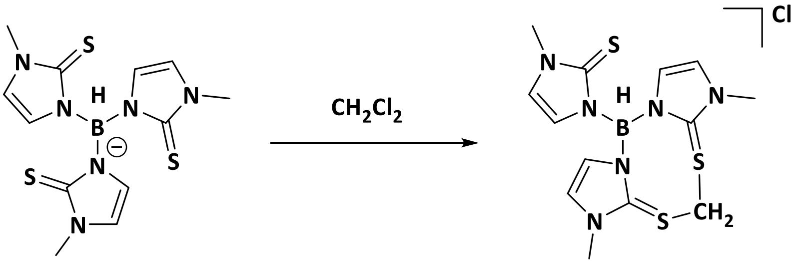

A132 **[A132.CH$_2$][Cl]**

Scheme 4.6: Addition of CH_2Cl_2 to thione ligrand reported by Hill[14]

4.2.2.5 Na$^+$ Binding

In addition to experiments with potassium, reactivity of **3** with 1 equivalent of $Na[BAr^F_4]$ was monitored by ^1H NMR spectroscopy. Binding of the Na^+ was observed by solvation of the $Na[BAr^F_4]$, complexation induced chemical shift changes and presence of the characteristic

$[BAr^F{}_4]^-$ resonances by ^1H NMR spectroscopy at δ 7.70 – 7.74 and 7.56. Despite multiple attempts, no crystals suitable for analysis by X-ray diffraction were obtained. Upon addition of excess $Na[BAr^F{}_4]$ ^1H NMR spectra indicated binding stoichiometries of greater than one $[BAr^F{}_4]^-$ per calix[4]arene, presumably a result of binding through the lower rim of the calix[4]arene.

4.2.2.6 Competition experiments

In order to help quantify the potassium binding strengths of **18**, **3**, **11a** and **12a** relative to **A2**, a series of competition experiments were carried out using a 10 mM solution of hosts and **$[A2{\cdot}K][BAr^F{}_4]$** in CD_2Cl_2 (**Scheme 4.6**).[‡] Solvents such as THF and 1,2-difluorobenzene were found to be competitive cation binders and therefore unsuitable for analysis. The resulting mixtures were in slow exchange and analysed using ^1H NMR spectroscopy (600 MHz) at 298 K with long relaxation delays (d1 = 10s). The corresponding mixtures were assigned by integration of the ^1H NMR spectra and equilibrium constants calculated and given in **Table 4.5**.

$$\mathbf{Host} + \mathbf{[A2{\cdot}K][BAr^F{}_4]} \rightleftharpoons \mathbf{[Host{\cdot}K][BAr^F{}_4]} + \mathbf{A2}$$

Scheme 4.6: Competition experiment equilibrium

Table 4.5: Equilibrium constants calculated from ^1H NMR spectra at 298 K

Host	**Equilibrium constant**
18	10
3	14
11a	3×10^{-3}
12a	3×10^{-3}

What is immediately clear from these results is that, binding strength increases in order **12a** ≈ **11a** << **A2** < **18** < **3**. This trend is in line with expectation; the binding of potassium by

---

[‡] Competition NMR experiments carried out and equilibrium constants calculated by Dr Richard Knighton, Post Doctoral Research Fellow, University of Warwick.

11a and **12a** is presumably destabilised by the electrostatic repulsion from the rhodium and iridium centres. Binding strength is then broadly proportional to the number of thione donors. No significant difference in binding strength between **11a** or **12a** was found, within error, suggesting that there is no meaningful stabilising interaction between the transition metal and potassium ion (no Z-type bonding) as a greater interaction would be expected for the heaver congener. VT ^{1}H NMR experiments were also recorded in attempt to probe the role of the thermodynamic parameters, however, the changes observed were too small to draw meaningful conclusions.

4.3 Conclusion

Monometallic rhodium(I) and iridium(I) complexes **11a** and **12a** were readily synthesised from 1,3-bis(imidazole-2-thione) functionalised calix[4]arene ligand **3**. These complexes were analysed in solution by ^{1}H, ^{13}C NMR spectroscopy, ESI-MS and in the solid state by microanalysis and X-ray diffraction. The solid-state structures of **11a** and **12a** demonstrate loss of π-stacking between the imidazole-2-thione donors compared to the free ligand **3**. Model complexes **11b** and **12b**, containing **I^{i}Pr$_2$Me$_2$S** were synthesised in parallel, and highlighted the flexibility of the calix[4]arene scaffold, which only results in relatively small changes to the S-M-S bond angles.

Reactivity of **11** and **12** with CO, H_2, bipy and **I^{i}Pr$_2$Me$_2$S** shed light into the binding of **3** and COD, in both cases the chelating COD ligand was easily displaced by CO and showed no reaction under 1 atm H_2. Addition of bipy revealed the reactivity differences between the Ir and Rh products, reaction of **11a** and **11b** both resulted in the subsititution of their respective ligands however reaction with Iridium analogues **12a** and **12b** resulted in the formation of adducts **16a** and **16b**. Imidazol-2-thione ligand **3** can be displaced by **I^{i}Pr$_2$Me$_2$S** in **11a** and **12a**, perhaps driven by relief of SMS bond strain, while the addition of bipy highlights the stronger binding of Ir compared to Rh and bipy compared to **3**.

Calix[4]arene species **A2**, **18**, **3**, **11a** and **12a** were all found to bind potassium cations, by reaction with K[BAr$^F{}_4$] and the resulting host-guest complexes were analysed in solution by ^{1}H and ^{13}C NMR spectroscopy and in the solid state by X-ray diffraction. Interrogation of crystallographic data demonstrated the potassium binding is mediated by interactions with S, O and arene donors. Despite electrostatic repulsion the cationic hosts **11a** and **12a** could bind K$^+$. Solution data indicated that potassium binding strength increases **11a** ~ **12a** < **A2** < **18** < **3** with no host-guest adducts observed for **I^{i}Pr$_2$Me$_2$S** or **11b** or **12b**. The formation of potassium adducts of **11a** and **12a** highlight the ability of calix[4]arene ligand scaffolds host to support otherwise unstable metal-metal systems.

4.4 Experimental

4.4.1 General considerations

Unless otherwise stated all manipulations were performed under an atmosphere of argon, using Schlenk and glove box techniques. Glassware was oven dried at 150 °C overnight and flame dried under vacuum prior to use. Anhydrous CH_2Cl_2, Et_2O, and pentane (<0.005% H_2O) were purchased from ACROS or Aldrich and freeze–pump–thaw degassed three times before being placed under argon. THF was dried over sodium/benzophenone, vacuum distilled, and freeze–pump–thaw degassed three times before being placed under argon. 1,2-$C_6H_4F_2$ was stored over neutral alumina for 12 hours, filtered, dried vacuum distilled from CaH_2 and freeze–pump–thaw degassed three times before being placed under argon over 3 Å molecular sieves. CD_2Cl_2 was dried over activated 3 Å sieves and freeze–pump–thaw degassed three times before being placed under argon. C_6D_6 was dried over Na, vacuum distilled, and freeze–pump–thaw degassed three times before being placed under argon. $[Rh(COD)Cl]_2$, $Na[BAr^F_4]$, $K[BAr^F_4]$ were synthesised using literature protocols.[53, 54] **A118** was prepared by Jack Emerson-King by adaption of literature protocols.[55, 56] All other solvents and reagents are commercial products and were used as received. NMR spectra were recorded on Bruker 300, 400, 600 Avance III HD, 400 Avance AV, 500 Avance III HD, 500 Avance AV and 700 Avance II HD spectrometers at 298 K unless otherwise stated. ^1H NMR spectra recorded in 1,2-$C_6H_4F_2$ were referenced using the highest intensity peak of the highest (δ 6.865) frequency fluoro-arene multiplets. $^{13}C\{^1H\}$ NMR spectra recorded in 1,2-$C_6H_4F_2$ were referenced using an internal sealed capillary of C_6D_6. Chemical shifts are quoted in ppm and coupling constants in Hz. IR spectra were recorded on a PerkinElmer Spectrum One FT-IR spectrometer at 293 K. ESI-MS analyses were recorded on Bruker Maxis Impact instrument or Brucker MicroTOF. Microanalyses were performed by Stephen Boyer at London Metropolitan University or Brian Addison at Elemental Microanalysis Ltd.

4.4.2 Preparation of isolated complexes

Synthesis of [(3)Rh(COD)][BAr$^F_4$] (11a)

A solution of **3** (201.8 mg, 0.2479 mmol), $[Rh(COD)Cl]_2$ (61.2 mg, 0.1241 mmol) in CH_2Cl_2 (10 mL) was stirred for one hour at RT, added to Na[BAr$^F_4$] (217.1 mg, 0.02450 mmol) stirred for a further hour, filtered, and layered with pentane (30 mL) for several days at RT. The mixture was filtered and the product dried *in vacuo*. Yield = 240.2 mg (52 %, yellow powder). **^{1}H NMR** (CH_2Cl_2, 600 MHz) δ 7.69 – 7.75 (m, 8H, Ar^F), 7.56 (s, 4H, Ar^F), 7.50 (s, 2H, Ar), 7.33 (d, $^3J_{HH}$ = 7.5, 2H, Ar), 7.15 (d, $^3J_{HH}$ = 7.5, 2H, Ar), 7.12 (t, $^3J_{HH}$ = 7.5 , 1H, Ar), 6.91 (t, $^3J_{HH}$ = 7.5, 1H, Ar), 6.85 (d, $^3J_{HH}$ = 2.3 , 2H, imid.), 6.78 (d, $^3J_{HH}$ = 2.3 , 2H, imid.), 6.11 (d, $^3J_{HH}$ = 2.8, 2H, Ar), 4.60 (d, $^2J_{HH}$ = 13.2, 2H, $ArCH_2Ar$), 4.56 (d, $^2J_{HH}$ = 13.2, 2H, $ArCH_2Ar$), 4.16 – 4.19 (m, 4H, OCH_2), 4.11 (s, 2H, COD{CH}), 3.86 (s, 2H, COD{CH}), 3.76 (s, 6H, NCH_3), 3.69 – 3.73 (m, 4H, OCH_2), 3.34 (d, $^2J_{HH}$ = 13.2, 2H, $ArCH_2Ar$), 3.22 (d, $^2J_{HH}$ = 13.3, 2H, $ArC\underline{H}_2Ar$), 2.60 (s, 2H, COD{CH}), 2.41 (s, 2H, COD{CH}), 2.02 – 2.11 (m, 4H, $C\underline{H}_2CH_2$), 1.92 – 2.11 (m, 8H, $C\underline{H}_2CH_2$, COD^{57}), 1.11 (t, $^3J_{HH}$ = 7.4 , 6H, $CH_2C\underline{H}_3$), 0.95 (app. q, 6H, $CH_2C\underline{H}_3$). **^{13}C{^{1}H} NMR** (CD_2Cl_2, 151 MHz) δ 162.3 (q, $^1J_{BC}$ = 50, Ar^F), 158.2 (Ar), 158.0 (Ar), 156.4 (C=S), 136.9 (Ar), 136.5 (Ar), 135.4 (Ar^F), 131.7, 130.2 (Ar), 129.4 (qq, $^2J_{FC}$ = 32, $^3J_{BC}$ = 3, Ar^F) 129.6 (Ar), 125.2 (q, $^1J_{FC}$ = 272, Ar^F) 124.8 (Ar), 123.6 (Ar), 123.1 (Ar), 121.1 (imid.), 118.0 (s, Ar^F), 82.9 (d, $^1J_{RhC}$ = 10, COD{CH}), 81.4 (d, $^1J_{RhC}$ = 12, COD{CH}), 78.6 (OCH_2), 77.2 (OCH_2), 77.1 (OCH_2), 37.2 (NCH_3), 32.3 (COD{CH_2}), 32.0 (COD{CH_2}), 31.6 (COD{CH_2}), 31.3 (COD{CH_2}), 24.1 ($\underline{C}H_2CH_3$), 23.4 ($\underline{C}H_2CH_3$), 11.1 ($CH_2\underline{C}H_3$), 10.1 ($CH_2\underline{C}H_3$). **ESI-MS** (CH_3CN, 180°C, 4 kV) Positive ion: 1027.3469 *m/z*, $[M]^+$ (calc. 1027.3732 *m/z*). **Anal.** Calcd. For $C_{88}H_{80}BF_{24}N_4O_4RhS_2$ (1890.4386 g·mol^{-1}): C,55.88; H, 4.26; N, 2.96. Found: C, 55.76; H, 4.18; N, 3.13.

***Cis*-[(3)Rh(CO)$_2$][BAr$^F_4$] (13a)**

A solution of **11a** (100.9 mg, 0.05334 mmol) in CH_2Cl_2 (10 mL) was stirred under CO (1 atm) for 2 hours. The solvent was removed *in vacuo* and the product washed with pentane and dried under vacuum. Yield = 24.6 mg (53 %, yellow powder). **^{1}H NMR** (CD_2Cl_2, 500 MHz) δ 7.71– 7.73 (m, 8H, Ar^F), 7.56 (s, 4H, Ar^F), 7.26 (d, $^3J_{HH}$ = 2.8, 2H, imid.), 7.18 (d, $^3J_{HH}$ = 7.5, 2H, Ar), 7.12 (d, $^3J_{HH}$ = 7.4, 2H, Ar), 7.03 (s, 4H, Ar), 6.95 (t, $^3J_{HH}$ = 7.5, 1H, Ar), 6.87 (t, $^3J_{HH}$ = 7.5, 1H, Ar), 6.46 (d, $^3J_{HH}$ = 2.9, 2H, imid.), 4.58 (d, $^2J_{HH}$ = 12.7, 4H, $ArCH_2Ar$), 4.04– 4.25 (m, 4H, OCH_2), 3.71– 3.81 (m, 4H, OCH_2), 3.71 (s, 6H, NCH_3), 3.32 (d, $^3J_{HH}$ = 12.7, 2H, $ArCH_2Ar$), 3.24 (d, $^2J_{HH}$ = 12.8, 2H, $ArCH_2Ar$), 1.92 – 2.18 (m, 4H, $C\underline{H}_2CH_3$), 1.92– 2.00 (m, 4H, $C\underline{H}_2CH_3$), 1.09 (t, $^3J_{HH}$ = 7.4, 6H, $CH_2C\underline{H}_3$), 0.99 (q, $^3J_{HH}$ = 7.7, 6H, $CH_2C\underline{H}_3$). **$^{13}C\{^1H\}$ NMR** (CD_2Cl_2, 126 MHz) 183.3 (d, $^1J_{RhC}$ = 69.7, CO), 162.3 (q, $^1J_{BC}$, 50, Ar^F), 135.4 (Ar^F), 130.0 (Ar) 129.4 (qq, $^2J_{FC}$=32, $^3J_{BC}$=3, Ar^F), 125.2 (q, $^1J_{FC}$=272, Ar^F), 125.0 (imid.), 121.9 (Ar), 121.7 (Ar), 118.1 (Ar^F), 78.9 (OCH_2), 77.3 (OCH_2), 77.1 (OCH_2), 37.1 (NCH_3), 23.7 ($\underline{C}H_2CH_3$),24.0 ($ArCH_2Ar$), 23.7 ($ArCH_2Ar$), 23.5 ($\underline{C}H_2CH_3$), 11.0 ($CH_2\underline{C}H_3$), 10.2 ($CH_2\underline{C}H_3$). **ESI-MS** (CH_3CN, 180°C, 3 kV) Positive ion: 976.2997 *m/z*, $[M]^+$ (calc. 976.2980 *m/z*). **IR** (CH_2Cl_2, cm^{-1}): ν(CO) 2068, 2001. **Anal.** Calcd. For $C_{82}H_{68}BF_{24}N_4O_6RhS_2$ (1838.33 $g{\cdot}mol^{-1}$): C, 53.55; H, 3.73; N, 3.05. Found: C, 53.52; H, 3.62; N, 3.28.

[(3)Ir(COD)][BAr^F_4] (12a)

A solution of 3 (149.8 mg, 0.1835 mmol), $[Ir(COD)Cl]_2$ (62.8 mg, 0.09345 mmol) in CH_2Cl_2 (10 mL) was stirred for one hour, added to Na[BAr^F_4] (161.0 mg, 0.1817 mmol) stirred for a further hour, filtered, and layered with pentane (30 mL) for several days at RT. The mixture was filtered and the product dried *in vacuo*. Yield = 163.2 mg (45 %, yellow crystals). **^1H NMR** (CD_2Cl_2, 600 MHz) δ 7.70 – 7.74 (m, 8H, Ar^F), 7.56 (s, 4H, Ar^F), 7.43 (s, 2H, Ar), 7.28 (d, $^3J_{HH}$ = 7.5, 2H, imid.), 7.14 (d, $^3J_{HH}$ = 7.5, 2H, imid.), 7.08 (t, $^3J_{HH}$ = 7.5, 1H, Ar), 6.98 – 6.91 (m, 4H, Ar), 6.89 (t, $^3J_{HH}$ = 7.5, 1H, Ar), 6.18 (d, $^3J_{HH}$ = 2.9, 2H, Ar), 4.59 (d, $^2J_{HH}$ = 12.9, 2H, $ArCH_2Ar$), 4.57 (d, $^2J_{HH}$ = 13.0, 2H, $ArCH_2Ar$), 4.25 – 4.12 (m, 4H), 3.73 (s, 4H), 3.73 – 3.69 (m, 2H), 3.66 – 3.43 (m, 2H), 3.32 (d, $^2J_{HH}$ = 13.0, 2H, $ArCH_2Ar$), 3.23 (d, $^2J_{HH}$ = 13.2, 2H, $ArCH_2Ar$), 2.40 (s, 2H, COD{CH}), 2.21 (s, 2H, COD{CH}), 2.05 – 2.11 (m, 4H, $C\underline{H}_2CH_3$), 1.93 – 1.98 (m, 4H, $C\underline{H}_2CH_3$), 1.69 (s, 2H, COD{CH_2}), 1.53 (s, 2H, COD{CH_2}), 1.11 (t, $^3J_{HH}$ = 7.4, 6H, $CH_2C\underline{H}_3$), 0.95 (app. q., 6H, $CH_2C\underline{H}_3$). **$^{13}C\{^1H\}$ NMR** (CD_2Cl_2, 151 MHz) δ 162.3 (q, $^1J_{BC}$= 50, Ar^F), 158.1, 157.8, 156.6 (NCN), 154.5, 136.7, 136.4, 136.10, 135.6, 135.4 (Ar^{F}), 131.6, 130.2, 129.6, 129.4 (qq, $^{2}J_{FC}$ = 32, $^{3}J_{BC}$ = 3, Ar^{F}) 125.2 (q, $^{1}J_{FC}$ = 272, Ar^{F}), 124.8, 123.9, 123.2, 121.8, 118.0 (Ar^{F}), 78.7 (OCH_2), 77.2 (OCH_2), 77.1 (OCH_2), 37.1 (NCH_3), 32.3 (ArC$\underline{H}_2$Ar), 31.6 (ArC$\underline{H}_2$Ar), 24.1($\underline{C}H_2CH_3$), 23.4 ($\underline{C}H_2CH_3$), 11.1 ($CH_2\underline{C}H_3$), 10.1 ($CH_2\underline{C}H_3$). **ESI-MS** (CH_3CN, 180°C, 4 kV) Positive ion: 1117.4331 *m/z*, $[M]^+$ (calc. 1117.4307). **Anal.** Calcd. For $C_{88}H_{80}BF_{24}N_4O_4IrS_2$ (1980.4960 g mol^{-1}): C, 53.36; H,4.07; N,2.83. Found: C, 53.33; H, 3.90; N, 2.91.

Synthesis of *cis*-[(3)Ir(CO)$_2$][BAr$^{F}_4$] (14a)

A solution *of* **12a** (26.0 mg, 0.01313 mmol) in CH_2Cl_2 (10 mL) was stirred for 16 hours under CO (1 atm) the solvent removed *in vacuo*. The residue was washed with pentane (3 × 10 mL) filtered and dried *in vacuo*. Yield = 14.6 mg (58 %, yellow powder). **^{1}H NMR** (CH_2Cl_2, 500 MHz) δ 7.83 – 7.73 (m, 8H, Ar^{F}), 7.60 (s, 4H, Ar^{F}), 7.26 – 7.22 (m, 2H), 7.20 (d, $^{3}J_{HH}$ = 7.5 , 2H, imid.), 7.16 (d, $^{3}J_{HH}$ = 7.5, 2H, Ar), 7.09 (s, 4H, Ar), 6.99 (d, $^{3}J_{HH}$ = 7.5, 1H, Ar), 6.91 (t, $^{3}J_{HH}$ = 7.5, 1H, Ar), 6.53 (d, $^{3}J_{HH}$ = 2.8, 2H, imid.), 4.62 (app. d, 4H, ArCH$_2$Ar), 4.23 – 4.09 (m, 4H), 3.86 – 3.69 (m, 17H), 3.81 (s, 6H, NCH_3), 3.35 (d, $^{2}J_{HH}$ = 12.7, 2H, , ArCH$_2$Ar), 3.29 (d, $^{2}J_{HH}$ = 12.8, 2H, ArCH$_2$Ar), 2.20 – 2.23 (m, 4H, $C\underline{H}_2CH_3$), 1.96 – 2.03 (m, 4H, $C\underline{H}_2CH_3$), 1.13 (t, $^{3}J_{HH}$ = 7.4, 6H, $CH_2C\underline{H}_3$), 1.04 (app. q, 6H, $CH_2C\underline{H}_3$). **^{13}C{^{1}H} NMR** (CD_2Cl_2, 126 MHz) δ 172.5 (CO), 162.3 (q, $^{1}J_{BC}$ = 50, Ar^{F}), 157.7 (Ar), 157.5 (Ar), 156.9 (NCN), 152.7 (Ar), 136.2 (Ar), 136.1 (Ar), 136.0 (Ar), 135.4 (Ar^{F}), 130.8, 130.0 (Ar), 129.4 (Ar), 129.4 (qq, $^{2}J_{FC}$ = 32, $^{3}J_{BC}$ = 3, Ar^{F}), 125.3 (imid), 125.2 (q, $^{1}J_{FC}$ = 272, Ar^{F}), 124.9 (Ar), 124.6 (imid), 123.5 (Ar), 122.1 (Ar), 121.7 (Ar), 118.0 (Ar^{F}), 79.0 (OCH_2), 77.3 (OCH_2), 77.1 (OCH_2), 37.1 (NCH_3), 31.7 (ArCH$_2$Ar), 31.5 (ArCH$_2$Ar), 24.0 ($\underline{C}H_2CH_3$), 23.7 ($\underline{C}H_2CH_3$), 23.5 ($\underline{C}H_2CH_3$), 11.0 ($CH_2\underline{C}H_3$), 10.2 ($CH_2\underline{C}H_3$), 10.2 ($CH_2\underline{C}H_3$). **ESI-MS** (CH_3CN, 180°C, 4 kV) Positive ion: 1065.3267 *m/z*, $[M]^+$ (calc. 1065.3265 *m/z*). **IR** (CH_2Cl_2, cm^{-1}): ν(CO) 2055, 1984. **Anal.** Calcd. For $C_{82}H_{68}BF_{24}N_4O_6IrS_2$ (1928.3919 g·mol^{-1}): C,51.07; H,3.55; N,2.91. Found: C,50.87; H,3.37; N,3.01.

[(I^{i}Pr$_2$Me$_2$S)$_2$Rh(COD)][BAr^F$_4$] (11b)

Adapted from procedure reported by Raubenheimer *et al.*[4]

A solution of I^{i}Pr$_2$Me$_2$S$_2$ (101.3 mg, 0.4775 mmol) and [Rh(COD)Cl]$_2$ (58.3 mg, 0.1182 mmol) was stirred in CH_2Cl_2 (10 mL) for one hour. The mixture was filtered onto Na[BAr^F$_4$] (231.4 mg, 0.2611 mmol) and stirred for a further two hours. The mixture was filtered, washed with heptane and dried *in vacuo*. Yield = 260.4 mg (74%, yellow powder).**^{1}H NMR** (CD_2Cl_2, 400 MHz) **^{1}H NMR** δ 7.71 – 7.72 (m, 8H, Ar^F), 7.56 (s, 4H, Ar^F), 5.46 (s, 4H, $C\underline{H}CH_3$), 3.78 (s, 4H, COD{CH}), 2.27 – 2.38 (m, 4H, COD{CH_2}), 2.22 (s, 12H, $CC\underline{H}_3$), 1.77 – 1.91 (m, 4H, COD{CH_2}), 1.51 (d, $^3J_{HH}$ = 7.1, 24H, $CHC\underline{H}_3$). **^{13}C{^{1}H} NMR** (CD_2Cl_2, 101 MHz) δ 162.3 (q, J_{BC} = 50, Ar^F), 152.2 (NCN), 135.4 (Ar^F$_4$), 129.4 (qq, $^2J_{FC}$ = 32, $^3J_{BC}$ = 3, Ar^F), 126.2 ($\underline{C}CH_3$), (q, $^1J_{FC}$ = 272, Ar^F), 118.0 (Ar^F), 81.1, (d, $^1J_{RhC}$ = 12.0, COD{CH}), 54.6 ($\underline{C}HCH_3$), 31.6 (COD{CH_2}), 21.4 ($CH\underline{C}H_3$), 10.9 ($C\underline{C}H_3$). **ESI-MS** (CH_3CN, 180 °C, 4 kV) Positive ion: 637.2509 *m/z* [M]$^+$ (Calculated 637.2839 *m/z*). **Anal.** Calcd. For $C_{62}H_{64}BF_{24}N_4RhS_2$ (1498.3337 g mol^{-1}): C, 49.68; H, 4.30; N, 3.74. Found: C, 49.83; H,4.16; N,3.75.

cis-[(I^{i}Pr$_2$Me$_2$S)$_2$Rh(CO)$_2$][BAr^F$_4$] (13b)

A solution of 11b (100.8 mg, 0.0673 mmol) in CH_2Cl_2 (10 mL) was stirred under an atmosphere of CO (atm) for 4 hours the solvent was removed *in vacuo*, the product washed with pentane (3 × 10 mL) and dried *in vacuo*. Recrystallised from CH_2Cl_2/pentane Yield= 15.1 mg (77%, orange powder). **^{1}H NMR** (CD_2Cl_2, 400 MHz) δ 7.80 – 7.66 (m, 8H, Ar^F), 7.56 (s, 4H, Ar^F), 5.48 (s, 4H, $C\underline{H}CH_3$), 2.27 (s, 12H, CCH_3), 1.55 (d, $^3J_{HH}$ = 7.1, 24H, $CHC\underline{H}_3$). **^{13}C{^{1}H} NMR** (CD_2Cl_2, 101 Hz) δ 183.7 (d, $^1J_{RhC}$ = 69, CO), 162.3 (q, $^1J_{BC}$ = 50, Ar^F), 146.8 (NCN), 135.4 (Ar^F), 129.4 (qq, Ar^F), 126.5 (imid), 118.0 (sept, $^3J_{FC}$ = 4, Ar^F), 52.4 ($\underline{C}H(CH_3)_2$), 21.1 ($CH(\underline{C}H_3)_2$), 10.9 ($C\underline{C}H_3$). **ESI-MS** (CH_3CN, 180°C, 4 kV) 583.1429 *m/z* [M]$^+$ positive ion (calc. 583.1642 *m/z* [M]$^+$). **IR** (CH_2Cl_2, cm^{-1}): ν(CO) 2067, 2002. **Anal.** Calcd. For $C_{56}H_{52}BF_{24}N_2O_2RhS_2$ (1446.2297 g mol^{-1}): C,46.49; H,3.62; N,3.87. Found: C,46.52; H,3.71; N,3.87.

[(I^{i}Pr$_2$Me$_2$S)$_2$Ir(COD)][BAr$^F{}_4$] (12b)

I^{i}Pr$_2$Me$_2$S (100.2 mg, 0.4718 mmol), [Ir(COD)Cl]$_2$ (74.6 mg, 0.1111 mmol) were stirred in CH_2Cl_2 (10 mL) and filtered onto Na[BAr$^F{}_4$] (232.0 mg, 0.2618 mmol) and stirred for a further hour. The yellow mixture was filtered, dried *in vacuo*, washed with heptane (2 x 10 mL) and recrystallised from CH_2Cl_2/pentane. Yield = 251.0 mg (67%, orange crystals). **^{1}H NMR** (400 MHz, CD_2Cl_2) δ 7.70 – 7.74 (m, 8H, Ar^F), 7.57 (s, 4H, Ar^F), 5.34 – 5.51 (m, 4H, $C\underline{H}CH_3$), 3.33 (s, 4H, COD{CH}), 2.25 (s, 12H, $C\underline{H}_3$), 2.06 – 2.20 (m, 4H, COD{CH_2}), 1.50 (d, $^3J_{HH}$ = 7.1, 24H, $CH\underline{H}_3$).**^{13}C{^{1}H} NMR** (101 MHz, CD_2Cl_2) δ 162.3 (q, Ar^F) , 149.2 (NCN), 135.4 (s, Ar^F), 129.4 (qq, Ar^F), 126.5 (NCC), 125.2 (q, $^1J_{FC}$= 272, Ar^F), 118.0 (sept, $^3J_{FC}$ = 4, Ar^F), 64.6 (COD{CH}), 52.1 (s, NCH), 32.0 (s, COD{CH_2}), 21.5 (s, $C\underline{C}H_3$), 10.9 (s, $C\underline{C}H_3$). **ESI-MS** (CH_3CN, 180 °C, 4 kV) 725.3248 *m/z* (calc. 725.3255 *m/z*). **Anal.** Calcd. For $C_{62}H_{64}BF_{24}IrN_4$ (1588.39 g mol^{-1}): C, 46.88; H, 4.06; N, 3.53 Found: C,47.02;H,4.17;N,3.58.

cis-[(I^{i}Pr$_2$Me$_2$S)$_2$Ir(CO)$_2$][BAr$^F{}_4$] (14b)

A solution of **12b** (100.3 mg, 0.06316 mmol) in CH_2Cl_2 (20 mL) was stirred for 4 hours under an atmosphere of CO (1 atm). The solvent was removed *in vacuo*, the solid washed with pentane (3 ×10 mL) and dried *in vacuo*. Yield = 15.1 mg (77%, yellow powder). **^{1}H NMR** (500 MHz, CD_2Cl_2) δ 7.71-7.73 (m, 8H, BAr^F), 7.56 (s, 4H, BAr^F), 5.48 (s, 4H, $C\underline{H}CH_3$), 2.31 (s, 12H, $CC\underline{H}_3$), 1.56 (d, J = 7.1 Hz, 20H, $CHC\underline{H}_3$).**^{13}C{^{1}H} NMR** (126 MHz, CD_2Cl_2) δ 173.0 (s, CO), 162.3 (q, $^1J_{BC}$ = 50, Ar^F), 147.5 (s, C=S), 135.4 (s, Ar^F), 129.4 (qq, $^2J_{FC}$ = 32, $^3J_{BC}$ = 3, Ar^F), 127.5 (s, $\underline{C}CH_3$) , 125.1 (q, $^1J_{FC}$ = 272, Ar^F), 118.0 (sept, $^3J_{FC}$ = 4, Ar^F), 52.6 (s, $\underline{C}HCH_3$), 21.1 ($CH\underline{C}H_3$), 10.8 ($C\underline{C}H_3$). **ESI-MS** (CH_3CN, 180 °C, 4 kV) 673.2215 *m/z* [M]$^+$ (Calc. 673.2214 *m/z*). **IR** (CH_2Cl_2, cm^{-1}): ν(CO) 2052, 1983. **Anal.** Calcd. For $C_{62}H_{64}BF_{24}IrN_4S_2$ (1588.39 g·mol^{-1}): C, 43.79;H, 3.41;N, 3.65 Found: C, 43.52; H, 3.29; N 3.71.

[A2·K][BAr$^F{}_4$]

A solution of **A2** (101.2 mg, 0.1707 mmol) and K[BAr$^F{}_4$] (170.1 mg, 0.1885 mmol) in CH_2Cl_2 (10 mL) was stirred for 16 hours at room temperature. The colourless solution was filtered and layered with pentane (30 mL) and stored at RT overnight. Yield = 203.2 mg (78 %, colourless crystals). **^{1}H NMR** (CD_2Cl_2, 400 MHz) δ 7.72 (s, 8H, BAr^F), 7.55 (s, 4H, BAr^F), 7.01 - 7.07 (m, 8H, Ar), 6.86-6.93 (m, 4H, Ar), 4.53 (d, $^2J_{HH}$ = 13.3, 4H, ArC$\underline{H}_2$Ar), 4.12 (t, $^3J_{HH}$ = 7.9, 8H, OCH_2), 3.47 (d, $^2J_{HH}$ = 13.4, 4H, ArC$\underline{H}_2$Ar), 1.88-2.01 (m, 8H, C$\underline{H}_2$CH$_3$), 0.98-1.06 (m, 12H, CH$_2$C$\underline{H}_3$). **^{13}C{^{1}H} NMR** (CD_2Cl_2, 101 MHz) 162.3 (q,$^1J_{BC}$= 51, Ar^F), 155.2 (Ar), 135.9 (Ar), 135.4 (s, Ar^F), 130.9 (Ar), 129.4 (qq, $^2J_{FC}$ = 32, $^3J_{BC}$ = 3, Ar^F), 128.4 (Ar), 126.2 (Ar), 125.2 (q, $^1J_{FC}$ = 272, Ar^F), 121.9 (Ar), 118.0 (sept, $^3J_{FC}$ = 4, Ar^F), 78.4 (OCH_2), 31.5 (ArC$\underline{H}_2$Ar), 23.4 ($\underline{C}$H$_2$CH$_3$), 10.3 (CH$_2\underline{C}$H$_3$). **ESI-MS** (CH_3CN, 180°C, 4 kV) 631.3186 *m/z* $[M]^+$ (calc. 631.3184 *m/z*). **Anal.** Calcd. For $C_{72}H_{60}BF_{24}KO_4$ (1494.38 g·mol^{-1}): C, 57.84; H, 4.05. Found: C, 57.69; H, 3.86.

[18-crown-6·K][BAr$^F{}_4$]

A solution of 18-crown-6 (155.0 mg, 0.5871 mmol) and K[BAr$^F{}_4$] (553.1 mg, 0.6131 mmol) were stirred in CH_2Cl_2 (20 mL) for 2 hours. The mixture was filtered and the colourless solution was layered with pentane resulting in the formation of large white crystals, which were dried *in vacuo.* Yield = 412.0 mg (60 %, white crystals). **^{1}H NMR** (400 MHz, CD_2Cl_2) δ 7.73 (s, 8H, BAr$^F{}_4$), 7.58 (s, 4H, BAr$^F{}_4$), 3.58 (s, 24H, OC$\underline{H}_2$). **^{13}C{^{1}H} NMR** (CD_2Cl_2, 101 MHz): δ 162.3 (q, $^1J_{BC}$ = 50, Ar^F 135.4 (s, Ar^F), 129.4 (qq, $^2J_{FC}$ = 32, $^3J_{BC}$ = 3, Ar^F), 125.2 (q, $^1J_{FC}$ = 272, Ar^F), 118.0 (sept, $^3J_{FC}$ = 4, Ar^F), 70.7 (s, O$\underline{C}$H$_2$). **ESI-MS** (CH_3CN, 180°C, 4 kV) Positive ion: 303.1189 *m/z*, $[M]^+$ (calc. 303.1204 *m/z*). **Anal.** Calcd.For $C_{44}H_{36}BF_{24}KO_6$ (1166.1859 g mol^{-1}): C, 45.30; H, 3.11; Found: C,45.33; H,2.94.

1-methylimidazolcalix[4]arene (17)

A mixture of A148 (167.0 mg, 0.2537 mmol) and iodomethane (0.1 mL, 1.606 mmol) in THF (1 mL) was heated at 80°C for 30 h. The product was precipitated by the addition of ethanol (10 mL), filtered and washed with diethyl ether (2 x 10 mL) and dried *in vacuo*. Yield = 181.0 mg (89 %, white solid). **^{1}H NMR** (CD_2Cl_2, 500 MHz) δ 9.88 (s, 1H, imid), 7.36 (m, 1H, imid), 7.01 – 7.09 (m, 4H, Ar), 6.85 (t, $^3J_{HH}$ = 7.5, 1H, Ar)., 6.46 (s, 2H, imid), 6.26 (d, $^3J_{HH}$ = 7.5, 2H, Ar), 6.08 (t, $^3J_{HH}$ = 7.5, 1H, Ar), 4.52 (d, $^2J_{HH}$ = 13.6, 2H, ArCH$_2$Ar), 4.46 (d, $^2J_{HH}$ = 13.3, 2H, ArCH$_2$Ar)., 4.12 (s, 3H, NCH$_3$), 3.89 – 4.08 (m, 4H, OCH$_2$), 3.81 (t, $^3J_{HH}$ = 6.9, 2H, OCH$_2$), 3.72 (t, $^3J_{HH}$ = 6.9, 2H, OCH$_2$), 3.27 (d, $^2J_{HH}$ = 13.6, 2H), 3.17 (d, $^2J_{HH}$ = 13.4, 2H, ArCH$_2$Ar)., 1.87 – 2.01 (m, 8H, C$\underline{H}_2$CH$_3$), 1.10 (t, $^3J_{HH}$ = 5.8, 3H, CH$_2$C$\underline{H}_3$), 1.07 (t, $^3J_{HH}$ = 5.8, 3H, CH$_2$C$\underline{H}_3$), 0.93 (t, $^3J_{HH}$ = 7.4, 6H, CH$_2$C$\underline{H}_3$).**^{13}C NMR** (CD$_2$Cl$_2$, 126 MHz) δ 158.0 (Ar), 156.6 (Ar), 137.76 (Ar), 137.2 (Ar), 136.0 (Ar), 135.6 (imid), 134.8 (Ar), 129.8 (Ar), 129.4 (Ar), 128.9 (Ar), 127.8 (Ar), 124.0 (imid), 122.8 (Ar), 121.8 (imid), 121.7 (Ar), 121.3 (Ar), 77.9 (OCH$_2$), 77.6 (OCH$_2$), 77.3 (OCH$_2$), 37.7 (NCH$_3$), 31.5 (ArCH$_2$Ar), 31.4 (ArCH$_2$Ar), 24.0 ($\underline{C}$H$_2$CH$_3$), 23.9 ($\underline{C}$H$_2$CH$_3$), 23.6 ($\underline{C}$H$_2$CH$_3$), 11.0 (CH$_2\underline{C}$H$_3$), 11.0 (CH$_2\underline{C}$H$_3$), 10.3 (CH$_2\underline{C}$H$_3$).**ESI-MS** (CH$_3$CN, 180°C, 3 kV) positive ion 637.4002 *m/z*, [M]$^+$ (calc 673.4000 *m/z*). **Anal.** Calcd. For $C_{44}H_{53}IN_2O_4$ (800.31 g·mol^{-1}): C,65.99; H,6.67; N,3.50. Found: C, 65.90; H, 6.64; N, 3.58.

imidazol-2-thione calix[4]arene (18)

A mixture of 17 (614.2 mg, 0.9121 mmol), K$_2$CO$_3$ (161.2 mg, 1.1663 mmol) and S$_8$ (34.4 mg, 0.1344 mmol) in ethanol (20 mL) was stirred at reflux for 16 hours. Solvent was removed *in vacuo* and the product extracted with CH$_2$Cl$_2$ (2 x 10 mL) and precipitated with excess pentane/hexane. Yield = 459.3 mg (71 %, white powder). **^{1}H NMR** (CD$_2$Cl$_2$, 500 MHz) δ 6.93 (d, $^3J_{HH}$ = 7.5, 4H, Ar), 6.77 (t, $^3J_{HH}$ = 7.5, 2H, Ar), 6.62 (d, $^3J_{HH}$ = 2.4, 1H, imid), 6.46 (s, 2H, Ar), 6.37 (d, $^3J_{HH}$ = 7.4, 2H, Ar), 6.29 – 6.32 (m, 6.5, 1H, Ar), 6.13 (d, $^2J_{HH}$ = 2.4, 1H, imid), 4.48 (app. t, $^3J_{HH}$ = 14, 4H, ArCH$_2$Ar), 3.90 – 4.06 (m, 4H, OCH$_2$), 3.84 (t, $^3J_{HH}$ = 7.0, 2H, OCH$_2$), 3.74 (t, $^3J_{HH}$ = 7.1, 2H, OCH$_2$), 3.51 (s, 3H, NCH$_3$), 3.23 (d, $^2J_{HH}$ = 13.5, 2H, ArCH$_2$Ar), 3.16 (d, $^2J_{HH}$ = 13.3, 2H, ArCH$_2$Ar), 1.85 – 2.06 (m, 8H, C$\underline{H}_2$CH$_3$), 1.08 (m, 1.05 – 1.11, 6H, CH$_2$C$\underline{H}_3$), 0.94 (t, $^3J_{HH}$ = 7.5, 6H, CH$_2$C$\underline{H}_3$). **^{13}C{^{1}H} NMR** (CD$_2$Cl$_2$, 126 MHz) δ 163.32 (NCN), 160.46 (imid), 157.87 (Ar), 156.59 (Ar), 156.03 (Ar), 136.89 (Ar), 136.40 (Ar), 135.51 (Ar), 134.86 (Ar), 133.01 (Ar), 129.32 (Ar), 129.13 (Ar), 128.01 (Ar), 125.54 (Ar), 122.53 (Ar), 122.34 (Ar), 118.54 (imid), 117.96 (imid), 77.76 (OCH$_2$), 77.64 (OCH$_2$), 77.29 (OCH$_2$), 35.52 (NCH$_3$), 31.44 (Ar$\underline{C}$H$_2$Ar), 24.03 ($\underline{C}$H$_2$CH$_3$), 23.65 ($\underline{C}$H$_2$CH$_3$), 11.01 (CH$_2\underline{C}$H$_3$), 10.36 (CH$_2\underline{C}$H$_3$). **ESI-MS** (CH$_3$CN, 180°C, 3 kV) positive ion 704.3364 *m/z* [M]$^+$ (calc. 704.3642 *m/z*). **Anal.** Calcd. For $C_{44}H_{51}N_4O_4S$ (704.36 g·mol^{-1}): C, 74.97; H, 7.44; N, 3.97. Found: C, 74.77; H, 7.29; N, 4.15.

[18·K][BAr^F$_4$]

A solution of **18** (20.2 mg, 0.02865 mmol) and K[BAr^F$_4$] (29.2 mg, 0.03236 mmol) in CH_2Cl_2 (10 mL) was stirred for 16 h. The mixture was filtered and the product was precipitated by addition of pentane (10 mL) and recrystallised from CH_2Cl_2/pentane and dried *in vacuo*. Yield = 25.4 mg (55 %, white crystals). **^{1}H NMR** (CD_2Cl_2, 500 MHz) δ 7.72 – 7.76 (m, 8H, Ar^F), 7.56 (s, 4H, Ar^F), 7.35 (d, $^3J_{HH}$ = 7.6, 1.7, 2H, Ar), 7.27 (d, $^3J_{HH}$ = 7.7, 2H, Ar), 7.14 (t, $^3J_{HH}$ = 7.6 , 2H, Ar), 6.73 – 6.82 (m, 3H, Ar), 6.70 – 6.71(m, 3H, Ar, imid), 6.63 (d, $^3J_{HH}$ = 2.4, 1H, imid), 4.57 (app. t, 4H, $ArCH_2Ar$), 4.39– 4.49 (m, 4H, OCH_2), 3.86 (t, $^3J_{HH}$ = 7.1, 2H, OCH_2), 3.81 (t, $^3J_{HH}$ = 7.1, 2H, OCH_2), 3.48 (app. t, 4H, $ArCH_2Ar$), 3.41 (s, 3H, NCH_3), 1.87 – 2.05 (m, 8H, $C\underline{H}_2CH_3$), 1.10 (app. q , 6H, $CH_2C\underline{H}_3$), 0.96 (t, $^3J_{HH}$ = 7.4, 6H, $CH_2C\underline{H}_3$). **^{13}C{^{1}H} NMR** (CD_2Cl_2, 126 MHz) δ 163.8 (NCN), 162.3 (q, $^1J_{BC}$ = 50, Ar^F), 157.4 (Ar), 157.2 (Ar), 153.4 (Ar), 136.8 (Ar), 136.2 (Ar), 136.1 (Ar), 135.4 (s, Ar^F), 134.8 (Ar), 134.5 (Ar), 131.9 (Ar), 131.4 (Ar), 130.2 (Ar), 129.6 (Ar), 129.4 (qq, $^2J_{FC}$ = 32, $^3J_{BC}$ = 3, Ar^F), 126.7 (Ar), 126.2 (Ar), 126.2 (Ar), 125.2 (Ar), (q, $^1J_{FC}$ = 272, Ar^F), 124.1 (Ar), 121.9 (Ar), 119.6 (imid), 118.0 (sept, $^3J_{FC}$ = 4, Ar^F), 117.9 (imid), 79.6 (OCH_2), 79.4 (OCH_2), 77.5 (OCH_2), 35.6 (NCH_3), 31.6 ($ArCH_2Ar$), 31.6 ($ArCH_2Ar$), 24.0 ($\underline{C}H_2CH_3$), 23.9 ($\underline{C}H_2CH_3$), 23.0 ($\underline{C}H_2CH_3$), 10.9 ($CH_2\underline{C}H_3$), 10.9 ($CH_2\underline{C}H_3$), 9.8 ($CH_2\underline{C}H_3$). **ESI-MS** (CH_3CN, 180°C, 4 kV) positive ion: 743.2924 *m/z* [M]$^+$ (calc. 743.3279 *m/z*). **Anal.** Calcd. For $C_{73}H_{55}BF_{24}KN_2O_4S$ (1561. 32g·mol^{-1}): C, 56.79; H, 4.01; N, 1.74. Found: C, 56.56; H, 3.90; N, 1.84. (56.13; H, 3.55; N, 1.79.)

[3·K][BAr^F$_4$]

A solution of **3** (51.2 mg, 0.0627 mmol) and K[BAr^F$_4$] (61.4 mg, 0.0680 mmol) in CH_2Cl_2 (10 mL) was stirred for 16 hours at RT. The colourless solution was filtered and layered with pentane (20 mL) at RT overnight. Yield = 92.4 mg (82 %, colourless crystals). **^{1}H NMR** (CD_2Cl_2, 400 MHz) δ 7.72 (s, 8H, Ar^F), 7.56 (s, 4H, Ar^F), 7.30 (d, $^3J_{HH}$ = 7.6, 4H, Ar), 7.12 (t, $^3J_{HH}$ = 7.6, 2H, Ar), 7.00

(s, 4H, Ar), 6.73 (d, $^3J_{HH}$=2.5, 2H, imid), 6.67 (d, $^3J_{HH}$ = 2.5, 2H, imid), 4.59 (d, $^2J_{HH}$ = 13.5 , 4H, ArCH$_2$Ar), 4.32 – 4.50 (m, 4H, OCH$_2$), 3.86 (t, $^3J_{HH}$ = 7.0 , 4H, OCH$_2$), 3.49 (d, $^2J_{HH}$ = 13.6 , 4H, ArCH$_2$Ar), 3.22 (s, 6H, NCH$_3$), 1.92 – 2.04 (m, 8H, $C\underline{H}_2CH_3$), 1.12 (t, $^3J_{HH}$ = 7.4, 6H, $CH_2C\underline{H}_3$), 0.96 (t, $^3J_{HH}$ = 7.4, 6H, $CH_2C\underline{H}_3$). **^{13}C{^{1}H} NMR** (CD$_2$Cl$_2$, 101 MHz) δ 164.16 (NCN), 162.3 (q, $^1J_{BC}$ = 50, Ar^F), 156.6 (Ar), 153.7 (Ar), 136.1 (Ar), 135.4 (s, Ar^F), 134.9, 134.1 (Ar), 132.0 (Ar), 129.4 (qq, $^2J_{FC}$ = 32, $^3J_{BC}$ = 3, Ar^F), 128.6 (Ar), 126.7 (Ar), 125.2 (q, $^1J_{FC}$ = 272, Ar^F), 118.8 (imid), 118.0 (sept, $^3J_{FC}$ = 4, Ar^F), 117.0 (imid), 79.5 (OCH$_2$), 77.5 (OCH$_2$), 35.4 (NCH$_3$), 31.9 (ArCH$_2$Ar), 24.0 ($\underline{C}H_2CH_3$), 23.0 ($\underline{C}H_2CH_3$), 10.9 ($CH_2\underline{C}H_3$), 9.9 ($CH_2\underline{C}H_3$). **ESI-MS** (CH$_3$CN, 180°C, 4 kV) Positive ion 855.3381 *m/z*, [M]$^+$ (calc 855.3375 *m/z*). **Anal.** Calcd. For $C_{80}H_{68}BF_{24}KN_4O_4S_2$ (1718.4029 g·mol^{-1}): C, 55.88; H, 3.99; N, 3.26 Found: C, 55.91;H, 3.91; N, 3.22.

[11a·K][BAr$^F_4$]

A solution of 11a (50.0 mg, 0.0252 mmol) and K[BAr$^F_4$] (113.6 mg, 0.126 mmol) in CH$_2$Cl$_2$ (10 mL) was stirred for 16 hours. The mixture was filtered and the solvent was removed *in vacuo*. The product washed with pentane and dried under vacuum. Yield = 32 % (9.0 mg, yellow powder). **^{1}H NMR** (CD$_2$Cl$_2$, 500 MHz) δ 7.70 – 7.74 (m, 16H, Ar^F), 7.56 (br, 8H, Ar^F), 7.46 (d, $^3J_{HH}$ = 7.6, 2H, Ar), 7.34 (d, $^3J_{HH}$ = 2.9, 2H, imid), 7.23 – 7.3(m, 3H, Ar), 7.06 (t, $^3J_{HH}$ = 7.6, 1H, Ar), 6.94 – 7.02 (m, 4H, Ar), 6.70 (d, $^3J_{HH}$ = 2.7 Hz, 2H, imid), 4.61 – 4.71 (m, 6H, ArCH$_2$Ar, COD{CH}), 4.41-4.46 (m, 2H, OCH$_2$), 33.82-3.97 (m, 4H, OCH$_2$), 3.75 (s, 6H, NCH$_3$), 3.69 (s, 1H, COD{CH}), 3.63 (d, $^2J_{HH}$ = 13.7 , 2H, ArCH$_2$Ar), 3.53 (d, $^2J_{HH}$ = 13.3, 2H, ArCH$_2$Ar), 3.20-3.25 (m, 2H, COD{CH}), 2.28-2.36 (m, 2H, COD{CH}), 2.04 – 1.63 (m, 14H, COD{CH$_2$}, CH$_2$CH$_3$), 1.10 (t, $^3J_{HH}$ = 7.4, 6H, CH$_2$CH$_3$), 1.01 (dt, $^3J_{HH}$ = 10.1, 7.4, 6H, CH$_2$CH$_3$). **^{13}C{^{1}H} NMR** (CD$_2$Cl$_2$, 126 MHz) δ 162.3 (q, $^1J_{BC}$ = 50, Ar^F), 135.4 (s, Ar^F), 1, 129.4 (qq, $^2J_{FC}$ = 32, $^3J_{BC}$ = 3, Ar^F), 125.2 (q, $^1J_{FC}$ = 272, Ar^F) 118.0 (sept, $^3J_{FC}$ = 4, Ar^F), 158.5 (NCN), 155.29 (Ar), 153.71(Ar), 137.37 (Ar), 136.69 (Ar), 136.30 (Ar), 135.97 (Ar), 135.36 (Ar), 132.70, 132.29, 131.44, 128.39, 127.88, 127.34, 127.17, 126.40, 126.23, 124.06, 123.05, 121.13, 84.15, 84.06, 80.21, 77.85, 76.67, 54.44, 37.4 (NCH3), 32.78, 31.34, 23.96 (COD{CH_2}), 23.15 (COD{CH_2}), 22.26 (COD{CH_2}), 9.99 (CH_2CH_3), 9.88 (CH_2CH_3). **Anal.** Calcd. For $C_{82}H_{68}BF_{24}KN_4O_4RhS_2$ (1934.24 g·mol^{-1}): C,51.59; H, 3.32; N, 2.01 Found: C, 51.63; H, 3.39; N, 2.13.

[12a·K][BAr^F$_4$]

A solution of **12a** (50.0 mg, 0.0252 mmol) and K[BAr^F$_4$] (113.6 mg, 0.126 mmol) in CH_2Cl_2 (10 mL) was stirred for 16 hours. The mixture was filtered and the solvent was removed *in vacuo* and the product washed with pentane and dried under vacuum. Yield = 9.0 mg (32 %, yellow powder). **^{1}H NMR** (CD_2Cl_2, 400 MHz) δ 7.70 – 7.74 (m, 8H, Ar^F), 7.56 (br, 4H, Ar^F), 7.37 (d, $^3J_{HH}$ = 7.6, 2H), 7.30 (d, $^3J_{HH}$ = 7.6, 2H, Ar), 7.14 (td, $^3J_{HH}$ = 7.6, 2.3, 2H, Ar), 7.06 (d, $^3J_{HH}$ = 2.3, 2H, Ar), 7.04 (d, $^3J_{HH}$ = 2.7, 2H, imid), 7.01 (d, $^3J_{HH}$ = 2.3, 2H, Ar), 6.86 (d, $^3J_{HH}$ = 2.7, 2H, imid), 4.73 – 4.81 (m, 2H, OCH_2), 4.68 (app.t, $^2J_{HH}$ = 13, 4H, $ArCH_2Ar$), 4.41 – 4.30 (m, 2H, OCH_2), 3.81 – 4.00 (m, 4H, OCH_2), 3.77 (s, 6H, NCH_3), 3.59 (d, $^2J_{HH}$ = 9.6, 2H, $ArCH_2Ar$), 3.55 (d, $^2J_{HH}$ = 9.6, 2H, $ArCH_2Ar$), 2.99 (s, 2H, COD{CH}), 2.44 (s, 2H, COD{CH}), 2.16 – 1.92 (m, 8H, CH_2CH_3), 1.73 – 1.86 (m, 2H, COD{CH}), 1.44 (d, $^3J_{HH}$ = 8.5, 2H, COD{CH}), 1.14 – 1.34 (m, 4H, COD{CH}), 0.94 – 1.13 (m, 12H, $CH_2C\underline{H}_3$).**^{13}C{^{1}H} NMR** (CD_2Cl_2, 126 MHz) δ 162.3 (q, $^1J_{BC}$ = 50, Ar^F), 158.8 9 (NCN), 137.3 (Ar), 137.2 (Ar), 135.7 (Ar), 135.4 (s, Ar^F), 132.3 (Ar), 132.1 (Ar), 131.3 (Ar), 129.4 (qq, $^2J_{FC}$ = 32, $^3J_{BC}$ = 3, Ar^F), 129.6 (Ar), 129.3 (Ar), 129.2 (Ar), 127.5 (Ar), 127.4 (Ar), 126.5 (imid), 126.0 (Ar), 125.2 (q, $^1J_{FC}$ = 272, Ar^F) 123.8 (Ar), 123.3 (Ar), 122.7 (Ar), 118.0 (sept, $^3J_{FC}$ = 4, Ar^F), 80.3 (OCH_2), 78.3 (OCH_2), 76.1 (OCH_2), 67.8 (COD{CH}), 65.9 (COD{CH}), 54.6, 37.3 (NCH_3), 33.0 (COD{CH}), 32.0 (COD{CH}), 31.6 (COD{CH}), 31.2 (COD{CH}), 24.0 (COD{CH}), 23.6 (COD{CH}), 21.9 (COD{CH}), 10.7 ($CH_2C\underline{H}_3$), 10.1 ($CH_2C\underline{H}_3$), 9.9 ($CH_2C\underline{H}_3$). **Anal.** Calcd. For $C_{82}H_{68}BF_{24}KN_4O_6IrS_2$ (2882.52 g·mol^{-1}): C, 49.99; H, 3.22; N, 1.94. Found: C, 49.86; H, 3.31; N, 2.02.

Synthesis of [I^{i}Pr$_2$Me$_2$S·CH$_2$Cl][BAr$^F{}_4$] (19)

A solution of **I^{i}Pr$_2$Me$_2$** (20.0 mg, 0.0942 mmol), K[BAr$^F{}_4$] (42.5 mg, 0.471 mmol) in CH_2Cl_2 (10 mL) was stirred for 16 hours at 50°C, filtered, and layered with pentane. The mixture was filtered and dried *in vacuo*. Yield = 31.4 mg (62 %, colourless crystals). **^{1}H NMR** (CH_2Cl_2, 400 MHz) δ 7.69 – 7.75 (m, 8H, Ar^F), 7.56 (s, 4H, Ar^F), 5.3 (m, 1H, $C\underline{H}CH_3$), 4.8 (s, H, $C\underline{H}_2Cl$), 2.4 (s, 6H, $CC\underline{H}_3$), 1.6 (d, 12H $C\underline{H}CH_3$). **^{13}C{^{1}H} NMR** (CD_2Cl_2, 101 MHz) δ 162.3 (q, $^1J_{BC}$ = 50, Ar^F), 135.4 (Ar^F), 131.7 ($\underline{C}CH_3$), 129.4 (qq, $^2J_{FC}$ = 32, $^3J_{BC}$ = 3, Ar^F) 125.2 (q, $^1J_{FC}$ = 272, Ar^F), 54.7 ($\underline{C}HCH_3$), 49.8 ($\underline{C}HCH_3$), 21.7 ($CH\underline{C}H_3$), 11.6 ($C\underline{C}H_3$).

4.4.3 NMR Experiments

Potassium binding stoichiometry

A mixture of 0.005 mmol reagent and incremental quantities of K[BAr$^F{}_4$] (0.5 equivalents; 0.0025 mmol, 2.3 mg; 1 equivalent; 0.005 mmol, 4.6 mg and 0.05 equivalents; 25 mmol, 23.0 mg) in CD_2Cl_2 (0.5 mL) under argon were agitated vigorously for 30 seconds and analysed by ^{1}H NMR spectroscopy. The ratio of host and complex was determined by integration of the ^{1}H NMR data.

Table 4.6: Potassium binding stoichiometry's determined by integration of ^{1}H NMR spectra *:*

Host	**0.5 eq.s of K[BAr$^F{}_4$]** **Host:[Host·K][BAr$^F{}_4$]**	**1.0 eq.s of K[BAr$^F{}_4$]** **Host:[Host·K][BAr$^F{}_4$]**	**5.0 eq.s of K[BAr$^F{}_4$]** **Host:[Host·K][BAr$^F{}_4$]**
A2	49:51	0:1	0:1
18	1.0:0.9	0.18:1.00	0:1
3	1.0:1.3	0.16:1.00	0:1
11a	1:1	0.22:1.00	0.13:1.00
12a	1.0:1.3	0.19:1.00	0.17:1.00

Potassium complexes of A2, 3, 17, 11a, 12a and 18-crown-6 general procedure

A solution of 0.005 mmol potassium was analysed by ^{1}H NMR spectroscopy. An excess of 18-crown-6 (~2 eq) was added which unanimously showed decoordination of the calix[4]arene binder and coordination of 18-crown-6 to K[BAr^F$_4$] observable by integration of the [BAr^F$_4$] resonance observed by ^{1}H NMR spectroscopy. These were in good agreement with expected values.

11a + I^{i}Pr$_2$Me$_2$

A solution of **11a** (9.5 mg, 5.00 mmol) and **I^{i}Pr$_2$Me$_2$** (2.1 mg, 10.00 mmol) in CD_2Cl_2 (0.5 mL) was analysed by ^{1}H NMR spectroscopy. The resulting mixture was analysed by ^{1}H NMR spectroscopy (400 MHz) which showed a ratio of 1:6 **11a**:**11b**

12a + I^{i}Pr$_2$Me$_2$

A solution of **12a** (mg, 5.00 mmol) and **I^{i}Pr$_2$Me$_2$** (2.1 mg, 10.00 mmol) in CD_2Cl_2 (0.5 mL) was analysed by ^{1}H NMR spectroscopy. The resulting mixture was analysed by ^{1}H NMR spectroscopy (400 MHz) which showed a ratio of 1: 2.4 **12a**:**12b**

Reaction with bipyridine

[(3)Rh(COD)][BAr^F$_4$] or [(I^{i}Pr$_2$Me$_2$S)$_2$Rh(COD)][BAr^F$_4$]

A solution of **I^{i}Pr$_2$Me$_2$S** complex (0.005 mmol) and bipy (0.8 mg, 0.005 mmol) in CD_2Cl_2 (0.5 mL) was analysed by ^{1}H NMR spectroscopy. This showed quantitative formation of [Rh(COD)(bipy)][BAr^F$_4$] and free **3**.

[(3)Ir(COD)][BAr^F$_4$]

A solution of **I^{i}Pr$_2$Me$_2$S** complex (0.005 mmol) and bipy (0.8 mg, 0.005 mmol) in CD_2Cl_2 (0.5 mL) was analysed by ^{1}H NMR spectroscopy. This showed quantitative formation of a single product thought to be [**(3)** Ir(COD)bipy][BAr^F$_4$] by observation of ^{1}H NMR and COSY NMR spectroscopy. This product was also formed by reaction of [Ir(COD)(bipy)][BAr^F$_4$] (6.6 mg, 0.005 mmol) and **3** (4.1 mg, 0.005 mmol) in CD_2Cl_2 (0.5 mL).

Hydrogenation attempt

A solution of **I^{i}Pr$_2$Me$_2$S** complex **11a**/**11b**/**12a**/**12b** (0.005 mmol) in CD_2Cl_2 (0.5 mL) was placed under an atmosphere of H_2 and monitored by ^{1}H NMR spectroscopy over 24 hours. A resonance indicating the presence of H_2 gas in solution was observed at 4.60 ppm however no reaction was observed in any case.

[(3)Ir(COD)][BAr^F$_4$] + 2 I^{i}Pr$_2$Me$_2$S

A solution of [**(3)**Ir(COD)][BAr^F$_4$] (9.9 mg, 0.005 mmol) and **I^{i}Pr$_2$Me$_2$S** (2.1 mg, 0.010 mmol) in CD_2Cl_2 (0.5 mL) was monitored by ^{1}H NMR spectroscopy Resulting in a mixture of **3**: [**(3)**Ir(COD)][BAr^F$_4$]:NHCS: [(NHCS)$_2$Ir(COD)][BAr^F$_4$] over time a fifth species was observed this has been attributed to the formation of [**(3)**Ir(COD)(NHCS)][BAr^F$_4$].

[(3)Rh(COD)][BAr^F$_4$] + 2 I^{i}Pr$_2$Me$_2$S

A solution of [**(3)**Rh(COD)][BAr^F$_4$] (9.5 mg, 0.005 mmol) and **I^{i}Pr$_2$Me$_2$S** (2.1 mg, 0.010 mmol) in CD_2Cl_2 (0.5 mL) was monitored by ^{1}H NMR spectroscopy for 24 hours. Resulting in a mixture of **3**: [**(3)**Rh(COD)][BAr^F$_4$]: **I^{i}Pr$_2$Me$_2$S**: [(**I^{i}Pr$_2$Me$_2$S**)$_2$Rh(COD)][BAr^F$_4$] 1: 8:8:1.

4.4.4 Crystallography

Structure determinations were carried out by Dr. A. B. Chaplin. Relevant crystallographic data are given in **Table 4.7** and **Table 4.8**. Data were collected on an Oxford Diffraction Gemini Ruby CCD or SuperNova AtlasS2 CCD diffractometer using graphite monochromated Mo Kα (λ = 0.71073 Å) or CuKα (λ = 1.54184 Å) radiation and a low-temperature device. Data were collected and reduced using CrysAlisPro. All non-hydrogen atoms were refined anisotropically using SHELXL,[58] through the Olex2 interface.

Table 4.7: Crystallographic data for **11a**, **12a**, **11b**, **12b** and **19**

	11a	**12a**	**11b**	**12b**	**19**
CCDC/ID	0229abc16s	0107abc14	0113abc14	0065abc14	0233abc16s
Figure	**Figure 4.8**	**Figure 4.8**	**Figure 4.8**	**Figure 4.8**	**Figure 4.18**
Formula	$C_{88}H_{80}BF_{24}N_4O_4RhS_2$	$C_{88}H_{80}BF_{24}N_4O_4IrS_2$	$C_{62}H_{64}BF_{24}N_4RhS_2$	$C_{62}H_{64}BF_{24}N_4IrS_2$	$C_{44}H_{34}BClF_{24}N_2S$
M	1891.40	1980.69	1499.01	1588.30	1125.05
Crystal System	monoclinic	monoclinic	Triclinic	Triclinic	orthorhombic
Space group	$P2_1/c$	$P2_1/c$	P-1	P-1	Pbca
Radiation	Mo Kα (λ = 0.71073 Å)	Mo Kα (λ = 0.71073 Å)	Mo Kα (λ = 0.71073 Å)	Mo Kα (λ = 0.71073 Å)	CuKα (λ = 1.54184 Å)
***T* [K]**	150(2)	150(2)	150(2)	150(2)	150(2)
***a* [Å]**	17.0807(2)	17.0555(3)	12.15660(17)	12.1169(4)	21.0239(6)
***b* [Å]**	13.79936(17)	13.80514(17)	15.5551(2)	15.5279(6)	19.1761(4)
***c* [Å]**	36.0546(10)	36.0149(6)	19.1376(3)	19.0942(6)	24.2192(6)
α[deg]	90	90	71.5985(13)	71.555(3)	90
β [deg]	94.3486(10)	94.4520(15)	79.1459(12)	79.098(3)	90
γ [deg]	90	90	79.6587(12)	79.588(3)	90
V [Å^3]	8473.10(17)	8454.3(2)	3344.28(9)	3318.2(2)	9764.1(4)
Z [Z']	4	4	2	2	8
Density [gcm^{-3}]	1.483	1.556	1.489	1.590	1.531
μ (mm^{-1})	0.357	1.735	0.426	2.184	2.255
θ range [deg]	6.196 to 52.744	6.438 to 52.744	5.97 to 52.742	5.986 to 52.7444	13.022 to 120.028
Reflns collected	84435	184417	79957	34737	68139
R_{int}	0.0441	0.1134	0.0371	0.0279	0.2197
Completeness	99.8	99.8	99.9	99.8	99.7
No. of data/restr/param	17305/504/1225	17259/405/1197	13665/532/952	13561/532/960	7224/639/804
R_1 [$I > 2\sigma(I)$]	0.0350	0.0365	0.0410	0.0323	0.0734
wR_2 [all data]	0.0848	0.0766	0.1142	0.0714	0.2292
GoF	1.018	1.016	1.051	1.038	0.985
Largest diff. pk and hole [eÅ^{-3}]	0.48/-0.68	0.64/-0.61	0.74/-0.69	1.45/-1.02	0.43/-0.44
Flack (*x*)	-0.024(5)	-	-	-	-

Table 4.8: *Crystallographic data for potassium complexes for 18-crown-6, **A2**, **17**, **3**, **11a**, **12a***

	[18-crown-6·K] $[\mathrm{BAr^F}_4]$	[A2·K]$[\mathrm{BAr^F}_4]$	[17·K]$[\mathrm{BAr^F}_4]$	[3·K]$[\mathrm{BAr^F}_4]$	[11a·K]$[\mathrm{BAr^F}_4]$	[12a·K]$[\mathrm{BAr^F}_4]$	
CCDC/ID	0184abc15	0182abc15a	0217abc16	0148abc15	0108abc14	0106abc14	
Figure	**Figure 4.10**	**Figure 4.12**	**Figure 4.14**	**Figure 4.14**	**Figure 4.16**	**Figure 4.16**	
Formula	$C_{44}H_{31}BF_{24}KO_6$	$C_{72}H_{60}BF_{24}KO_4$	$C_{76}H_{64}BF_{24}KN_2O_4S$	$C_{80}H_{68}BF_{24}KN_4O_4S_2$	$C_{120}H_{92}B2F_{48}KN_4O_4RhS_2$	$C_{120}H_{92}B_2F_{48}KN_4O_4IrS_2$	
M	1161.60	1495.11	1607.26	1719.41	2793.72	2883.01	
Crystal System	tetragonal	tetragonal	monoclinic	monoclinic	Monoclinic	Monoclinic	
Space group	$P4_1$	$I4_1/a$	$P2_1/n$	$P2_1/c$	Cc	Cc	
Radiation	CuKα (λ = 1.54178 Å)	CuKα (λ = 1.54178 Å)	Mo Kα (λ = 0.71073 Å)	CuKα (λ = 1.54178 Å)	Mo Kα (λ = 0.71073 Å)	Mo Kα (λ = 0.71073 Å)	
***T* [K]**	150(2)	150(2)	150(2)	150(2)	150(2)	150(2)	
***a* [Å]**	10.35845(7)	18.2071(3)	21.8843(3)	19.56163(10)	21.1080(2)	21.0354	
***b* [Å]**	10.35845(7)	18.2071(3)	13.02630(12)	18.55522(11)	30.0680(2)	30.0638(2)	
***c* [Å]**	46.9994(5)	20.3230(4)	27.6180(3)	21.98471(12)	20.1929(2)	20.2173(2)	
α[deg]	90	90	90	90	90	90	
β [deg]	90	90	108.4047(12)	97.5122(5)	109.3759(12)	109.3840(14)	
γ [deg]	90	90	90	90	90	90	
***V* [Å^3]**	5042.92(9)	6737.0(3)	7470.40(15)	7911.31	12090.1(2)	12060.7(2)	
***Z* [*Z'*]**	4	4	4	4	4	4	
Density [gcm^{-3}]	1.530	1.474	1.429	1.444	1.535	1.588	
μ (mm^{-1})	2.157	1.729	0.209	2.047	0.339	1.205	
θ range [deg]	12.658 to 133.18	13.056 to 133.14	5.948 to 52.436	12.968 to 149.004	6.694 to 52.742	6.696 to 52.744	
Reflns collected	29477	13213	183708	66723	130874	116009	
R_{int}	0.0259	0.0286	0.0466	0.0369	0.0392	0.0472	
Completeness	99.8	99.8	99.9	99.8	99.8	99.8	
No. of data/restr/param	8753/1600/987	2982/427/403	15254/610/1109	16145/441/1133	24663/1358/1924	24628/1145/1852	
R_1 [$I > 2\sigma(I)$]	0.0532	0.0949	0.0458	0.0473	0.0347	0.0303	
wR_2 [all data]	0.1205	0.3268	0.1251	0.1287	0.0891	0.0718	
GoF	1.023	1.122	1.037	1.030	1.030	1.023	
Largest diff. pk and hole [eÅ^{-3}]	0.35/-0.28	0.45/-0.50	0.74/-0.53	0.62/-0.48	0.64/-0.26	0.64/-0.40	
Flack (*x*)	0.008(4)	-	-	-	0.024(5)	-0.0162(13)	

4.5 References

1. N. Kuhn and T. Kratz, *Synthesis*, 1993, **1993**, 561-562.

2. S. R. Page, C. E. Sheard, M. Herbert, M. Hopton and W. J. Jeffcoate, *Clinical Endocrinology*, 1996, **45**, 511-515.

3. D. J. Williams, D. Vanderveer, R. L. Jones and D. S. Menaldino, *Inorg. Chim. Acta*, 1989, **165**, 173-178.

4. A. Neveling, G. R. Julius, S. Cronje, C. Esterhuysen and H. G. Raubenheimer, *Dalton Trans.*, 2005, 181-192.

5. M. Imran, B. Neumann, H.-G. Stammler, U. Monkowius, M. Ertl and N. W. Mitzel, *Dalton Trans.*, 2014, **43**, 1267-1278.

6. W.-G. Jia, Y.-C. Dai, H.-N. Zhang, X. Lu and E.-H. Sheng, *RSC Advances*, 2015, **5**, 29491-29496.

7. G. E. Tyson, K. Tokmic, C. S. Oian, D. Rabinovich, H. U. Valle, T. K. Hollis, J. T. Kelly, K. A. Cuellar, L. McNamara, N. I. Hammer, C. E. Webster, A. G. Oliver and M. Zhang, *Dalton Trans.*, 2015.

8. B. S. Stadelman, M. M. Kimani, C. A. Bayse, C. D. McMillen and J. L. Brumaghim, *Dalton Trans.*, 2016, **45**, 4697-4711.

9. M. V. Baker, S. K. Brayshaw, B. W. Skelton and A. H. White, *Inorg. Chim. Acta*, 2004, **357**, 2841-2849.

10. T. Matsuda, M. Shigeno and M. Murakami, *Chem. Lett.*, 2006, **35**, 288-289.

11. M. Jagenbrein, K. Y. Monakhov and P. Braunstein, *J. Organomet. Chem.*, 2015, **796**, 11-16.

12. J. R. Miecznikowski, W. Lo, M. A. Lynn, S. Jain, L. C. Keilich, N. F. Kloczko, B. E. O'Loughlin, A. P. DiMarzio, K. M. Foley, G. P. Lisi, D. J. Kwiecien, E. E. Butrick, E. Powers and R. Al-Abbasee, *Inorg. Chim. Acta*, 2012, **387**, 25-36.

13. J. Reglinski, M. D. Spicer, M. Garner and A. R. Kennedy, *J. Am. Chem. Soc*, 1999, **121**, 2317-2318.

14. M. D. Spicer and J. Reglinski, *Eur.J. Inorg.Chem.*, 2009, 1553-1574.

15. S. L. De Wall, E. S. Meadows, L. J. Barbour and G. W. Gokel, *Proc. Natl. Acad. Sci. U.S.A.*, 2000, **97**, 6271-6276.

16. L. N. Appelhans, D. Zuccaccia, A. Kovacevic, A. R. Chianese, J. R. Miecznikowski, A. Macchioni, E. Clot, O. Eisenstein and R. H. Crabtree, *J. AM. CHEM. SOC.*, 2005, 16299-16311.

17. A. Verdian-Doghaei, M. R. Housaindokht and K. Abnous, *Analytical Biochemistry*, 2014, **466**, 72-75.

18. C. Xu, L. Yuan, X. Shen and M. Zhai, *Dalton Trans.*, 2010, **39**, 3897-3902.

19. D.-S. Guo, V. D. Uzunova, X. Su, Y. Liu and W. M. Nau, *Chem. Sci.*, 2011, **2**, 1722-1734.

20. P. E. Georghiou, S. Rahman, G. Valluru, L. N. Dawe, S. M. S. Rahman, A. N. Alodhayb and L. Y. Beaulieu, *New J. Chem.*, 2013, **37**, 1298-1301.

21. A. Sigel, H. Sigel and R. K. O. Sigel, *The Alkali Metal Ions: Their Role for Life*, Springer, 2016.

22. M. J. Page and E. Di Cera, *Physiol. Rev.*, 2006, **86**, 1049.

23. C. A. Austin and M. T. Rodgers, *J. Phys. Chem. A*, 2014, **118**, 5488-5500.

24. C. J. Pedersen, *J. Am. Chem. Soc*, 1967, **89**, 7017-7036.

25. C. J. Pedersen, *J. Am. Chem. Soc*, 1967, **89**, 2495-2496.

26. G. W. Gokel, W. M. Leevy and M. E. Weber, *Chem. Rev.*, 2004, **104**, 2723-2750.

27. J. M. Lehn, *Angew. Chem. Int. Ed.*, 1970, **9**, 175-175.

28. P. B. Smith, J. L. Dye, J. Cheney and J. M. Lehn, *J. Am. Chem. Soc*, 1981, **103**, 6044-6048.

29. *Cation Binding by Macrocycles: Complexation of Cationic Species by Crown Ethers*, Taylor & Francis, 1990.

30. N. G. Khusainova, S. M. Rybakov, D. A. Safin, D. B. Krivolapov and I. A. Litvinov, *Z. Anorg. Allg. Chem*, 2008, **634**, 1836-1838.

31. S. Faulkner, R. Kataky, D. Parker and A. Teasdale, *J. Chem. Soc., Perkin Trans. 2*, 1995, 1761-1769.

32. G. McSkimming, J. H. R. Tucker, H. Bouas-Laurent, J.-P. Desvergne, S. J. Coles, M. B. Hursthouse and M. E. Light, *Chem. Eur. J.*, 2002, **8**, 3331-3342.

33. D. Liu, D. Wang, M. Wang, Y. Zheng, K. Koynov, G. K. Auernhammer, H.-J. Butt and T. Ikeda, *Macromolecules*, 2013, **46**, 4617-4625.

34. J. P. Chinta, B. Ramanujam and C. P. Rao, *Coord. Chem. Rev.*, 2012, **256**, 2762-2794.

35. M. Yamada, Y. Shimakawa and F. Hamada, *Tetrahedron*, 2011, **67**, 7392-7399.

36. K. Iwamoto and S. Shinkai, *J. Org. Chem.*, 1992, **57**, 7066-7073.

37. S. E. Matthews, P. Schmitt, V. Felix, M. G. B. Drew and P. D. Beer, *J. Am. Chem. Soc.*, 2002, **124**, 1341-1353.

38. A. Ikeda and S. Shinkai, *J. Am. Chem. Soc*, 1994, **116**, 3102-3110.

39. P. D. Beer, M. G. B. Drew, P. A. Gale, P. B. Leeson and M. I. Ogden, *J. Chem. Soc., Chem. Commun.*, 1994, 3479-3485.

40. E. Ghidini, F. Ugozzoli, R. Ungaro, S. Harkema, A. Abu El-Fadl and D. N. Reinhoudt, *J. Am. Chem. Soc.*, 1990, **112**, 6979-6985.

41. Y. Li, H. Zhao, X. Mao, X. Pan and J. Wu, *Dalton Trans.*, 2016, **45**, 9636-9645.

42. J. M. Harrowfield, M. I. Ogden, W. R. Richmond and A. H. White, *J. Chem. Soc., Chem. Commun.*, 1991, 1159-1161.

43. A. Casnati, M. Fochi and A. Pochini, *Gazz. Chim. Ital.*, 1996, 99-106.

44. A. Ikeda, M. Yoshimura, P. Lhotak and S. Shinkai, *J. Chem. Soc., Perkin Trans. 1*, 1996, 1945-1950.

45. E. Brenner, D. Matt, M. Henrion, M. Teci and L. Toupet, *Dalton Trans.*, 2011, **40**, 9889-9898.

46. J. W. Steed and J. L. Atwood, in *Supramol. Chem.*, John Wiley & Sons, Ltd, 2009, 105-222.

47. *Structural Inorganic Chemistry*, Clarendon Press, Oxford, 1984.

48. S. K. Murphy, A. Bruch and V. M. Dong, *Chem. Sci.*, 2015, **6**, 174-180.

49. M. J. Krause and R. G. Bergman, *Organometallics*, 1986, **5**, 2097-2108.

50. T. Irrgang, D. Friedrich and R. Kempe, *Angew. Chem. Int. Ed.*, 2011, **50**, 2183-2186.

51. C. Tejel, M. A. Ciriano, M. P. del Río, D. G. H. Hetterscheid, N. Tsichlis Spithas, J. M. M. Smits and B. de Bruin, *Chem. Eur. J.*, 2008, **14**, 10932-10936.

52. I. R. Crossley, A. F. Hill, E. R. Humphrey, M. K. Smith, N. Tshabang and A. C. Willis, *Chem. Comm.*, 2004, 1878-1879.

53. G. Giordano and R. H. Crabtree, *Inorg. Synth.*, 1990, **28**, 88-90.

54. W. E. Buschmann and J. J. Miller, *Inorg. Synth.*, 2002, **33**, 83-85.

55. M. Larsen and M. Jørgensen, *J. Org. Chem.*, 1996, **61**, 6651-6655.

56. I. Dinarès, C. G. Miguel, N. Mesquida and E. Alcalde, *J. Org. Chem.*, 2008, **74**, 482–485.

57. R. E. Andrew, C. M. Storey and A. B. Chaplin, *Dalton Trans.*, 2016, **45**, 8937-8944.

58. G. M. Sheldrick, *Acta Cryst.*, 2008, **A64**, 112-122.

5.0 Summary and outlook

Despite the long period of investigation since the elucidation of their structure in the 1940s relatively few calix[4]arene complexes bearing transition metals over the calix[4]arene cavity have been reported. In particular there are few examples of NHC and no examples of NHCS-calix[4]arene complexes have been reported.

This thesis describes the preparation of bi- and mono-metallic calix[4]arene-NHC complexes (**4a**, **5a**, **7a** and **8a**) and calix[4]arene–thione complexes (**11a** and **12a**). Their structural properties have been studied by NMR spectroscopy and X-ray analysis and by comparison to model complexes containing the **I^{i}Pr$_2$Me$_2$** and **I^{i}Pr$_2$Me$_2$S** ligands.

Synthesis of 1,3-imidazolinium functionalised calix[4]arenes proved challenging due to the low selectivity for the synthesis of the 1,3-dinitrocalix[4]arene **A82** by nitration of *p-tert*butylcalix[4]arene **A2** or calix[4]arene **A19**. However, adaption of literature procedures resulted, in the synthesis of 1,3-imidazolium pro-ligand **2a.2HI** over a six step synthesis pathway with an overall yield of 7%.

Reaction of **2a** with Rh(I) precursors [Rh(COD)Cl]$_2$ and [Rh(CO)$_2$Cl]$_2$ resulted in the formation of bimetallic complexes, featuring discrete Rh(COD)I and Rh(CO)$_2$I centres (**4a** and **5a**). Transmetallation from the isolated silver complex **6a** resulted in the formation of μ-Cl bridged complexes **7a** and **8a** (**Scheme 5.1**). These structures highlight the flexibility of the calix[4]arene scaffold, which underwent significant conformational distortion as a result of charge repulsion (**2a.2HI**), π-stacking of the imidazolylidene rings (**4a**), *trans*-coordination to silver (**6a**), or presence of a bridging μ^2-Cl ligand (**8a**).

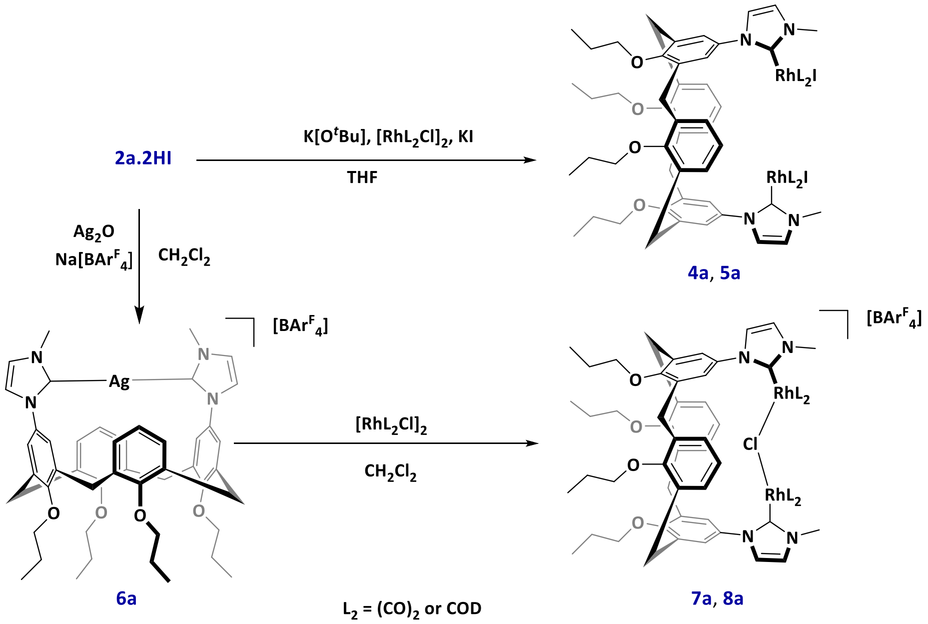

Scheme 5.1: Formation of bimetallic calix[4]arene complexes from **2a.2HI**

Imidazole-2-thione functionalised calix[4]arene **3** was synthesised by deprotonation using a weak base and addition of elemental sulfur. Ligand **3** was subsequently used in the formation of mononuclear Rh and Ir COD complexes **11a** and **12a** which were fully characterised in solution and in the solid state (**Scheme 5.2**). These showed excellent agreement with the **I^{i}Pr$_2$Me$_2$S** model complexes. **3** was found to bind more weakly to the transition metal centres than their **I^{i}Pr$_2$Me$_2$S** based analogues; this was presumed to be a result of the strain associated with the S-M-S bonds angles, which were slightly smaller in **11a** and **12a** than those for the corresponding complexes of **I^{i}Pr$_2$Me$_2$S (11b** and **12b)**.

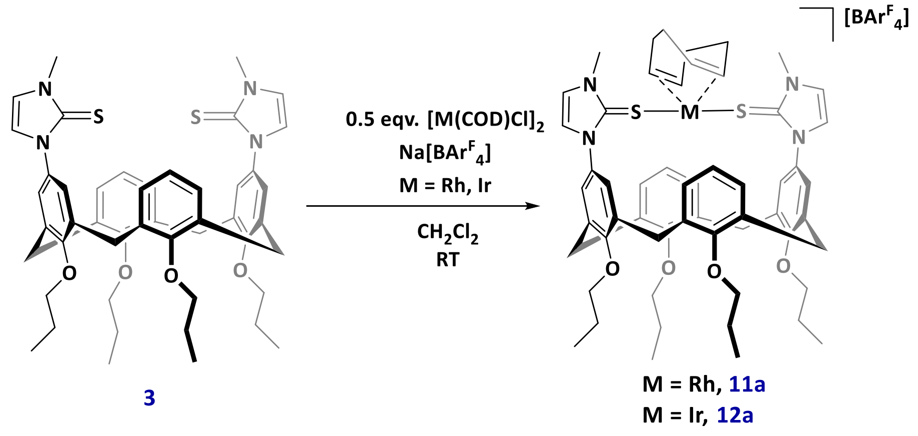

Scheme 5.2: Synthesis of imidazole-2-thione complexes **11a** and **12a**

Isolated calix[4]arene species, most interestingly the rhodium(I) and iridium(I) complexes **11a** and **12a** showed a good affinity for the binding of potassium cations, and could be formed easily by the addition of $K[BAr^F_4]$. These potassium complexes were all analysed in solution and the solid state, which confirmed the presence of the potassium guest within the calix[4]arene cavity. Evidence for π-dontation from calix[4]arene scaffold, donation from ether functionalities and chelation from thione donors, where present, were evident from X-ray diffraction and NMR spectra. Although encapsulation of potassium cations with calix[4]arene species have been previously reported, few examples exist with the cation is bound deeply inside the cavity, and to the writers knowledge no previous examples with potassium cations held in close proximity to a transition metal cation have been reported.

Formation of the potassium adducts of **11a** and **12a** highlight the potential for encapsulation of otherwise weakly binding substrates within the calix[4]arene cavity in order to probe interactions with transition metal centres bound on the upper rim.

Current work is being carried out in the Chaplin group to achieve this by functionalization of the upper rim with phosphinomethyl donors and subsequent coordination with rhodium precursors. Calix[4]arene ligands adapted with pincer functionalities on the upper rim to minimise distortion of the calix[4]arene scaffold may also be targeted as a means to favour the formation of monometallic chelated complexes (**Figure 5.1**).

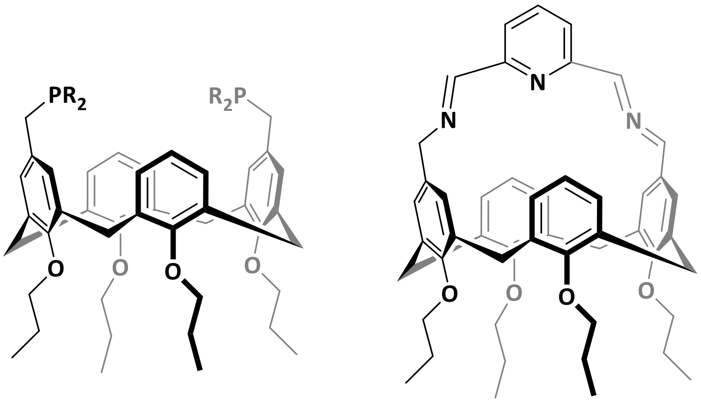

Figure 5.1: Calix[4]arene ligands being developed in the Chaplin group